

**Development, Application and Mechanistic Investigation of Palladium Catalyzed
Aerobic Oxidative Amination Methods**

By

Adam B. Weinstein

A dissertation submitted in partial fulfillment of
the requirements for the degree of

Doctor of Philosophy

(Chemistry)

at the

UNIVERSITY OF WISCONSIN–MADISON

2014

Date of final oral examination: 05/08/2014

The dissertation is approved by the following members of the Final Oral Committee:

Shannon S. Stahl, Professor, Chemistry

Clark R. Landis, Professor, Chemistry

Steve D. Burke, Professor, Chemistry

Jennifer M. Schomaker, Assistant Professor, Chemistry

Ive Hermans, Associate Professor, Chemistry

**Development, Application and Mechanistic Investigation of Palladium Catalyzed
Aerobic Oxidative Amination Methods**

By

Adam B. Weinstein

Under the supervision of Professor Shannon S. Stahl

at the University of Wisconsin-Madison

Abstract

Palladium catalyzed oxidative transformations that employ readily available molecular oxygen as the stoichiometric oxidant enable economic synthetic routes to complex organic targets. This thesis focuses on the development of aerobic oxidative transformations that generate carbon–nitrogen bonds. Chapters 2 and 3 describe research projects that have expanded the scope and mechanistic understanding of reactions that involve amidopalladation of alkenes (aza-Wacker reactions). Chapters 4, 5 and 6 describe research projects that have targeted the discovery of aryl C–H amination reactions. Palladium catalyzed aerobic C–H amination reactions have limited precedent. Several approaches to address this challenge were tested, and promising results are discussed.

Acknowledgements

I thank my advisor, Shannon Stahl, whose unwavering enthusiasm for science has been a consistent source of inspiration during my graduate studies. With Shannon's guidance and based on his example, I have learned to experiment with rigor, to speculate with a creative impulse, and to communicate with clarity and passion.

I thank all of my colleagues in the Stahl Group, whose professionalism and friendship have helped make these years of study enjoyable. The sharing of ideas and knowledge within the labs has been intellectually stimulating, and the sharing of beers sampled from around our town has been emotionally rewarding.

I thank the undergraduate chemistry students, Zhi Xu Tan and David Schuman, who I've had the privilege of mentoring. Their devotion to their work has helped motivate me in my own studies, and their sharp intellect has kept me honest.

I thank the UW–Madison chemistry department for sustaining and facilitating my research efforts. I especially thank the NMR Spectroscopy facility managers, Drs. Charlie Fry, Monika Ivancic and Bob Shanks, who have maintained a state-of-the-art facility that has been of critical importance for the research described in this thesis. I also thank my thesis committee members and the other faculty members of the department for establishing our vibrant community and for providing insight and perspective during various seminars and meetings.

Finally, I thank you, for your interest in this volume of work. This was the best I could do.

Adam B. Weinstein

May 1st, 2014

Table of Contents

Abstract	i
Acknowledgements	ii
Table of Contents	iii
List of Schemes	vii
List of Tables	x
List of Figures	xi
Abbreviations and Acronyms	xii
Chapter 1. <i>A Survey of Issues Concerning the Development of Palladium Catalyzed Aerobic Oxidation of Alkenes and C–H Bonds</i>	1
1.1 The Aerobic Palladium Oxidase Paradigm	2
1.2 Aerobic Oxidation of Alkenes	2
1.2.1 The Wacker Process	2
1.2.2 Wacker-Type Reactions	3
1.2.3 The Stereochemical Course of Nucleopalladation of an Alkene	5
1.3 Aerobic Oxidation of C–H Bonds	6
1.3.1 C–H Activation, C–X Reductive Elimination, and the Oxidant Problem	6
1.3.2 Strategies for Overcoming the Oxidant Problem	9
1.3.2.1 Ligand Promoted Aerobic C–H Functionalizations	9
1.3.2.2 Redox Co-catalysts	13
1.3.2.3 Trapping of Strong Peroxide Oxidants Derived from O ₂	15
1.4 References and Notes	17
Chapter 2. <i>Synthesis of Vicinal Aminoalcohols by Stereoselective Aza-Wacker Cyclizations: Access to (–)-Acosamine by Redox Relay</i>	21
2.1 Introduction	22

2.2	Results and Discussion	23
2.3	Acknowledgements	29
2.4	Experimental Details and Supporting Information	30
2.4.1	General considerations	30
2.4.2	Preparation of <i>O</i> -acetyl hemiaminal tethering reagents	30
2.4.3	Preparation of <i>O</i> -allyl hemiaminal substrates	31
2.4.4	Aza-Wacker cyclization of <i>O</i> -allyl hemiaminal substrates	42
2.4.5	Allylic <i>N</i> -tosyl carbamate and <i>N</i> -allyl hemiaminal substrates	49
2.4.6	Deprotection of 5b and 6j	51
2.4.7	NOESY-1D analysis of 6a and 6j	53
2.4.8	Synthesis of (–)- <i>N</i> -Cbz- <i>O</i> -methylacosamine, COSY analysis	55
2.5	References and Notes	63
Chapter 3.	<i>Reconciling the Stereochemical Course of Nucleopalladation with the Development of Enantioselective Wacker-Type Cyclizations</i>	67
3.1	Introduction	68
3.2	Results and Discussion	70
3.3	Acknowledgements	76
3.4	Experimental Details and Supporting Information	77
3.4.1	General considerations	77
3.4.2	Experimental procedures and data for the determination of <i>trans</i> -vs. <i>cis</i> -AP	77
3.4.3	Stereoselective synthesis of deuterium labeled substrate probe	86
3.4.4	Synthesis of protio intermediates and analogues	90
3.4.5	Characterization of stereochemical purity of the deuterated substrate probe	93
3.4.6	Synthesis of pyridine-oxazoline ligand	96

3.4.7 Use of cyclopentenyl deuterated substrate probe	99
3.5 References and Notes	101
Chapter 4. <i>Synthesis of Indole-2-carboxylates via Palladium-Catalyzed Aryl C–H Amination Reactions</i>	106
4.1 Introduction	107
4.2 Results and Discussion	109
4.3 Experimental Details and Supporting Information	112
4.3.1 General considerations	112
4.3.2 Preparation of 2-acetamide-3-aryl-ethylacrylate substrates	112
4.3.3 Preparation of indole-2-carboxylates	114
4.4 References and Notes	117
Chapter 5. <i>Design of 8-Aryl Quinoline Ligands for Palladium-Catalyzed Aryl C–H Amination Reactions</i>	120
5.1 Introduction	121
5.2 Results and Discussion	123
5.3 Experimental Details and Supporting Information	129
5.3.1 General considerations	129
5.3.2 General procedures for reaction screening	129
5.3.3 Benzenesulfonyl-protected 2-aminobiphenyl and carbazole	130
5.3.4 Synthesis of 8-aryl-quinoline ligands	131
5.4 References and Notes	139
Chapter 6. <i>Powerful Peroxide Oxidants Derived from Molecular Oxygen for Palladium-Catalyzed Aryl C–H Amination Reactions</i>	141
6.1 Introduction	142
6.2 Results and Discussion	144
6.3 Experimental Details and Supporting Information	153

6.3.1 General considerations	153
6.3.2 General procedure for reaction set up	153
6.3.3 Benzenesulfonyl-protected 2-aminobiphenyl and carbazole	154
6.3.4 Typical crude ^1H NMR spectrum and isolation of 1,4-dioxane autoxidation byproducts	155
6.4 References and Notes	157
Appendix 1. <i>NMR Spectra for Chapter 2</i>	161
Appendix 2. <i>NMR Spectra for Chapter 3</i>	208
Appendix 3. <i>NMR Spectra for Chapter 4</i>	222
Appendix 4. <i>NMR Spectra for Chapter 5</i>	227

List of Schemes

Scheme 1.1.	The Pd ^{II} /Pd ⁰ aerobic oxidase paradigm.	2
Scheme 1.2.	The Wacker Process.	3
Scheme 1.3.	Nucleopalladation of an alkene and the diverse reactivity of Pd ^{II} –alkyl species.	4
Scheme 1.4.	Aza-Wacker cyclization of γ -hexenyl tosylamides.	5
Scheme 1.5.	The stereochemical course of nucleopalladation of an alkene.	6
Scheme 1.6.	Comparative analysis of a) Pd ⁰ /Pd ^{II} cross couplings, b) Pd ^{II} /Pd ⁰ aerobic oxidative couplings and c) Pd ^{II} /Pd ^{IV} oxidative couplings.	7
Scheme 1.7.	Arylation of anilides using dimethylsulfoxide supported Pd ^{II} /Pd ⁰ catalysis.	9
Scheme 1.8.	Dimethylsulfoxide as the solvent stabilizes Pd ⁰ at high temperatures.	10
Scheme 1.9.	2-Fluoropyridine supported Pd catalyst balances C–H activation and reductive elimination steps with stabilization and reoxidation of Pd ⁰ .	11
Scheme 1.10.	4,5-Diazafluorenone promotes aerobic allylic acetoxylation.	12
Scheme 1.11.	4,5-Diazafluorenone promotes reductive elimination of allyl acetate.	13
Scheme 1.12.	Standard reduction potentials of O ₂ and H ₂ O ₂ .	13
Scheme 1.13.	Proposed mechanism of Pd ^{II} /NO ₂ co-catalyzed aerobic sp ³ C–H acetoxylation.	15
Scheme 1.14.	Palladium-catalyzed aryl C–H hydroxylation with O ₂ -derived peroxide.	16
Scheme 2.1.	a) Detachable tethered nucleophile approach for the synthesis of vicinal aminoalcohols from allylic alcohols. b) Aminosugars in natural product antibiotic and anticancer agents. Z = benzyloxycarbonyl (Cbz) or <i>tert</i> -butoxycarbonyl (Boc).	23
Scheme 2.2.	Transformation of primary allylic alcohols into vicinal aminoalcohols. PTS = pyridinium <i>p</i> -tolueneulfonate.	25

Scheme 2.3.	Transformation of enantioenriched allylic alcohol to the oxazolidine with no epimerization. rsm = recovered starting material.	27
Scheme 2.4.	Retrosynthetic analysis of 2-deoxy-3-aminosugars with application of aza-Wacker cyclization and redox-relay.	28
Scheme 2.5.	Synthesis of (–)- <i>N</i> -Cbz- <i>O</i> -methylacosamine	28
Scheme 3.1.	Stereochemical pathways for alkene nucleopalladation.	69
Scheme 3.2.	Pyrox-ligated palladium catalysts for enantioselective aza-Wacker cyclizations.	70
Scheme 3.3.	Cyclization of substrate 3-D-4 with chiral catalyst.	70
Scheme 3.4.	a) Mechanistic pathways for the reaction of 6-D-1 and b) mathematical relationships used to determine the yields of products A-D.	71
Scheme 3.5.	Experimental data and <i>trans</i> : <i>cis</i> -AP selectivity obtained from oxidative cyclization of substrate 6-D-1 with the optimized chiral catalyst conditions.	73
Scheme 3.6.	Experimental data and <i>trans</i> : <i>cis</i> -AP selectivity obtained from oxidative cyclization of substrate 6-D-1 with a Pd(pyrox)(OAc) ₂ catalyst system (refer to Scheme 3.5 for depiction of the reaction).	74
Scheme 3.7.	Potential isomerizations when using substrate probe 6-D-S1	79
Scheme 3.8.	Application of novel deuterated substrate probe	80
Scheme 3.9.	Raw experimental data: Pd(OAc) ₂ / pyridine catalyst system.	81
Scheme 3.10.	Raw experimental data: Pd(TFA) ₂ / (<i>S</i>)-pyrox catalyst system.	82
Scheme 3.11.	Raw experimental data: Pd(TFA) ₂ / (<i>R</i>)-pyrox catalyst system.	82
Scheme 3.12.	Raw experimental data: Pd(OAc) ₂ / (<i>S</i>)-pyrox catalyst system.	83
Scheme 3.13.	Raw experimental data: Pd(TFA) ₂ / no ligand catalyst system.	83
Scheme 3.14.	Raw experimental data: Pd(OAc) ₂ / no ligand catalyst system.	84
Scheme 3.15.	Attempt to study reactivity with modified pyrox ligand.	85
Scheme 3.16.	Characterization of stereochemical purity of probe 6-D-S1.	96

Scheme 4.1.	Prior examples of intramolecular palladium catalyzed aryl C–H aminations.	108
Scheme 4.2.	An aerobic aryl C–H amination reaction for the synthesis of indole-2-carboxylates from readily accessible 2-acetamido-3-aryl-acrylates.	109
Scheme 5.1.	Mechanistic manifolds for Pd ^{II} /Pd ⁰ -catalyzed construction of aryl C–N bonds.	121
Scheme 5.2.	Design of oxidatively stable 8-aryl-quinoline ligands that mimic the architecture of biaryl phosphine ligands.	123
Scheme 5.3.	Palette of electronically diverse 8-aryl-quinoline ligands.	124
Scheme 5.4.	a) Carbazole synthesis with 4-OMe-SQuin ligated Pd ^{II} catalyst at elevated oxygen pressure. b) Attempted extension to substrates for indole synthesis failed.	127
Scheme 6.1.	The oxidant problem in Pd ^{II} /Pd ^{IV} catalysis of aryl C–H amination reactions.	142
Scheme 6.2.	a) Discovery of a positive effect of peroxide species in carbazole synthesis. b) Dioxane decomposition by autoxidation.	144
Scheme 6.3.	a) Generation of activated peroxide by reduction of O ₂ and <i>in situ</i> trapping. b) Autoxidation of dioxane initiated by activated trapped peroxide.	148
Scheme 6.4.	Mechanistic pathways for a) further peroxide activation b) decomposition of dioxane and c) decomposition of glycolic acid.	150
Scheme 6.5.	Proposed mechanism for substrate oxidation via Pd ^{IV} /Pd ^{II} catalysis with an <i>in situ</i> generated peroxide as the oxidant.	151

List of Tables

Table 1.1. Co-catalytic nitrate in aerobic sp^3 C–H acetoxylation.	14
Table 2.1. Evaluation of diastereoselective oxidative cyclization of substrates derived from an allylic alcohol or an allylic amine.	24
Table 2.2. Diastereoselective synthesis of oxazolidines from cyclization of secondary <i>O</i> -allyl hemiaminals.	26
Table 3.1. Summary of amidopalladation studies with pyrox-ligated and ligand-free catalysts.	75
Table 4.1. Investigation of dimethylsulfoxide-based palladium catalyst systems for intramolecular aerobic C–H amination of 2-acetamido-3-phenyl-ethylacrylate.	110
Table 4.2. a) Preliminary investigation of the scope of intramolecular aerobic C–H amination of 2-acetamido-3-aryl-ethylacrylates. b) Ineffective substrates.	111
Table 6.1. Investigation of additive effects on carbazole synthesis with a $\text{Pd}(\text{OAc})_2$ / DAF / 1 atm O_2 catalyst system.	146

List of Figures

- Figure 5.1.** Ligand screen for carbazole synthesis (solvent = benzene; temperature = 60 °C). Yield of product was determined by ^1H NMR spectroscopic analysis of the reaction mixture using phenyltrimethylsilane as the internal standard. 125
- Figure 5.2.** Ligand screen for carbazole synthesis (solvent = dioxane; temperature = 80 °C). Yield of product was determined by ^1H NMR spectroscopic analysis of the reaction mixture using phenyltrimethylsilane as the internal standard. 126
- Figure 6.1.** Ligand screen for carbazole synthesis in the presence of glycolic acid and dioxane solvent. Yield of product was determined by ^1H NMR spectroscopic analysis of the reaction mixture using phenyltrimethylsilane as the internal standard. 147

Abbreviations and Acronyms

atm	atmosphere
equiv	equivalents
rsm	recovered starting material
TON	turnover number
NMR	nuclear magnetic resonance
NOESY	Nuclear Overhauser effect spectroscopy
NP	nucleopalladation
AP	amidopalladation
pyr	pyridine
DMSO	dimethylsulfoxide
pyrox	pyridyl-oxazoline
DAF	4,5-diazafluorenone
bpy	2,2'-bipyridine
Ts	toluenesulfonyl
Cbz	benzyloxycarbonyl
Boc	<i>tert</i> -butoxycarbonyl
M.S.	molecular sieves

Chapter 1

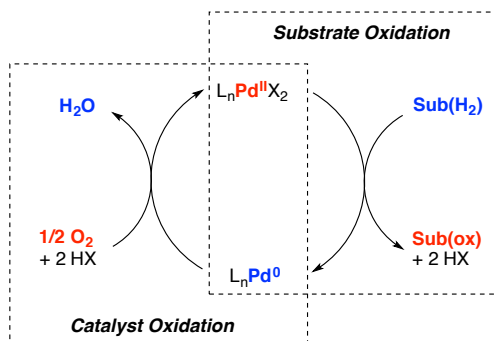
A Survey of Issues Concerning the Development of Palladium

Catalyzed Aerobic Oxidation of Alkenes and C–H Bonds

1.1 The Aerobic Palladium Oxidase Paradigm

The oxidative functionalization of organic substrates allows for streamlined conversion of simple feedstock chemicals into complex target structures.¹ These transformations face several key challenges, including problems with chemo- regio- and stereoselectivity, and with the cost and environmental detriment of the reagents required for the oxidation processes. Our goal is to develop palladium catalysts that mediate the selective two-electron oxidative transformation of a substrate with the two-electron reduction of molecular oxygen (Scheme 1.1).² The availability of molecular oxygen and the environmentally benign nature of the byproduct of its reduction (water) make it an attractive choice as a terminal oxidant. The strategies and challenges associated with the implementation of this paradigm will be discussed below in the context of the oxidative transformations that are relevant to the research presented in this thesis.

Scheme 1.1. The Pd^{II}/Pd⁰ aerobic oxidase paradigm.



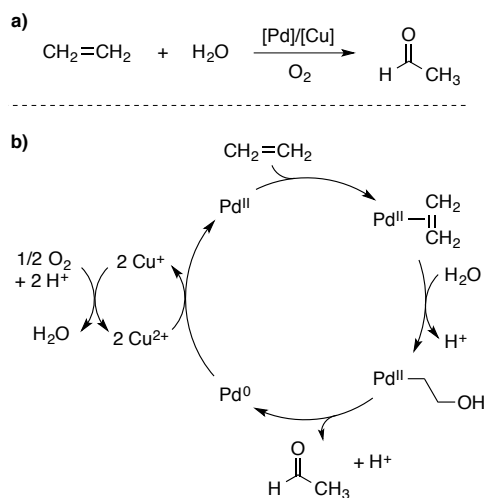
1.2 Aerobic Oxidation of Alkenes

1.2.1. The Wacker Process

The most prominent example of a palladium-catalyzed aerobic oxidation reaction is the Wacker Process, which is the industrial-scale transformation of ethylene gas and water to acetaldehyde in the presence of molecular oxygen and catalytic palladium and copper (Scheme 1.2a).³ The catalytic mechanism involves oxypalladation of ethylene with Pd^{II} and water to

generate a Pd^{II} -alkyl intermediate, which can undergo reductive elimination to give acetaldehyde and Pd^0 . Cu^{II} oxidizes the Pd^0 species to Pd^{II} , and Cu^{II} is regenerated rapidly in the presence of O_2 (Scheme 1.2b).

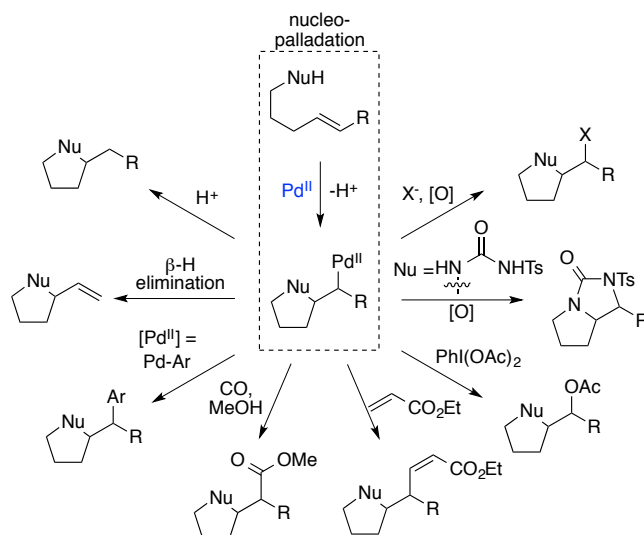
Scheme 1.2. The Wacker Process.



1.2.2. Wacker-Type Reactions

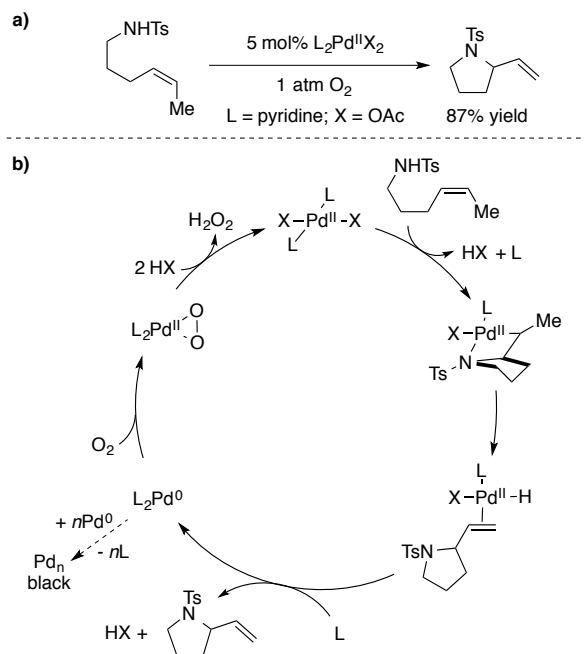
Since its discovery in the 1950's, the Wacker Process has served as the prototypical example for palladium catalyzed oxidative functionalization of alkenes, and a wide range of Wacker-type reactions have been developed.⁴ Wacker-type reactions are defined here as transformations that involve nucleopalladation of an alkene to generate a Pd^{II} -alkyl intermediate. Nucleopalladation of alkenes has proven to be an exceptionally versatile mode of reactivity, as a variety of nitrogen-, oxygen-, and carbon-based nucleophiles have been employed. Moreover, the Pd^{II} -alkyl intermediate that results from nucleopalladation of an alkene is amenable to a broad range of synthetic elaborations, enabling access to diverse structures (Scheme 1.3).

Scheme 1.3. Nucleopalladation of an alkene and the diverse reactivity of Pd^{II}-alkyl species.



Of particular relevance to the research described in this thesis, aza-Wacker cyclization of a nitrogen nucleophile onto a tethered alkene yields *N*-heterocycles.⁵ For example, our group reported that a (pyridine)₂Pd(OAc)₂ catalyst system could mediate the oxidative cyclization of γ -hexenyl tosylamides to pyrrolidines under an atmosphere of oxygen (Scheme 1.4a).⁶ This transformation involves amidopalladation of the alkene to generate a Pd-alkyl species, followed by β -hydride elimination, dissociation of product, and reductive elimination of an equivalent of acid. The Pd⁰ species represents a critical juncture in the catalytic mechanism, as unproductive aggregation of Pd⁰ to Pd black (catalyst death) competes with reaction with O₂ and ultimately regeneration of the active Pd^{II} catalyst. Neutral donor ligands, such as pyridine and dimethylsulfoxide, stabilize the Pd⁰ species and help prevent formation of Pd black.⁷ Chapter 2 of this thesis describes the application of aza-Wacker cyclizations to the stereoselective synthesis of vicinal amino alcohol derivatives from allylic alcohol precursors.

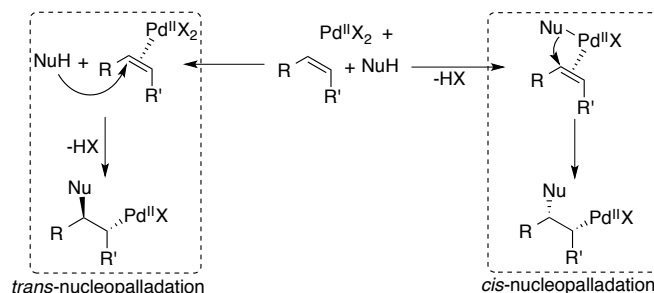
Scheme 1.4. Aza-Wacker cyclization of γ -hexenyl tosylamides.



1.2.3. The Stereochemical Course of Nucleopalladation of an Alkene

Wacker-type reactions are characterized by the nucleopalladation event, in which carbon–nucleophile and carbon–palladium bonds are formed at the olefinic carbons. In many cases, two stereogenic centers are generated during this process, and the relative and absolute configuration of these stereogenic centers typically translates into the final product of the transformation. The stereochemical course of nucleopalladation has been a topic of great intrigue, because two mechanistically distinct stereochemical pathways are possible.⁸ In a *trans*-nucleopalladation, the electrophilic Pd^{II} center activates the alkene for nucleophilic attack from the opposite face, resulting in a Pd–alkyl intermediate in which Pd and the nucleophile are *anti* with respect to each other (Scheme 1.5, left pathway). In a *cis*-nucleopalladation, both the alkene and the nucleophile bind the Pd^{II} center, and migratory insertion of the alkene into the Pd–nucleophile bond results in a Pd–alkyl intermediate in which Pd and the nucleophile are *syn* with respect to each other (Scheme 1.5, right pathway).

Scheme 1.5. The stereochemical course of nucleopalladation of an alkene.



The distinction between these two stereochemical pathways has been the subject of extensive study, and the nature of oxypalladation in the traditional Wacker Process is still under debate. The stereochemical pathway of Wacker-type reactions that lead to products with stereogenic centers is often characterized with cleverly designed substrate probes.⁹ Such studies have revealed that *cis*- and *trans*-NP processes are both prevalent, and thus the selectivity between the *trans*- and *cis*-NP pathways is an important consideration in the development of stereoselective Wacker-type reactions. Chapter 3 of this thesis describes an investigation of the factors that affect the selectivity for *cis*- and *trans*-amidopalladation in the context of an *asymmetric* aza-Wacker cyclization.

1.3 Aerobic Oxidation of C–H bonds

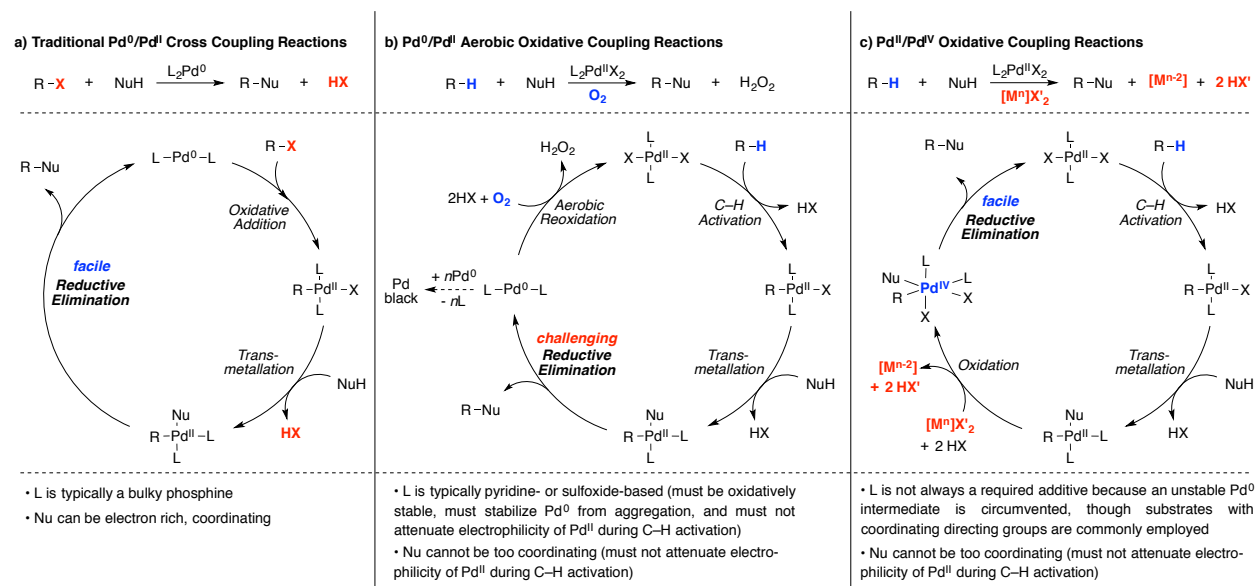
1.3.1. C–H Activation, C–X Reductive Elimination, and the Oxidant Problem

A major limitation in the scope of reactivity amenable to aerobic palladium oxidase catalysis is direct C–H bond activation followed by C–C, C–O or C–N bond forming reductive elimination. Apparently, transformations that terminate in β -hydride elimination, such as the aza-Wacker reactions discussed above and oxidative Heck-type reactions,¹⁰ are more compatible with aerobic regeneration of the active Pd^{II} catalyst than are the direct C–H functionalization reactions.¹¹ While relatively few synthetically useful examples of palladium catalyzed aerobic C–H functionalization exist, examples that take advantage of strong chemical oxidant additives

are more prevalent.¹² This is unfortunate, because the advantages of direct C–H functionalization in streamlining the synthesis of complex targets are partially negated by the wasteful byproducts of these strong chemical oxidants. Explanations for the origin of this challenge, which we term "the oxidant problem," and strategies to address it, are discussed below.

To establish the potential origins of the "oxidant problem" in palladium catalyzed C–H functionalization reactions, a comparative analysis of generic mechanisms for traditional cross coupling and oxidative coupling reactions is worthwhile (Scheme 1.6). In traditional cross coupling reactions, such as Suzuki or Buchwald-Hartwig couplings, a Pd^0 species undergoes oxidative addition into a carbon–halogen bond, transmetalation with a nucleophilic species, and reductive elimination to generate the carbon–nucleophile bond (Scheme 1.6a).¹³ The oxidative addition process is accelerated by the presence of electron-rich, donating ligands bound to Pd^0 .¹⁴ With that in mind, a bulky phosphine ligand is often employed as a strongly coordinating neutral donor ligand, and highly basic nucleophiles are compatible. The reductive elimination process

Scheme 1.6. Comparative analysis of a) $\text{Pd}^0/\text{Pd}^{\text{II}}$ cross couplings, b) $\text{Pd}^{\text{II}}/\text{Pd}^0$ aerobic oxidative couplings and c) $\text{Pd}^{\text{II}}/\text{Pd}^{\text{IV}}$ oxidative couplings.



benefits from these choices in phosphine ligand and nucleophilic coupling partner. Bulky phosphine ligands accelerate the rate of reductive elimination by crowding the Pd square plane and favoring the lower coordination number that follows reductive elimination,¹⁵ and electron rich nucleophilic coupling partners undergo reductive elimination faster than electron poor coupling partners.¹⁶ These features of traditional cross coupling reactions account for the facile reductive elimination that occurs in these systems as compared to the difficult reductive elimination that must occur in oxidative cross coupling reactions. In aerobic oxidative coupling reactions, Pd^{II} catalysts perform C–H activation, metallation with a nucleophilic species, and reductive elimination of carbon–nucleophile bonds to afford Pd⁰ species that must be trapped by O₂ prior to degradation to Pd black (Scheme 1.6b). In contrast to the oxidative addition process in traditional cross coupling reactions, Pd^{II} mediated C–H activation typically proceeds through an electrophilic cyclometalation-deprotonation mechanism¹⁷ and is not compatible with presence of strongly donating neutral ligands or nucleophilic partners. Moreover, the bulky phosphine ligands that have enabled highly efficient cross coupling reactions are not expected to be stable under oxidizing conditions. Instead, pyridine- or sulfoxide-based ligands are often employed. These considerations suggest that a difficult reductive elimination step may account for the challenge in the development of aerobic oxidative coupling reactions. The non-aerobic oxidative coupling reactions that have been developed in recent years circumvent this challenging reductive elimination step (as well as the unstable Pd⁰ intermediate) by employing chemical oxidants that are capable of promoting the oxidation of Pd^{II} to high-valent species, such as Pd^{IV} (Scheme 1.6c).¹⁸ Reductive elimination from an electrophilic high-valent Pd centers is expected to be more favorable than reductive elimination from the corresponding Pd^{II} center.

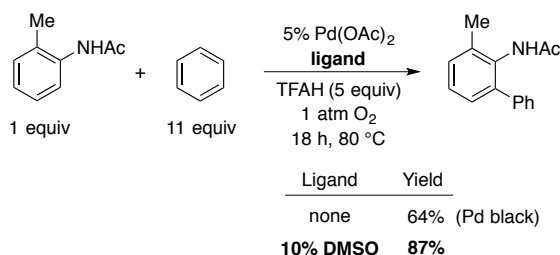
1.3.2. Strategies for Overcoming the Oxidant Problem

1.3.2.1. Ligand Promoted Aerobic C–H Functionalizations

The discovery of new ligand-supported Pd catalyst systems for aerobic C–H functionalization reactions is a central goal of our research efforts. The presence of a suitable neutral donor ligand is critical to the stabilization of the Pd⁰ intermediate and prevention of catalyst death, and our challenge is the identification of ligands that satisfy this function and are compatible with electrophilic C–H activation and reductive elimination. Several successful examples are mentioned below.

Buchwald and coworkers reported the *ortho* arylation of anilides using catalytic Pd(OAc)₂ in the presence of trifluoroacetic acid and 1 atm of O₂ (Scheme 1.7).¹⁹ The authors noted that Pd black was observed, and addition of dimethylsulfoxide (two equivalents with respect to Pd) helped prevent catalyst decomposition and improved the yield and reproducibility of the reaction. This is a straightforward example of the identification of a suitable ligand for the stabilization of Pd⁰ intermediates in an aerobic oxidation reaction, and it is significant in light of the scarcity of aerobic aryl C–H coupling reactions.

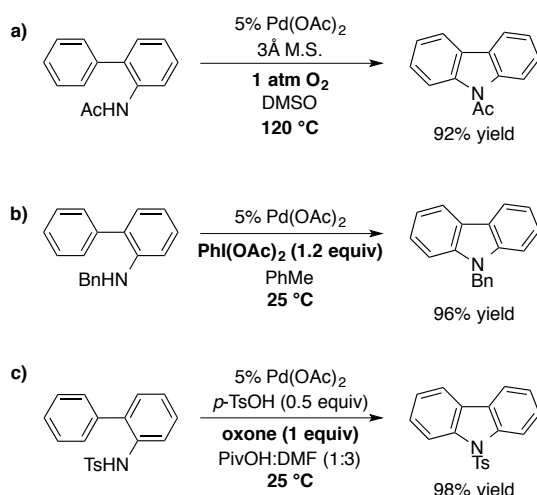
Scheme 1.7. Arylation of anilides using dimethylsulfoxide supported Pd^{II}/Pd⁰ catalysis.



In separate research efforts executed by Buchwald and coworkers, Pd(OAc)₂ was used in dimethylsulfoxide (as the solvent) for the synthesis of carbazoles via intramolecular aryl C–H amination of 2-acetamido-biphenyl substrates.²⁰ Pd(OAc)₂ has been shown to form nanoparticles in dimethylsulfoxide,²¹ and these may act as robust reservoirs of Pd⁰ and accommodate the high

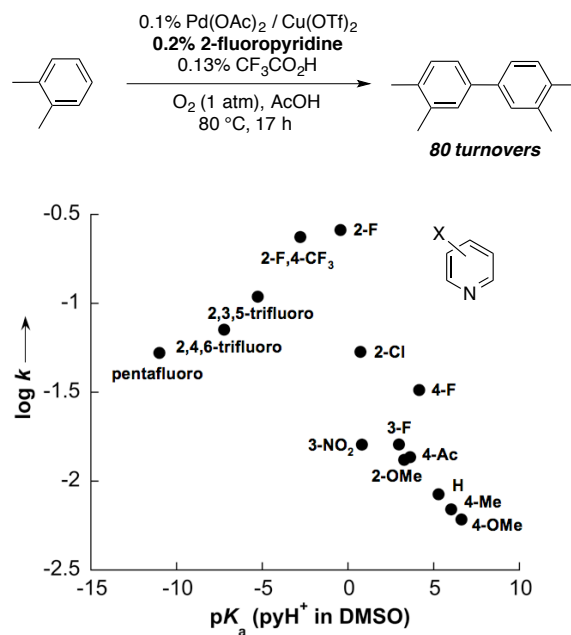
temperatures that are employed in this reaction. This transformation is noteworthy for being the only reported example of an aerobic aryl C–H amination, though the scope is limited and reactivity diminishes when the temperature is lowered from 120 °C. Alternative methods that have been reported in the literature for carbazole synthesis from analogous substrates have employed ambient temperatures and stronger oxidants, such as $\text{PhI}(\text{OAc})_2$ (Scheme 1.8b)²² and oxone (Scheme 1.8c).²³

Scheme 1.8. Dimethylsulfoxide as the solvent stabilizes Pd^0 at high temperatures.

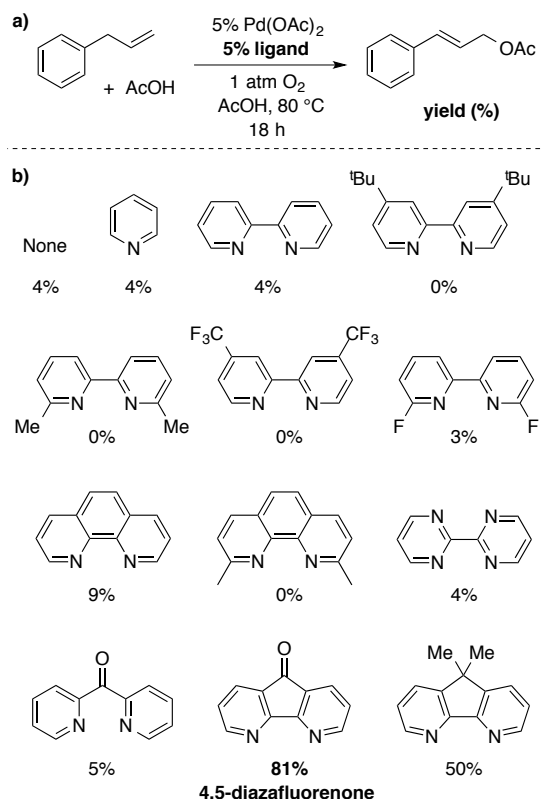


A report from our group described the aerobic homocoupling of *o*-xylene using catalytic Pd, Cu and pyridine ligand.²⁴ 2-Fluoropyridine was found to be especially effective at promoting this reactivity. A plot of the initial rate of reaction versus the pK_a of pyH^+ for various pyridine derivatives that were tested indicated that the electronics of 2-fluoropyridine were finely tuned for this reaction. These results support the idea that the neutral donor ligand must be sufficiently donating to stabilize Pd^0 and promote reoxidation by O_2 and sufficiently electron poor to facilitate C–H activation and reductive elimination steps.

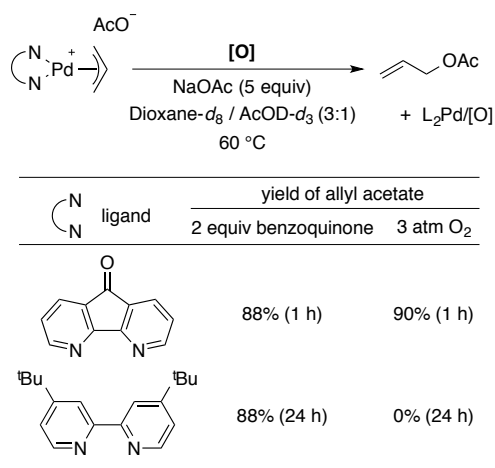
Scheme 1.9. 2-Fluoropyridine supported Pd catalyst balances C–H activation and reductive elimination steps with stabilization and reoxidation of Pd⁰.



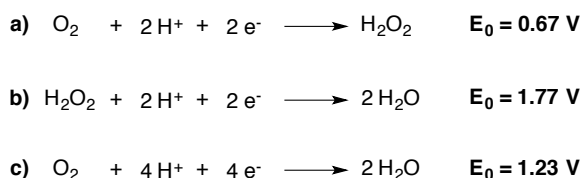
In 2010, our group first reported on the remarkable utility of 4,5-diazafluorenone (DAF) as a novel ligand for promotion of palladium oxidase chemistry. DAF was found to promote the allylic acetoxylation of terminal olefins (Scheme 1.10).²⁵ A screen of common pyridine-based ligands highlighted the ability of the diazafluorene ligand scaffold to enable reactivity.

Scheme 1.10. 4,5-Diazafluorenone promotes aerobic allylic acetoxylation.

Mechanistic studies to elucidate the origin of the promoting effect of DAF on this and other oxidative transformations are in progress. A test of the stoichiometric reactivity of a DAF-ligated π -allyl-Pd^{II} complex and a *t*Bu₂bpy-ligated π -allyl-Pd^{II} complex showed that reductive elimination of allyl acetate readily occurred from the DAF-ligated complex under aerobic conditions, while the *t*Bu₂bpy-ligated π -allyl-Pd^{II} complex required the presence of benzoquinone to help promote the reductive elimination (Scheme 1.11). These results provide early evidence that DAF is responsible for facilitating a difficult reductive elimination step under aerobic conditions.

Scheme 1.11. 4,5-Diazafluorenone promotes reductive elimination of allyl acetate.**1.3.2.2. Redox Co-catalysts**

As discussed above, the ability to access high-valent Pd^{III} or Pd^{IV} intermediates greatly facilitates reductive elimination steps in oxidative coupling reactions.¹² Unfortunately, molecular oxygen is not expected to be able to carry out the oxidation of catalytically relevant Pd^{II} species in the oxidative coupling reactions of interest.²⁶ This can be attributed to the relatively small reduction potential associated with the two-electron reduction of O₂ to H₂O₂ (Scheme 1.12a) compared to that of H₂O₂ to H₂O (Scheme 1.12b), where the majority of the oxidizing power of molecular oxygen is held.²⁷ The reduction potential for the overall four-electron conversion of O₂ to water highlights that O₂ is sufficiently oxidizing to generate high-valent Pd species, but only if the four-electron process can be accessed kinetically (Scheme 1.12c). Indeed, the reduction potential of PhI(OAc)₂, which is known to generate high-valent Pd species, is comparable to that of the four electron reduction of O₂.²⁸

Scheme 1.12. Standard reduction potentials of O₂ and H₂O₂.

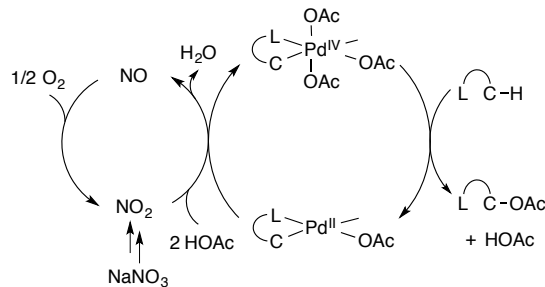
A strategy for harnessing the four-electron reduction of O₂ in a palladium catalyzed two-electron oxidation reaction is to use an appropriate redox co-catalyst.²⁹ Sanford and coworkers reported an example of this strategy in which catalytic nitrate was employed in conjunction with Pd(OAc)₂ for sp³ C–H acetoxylation reactions.³⁰ The authors had previously found that PhI(OAc)₂³¹ and K₂S₂O₈³² were capable of promoting this transformation (Table 1.1, entries 1-2). Air, with and without co-catalytic copper (cf. the Wacker Process, Scheme 1.2), was not effective (entries 3-4). Based on prior studies by Campora that demonstrated the ability of NO₂ to oxidize Pd^{II} to well-defined Pd^{IV} complexes,³³ the authors tested co-catalytic NaNO₃ and were able to obtain comparable yields to those reported in their prior studies with stoichiometric chemical oxidants (entries 5-6).

Table 1.1. Co-catalytic nitrate in aerobic sp³ C–H acetoxylation.

entry	oxidant	redox co-cat.	yield (%)
1	PhI(OAc) ₂	none	75
2	K ₂ S ₂ O ₈	none	63
3	air	none	0
4	air	Cu(OAc) ₂ (10%)	1
5	air	NaNO ₃ (10%)	53
6	1 atm O ₂	NaNO ₃ (10%)	70

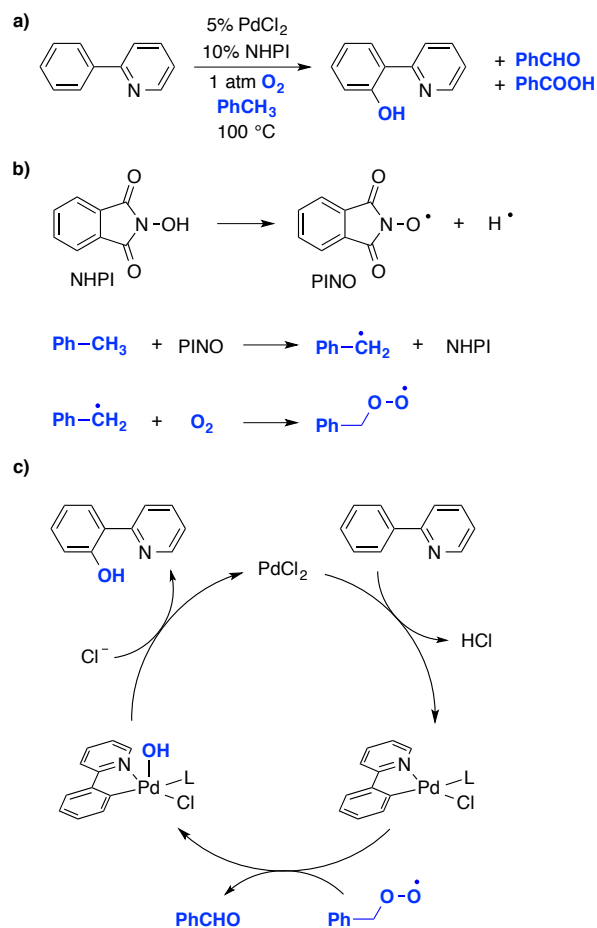
The proposed mechanism of this transformation invokes the ability of NO₂ to oxidize a Pd^{II} species to Pd^{IV} with generation of NO (Scheme 1.13). Molecular oxygen then reacts with two equivalents of NO to regenerate two equivalents of NO₂. This reactivity between NO and O₂ takes full advantage of the four-electron oxidizing power of molecular oxygen.

Scheme 1.13. Proposed mechanism of Pd^{II}/NO₂ co-catalyzed aerobic sp³ C–H acetoxylation.



1.3.2.3. Trapping of Strong Peroxide Oxidants Derived from O₂

A final approach to solving the "oxidant problem" also involves a strategy for harnessing the four-electron oxidizing power of O₂. As mentioned above, the initial two electron reduction of O₂ to H₂O₂ holds limited potential, while the two electron reduction of H₂O₂ to H₂O holds significant potential (cf. Scheme 1.12).³⁴ A tactic for accessing the oxidizing power of hydrogen peroxide rather than O₂ is to employ a reductive trap for in situ conversion of O₂ to a reactive peroxide species.³⁵ Jiao and coworkers reported an example in which aerobic aryl C–H hydroxylation of 2-phenylpyridine derivatives could be carried out with catalytic Pd and N-hydroxyphthalimide (NHPI) in toluene (Scheme 1.14a).³⁶ The authors noted that significant amounts of benzaldehyde and benzoic acid were formed during the reaction, and an experiment with labeled ¹⁸O₂ indicated that the hydroxyl oxygen atom in the product is derived from molecular oxygen. These results led the authors to propose that NHPI initiates the reaction by generation of a phthalimide *N*-oxyl radical (PINO) that can abstract a hydrogen atom from toluene (Scheme 1.14b). The tolyl radical can trap O₂ as a peroxo species that is capable of transferring an oxygen atom to the cyclometalated (2-phenylpyridine)Pd^{II} complex. The resulting high-valent Pd species can reductively eliminate the aryl–OH bond (Scheme 1.14c).

Scheme 1.14. Palladium-catalyzed aryl C–H hydroxylation with O₂-derived peroxide.

Chapters 4, 5 and 6 of this thesis explore some of the strategies discussed above in the development of aerobic aryl C–H amination reactions.

1.4 References and Notes

1. Burns, N. Z.; Baran, P. S.; Hoffmann, R. W. *Angew. Chem. Int. Ed.* **2009**, *48*, 2854.
2. Stahl, S. S. *Angew. Chem. Int. Ed.* **2004**, *43*, 3400.
3. (a) Smidt, J.; Hafner, R.; Jira, S.; Sedlmeier, S.; Sieber, R.; Rüttinger, R.; Kojer, H. *Angew. Chem.* **1959**, *71*, 176. (b) Smidt, J.; Hafner, R.; Jira, S.; Sieber, R.; Sedlmeier, S.; Sabel, A. *Angew. Chem. Int. Ed.* **1962**, *1*, 80.
4. (a) Henry, P. M. in *Palladium Catalyzed Oxidation of Hydrocarbons*, Vol. 2, D. Reidel Publishing Co., Dordrecht, The Netherlands, **1980**. (b) Backvall, J. E. *Acc. Chem. Res.* **1983**, *16*, 335. (c) Zeni, G.; Larock, R. C. *Chem. Rev.* **2004**, *104*, 2285. (d) Beccalli, E. M.; Broggini, G.; Martinelli, M.; Sottocornola, S. *Chem. Rev.* **2007**, *107*, 5318. (e) Minatti, A.; Muñiz, K. *Chem. Soc. Rev.* **2007**, *36*, 1142. (f) Jensen, K. H.; Sigman, M. S. *Org. Biomol. Chem.* **2008**, *6*, 4083.
5. Kotov, V.; Scarborough, C. C.; Stahl, S. S. *Inorg. Chem.* **2007**, *46*, 1910.
6. Fix, S. R.; Brice, J. L.; Stahl, S. S. *Angew. Chem. Int. Ed.* **2002**, *41*, 164.
7. (a) Ye, X. A.; Liu, G. S.; Popp, B. V.; Stahl, S. S. *J. Org. Chem.* **2011**, *76*, 1031. (b) Steinhoff, B. A.; Stahl, S. S. *J. Am. Chem. Soc.* **2006**, *128*, 4348. (c) Stahl, S. S.; Thorman, J. L.; Nelson, R. C.; Kozee, M. A. *J. Am. Chem. Soc.* **2001**, *123*, 7188.
8. Keith, J. A.; Henry, P. M. *Angew. Chem. Int. Ed.* **2009**, *48*, 9038.
9. McDonald, R. I.; Liu, G. S.; Stahl, S. S. *Chem. Rev.* **2011**, *111*, 2981.
10. (a) Jung, Y. C.; Mishra, R. K.; Yoon, C. H.; Jung, K. W. *Org. Lett.* **2003**, *5*, 2231. (b) Andappan, M. M. S.; Nilsson, P.; von Schenck, H.; Larhed, M. *J. Org. Chem.* **2004**, *69*,

-
5212. (c) Wang, D. H.; Engle, K. M.; Shi, B. F.; Yu, J. Q. *Science* **2010**, 327, 315. (d) Mei, T. -S.; Werner, E. W.; Burckle, A. J.; Sigman, M. S. *J. Am. Chem. Soc.* **2013**, 135, 6830.
11. (a) Campbell, A. N.; Stahl, S. S. *Acc. Chem. Res.* **2012**, 45, 851. (b) Gligorich, K. M.; Sigman, M. S. *Chem. Commun.* **2009**, 3854.
12. (a) Muñiz, K. *Angew. Chem. Int. Ed.* **2009**, 48, 9412. (b) Powers, D. C.; Ritter, T. *Acc. Chem. Res.* **2012**, 45, 840. (c) Hickman, A. J.; Sanford, M. S. *Nature* **2012**, 484, 177.
13. (a) Littke, A. F.; Fu, G. C. *Angew. Chem. Int. Ed.* **2002**, 41, 4176. (b) Surry, D. S.; Buchwald, S. L. *Angew. Chem. Int. Ed.* **2008**, 47, 6338. (c) Hartwig, J. F. *Acc. Chem. Res.* **2008**, 41, 1534. (d) Martin, R.; Buchwald, S. L. *Acc. Chem. Res.* **2008**, 41, 1461.
14. (a) Hamann, B. C.; Hartwig, J. F. *J. Am. Chem. Soc.* **1998**, 120, 3694. (b) Hartwig, J. F. *Angew. Chem. Int. Ed.* **1998**, 37, 2047. (c) Alcazar-Roman, L. M.; Hartwig, J. F. *J. Am. Chem. Soc.* **2001**, 123, 12905.
15. (a) Yamashita, M.; Hartwig, J. F. *J. Am. Chem. Soc.* **2004**, 126, 5344. (b) Fujita, K.; Yamashita, M.; Puschmann, F.; Alvarez-Falcon, M. M.; Incarvito, C. D.; Hartwig, J. F. *J. Am. Chem. Soc.* **2006**, 128, 9044.
16. (a) Driver, M. S.; Hartwig, J. F. *J. Am. Chem. Soc.* **1995**, 117, 4708. (b) Driver, M. S.; Hartwig, J. F. *J. Am. Chem. Soc.* **1997**, 119, 8232. (c) Yamashita, M.; Vicario, J. V. C.; Hartwig, J. F. *J. Am. Chem. Soc.* **2003**, 125, 16347. (e) Hartwig, J. F. *Inorg. Chem.* **2007**, 46, 1936.
17. (a) Davies, D. L.; Donald, S. M. A.; Macgregor, S. A. *J. Am. Chem. Soc.* **2005**, 127, 13754. (b) Lafrance, M.; Gorelsky, S. I.; Fagnou, K. *J. Am. Chem. Soc.* **2007**, 129, 14570. (c) Gorelsky, S. I.; Lapointe, D.; Fagnou, K. *J. Am. Chem. Soc.* **2008**, 130, 10848.

-
18. See ref. 12 and: (a) Canty, A. J.; Denney, M. C.; Skelton, B. W.; White, A. H. *Organometallics* **2004**, *23*, 1122. (b) Dick, A. R.; Kampf, J. W.; Sanford, M. S. *J. Am. Chem. Soc.* **2005**, *127*, 12790. (c) Deprez, N. R.; Sanford, M. S. *Inorg. Chem.* **2007**, *46*, 1924. (d) Powers, D. C.; Ritter, T. *Nat. Chem.* **2009**, *1*, 302. (e) Deprez, N. R.; Sanford, M. S. *J. Am. Chem. Soc.* **2009**, *131*, 11234. (f) Powers, D. C.; Lee, E.; Ariafard, A.; Sanford, M. S.; Yates, B. F.; Canty, A. J.; Ritter, T. *J. Am. Chem. Soc.* **2012**, *134*, 12002.
19. Brasche, G.; Garcia-Fortanet, J.; Buchwald, S. L. *Org. Lett.* **2008**, *10*, 2207.
20. (a) Tsang, W. C. P.; Munday, R. H.; Brasche, G.; Zheng, N.; Buchwald, S. L. *J. Org. Chem.* **2008**, *73*, 7603. (b) Tsang, W. C. P.; Zheng, N.; Buchwald, S. L. *J. Am. Chem. Soc.* **2005**, *127*, 14560.
21. van Benthem, R. A. T. M.; Hiemstra, H.; Vanleeuwen, P. W. N. M.; Geus, J. W.; Speckamp, W. N. *Angew. Chem. Int. Ed.* **1995**, *34*, 457.
22. Jordan-Hore, J. A.; Johansson, C. C. C.; Gulias, M.; Beck, E. M.; Gaunt, M. J. *J. Am. Chem. Soc.* **2008**, *130*, 16184.
23. Youn, S. W.; Bihn, J. H.; Kim, B. S. *Org. Lett.* **2011**, *13*, 3738.
24. Izawa, Y.; Stahl, S. S. *Adv. Synth. Catal.* **2010**, *352*, 3223.
25. Campbell, A. N.; White, P. B.; Guzei, I. A.; Stahl, S. S. *J. Am. Chem. Soc.* **2010**, *132*, 15116.
26. For well defined studies in which high-valent Pd complexes are accessed with molecular oxygen as the oxidant, see: (a) Khusnutdinova, J. R.; Rath, N. P.; Mirica, L. M. *J. Am. Chem. Soc.* **2012**, *134*, 2414. (b) Khusnutdinova, J. R.; Qu, F. R.; Zhang, Y.; Rath, N. P.; Mirica, L. M. *Organometallics* **2012**, *31*, 4627. (c) Mirica, L. M.; Khusnutdinova, J. R. *Coord. Chem. Rev.* **2013**, *257*, 299. (d) Qu, F. R.; Khusnutdinova, J. R.; Rath, N. P.; Mirica, L. M. *Chem. Commun.* **2014**, *50*, 3036.

-
27. Yeager, E. *J. Mol. Catal.* **1986**, *38*, 5.
28. Giffard, H.; Mabon, G.; Leclair, E.; Mercier, N.; Allain, M.; Gorgues, A.; Molinie, P.; Neilands, O.; Krief, P.; Khodorkovsky, V. *J. Am. Chem. Soc.* **2001**, *123*, 3852.
29. For a review of redox co-catalysis, see: Piera, J.; Backvall, J. E. *Angew. Chem. Int. Ed.* **2008**, *47*, 3506.
30. Stowers, K. J.; Kubota, A.; Sanford, M. S. *Chem. Sci.* **2012**, *3*, 3192.
31. Desai, L. V.; Hull, K. L.; Sanford, M. S. *J. Am. Chem. Soc.* **2004**, *126*, 9542.
32. Desai, L. V.; Malik, H. A.; Sanford, M. S. *Org. Lett.* **2006**, *8*, 1141.
33. Campora, J.; Palma, P.; del Rio, D.; Carmona, E.; Graiff, C.; Tiripicchio, A. *Organometallics* **2003**, *22*, 3345.
34. For well defined studies of the ability to access high-valent Pd complexes in catalytically relevant systems using hydrogen peroxide as the oxidant, see: (a) Oloo, W.; Zavalij, P. Y.; Zhang, J.; Khaskin, E.; Vedernikov, A. N. *J. Am. Chem. Soc.* **2010**, *132*, 14400. (b) Vedernikov, A. N. *Acc. Chem. Res.* **2012**, *45*, 803.
35. (a) Clerici, M. G.; Ingallina, P. *Catal. Today* **1998**, *41*, 351. (b) Mukaiyama, T.; Yamada, T. *Bull. Chem. Soc. Jpn.* **1995**, *68*, 17. (c) Murahashi, S. I.; Oda, Y.; Naota, T. *J. Am. Chem. Soc.* **1992**, *114*, 7913.
36. Yan, Y. P.; Feng, P.; Zheng, Q. Z.; Liang, Y. F.; Lu, J. F.; Cui, Y. X.; Jiao, N. *Angew. Chem. Int. Ed.* **2013**, *52*, 5827.

Chapter 2

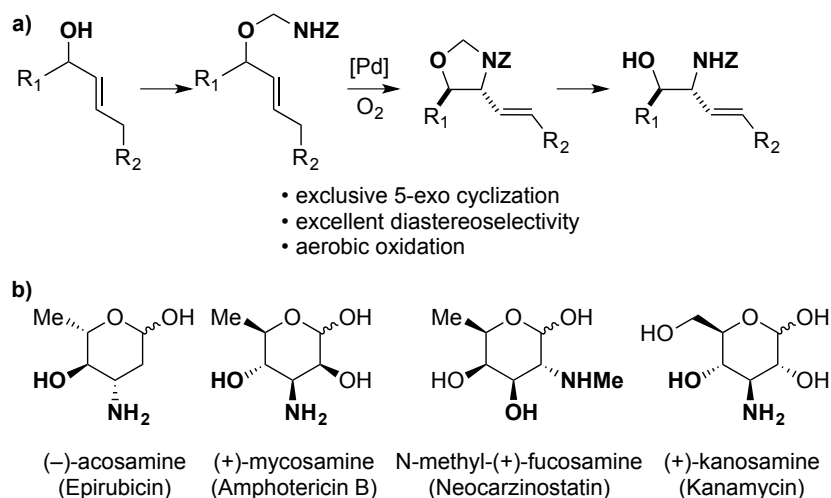
Synthesis of Vicinal Aminoalcohols by Stereoselective Aza-Wacker Cyclizations: Access to (–)-Acosamine by Redox Relay

This work has been published: Weinstein, A. B.; Schuman, D. P.; Tan, Z. X.; Stahl, S. S. *Angew. Chem. Int. Ed.* **2013**, 52, 11867–11870.

2.1 Introduction

The stereoselective synthesis of vicinal aminoalcohols from simple starting materials is a prominent challenge in organic chemistry. The prevalence of the vicinal aminoalcohol moiety in biologically active molecules, as well as the difficulty with which the 1,2-oxidation pattern can be synthesized, has justified the development of a diverse array of approaches to access these molecules.¹ Intermolecular oxidative difunctionalization of alkenes is an appealing strategy for the generation of the 1,2-aminoxyoxygenation pattern, but methods with a combination of high stereo- and regioselectivity and diverse scope remain elusive. Examples include Sharpless asymmetric aminohydroxylation,² metal-catalyzed activation of oxaziridines,³ and palladium-catalyzed aminoacetoxylation reactions that employ hypervalent iodine oxidants.⁴ Our interest in palladium-catalyzed *aerobic* oxidation of alkenes (Wacker-type reactions) prompted us to investigate new methods for the synthesis of vicinal aminoalcohols from readily available, stereochemically defined starting materials. Here, we employ a detachable, tethered nitrogen nucleophile to generate the 1,2-aminoxyoxygenation pattern from allylic alcohols via an aza-Wacker cyclization (Scheme 2.1a).^{5,6,7} The cyclization step forms 5-membered oxazolidine products and exhibits high levels of diastereoselectivity. This strategy is amenable to the *de novo* synthesis of aminosugars, which are key substructures of several antibiotic and anticancer natural products (Scheme 2.1b).⁸ Implementation of a redox-relay approach⁹ enables rapid synthesis of (–)-acosamine and highlights the utility of this method.

Scheme 2.1. a) Detachable tethered nucleophile approach for the synthesis of vicinal aminoalcohols from allylic alcohols. b) Aminosugars in natural product antibiotic and anticancer agents. Z = benzyloxycarbonyl (Cbz) or *tert*-butoxycarbonyl (Boc).



2.2 Results and Discussion

We began our studies with an assessment of the reactivity and diastereoselectivity of Wacker cyclization when using distinct tethering units for the attachment of oxygen or nitrogen nucleophiles to secondary allylic amine or allylic alcohol substrates (Table 2.1). These efforts included the allylic *N*-tosyl carbamate **1** (entries 1-3) and *N*-allyl hemiaminal **3** (entries 4-6) substrates, reported previously by Bäckvall^{5f} and Hiemstra,^{5a} as well as aminal **5a**. Assessment of a variety of catalyst conditions for aerobic oxidative cyclization revealed Pd^{II}/dimethylsulfoxide-based catalysts to be the most promising.¹⁰ Effective catalyst systems included Pd(DMSO)₂(TFA)₂ in THF,^{10c} which is effective at ambient temperature (condition **A**), Pd(TFA)₂ in DMSO, which is compatible with higher reaction temperatures (condition **B**), and Pd(OAc)₂ in DMSO, resembling conditions originally discovered by Larock^{10a} and Hiemstra^{10b} (condition **C**). Allylic *N*-tosyl carbamate substrate **1** was susceptible to decomposition under these direct aerobic reoxidation conditions.¹¹ When cyclization to oxazolidinone **2** occurred (e.g., entry 2), only modest diastereoselectivity was observed. *N*-Allyl hemiaminal **3** cyclized to the

corresponding oxazolidine **4** in moderate yields, but the diastereoselectivity of the transformation was poor.¹² *O*-Allyl hemiaminals are an appealing class of substrates because they may be synthesized directly from allylic alcohols, but they have not been tested previously in Wacker-type cyclizations. The benzyl carbamate (Cbz) derivative **5a**, underwent cyclization in excellent yield and good diastereoselectivity to afford the *trans* oxazolidine **6a** (entries 7-9). Conditions **A** and **B** were particularly effective.

Table 2.1. Evaluation of diastereoselective oxidative cyclization of substrates derived from an allylic alcohol or an allylic amine.

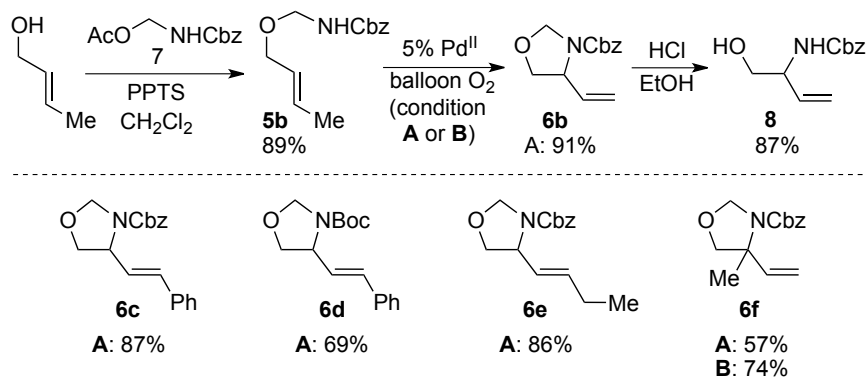
entry	substrate	major product	conditions ^[a]	yield (%) / d.r. ^[b]
1			A	0 / nd
2			B	11 / 3.5:1 ^[c]
3	1	2	C	0 / nd
4			A	34 / 1.6:1
5			B	51 / 1.6:1
6	3	4	C	67 / 1.8:1
7			A	93 / 9:1
8			B	94 / 8:1
9	5a	6a	C	77 / 5:1

[a] Catalyst conditions **A**: 5 mol% Pd(TFA)₂, 20 mol% DMSO, 20 mol% NaOBz, 3Å M.S., THF (0.1 M), 25 °C, 24 h, 1 atm O₂. Catalyst condition **B**: 5 mol% Pd(TFA)₂, 20 mol% NaOBz, 3Å M.S., DMSO (0.1 M), 60 °C, 24 h, 1 atm O₂. Catalyst condition **C**: 5 mol% Pd(OAc)₂, DMSO (0.1 M), 60 °C, 24 h, 1 atm O₂.
 [b] Yield / diastereomeric ratio based on ¹H NMR spectroscopic analysis of the crude reaction mixture with phenyltrimethylsilane as the internal standard. [c] Isolated yield. Diastereomeric ratio based on ¹H NMR analysis of the purified products. Boc = *tert*-butoxycarbonyl, Bz = benzoyl, Cbz = benzyloxycarbonyl, DMSO = dimethylsulfoxide, M.S. = molecular sieves, THF = tetrahydrofuran, TFA = trifluoroacetic acid, Ts = 4-toluenesulfonyl.

The three-step detachable tethered nucleophile approach for the conversion of *trans* crotyl alcohol to vicinal aminoalcohol derivative **8** is illustrated in Scheme 2.2. *Trans*-crotyl alcohol is

readily converted to the corresponding *O*-allyl hemiaminal, and aza-Wacker cyclization proceeds smoothly at ambient temperature (condition **A**). The oxazolidine ring is unmasked under acidic conditions. Several additional primary *O*-allyl hemiaminal substrates were similarly effective. Comparison of benzyl and *tert*-butyl carbamate (Cbz- and Boc-) *O*-allyl hemiaminals revealed that the Cbz-derived nitrogen nucleophile is more effective (cf. **6c** and **6d**). A propyl-substituted alkene produced oxazolidine **6e** with negligible alkene isomerization.¹³ Finally, reaction with a trisubstituted alkene affords a tertiary C–N bond (cf. **6f**); condition **B** was more effective than condition **A** in this reaction.

Scheme 2.2. Transformation of primary allylic alcohols into vicinal aminoalcohols. PPTS = pyridinium *p*-toluenesulfonate.



We next explored the scope of the diastereoselective cyclization of *O*-allyl hemiaminals derived from secondary alcohols (Table 2.2). Both *trans* and *cis* allylic alcohols are good substrates and afford the same *trans*-4,5-disubstituted oxazolidine (entries 2-3). The effectiveness of the *trans*-allylic alcohol substrate is noteworthy because such substrates are more readily accessible than the *cis* analog; however, higher diastereoselectivity can be achieved with the *cis* substrate. Increasing the size of the secondary allylic substituent improves the diastereoselectivity, and condition **B** provides higher reactivity with these more sterically encumbered substrates (entries 4-6). Cyclic *O*-allyl hemiaminals **5j** and **5k** yield the *cis* ring-

Table 2.2. Diastereoselective synthesis of oxazolidines from cyclization of secondary *O*-allyl hemiaminals.

entry	substrate	product	conditions ^[a]	yield (%) / d.r. ^[b]
1			A	86 / 12:1
2	5a	6a	B	88 / 11:1
3			B	73 / >20:1
4			A	72 / >20:1
5	5h	6h	B	85 / >20:1
6			B	75 / >20:1
7			B	78 / >20:1
8			B	59 / >20:1
9			B	53 / >20:1
10			B	62 / 9:1
11			B	74 / 19:1
12			B	75 / 9:1
	5o	6o		

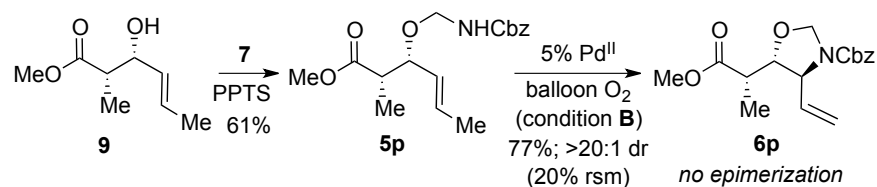
[a] See Table 2.1 for descriptions of catalyst conditions **A** and **B**.

[b] Isolated yields. Diastereomeric ratio based on ¹H NMR spectroscopic analysis of the isolated material. Relative configurations of **6a** and **6j** were assigned by NOESY-1D spectroscopic analysis (other structures assigned by analogy).

fused products in good yields (entries 7-8). Allylic alcohols derived from aldol additions to crotonaldehyde also provide effective *O*-allyl hemiaminal substrates (entries 9-12). Ketone adduct **5l** is prone to decomposition under the reaction conditions and provided only modest yield of oxazolidine **6l**, but the Weinreb amide **5m**, ethyl ester **5n**, and dimethylamide **5o** are well-tolerated.

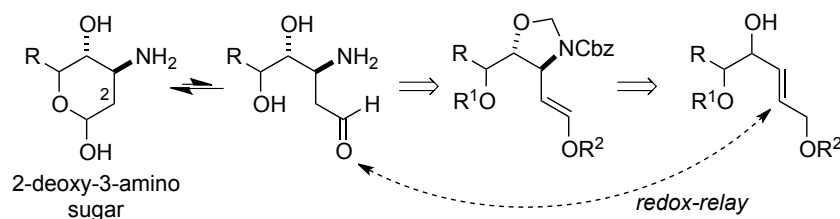
The aldol reaction is one of many potential routes to enantioenriched allylic alcohols¹⁴ and thus can provide access to enantioenriched aminoalcohol derivatives in connection with our method. Asymmetric aldol chemistry enabled the synthesis of enantioenriched allylic alcohol **9** from crotonaldehyde,¹⁵ which was converted to the corresponding *O*-allyl hemiaminal **5p** and cyclized cleanly to oxazolidine **6p** (Scheme 2.3). Oxazolidine **6p** was obtained with exquisite diastereoselectivity and no epimerization of the α -methyl stereocenter.

Scheme 2.3. Transformation of enantioenriched allylic alcohol to the oxazolidine with no epimerization. rsm = recovered starting material.



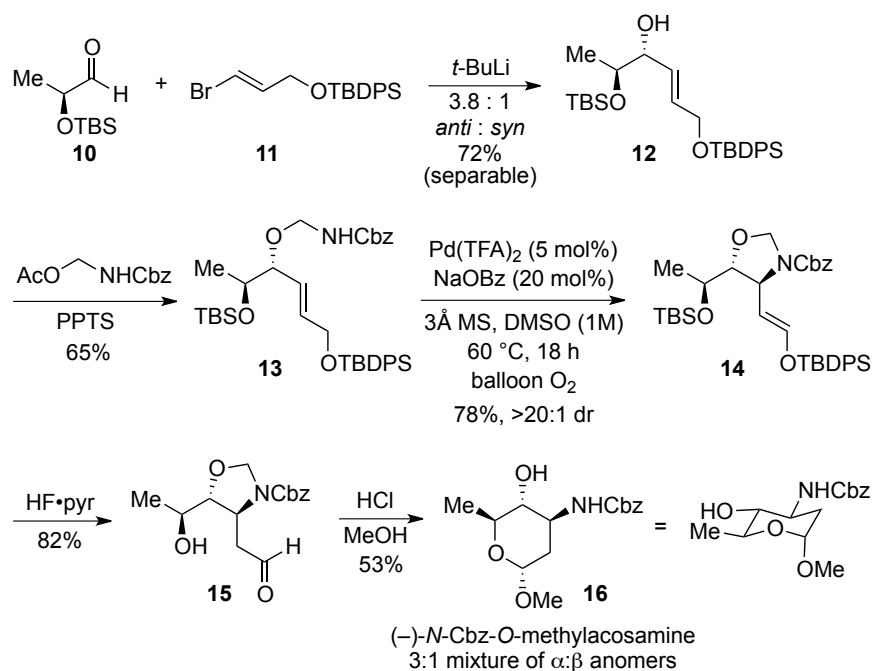
The utility of this method is illustrated in the synthesis of the 2-deoxy-3-aminosugar (–)-acosamine.¹⁶ 2-Deoxy-3-aminosugars can be obtained via synthesis of the corresponding acyclic 1,3-aminoaldehyde precursor. We envisioned that the aminoaldehyde could be accessed rapidly by employing our cyclization in a redox-relay sequence, whereby cyclization of an *O*-allyl hemiaminal derived from a *bis*-allylic alcohol precursor would generate a masked aldehyde intermediate (Scheme 2.4). Transfer of the olefin redox equivalent via β -hydride elimination from the second allylic alcohol position would form an enol ether and expedite elaboration of the oxazolidine to the desired aminosugar target.

Scheme 2.4. Retrosynthetic analysis of 2-deoxy-3-aminosugars with application of aza-Wacker cyclization and redox-relay.



This redox-relay strategy enabled the synthesis of (–)-*N*-Cbz-*O*-methylicosamine, a conveniently isolated derivative of acosamine, from TBS-protected (–)-lactaldehyde in five steps (Scheme 2.5). First, vinyl lithium addition of silyl-protected allylic alcohol **11** to lactaldehyde **10** yielded **12** with the desired stereochemistry. Installation of the *O*-allyl hemiaminal and aza-Wacker cyclization provided the silyl enol ether **14** with good efficiency as a single diastereomer.¹⁷ The silyl enol ether and secondary TBS-ether were removed to unveil the free aldehyde and alcohol. Finally, the oxazolidine ring was opened under acidic conditions with concomitant formation of the methyl-protected cyclic acetal **16** [(–)-*N*-Cbz-*O*-methylicosamine].

Scheme 2.5. Synthesis of (–)-*N*-Cbz-*O*-methylicosamine



This rapid and redox economical synthesis of (–)-acosamine illustrates a versatile approach that could be applied to a variety of other aminosugar derivatives.

In summary, we have demonstrated that aza-Wacker cyclizations can be used to synthesize stereodefined vicinal aminoalcohols from allylic alcohol precursors by employing a detachable tethered nucleophile approach. These oxidative functionalization reactions are operationally simple and the catalytic reactions give clean conversion of starting material to desired product. The diversity of methods for the asymmetric synthesis of allylic alcohols makes the diastereoselective transformation described here particularly apt for application to a variety of contexts.

2.3 Acknowledgements

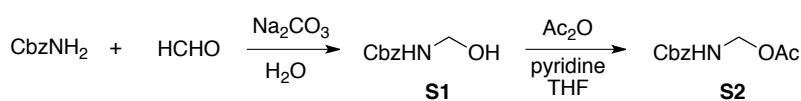
We thank the NIH (R01 GM67173) and Organic Syntheses (ACS Division of Organic Chemistry fellowship for A.B.W.) for financial support of this work. Spectroscopic instrumentation was partially funded by the NSF (CHE-1048642, CHE-0342998, CHE-9208463).

2.4 Experimental Details and Supporting Information

2.4.1. General considerations

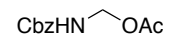
All commercially available compounds were purchased and used as received, unless otherwise noted. Solvents were dried over alumina columns prior to use; however, purification and drying of commercial solvents is not required for the catalytic reactions described here. Dimethylsulfoxide (DMSO) was purchased from Aldrich and stored over molecular sieves. ^1H and ^{13}C NMR spectra were recorded on Bruker or Varian 300 MHz, 400 MHz or 500 MHz spectrometers and chemical shifts are given in parts per million relative to internal tetramethylsilane (0.00 ppm for ^1H) or CDCl_3 (77.16 ppm for ^{13}C). Flash chromatography was carried out with SiliaFlash® P60 (Silicycle, particle size 40-63 μm , 230-400 mesh) or by using a CombiFlash Rf® automated chromatography system with reusable high performance silica columns (RediSep® Rf Gold Silica, 20-40 μm spherical particles).

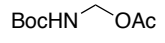
2.4.2. Preparation of *O*-acetyl hemiaminal tethering reagents



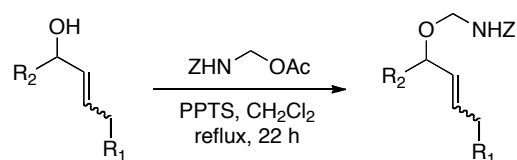
S1: Procedure adapted from literature precedence.¹⁸ Benzyl carbamate (1 equiv, 33.1 mmol, 5 g) and sodium carbonate (0.5 equiv, 16.5 mmol, 1.75 g) were weighed into a 250 ml round bottom flask. Water (55 ml) was added, followed by formaldehyde solution (37 wt. % in H_2O , 1.38 equiv, 45.5 mmol, 3.38 ml). The mixture was heated to reflux with stirring until the solids dissolved, then allowed to cool to room temperature (product begins to precipitate as a white solid almost immediately) and stirred for 5 h. The reaction mixture was extracted with 50 ml dichloromethane 3x, and combined organics washed with brine, dried over MgSO_4 , filtered

and concentrated *in vacuo*. Recrystallization from dichloromethane/hexanes afforded 4.35 g white needles (73% yield).

 **S2**: White crystalline solid **S1** (1 equiv., 15 mmol, 2.7 g) was dissolved in THF (0.22 M, 70 ml). Pyridine (2 equiv., 30 mmol, 2.8 ml) and acetic anhydride (6 equiv., 69 mmol, 7.2 ml) were added sequentially via syringe at room temperature. The clear solution was stirred for 8 h at room temperature and then concentrated *in vacuo*. The resulting oil was purified on silica using hexanes : ethyl acetate as the eluent, to afford the product (3.23 g, 98% yield) as a clear oil. ¹H NMR (300 MHz, CDCl₃) δ 7.36 (m, 5H), 5.91 (bs, 1H), 5.21 (d, *J* = 7.5 Hz, 2H), 5.15 (s, 2H), 2.07 (s, 3H); ¹³C NMR (75 MHz, CDCl₃) δ 171.77, 155.87, 135.89, 128.62, 128.40, 128.30, 67.39, 66.71, 21.00; HRMS (ESI) calculated for [C₁₁H₁₃NO₄ + Na]⁺ requires *m/z* 246.0737, found 246.0735.

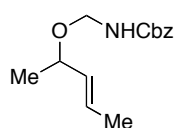
 **S3**: Prepared as described previously.¹⁹

2.4.3. Preparation of *O*-allyl hemiaminal substrates

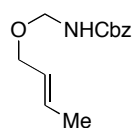


General procedure: A 100 ml 3-necked round bottom flask equipped with a stir bar and reflux condenser was flame dried and purged with nitrogen, then charged with pyridinium *p*-toluene sulfonate (0.1 equiv). The allylic alcohol (1 equiv) was then added via cannula as a solution in dry CH₂Cl₂ under nitrogen. Tethering reagent (**S2**, 1.5 equiv, or **S3**, 1 equiv) was added via cannula as a solution in dry CH₂Cl₂ under nitrogen. The reaction mixture was diluted to a

concentration of 0.1 M allylic alcohol in CH₂Cl₂. The reaction mixture was heated to reflux for approximately 22 hours. The yellow-orange reaction mixture was then allowed to cool to room temperature, transferred to a separatory funnel, diluted three-fold with pentanes and washed with water and then brine. The organic layer was dried over MgSO₄ and concentrated *in vacuo*. The yellow-orange oil was purified on silica. Typically, purification was performed on silica using a CombiFlash Rf automated chromatography system with a gradient of ethyl acetate in hexanes. Often, this afforded a yellow oil, which could be further purified manually on silica with a toluene:acetone solvent system.

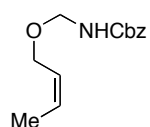


5a: Prepared from commercially available *trans*-3-penten-2-ol (3.4 mmol) and **S2** according to the general procedure. Purification on silica using a CombiFlash Rf system with a gradient (0-30%) of ethyl acetate in hexanes, followed by manual purification on silica with a 20:1 toluene:acetone solvent system, afforded the product (672 mg, 79% yield) as a clear oil. ¹H NMR (300 MHz, CDCl₃) δ 7.35 (m, 5H), 5.68 (dq, *J* = 12.8, 6.3 Hz, 1H), 5.44 (bs, 1H), 5.36 (dd, *J* = 15.0, 8.0 Hz, 1H), 5.12 (s, 2H), 4.70 (dd, *J* = 10.7, 7.7 Hz, 1H), 4.61 (dd, *J* = 10.6, 6.5 Hz, 1H), 4.00 (p, *J* = 6.4 Hz, 1H), 1.69 (d, *J* = 6.2 Hz, 3H), 1.22 (d, *J* = 6.4 Hz, 3H); ¹³C NMR (75 MHz, CDCl₃) δ 156.26, 136.32, 132.77, 128.57, 128.23, 128.18, 128.08, 74.08, 69.91, 66.94, 21.64, 17.71; HRMS (ESI) calculated for [C₁₄H₁₉NO₃ + Na]⁺ requires *m/z* 272.1258, found 272.1250.

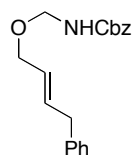


5b: Prepared from *trans*-2-buten-1-ol²⁰ (1.76 mmol) and **S2** according to the general procedure. Purification on silica using a gradient (0-30%) of ethyl acetate in hexanes afforded the product (369 mg, 89% yield) as a clear oil. ¹H NMR (300 MHz, CDCl₃) δ 7.36 (m,

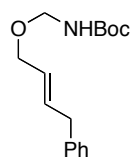
5H), 5.73 (dq, $J = 14.7, 6.8$ Hz, 1H), 5.56 (dt, $J = 14.7, 6.3$ Hz, 1H), 5.47 (bs, 1H), 5.13 (s, 2H), 4.69 (d, $J = 7.2$ Hz, 2H), 3.97 (d, $J = 6.3$ Hz, 2H), 1.71 (d, $J = 6.6$ Hz, 3H); ^{13}C NMR (75 MHz, CDCl_3) δ 156.39, 136.29, 130.20, 128.68, 128.38, 128.30, 127.08, 71.71, 68.96, 67.15, 17.91; HRMS (ESI) calculated for $[\text{C}_{13}\text{H}_{17}\text{NO}_3 + \text{Na}]^+$ requires m/z 258.1101, found 258.1104.



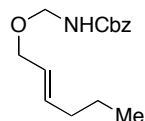
cis-5b: Prepared from *cis*-2-buten-1-ol²¹ (3.5 mmol) and **S2** according to the general procedure. Purification on silica using a gradient (0-30%) of ethyl acetate in hexanes afforded the product (636 mg, 77% yield) as a clear oil. ^1H NMR (300 MHz, CDCl_3) δ 7.44 – 7.27 (m, 5H), 5.67 (dq, $J = 13.5, 6.8$ Hz, 1H), 5.59 – 5.49 (m, 1H), 5.48 (bs, 1H), 5.14 (s, 2H), 4.71 (d, $J = 7.1$ Hz, 2H), 4.11 (d, $J = 6.5$ Hz, 2H), 1.65 (d, $J = 6.4$ Hz, 3H); ^{13}C NMR (101 MHz, CDCl_3) δ 156.40, 136.25, 128.66, 128.44, 128.36, 128.29, 126.39, 72.01, 67.13, 63.62, 13.30; HRMS (ESI) calculated for $[\text{C}_{13}\text{H}_{17}\text{NO}_3 + \text{Na}]^+$ requires m/z 258.1101, found 258.1109.



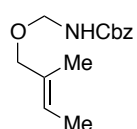
5c: Prepared from the crotyl alcohol²² (2.83 mmol) and **S2** according to the general procedure. Purification on silica using a gradient (0-30%) of ethyl acetate in hexanes, followed by purification with a 15:1 toluene:acetone solvent system, and finally purification using a gradient (0-20%) of acetone in hexanes afforded the product (647 mg, 73% yield) as a clear oil. ^1H NMR (300 MHz, CDCl_3) δ 7.35 (m, 5H), 7.32 – 7.24 (m, 2H), 7.23 – 7.13 (m, 3H), 5.88 (dt, $J = 14.4, 6.7$ Hz, 1H), 5.60 (dt, $J = 12.4, 5.3$ Hz, 1H), 5.44 (bs, 1H), 5.12 (s, 2H), 4.70 (d, $J = 7.2$ Hz, 2H), 4.02 (d, $J = 6.1$ Hz, 2H), 3.38 (d, $J = 6.7$ Hz, 2H); ^{13}C NMR (75 MHz, CDCl_3) δ 156.41, 140.00, 136.26, 133.46, 128.72, 128.70, 128.59, 128.40, 128.31, 127.33, 126.27, 71.88, 68.79, 67.19, 38.84; HRMS (ESI) calculated for $[\text{C}_{19}\text{H}_{21}\text{NO}_3 + \text{Na}]^+$ requires m/z 334.1414, found 334.1400.



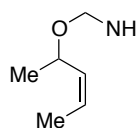
5d: Prepared from the crotyl alcohol²² (2.86 mmol) and **S3** according to the general procedure. Purification on silica using a gradient (0-30%) of ethyl acetate in hexanes, followed by purification with a 25:1 toluene:acetone solvent system, and finally purification using a gradient (0-20%) of acetone in hexanes afforded the product (202 mg, 25% yield) as a clear oil. ¹H NMR (300 MHz, CDCl₃) δ 7.33 – 7.25 (m, 2H), 7.19 (td, *J* = 6.7, 1.7 Hz, 3H), 5.89 (dt, *J* = 14.7, 6.6, 1.3 Hz, 1H), 5.62 (dt, *J* = 15.2, 6.1, 1.5 Hz, 1H), 5.24 (bs, 1H), 4.63 (d, *J* = 7.2 Hz, 2H), 4.00 (d, *J* = 6.1 Hz, 2H), 3.39 (d, *J* = 6.7 Hz, 2H), 1.45 (s, 9H); ¹³C NMR (75 MHz, CDCl₃) δ 155.68, 140.05, 133.19, 128.72, 128.57, 127.55, 126.24, 80.12, 71.55, 68.61, 38.85, 28.44; HRMS (ESI) calculated for [C₁₆H₂₃NO₃ + Na]⁺ requires *m/z* 300.1571, found 300.1572.



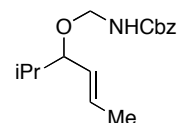
5e: Prepared from commercially available *trans*-2-hexen-1-ol (2.95 mmol) and **S2** according to the general procedure. Purification on silica using a gradient (0-30%) of ethyl acetate in hexanes, followed by purification with a 18:1 toluene:acetone solvent system, and finally purification using a gradient (0-20%) of acetone in hexanes afforded the product (509 mg, 66% yield) as a clear oil. ¹H NMR (300 MHz, CDCl₃) δ 7.42 – 7.28 (m, 5H), 5.72 (dt, *J* = 13.9, 6.6 Hz, 1H), 5.60 – 5.48 (m, 1H), 5.46 (bs, 1H), 5.13 (s, 2H), 4.70 (d, *J* = 7.1 Hz, 2H), 3.99 (d, *J* = 6.3 Hz, 2H), 2.02 (q, *J* = 7.2 Hz, 2H), 1.40 (h, *J* = 7.4 Hz, 2H), 0.90 (t, *J* = 7.3 Hz, 3H); ¹³C NMR (75 MHz, CDCl₃) δ 156.39, 136.26, 135.14, 128.60, 128.28, 128.22, 125.86, 71.65, 68.98, 67.05, 34.43, 22.26, 13.76; HRMS (ESI) calculated for [C₁₅H₂₁NO₃ + Na]⁺ requires *m/z* 286.1414, found 286.1428.



5f: Prepared from the crotyl alcohol²³ (4.0 mmol) and **S2** according to the general procedure. Purification on silica using a gradient (0-40%) of ethyl acetate in hexanes, followed by purification with a 15:1 toluene:acetone solvent system afforded the product (831 mg, 83% yield) as a clear oil. ¹H NMR (300 MHz, CDCl₃) δ 7.42 – 7.29 (m, 5H), 5.50 (m, 1H), 5.44 (bs, 1H), 5.13 (s, 2H), 4.67 (d, *J* = 7.1 Hz, 2H), 3.91 (s, 2H), 1.68 – 1.56 (m, 6H); ¹³C NMR (101 MHz, CDCl₃) δ 156.37, 136.29, 132.58, 128.67, 128.36, 128.29, 123.13, 74.50, 71.63, 67.11, 53.56, 13.77, 13.33; HRMS (ESI) calculated for [C₁₄H₁₉NO₃ + H]⁺ requires *m/z* 250.1438, found 250.1428.

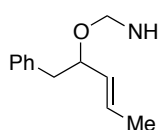


5g: Prepared from *cis*-3-penten-2-ol²⁴ (2.5 mmol) and **S2** according to the general procedure. Purification on silica using a CombiFlash Rf system with a gradient (0-30%) of ethyl acetate in hexanes, followed by manual purification on silica with a 20:1 toluene:acetone solvent system, afforded the product (350 mg, 56% yield) as a clear oil. ¹H NMR (400 MHz, CDCl₃) δ 7.44 – 7.28 (m, 5H), 5.58 (dt, *J* = 13.8, 6.9 Hz, 1H), 5.48 (bs, 1H), 5.41 – 5.26 (m, 1H), 5.12 (s, 2H), 4.73 – 4.56 (m, 2H), 4.46 (dq, *J* = 12.6, 6.7 Hz, 1H), 1.65 (d, *J* = 6.6 Hz, 3H), 1.21 (d, *J* = 6.2 Hz, 3H); ¹³C NMR (101 MHz, CDCl₃) δ 156.21, 136.33, 132.70, 128.63, 128.31, 126.61, 70.35, 68.68, 67.04, 21.38, 13.25; HRMS (ESI) calculated for [C₁₄H₁₉NO₃ + Na]⁺ requires *m/z* 272.1258, found 272.1248.

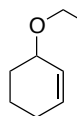


5h: Prepared from the crotyl alcohol²⁵ (3.7 mmol) and **S2** according to the general procedure. Purification on silica using a gradient (0-30%) of ethyl acetate in hexanes, followed by purification with a 20:1 toluene:acetone solvent system, afforded the product (543 mg, 53% yield) as a clear oil. ¹H NMR (300 MHz, CDCl₃) δ 7.35 (d, *J* = 3.9 Hz,

5H), 5.66 (dq, $J = 12.9, 6.3$ Hz, 1H), 5.41 (bs, 1H), 5.30 (dd, $J = 15.4, 8.7$ Hz, 1H), 5.12 (s, 2H), 4.70 (dd, $J = 10.8, 7.9$ Hz, 1H), 4.59 (dd, $J = 10.5, 6.1$ Hz, 1H), 3.47 (t, $J = 7.6$ Hz, 1H), 1.72 (d, $J = 6.4$ Hz, 3H), 1.67 – 1.62 (m, 1H), 0.85 (dd, $J = 18.1, 6.9$ Hz, 6H); ^{13}C NMR (75 MHz, CDCl_3) δ 156.28, 136.42, 129.87, 129.75, 128.59, 128.25, 128.19, 83.88, 70.23, 66.90, 32.67, 18.76, 18.43, 17.88; HRMS (ESI) calculated for $[\text{C}_{16}\text{H}_{23}\text{NO}_3 + \text{Na}]^+$ requires m/z 300.1571, found 300.1563.

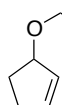


5i: Prepared from the crotyl alcohol²⁶ (3.3 mmol) and **S2** according to the general procedure. Purification on silica using a gradient (0-30%) of ethyl acetate in hexanes, followed by purification with a 20:1 toluene:acetone solvent system, afforded the product (701 mg, 65% yield) as a clear oil. ^1H NMR (400 MHz, CDCl_3) δ 7.39 – 7.29 (m, 5H), 7.25 – 7.11 (m, 5H), 5.64 (dq, $J = 13.3, 6.4$ Hz, 1H), 5.38 (dd, $J = 15.6, 8.0$ Hz, 1H), 5.19 (bs, 1H), 5.09 (s, 2H), 4.66 (dd, $J = 10.8, 7.9$ Hz, 1H), 4.56 (dd, $J = 10.7, 6.3$ Hz, 1H), 4.05 (q, $J = 7.4$ Hz, 1H), 2.84 (dd, $J = 13.7, 7.5$ Hz, 1H), 2.74 (dd, $J = 13.7, 5.7$ Hz, 1H), 1.67 (d, $J = 6.5$ Hz, 3H); ^{13}C NMR (101 MHz, CDCl_3) δ 156.26, 138.54, 136.38, 130.99, 129.67, 129.27, 128.67, 128.34, 128.26, 128.19, 126.21, 79.38, 70.28, 66.96, 42.45, 17.86; HRMS (ESI) calculated for $[\text{C}_{20}\text{H}_{23}\text{NO}_3 + \text{Na}]^+$ requires m/z 348.1571, found 348.1555.

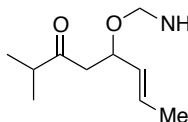


5j: Prepared from commercially available 2-cyclohexen-1-ol (2.0 mmol) and **S2** according to the general procedure. Purification on silica using a gradient (0-30%) of ethyl acetate in hexanes afforded the product (361 mg, 69% yield) as a clear oil. ^1H NMR (400 MHz, CDCl_3) δ 7.43 – 7.28 (m, 5H), 5.91 – 5.81 (m, 1H), 5.79 – 5.69 (m, 1H), 5.53 (bs, 1H), 5.13 (s, 2H), 4.76 (dd, $J = 7.2, 2.9$ Hz, 2H), 4.12 – 4.02 (m, 1H), 2.10 – 1.89 (m, 2H), 1.89 – 1.49

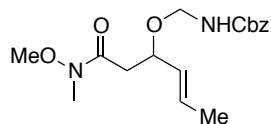
(m, 4H); ^{13}C NMR (101 MHz, CDCl_3) δ 156.38, 136.30, 131.41, 128.65, 128.34, 128.28, 127.54, 70.53, 70.44, 67.09, 28.76, 25.21, 19.17; HRMS (ESI) calculated for $[\text{C}_{15}\text{H}_{19}\text{NO}_3 + \text{Na}]^+$ requires m/z 284.1258, found 284.1252.



5k: Prepared from the 2-cyclopenten-1-ol²⁷ (3.0 mmol) and **S2** according to the general procedure. Purification on silica using a gradient (0-40%) of ethyl acetate in hexanes, followed by purification with a 20:1 toluene:acetone solvent system, afforded the product (314 mg, 42% yield) as a clear oil. ^1H NMR (400 MHz, CDCl_3) δ 7.50 – 7.28 (m, 5H), 6.03 – 6.00 (m, 1H), 5.90 – 5.77 (m, 1H), 5.47 (bs, 1H), 5.14 (s, 2H), 4.74 (d, J = 7.0 Hz, 3H), 2.54 – 2.40 (m, 1H), 2.33 – 2.12 (m, 2H), 1.79 (td, J = 9.0, 4.3 Hz, 1H); ^{13}C NMR (101 MHz, CDCl_3) δ 156.38, 136.28, 136.12, 130.77, 128.65, 128.35, 128.29, 82.95, 71.03, 67.10, 31.13, 30.25; HRMS (ESI) calculated for $[\text{C}_{14}\text{H}_{17}\text{NO}_3 + \text{NH}_4]^+$ requires m/z 265.1574, found 265.1550.

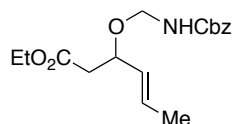


5l: Prepared from the crotyl alcohol²⁸ (2.84 mmol) and **S2** according to the general procedure. Purification on silica using a gradient (0-40%) of ethyl acetate in hexanes, followed by purification with a 9:1 toluene:acetone solvent system, afforded the product (547 mg, 60% yield) as a clear oil. ^1H NMR (400 MHz, CDCl_3) δ 7.40 – 7.30 (m, 5H), 5.75 (dq, J = 13.2, 6.4 Hz, 1H), 5.44 (bs, 1H), 5.34 (dd, J = 15.7, 7.9 Hz, 1H), 5.13 (s, 2H), 4.63 (dd, J = 7.0, 2.3 Hz, 2H), 4.35 (td, J = 8.2, 4.5 Hz, 1H), 2.79 (dd, J = 16.2, 8.4 Hz, 1H), 2.56 (p, J = 6.9 Hz, 1H), 2.47 (dd, J = 16.2, 4.7 Hz, 1H), 1.69 (d, J = 6.1 Hz, 3H), 1.06 (d, J = 6.9 Hz, 6H); ^{13}C NMR (101 MHz, CDCl_3) δ 212.19, 156.25, 136.41, 130.25, 129.51, 128.60, 128.23, 74.13, 70.37, 66.95, 46.43, 41.58, 17.94, 17.87, 17.82; HRMS (ESI) calculated for $[\text{C}_{18}\text{H}_{25}\text{NO}_4 + \text{H}]^+$ requires m/z 320.1857, found 320.1853.



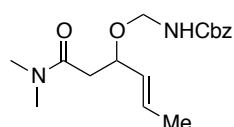
5m: Prepared from the crotyl alcohol²⁹ (2.3 mmol) and **S2** according to the general procedure. Purification on silica using a gradient (0-85%) of

ethyl acetate in hexanes afforded the product (418 mg, 54% yield) as a clear oil. ¹H NMR (400 MHz, CDCl₃) δ 7.47 – 7.28 (m, 5H), 5.78 (dq, *J* = 13.3, 6.5 Hz, 1H), 5.66 (bs, 1H), 5.41 (dd, *J* = 15.5, 7.9 Hz, 1H), 5.12 (d, *J* = 4.3 Hz, 2H), 4.66 (q, *J* = 10.7, 8.4 Hz, 2H), 4.38 (td, *J* = 8.3, 4.5 Hz, 1H), 3.65 (s, 3H), 3.15 (s, 3H), 2.84 (dd, *J* = 15.7, 8.6 Hz, 1H), 2.44 (dd, *J* = 15.5, 4.5 Hz, 1H), 1.70 (d, *J* = 6.6 Hz, 3H); ¹³C NMR (101 MHz, CDCl₃) δ 171.70, 156.20, 136.47, 130.39, 129.39, 128.57, 128.22, 128.19, 74.57, 70.68, 66.84, 61.38, 38.40, 32.10, 17.84; HRMS (ESI) calculated for [C₁₇H₂₄N₂O₅ + H]⁺ requires *m/z* 337.1758, found 337.1754.



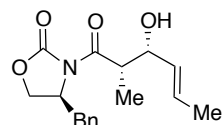
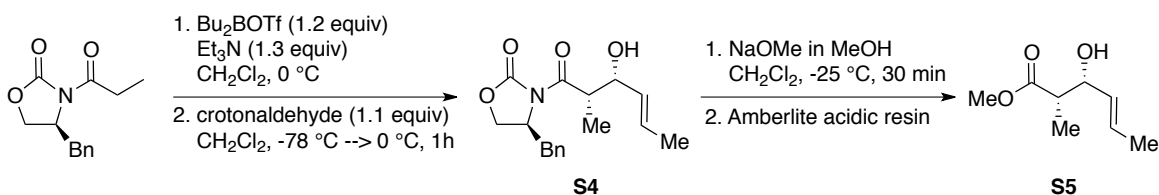
5n: Prepared from the crotyl alcohol³⁰ (5 mmol) and **S2** according to the general procedure. Purification on silica using a gradient (0-40%) of ethyl

acetate in hexanes afforded the product (795 mg, 49% yield) as a clear oil. ¹H NMR (400 MHz, CDCl₃) δ 7.46 – 7.29 (m, 5H), 5.79 (dq, *J* = 13.2, 6.4 Hz, 1H), 5.42 (bs, 1H), 5.40 – 5.27 (m, 1H), 5.13 (d, *J* = 3.1 Hz, 2H), 4.71 (dd, *J* = 10.8, 7.7 Hz, 1H), 4.63 (dd, *J* = 10.7, 6.3 Hz, 1H), 4.31 (td, *J* = 8.3, 4.9 Hz, 1H), 4.12 (q, *J* = 7.1 Hz, 2H), 2.57 (dd, *J* = 15.3, 8.5 Hz, 1H), 2.43 (dd, *J* = 15.1, 5.0 Hz, 1H), 1.70 (d, *J* = 6.5 Hz, 3H), 1.23 (t, *J* = 7.1 Hz, 3H); ¹³C NMR (101 MHz, CDCl₃) δ 170.96, 156.25, 136.35, 130.21, 129.74, 128.62, 128.28, 128.24, 74.65, 70.20, 66.99, 60.58, 41.31, 17.83, 14.31; HRMS (ESI) calculated for [C₁₇H₂₃NO₅ + NH₄]⁺ requires *m/z* 339.1915, found 339.1926.



50: Prepared from the crotyl alcohol³¹ (1.46 mmol) and **S2** according to the general procedure. Purification on silica using a gradient (40-100%) of ethyl

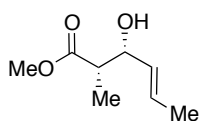
acetate in hexanes (230 mg, 49% yield) as a clear oil. ¹H NMR (400 MHz, CDCl₃) δ 7.43 – 7.29 (m, 5H), 5.77 (dq, *J* = 13.2, 6.5 Hz, 1H), 5.67 (bs, 1H), 5.41 (dd, *J* = 15.2, 7.4 Hz, 1H), 5.12 (d, *J* = 3.6 Hz, 2H), 4.71 (dd, *J* = 10.6, 6.7 Hz, 1H), 4.63 (dd, *J* = 10.6, 7.0 Hz, 1H), 4.39 (td, *J* = 8.0, 4.3 Hz, 1H), 2.97 (s, 3H), 2.92 (s, 3H), 2.68 (dd, *J* = 15.4, 8.4 Hz, 1H), 2.35 (dd, *J* = 15.4, 4.3 Hz, 1H), 1.70 (d, *J* = 5.6 Hz, 3H); ¹³C NMR (101 MHz, CDCl₃) δ 170.53, 156.22, 136.50, 130.58, 129.10, 128.59, 128.25, 128.20, 75.29, 70.92, 66.85, 39.78, 37.54, 35.57, 17.86; HRMS (ESI) calculated for [C₁₇H₂₄N₂O₄ + H]⁺ requires *m/z* 321.1809, found 321.1812.



S4: Procedure adapted from literature precedence.^{15b} A dry 100 ml round

bottom flask equipped with a stir bar was charged with (*S*)-(+)-4-benzyl-3-propionyl-2-oxazolidinone (1 equiv, 4.29 mmol, 1 g) and evacuated and back-filled with nitrogen. Dry dichloromethane (9 ml, 0.46M) was added via syringe, and the reaction mixture was cooled to 0 °C. Dibutylboron triflate (1M in CH₂Cl₂, 1.18 equiv, 5.06 mmol, 5 ml) was added via syringe, followed by dropwise addition of triethylamine (freshly distilled from CaH₂, 1.32 equiv, 5.66 mmol, 0.79 ml). The reaction mixture was cooled to -78 °C, and crotonaldehyde (1.11 equiv, 4.76 mmol, 0.4 ml) was added dropwise via syringe. The reaction mixture was allowed to stir for 20 minutes at -78 °C and was then warmed to 0 °C and stirred for an additional 1 hour. The reaction was quenched with approximately 16 ml of 1:3 (pH 7 phosphate

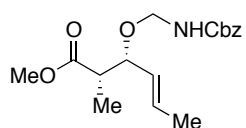
buffer):(MeOH). An additional 12 ml of a 2:1 mixture of (MeOH):(30% aqueous H₂O₂) was added and allowed to stir for 1 hour. This mixture was transferred to a separatory funnel, partitioned with additional water and extracted 3x with diethyl ether. The combined organics were washed with a 5% aqueous solution of sodium bicarbonate, brine, and then dried over MgSO₄ and concentrated to oil. Purification on silica with a CombiFlash Rf automated chromatography system using a 0-50% EtOAc/hexanes solvent program afforded the product (1.17 g, 90% yield) as a clear oil. ¹H NMR (500 MHz, CDCl₃) δ 7.34 (dd, *J* = 8.0, 6.5 Hz, 2H), 7.31 – 7.26 (m, 1H), 7.23 – 7.19 (m, 2H), 5.77 (dq, *J* = 13.0, 6.5 Hz, 1H), 5.52 (ddd, *J* = 15.4, 6.3, 1.8 Hz, 1H), 4.70 (ddt, *J* = 10.4, 6.9, 3.2 Hz, 1H), 4.43 (s, 1H), 4.22 (dd, *J* = 9.1, 7.6 Hz, 1H), 4.19 (dd, *J* = 9.1, 3.1 Hz, 1H), 3.86 (qd, *J* = 7.0, 3.7 Hz, 1H), 3.26 (dd, *J* = 13.4, 3.4 Hz, 1H), 2.79 (dd, *J* = 13.4, 9.5 Hz, 1H), 2.75 (s, 1H), 1.72 (d, *J* = 6.7 Hz, 3H), 1.25 (d, *J* = 7.0 Hz, 3H); ¹³C NMR (126 MHz, CDCl₃) δ 176.80, 153.27, 135.18, 130.23, 129.56, 129.10, 128.46, 127.56, 72.92, 66.31, 55.31, 42.94, 37.94, 17.92, 11.40; HRMS (ESI) calculated for [C₁₇H₂₁NO₄ + Na]⁺ requires *m/z* 326.1363, found 326.1368.



S5: Procedure adapted from literature precedence.³² A dry 100 ml round bottom flask was charged with oxazolidinone **S4** (1 equiv, 2.26 mmol, 687 mg)

and a stir bar and evacuated and back-filled with nitrogen. Dry dichloromethane (15 ml, 0.15M) was added via syringe, and the reaction mixture was cooled to -25 °C. Sodium methoxide (freshly prepared, 0.42M in MeOH, 1.1 equiv, 2.5 mmol, 5.9 ml) was added dropwise via syringe over the course of 10 minutes. The reaction mixture was allowed to stir for 15 minutes at -25 °C, and then was quenched with the addition of amberliteTM acidic resin. The resin was removed with filtration, rinsed with additional CH₂Cl₂, and the combined organics were dried

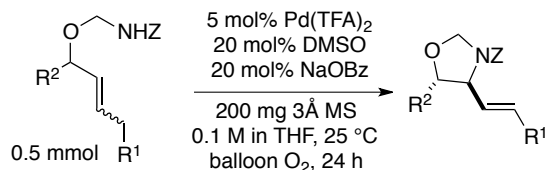
over MgSO_4 and concentrated to oil. Purification on silica with a 3:1 hexanes:EtOAc solvent system afforded the product (211 mg, 59% yield) as a clear oil. ^1H NMR (300 MHz, CDCl_3) δ 5.74 (dq, $J = 15.2, 6.5, 1.1$ Hz, 1H), 5.48 (ddq, $J = 15.3, 6.8, 1.6$ Hz, 1H), 4.31 (q, $J = 5.1$ Hz, 1H), 3.71 (s, 3H), 2.63 (qd, $J = 7.2, 4.4$ Hz, 1H), 2.47 (d, $J = 4.9$ Hz, 1H), 1.71 (ddd, $J = 6.5, 1.6, 0.9$ Hz, 3H), 1.17 (d, $J = 7.2$ Hz, 3H); ^{13}C NMR (126 MHz, CDCl_3) δ 175.95, 130.32, 128.62, 73.43, 51.93, 45.07, 17.92, 11.69; HRMS (ESI) calculated for $[\text{C}_8\text{H}_{14}\text{O}_3 + \text{NH}_4]^+$ requires m/z 176.1282, found 176.1275.



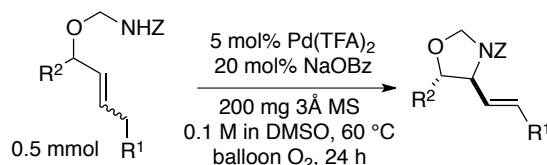
5p: Prepared from crotyl alcohol **S5** (1 equiv, 1.33 mmol, 211 mg) and **S2** according to the general procedure. Purification on silica with a 3:1

hexanes:EtOAc solvent system, followed by further purification on silica with a 9:1 toluene:acetone column, afforded the product (262 mg, 61% yield) as a clear oil. ^1H NMR (500 MHz, CDCl_3) δ 7.42 – 7.30 (m, 5H), 5.75 (dq, $J = 13.1, 6.4$ Hz, 1H), 5.39 (dd, $J = 15.3, 8.3$ Hz, 1H), 5.34 (bs, 1H), 5.13 (d, $J = 2.2$ Hz, 2H), 4.69 (dd, $J = 10.9, 8.0$ Hz, 1H), 4.61 (dd, $J = 10.9, 6.2$ Hz, 1H), 4.07 (t, $J = 7.3$ Hz, 1H), 3.63 (s, 3H), 2.58 (p, $J = 6.5$ Hz, 1H), 1.71 (d, $J = 6.5$ Hz, 3H), 1.15 (d, $J = 7.1$ Hz, 3H); ^{13}C NMR (126 MHz, CDCl_3) δ 174.69, 156.26, 136.33, 130.90, 128.69, 128.55, 128.38, 128.30, 79.20, 70.24, 67.07, 51.73, 45.14, 17.95, 12.46; HRMS (ESI) calculated for $[\text{C}_{17}\text{H}_{23}\text{NO}_5 + \text{NH}_4]^+$ requires m/z 339.1915, found 339.1914.

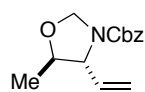
2.4.4. Aza-Wacker cyclization of *O*-allyl hemiaminal substrates



General procedure (Condition A): A 100 ml 3-necked round bottom flask equipped with a stir bar (3/4" x 3/8", egg-shaped, Teflon) and a reflux condenser was charged with pulverized sodium benzoate (0.2 equiv, 0.1 mmol, 14.4 mg) and powdered 3Å molecular sieves (200 mg, not activated³³). The apparatus was evacuated and backfilled with O₂ from a balloon 3x. Oxygen from a balloon was bubbled through 20-30 ml of THF prior to use. A stock solution of DMSO in THF (28.4 ul in 12 ml THF) was prepared. This DMSO/THF stock solution was used to prepare a Pd(TFA)₂/DMSO/THF stock solution, such that a 3 ml portion would contain Pd(TFA)₂ (0.05 equiv, 0.025 mmol, 8.3 mg) and DMSO (0.2 equiv, 0.1 mmol, 7.1 ul). 3 ml of this stock was added to the reaction vessel via syringe. The mixture was allowed to stir for 10 minutes at room temperature, at which time the substrate (1 equiv, 0.5 mmol) was added in a total volume of 2 ml of THF via syringe. The reaction vessel was submerged in an oil bath held at 25-27 °C and stirred *vigorously* under a balloon of O₂ for 24 hrs. (*NOTE*: Efficient gas-liquid mixing is critical to prevent catalyst death via aggregation of Pd black. Use of an over-sized reaction vessel and stir bar helps ensure adequate mixing.) The reaction mixture was then poured over a plug of basic alumina and washed through with ethyl acetate. The resulting clear solution was concentrated *in vacuo* and purified on silica using a CombiFlash Rf automated chromatography system with a 0-30% gradient of ethyl acetate in hexanes, unless otherwise noted.

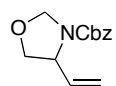


General procedure (Condition B): A 100 ml 3-necked round bottom flask equipped with a stir bar (3/4" x 3/8", egg-shaped, Teflon) and a reflux condenser was charged with the substrate (1 equiv, 0.5 mmol), pulverized sodium benzoate (0.2 equiv, 0.1 mmol, 14.4 mg) and powdered 3Å molecular sieves (200 mg, not activated³³). The apparatus was evacuated and backfilled with O₂ from a balloon 3x. A 5 ml stock solution containing Pd(TFA)₂ (0.05 equiv, 0.025 mmol, 8.3 mg) in DMSO was added via syringe. The reaction vessel was submerged in an oil bath held at 60 °C and stirred *vigorously* under a balloon of O₂ for 24 hrs. (*NOTE:* Under these conditions, catalyst death via aggregation to Pd black is less problematic due to the ability of DMSO to stabilize Pd⁰. However, efficient gas-liquid mixing is still critical to prevent slow mass-transport limited kinetics.³⁴ Use of an over-sized reaction vessel and stir bar helps ensure adequate mixing.) The reaction mixture was cooled to room temperature and then partitioned between ether and water (approximately 50 ml of each). The aqueous layer was re-extracted an additional 2x with ether. The combined organics were washed with brine, dried over MgSO₄ and concentrated *in vacuo*. The resulting oil was purified on silica using a CombiFlash Rf automated chromatography system with a 0-30% gradient of ethyl acetate in hexanes, unless otherwise noted.

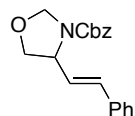


6a: From **5a** – Condition **A**: clear oil, 98 mg major (*trans*) diastereomer, 79% yield; 8 mg minor (*cis*) diastereomer, 6% yield (12:1 dr). Condition **B**: clear oil, 101 mg major (*trans*) diastereomer, 81% yield; 9 mg minor (*cis*) diastereomer, 7% yield (11:1 dr). From **5g** – Condition **B**: 73% yield (>20:1 dr). See below for NOESY-1d analysis. *Major (trans) Diastereomer*: ¹H NMR (300 MHz, CDCl₃) δ 7.43 – 7.28 (m, 5H), 5.74 (ddd, *J* = 17.0, 10.0, 6.9

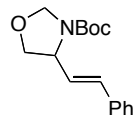
Hz, 1H), 5.35 (m, 1H), 5.23 (m, 2H), 5.17 (d, $J = 12.4$ Hz, 1H), 5.10 (d, $J = 12.4$ Hz, 1H), 4.75 (d, $J = 4.6$ Hz, 1H), 3.86 (m, 1H), 3.82 (m, 1H), 1.34 (d, $J = 6.0$ Hz, 3H); ^{13}C NMR (75 MHz, CDCl_3) δ 154.16, 136.47, 135.19, 128.58, 128.17, 128.07, 118.07, 80.37, 78.71, 67.19, 65.45, 17.04; HRMS (ESI) calculated for $[\text{C}_{14}\text{H}_{17}\text{NO}_3 + \text{Na}]^+$ requires m/z 270.1101, found 270.1106; *Minor Diastereomer*: ^1H NMR (300 MHz, CDCl_3) δ 7.35 (m, 5H), 5.70 (ddd, $J = 17.2, 10.3, 7.5$ Hz, 1H), 5.34 – 5.22 (m, 2H), 5.17 (d, $J = 13.6$ Hz, 1H), 5.11 (d, $J = 12.5$ Hz, 1H), 5.04 (d, $J = 12.5$ Hz, 1H), 4.86 (d, $J = 14.8$ Hz, 1H), 4.34 – 4.20 (m, 1H), 4.14 (p, $J = 5.9, 5.4$ Hz, 1H), 1.22 (d, $J = 6.3$ Hz, 3H).



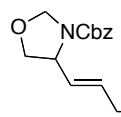
6b: From **5b**: Condition A: clear oil, 106 mg, 91% yield. From *cis*-**5b**: Condition A: clear oil, 105 mg, 90% yield. ^1H NMR (300 MHz, CDCl_3) δ 7.35 (m, 5H), 5.80 (ddd, $J = 17.1, 10.2, 6.8$ Hz, 1H), 5.27 (m, 1H), 5.25 – 5.12 (m, 2H), 5.12 (d, $J = 12.4$ Hz, 1H), 5.04 (m, 1H), 4.86 (d, $J = 4.1$ Hz, 1H), 4.40 (m, 1H), 4.12 (dd, $J = 8.7, 6.6$ Hz, 1H), 3.78 (dd, $J = 8.8, 4.4$ Hz, 1H); ^{13}C NMR (75 MHz, CDCl_3) δ 153.45, 136.38, 135.50, 128.51, 128.13, 127.98, 117.13, 79.14, 72.31, 67.10, 57.95; HRMS (ESI) calculated for $[\text{C}_{13}\text{H}_{15}\text{NO}_3 + \text{Na}]^+$ requires m/z 256.0945, found 256.0949.



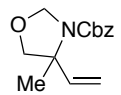
6c: Condition A: clear oil, 135 mg, 87% yield, >20:1 *trans:cis* alkene isomer. ^1H NMR (300 MHz, CDCl_3) δ 7.43 – 7.20 (m, 10H), 6.55 (m, 1H), 6.13 (dd, $J = 15.7, 7.3$ Hz, 1H), 5.19 (d, $J = 12.3$ Hz, 1H), 5.09 (m, 2H), 4.94 (m, 1H), 4.55 (m, 1H), 4.19 (t, $J = 7.4$ Hz, 1H), 3.87 (dd, $J = 8.8, 4.5$ Hz, 1H); ^{13}C NMR (75 MHz, CDCl_3) δ 153.55, 136.37, 132.80, 128.64, 128.59, 128.16, 128.12, 127.99, 126.68, 79.58, 72.96, 67.26, 57.90; HRMS (ESI) calculated for $[\text{C}_{19}\text{H}_{19}\text{NO}_3 + \text{H}]^+$ requires m/z 310.1438, found 310.1440.



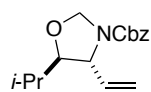
6d: Condition **A**: clear oil, 95 mg, 69% yield (a 0-20% hexanes:acetone solvent program was used for purification). ^1H NMR (300 MHz, CDCl_3) δ 7.44 – 7.15 (m, 5H), 6.57 (d, J = 15.8 Hz, 1H), 6.11 (dd, J = 15.5, 7.5 Hz, 1H), 5.02 (s, 1H), 4.86 (s, 1H), 4.46 (bs, 1H), 4.18 (t, J = 6.8 Hz, 1H), 3.84 (dd, J = 8.8, 4.6 Hz, 1H), 1.45 (s, 9H); ^{13}C NMR (75 MHz, CDCl_3) δ 153.10, 136.60, 132.34, 128.68, 127.86, 127.36, 126.58, 80.50, 79.38, 72.92, 57.84, 28.53; HRMS (ESI) calculated for $[\text{C}_{16}\text{H}_{21}\text{NO}_3 + \text{Na}]^+$ requires m/z 298.1414, found 298.1410.



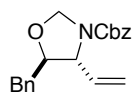
6e: Condition **A**: clear oil, 113 mg, 86% yield. ^1H NMR (300 MHz, CDCl_3) δ 7.41 – 7.28 (m, 5H), 5.71 (m, 1H), 5.38 (dd, J = 15.3, 7.4 Hz, 1H), 5.20 (d, J = 12.4 Hz, 1H), 5.09 (d, J = 12.4 Hz, 1H), 5.03 (s, 1H), 4.84 (d, J = 4.2 Hz, 1H), 4.36 (m, 1H), 4.10 (dd, J = 8.7, 6.6 Hz, 1H), 3.73 (dd, J = 8.7, 4.7 Hz, 1H), 2.04 (p, J = 9.0, 7.9 Hz, 2H), 0.97 (t, J = 7.4 Hz, 3H); ^{13}C NMR (75 MHz, CDCl_3) δ 153.53, 136.53, 135.67, 128.53, 128.12, 127.99, 126.22, 79.24, 73.01, 67.04, 57.64, 25.22, 13.31; HRMS (ESI) calculated for $[\text{C}_{15}\text{H}_{19}\text{NO}_3 + \text{H}]^+$ requires m/z 262.1438, found 262.1436.



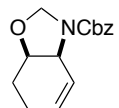
6f: Condition **A**: clear oil, 71 mg, 57% yield, recovered starting material (35%). Condition **B**: clear oil, 91 mg, 74% yield. ^1H NMR (400 MHz, CDCl_3) δ 7.35 (m, 5H), 5.94 (m, 1H), 5.26 – 4.90 (m, 6H), 3.88 (d, J = 8.6 Hz, 1H), 3.77 (d, J = 8.7 Hz, 1H), 1.56 (s, 3H); ^{13}C NMR (101 MHz, CDCl_3) δ 151.74, 140.04, 139.39, 136.55, 128.58, 128.13, 128.03, 114.68, 80.95, 80.25, 79.92, 79.31, 67.02, 66.68, 61.91, 21.36, 20.55; HRMS (ESI) calculated for $[\text{C}_{14}\text{H}_{17}\text{NO}_3 + \text{H}]^+$ requires m/z 248.1282, found 248.1290.



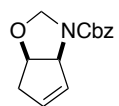
6h: Condition **A**: clear oil, 99 mg, 72% yield (>20:1 dr), 30 mg recovered starting material (22%). Condition **B**: clear oil, 118 mg, 85% yield (>20:1 dr). ^1H NMR (300 MHz, CDCl_3) δ 7.34 (m, 5H), 5.76 (ddd, $J = 17.1, 10.2, 7.0$ Hz, 1H), 5.28 (m, 3H), 5.18 (d, $J = 12.4$ Hz, 1H), 5.11 (d, $J = 12.4$ Hz, 1H), 4.73 (d, $J = 4.6$ Hz, 1H), 4.14 (m, 1H), 3.54 (t, $J = 6.3$ Hz, 1H), 1.87 (dq, $J = 13.5, 6.7$ Hz, 1H), 0.97 (dd, $J = 6.7, 4.4$ Hz, 6H); ^{13}C NMR (75 MHz, CDCl_3) δ 153.75, 136.50, 136.09, 128.59, 128.19, 128.08, 117.36, 89.04, 78.41, 67.23, 61.13, 30.65, 19.07, 18.17; HRMS (ESI) calculated for $[\text{C}_{16}\text{H}_{21}\text{NO}_3 + \text{Na}]^+$ requires m/z 298.1414, found 298.1409.



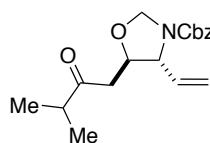
6i: Condition **B**: clear oil, 122 mg, 75% yield (>20:1 dr), recovered starting material (16%). ^1H NMR (400 MHz, CDCl_3) δ 7.53 – 7.05 (m, 10H), 5.68 (ddd, $J = 17.1, 10.2, 7.0$ Hz, 1H), 5.24 (m, 3H), 5.16 (d, $J = 12.4$ Hz, 1H), 5.11 (d, $J = 12.4$ Hz, 1H), 4.74 (d, $J = 4.7$ Hz, 1H), 4.00 (dd, $J = 16.4, 10.5$ Hz, 2H), 2.93 (d, $J = 6.2$ Hz, 2H); ^{13}C NMR (101 MHz, CDCl_3) δ 153.90, 137.20, 136.41, 135.09, 129.36, 128.61, 128.58, 128.20, 127.93, 126.87, 117.88, 84.92, 78.75, 67.23, 63.16, 38.21; HRMS (ESI) calculated for $[\text{C}_{20}\text{H}_{21}\text{NO}_3 + \text{H}]^+$ requires m/z 324.1595, found 324.1611.



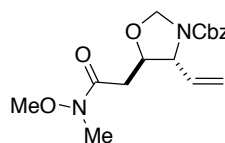
6j: Condition **B**: clear oil, 102 mg, 78% yield (>20:1 dr), recovered starting material (21%). ^1H NMR (400 MHz, CDCl_3) δ 7.46 – 7.27 (m, 5H), 5.97 – 5.54 (m, 2H), 5.16 (s, 2H), 5.04 – 4.81 (m, 2H), 4.32 (m, 2H), 2.19 (dddt, $J = 16.1, 10.2, 4.8, 2.4$ Hz, 1H), 2.13 – 2.04 (m, 1H), 2.00 – 1.89 (m, 1H), 1.75 (m, 1H); ^{13}C NMR (101 MHz, CDCl_3) δ 153.14, 136.57, 129.62, 128.66, 128.25, 128.11, 123.66, 78.12, 75.72, 67.06, 52.65, 24.38, 19.32; HRMS (ESI) calculated for $[\text{C}_{15}\text{H}_{17}\text{NO}_3 + \text{Na}]^+$ requires m/z 282.1101, found 282.1113.



6k: Condition **B**: clear oil, 72 mg, 59% yield (>20:1 dr), recovered starting material (19%). ^1H NMR (400 MHz, CDCl_3) δ 7.45 – 7.28 (m, 5H), 6.01 – 5.66 (m, 2H), 5.17 (d, J = 1.8 Hz, 2H), 5.00 (d, J = 4.3 Hz, 1H), 4.97 – 4.70 (m, 2H), 2.63 (dd, J = 18.4, 5.9 Hz, 1H), 2.53 (dt, J = 18.4, 1.8 Hz, 1H); ^{13}C NMR (101 MHz, CDCl_3) δ 153.12, 136.48, 132.52, 128.64, 128.50, 128.25, 128.10, 80.47, 77.71, 67.20, 65.42, 38.67; HRMS (ESI) calculated for $[\text{C}_{14}\text{H}_{15}\text{NO}_3 + \text{H}]^+$ requires m/z 246.1125, found 246.1131.

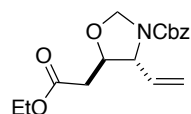


6l: Condition **B**: clear oil, 84 mg, 53% yield (>20:1 dr), recovered starting material (24%). ^1H NMR (400 MHz, CDCl_3) δ 7.34 (d, J = 5.2 Hz, 5H), 5.79 (ddd, J = 17.2, 10.2, 7.2 Hz, 1H), 5.38 – 5.20 (m, 3H), 5.16 (d, J = 12.4 Hz, 1H), 5.11 (d, J = 12.4 Hz, 1H), 4.78 (d, J = 4.6 Hz, 1H), 4.31 – 4.23 (m, 1H), 3.99 (t, J = 6.9 Hz, 1H), 2.86 (dd, J = 16.7, 7.8 Hz, 1H), 2.68 (m, 1H), 2.61 (dt, J = 13.9, 6.7 Hz, 1H), 1.11 (d, J = 7.0 Hz, 6H); ^{13}C NMR (126 MHz, CDCl_3) δ 211.39, 153.64, 136.32, 128.64, 128.60, 128.25, 127.98, 118.07, 79.60, 78.74, 67.31, 63.49, 42.25, 41.59, 17.98, 17.94; HRMS (ESI) calculated for $[\text{C}_{18}\text{H}_{23}\text{NO}_4 + \text{H}]^+$ requires m/z 318.1700, found 318.1707.

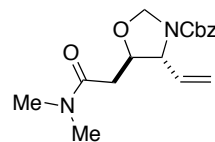


6m: Condition **B**: Purified over basic alumina with a 30-100% EtOAc/hexanes solvent program to afford clear oil, 104 mg, 62% yield (9:1 dr). ^1H NMR (400 MHz, CDCl_3) δ 7.35 (m, 5H), 5.81 (ddd, J = 17.2, 10.2, 7.1 Hz, 1H), 5.39 – 5.20 (m, 3H), 5.17 (d, J = 12.4 Hz, 1H), 5.11 (d, J = 12.4 Hz, 1H), 4.81 (d, J = 4.6 Hz, 1H), 4.32 (ddd, J = 7.8, 6.2, 4.8 Hz, 1H), 4.10 (t, J = 6.7 Hz, 1H), 3.68 (s, 3H), 3.19 (s, 3H), 2.88 (dd, J = 15.9, 8.0 Hz, 1H), 2.65 (dd, J = 15.8, 4.9 Hz, 1H); ^{13}C NMR (101 MHz, CDCl_3) δ 170.65,

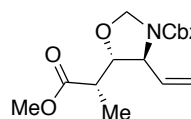
153.68, 136.31, 134.70, 128.55, 128.16, 127.94, 118.29, 79.80, 78.63, 67.23, 63.31, 61.45, 34.48, 32.11; HRMS (ESI) calculated for $[C_{17}H_{22}N_2O_5 + H]^+$ requires m/z 335.1602, found 335.1612.



6n: Condition **B**: clear oil, 119 mg, 74% yield (19:1 dr), recovered starting material (22%). 1H NMR (400 MHz, $CDCl_3$) δ 7.35 (m, 5H), 5.78 (ddd, J = 17.3, 10.2, 7.3 Hz, 1H), 5.40 – 5.20 (m, 3H), 5.17 (d, J = 12.4 Hz, 1H), 5.11 (d, J = 12.4 Hz, 1H), 4.81 (d, J = 4.6 Hz, 1H), 4.23 (q, J = 6.4 Hz, 1H), 4.16 (q, J = 7.2 Hz, 2H), 4.05 (t, J = 6.9 Hz, 1H), 2.64 (d, J = 6.6 Hz, 2H), 1.26 (t, J = 7.1 Hz, 3H); ^{13}C NMR (101 MHz, $CDCl_3$) δ 170.18, 153.70, 136.30, 134.73, 128.62, 128.26, 128.02, 118.26, 80.13, 78.83, 67.36, 63.26, 61.10, 37.23, 14.27; HRMS (ESI) calculated for $[C_{17}H_{21}NO_5 + H]^+$ requires m/z 320.1493, found 320.1500.



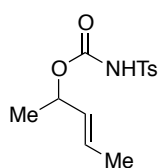
6o: Condition **B**: Purified over basic alumina with a 35-100% EtOAc/hexanes solvent program to afford clear oil, 120 mg, 75% yield (9:1 dr). 1H NMR (400 MHz, $CDCl_3$) δ 7.35 (m, 5H), 5.84 (ddd, J = 17.1, 10.2, 6.9 Hz, 1H), 5.40 – 5.20 (m, 3H), 5.17 (d, J = 12.4 Hz, 1H), 5.11 (d, J = 12.4 Hz, 1H), 4.82 (d, J = 4.7 Hz, 1H), 4.36 (dt, J = 7.2, 5.6 Hz, 1H), 4.12 (t, J = 6.4 Hz, 1H), 3.00 (s, 3H), 2.95 (s, 3H), 2.72 (dd, J = 15.7, 7.2 Hz, 1H), 2.55 (dd, J = 15.9, 5.4 Hz, 1H); ^{13}C NMR (101 MHz, $CDCl_3$) δ 169.48, 153.76, 136.35, 134.95, 128.59, 128.21, 128.02, 117.85, 80.77, 78.69, 67.28, 63.31, 37.43, 35.83, 35.51; HRMS (ESI) calculated for $[C_{17}H_{22}N_2O_4 + H]^+$ requires m/z 319.1653, found 319.1645.



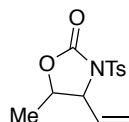
6p: Condition **B**: clear oil, 123 mg, 77% yield (>20:1 dr), recovered starting material (20%). 1H NMR (500 MHz, $CDCl_3$) δ 7.34 (m, 5H), 5.76 (ddd, J =

17.1, 10.1, 7.0 Hz, 1H), 5.35 – 5.20 (m, 3H), 5.17 (d, $J = 12.4$ Hz, 1H), 5.11 (d, $J = 12.4$ Hz, 1H), 4.78 (d, $J = 4.5$ Hz, 1H), 4.26 – 4.15 (m, 1H), 4.04 (dd, $J = 7.1, 5.4$ Hz, 1H), 3.67 (s, 3H), 2.69 (p, $J = 7.0$ Hz, 1H), 1.26 (d, $J = 7.0$ Hz, 3H); ^{13}C NMR (126 MHz, CDCl_3) δ 173.92, 153.61, 136.35, 135.14, 128.64, 128.26, 127.95, 117.74, 84.27, 78.60, 67.38, 61.67, 52.08, 41.87, 12.97; HRMS (ESI) calculated for $[\text{C}_{17}\text{H}_{21}\text{NO}_5 + \text{H}]^+$ requires m/z 320.1493, found 320.1494.

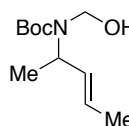
2.4.5. Allylic *N*-tosyl carbamate and *N*-allyl hemiaminal substrates



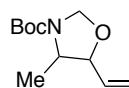
1: Procedure adapted from literature precedence.³⁵ An oven dried 50 ml round bottom flask equipped with a stir bar was evacuated and back-filled with nitrogen and charged with 3-penten-1-ol (1 equiv, 1.96 mmol, 0.2 ml) and 5 ml dry dichloromethane (0.4M). *p*-Toluenesulfonyl isocyanate (1.2 equiv, 2.35 mmol, 0.36 ml) was added via syringe. The reaction mixture was stirred at room temperature for 30 minutes, then transferred to a separatory funnel, diluted with additional dichloromethane and partitioned with water. The aqueous layer was re-extracted 2x with dichloromethane, and the combined organics were washed with brine, dried over MgSO_4 , and concentrated to oil. Purification on silica using a CombiFlash Rf automated chromatography system with a 0-50% ethyl acetate in hexanes solvent program afforded the product (494 mg, 89% yield) as a viscous clear oil. ^1H NMR (500 MHz, CDCl_3) δ 7.92 (d, $J = 8.3$ Hz, 2H), 7.53 (bs, 1H), 7.34 (d, $J = 8.2$ Hz, 2H), 5.67 (dq, $J = 15.3, 6.6, 0.8$ Hz, 1H), 5.36 (ddd, $J = 15.3, 7.1, 1.7$ Hz, 1H), 5.17 (p, $J = 6.6$ Hz, 1H), 2.45 (s, 3H), 1.65 (dd, $J = 6.5, 1.1$ Hz, 3H), 1.24 (d, $J = 6.4$ Hz, 3H); ^{13}C NMR (126 MHz, CDCl_3) δ 149.91, 145.08, 135.74, 129.78, 129.66, 129.58, 128.55, 74.95, 21.82, 20.30, 17.77; HRMS (ESI) calculated for $[\text{C}_{13}\text{H}_{17}\text{NO}_4\text{S} + \text{NH}_4]^+$ requires m/z 301.1217, found 301.1207.



2: Substrate **1** was reacted according to the general procedure for condition **B** (section IV). Following the extraction, purification on silica using a CombiFlash Rf automated chromatography system with a 0-50% ethyl acetate in hexanes solvent program afforded the product (16 mg, 11% yield) as a clear oil and as a 3.5:1 mixture of *cis* and *trans* isomers. Characterization data matched literature precedent for this compound.³⁶ Two byproducts were also isolated: 56 mg of TsNH₂ (accounting for 66% of the molar balance) and 13 mg of (*E*)-4-methyl-*N*-(pent-3-en-2-yl)benzenesulfonamide (accounting for 11% of the molar balance). Condition **A** [5 mol% Pd(TFA)₂, 20 mol% DMSO, 20 mol% NaOBz, 3 Å M.S., 0.1M in THF, 25 °C, 24 hr] and condition **C** [5 mol% Pd(OAc)₂, 0.1M in DMSO, 60 °C, 24 hr] were tested on 0.1 mmol scale in a custom parallel reactor that allows for orbital agitation and supplies 1 atm of O₂. After work-up, the crude materials were analyzed by ¹H NMR with trimethylphenylsilane as an internal standard, and 0% of the desired oxazolidinone was observed.



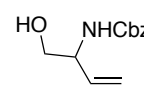
3: Prepared as described previously; characterization data matched literature precedent.³⁷ ¹H NMR (300 MHz, CDCl₃) δ 5.66 – 5.33 (m, 2H), 4.75 (dd, *J* = 11.1, 6.6 Hz, 1H), 4.58 (dd, *J* = 11.1, 8.5 Hz, 1H), 1.70 (dd, *J* = 4.8, 1.4 Hz, 3H), 1.49 (s, 9H), 1.26 (d, *J* = 6.9 Hz, 3H).



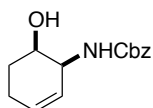
4: Condition **A** [5 mol% Pd(TFA)₂, 20 mol% DMSO, 20 mol% NaOBz, 3 Å M.S., 0.1M in THF, 25 °C, 24 hr], condition **B** [5 mol% Pd(TFA)₂, 20 mol% NaOBz, 3 Å M.S., 0.1M in DMSO, 60 °C, 24 hr], and condition **C** [5 mol% Pd(OAc)₂, 0.1M in DMSO, 60 °C, 24 hr] were tested on 0.08 mmol scale in a custom parallel reactor that allows for orbital agitation and supplies 1 atm of O₂. After work-up, the crude materials were analyzed by ¹H

NMR with trimethylphenylsilane as an internal standard. ^1H NMR spectroscopic data matched prior report for this compound.³⁸ *Trans* isomer: ^1H NMR (300 MHz, CDCl_3) δ 5.87 (ddd, J = 17.2, 10.4, 6.8 Hz, 1H), 5.36 (dd, J = 7.3, 1.1 Hz, 1H), 5.28 (dd, J = 10.3, 1.1 Hz, 1H), 5.14 (m, 1H), 4.69 (d, J = 4.5 Hz, 1H), 4.02 (t, J = 6.8 Hz, 1H), 3.55 (m, 1H), 1.47 (s, 9H), 1.27 (d, J = 7.0 Hz, 3H). *Cis* isomer: ^1H NMR (300 MHz, CDCl_3) δ 5.83 (ddd, J = 17.2, 10.4, 6.6 Hz, 1H), 5.42 (dd, J = 7.1, 1.3 Hz, 1H), 5.32 (dd, J = 12.4, 1.6 Hz, 1H), 4.94 (m, 1H), 4.80 (m, 1H), 4.44 (t, J = 6.3 Hz, 1H), 3.94 (m, 1H), 1.47 (s, 9H), 1.09 (d, J = 6.6 Hz, 3H).

2.4.6. Deprotection of **6b** and **6j**

 **7**: Oxazolidine **6b** (1 equiv, 0.549 mmol, 128 mg) was weighed into a 50 ml round bottom flask and dissolved in 5.5 ml of ethanol (0.1M). HCl (5 M, 50 equiv, 27.4 mmol, 5.5 ml) was added, and the reaction vessel was equipped with a stir bar and reflux condenser and heated to 80-85 °C (reflux) for 1 hour. After cooling to room temperature, the reaction mixture was diluted with ethyl acetate and quenched with a saturated aqueous solution of sodium bicarbonate. The aqueous layer was extracted a total of 3x with ethyl acetate, and the combined organics were then washed with brine, dried over MgSO_4 and concentrated to oil. Purification on silica with a CombiFlash Rf automated chromatography system using a 0-100% EtOAc/hexanes solvent program afforded the product (105 mg, 87% yield) as a clear oil, which solidified at room temperature. ^1H NMR (500 MHz, CDCl_3) δ 7.41 – 7.27 (m, 5H), 5.79 (ddd, J = 16.4, 10.5, 5.3 Hz, 1H), 5.34 (d, J = 8.4 Hz, 1H), 5.25 (d, J = 17.4 Hz, 1H), 5.21 (d, J = 10.6 Hz, 1H), 5.09 (s, 2H), 4.36 – 4.22 (m, 1H), 3.73 – 3.64 (m, 1H), 3.60 (dd, J = 11.4, 5.5 Hz, 1H), 2.64 (s, 1H); ^{13}C NMR (126 MHz, CDCl_3) δ 156.52, 136.36, 135.20, 128.62, 128.27, 128.21,

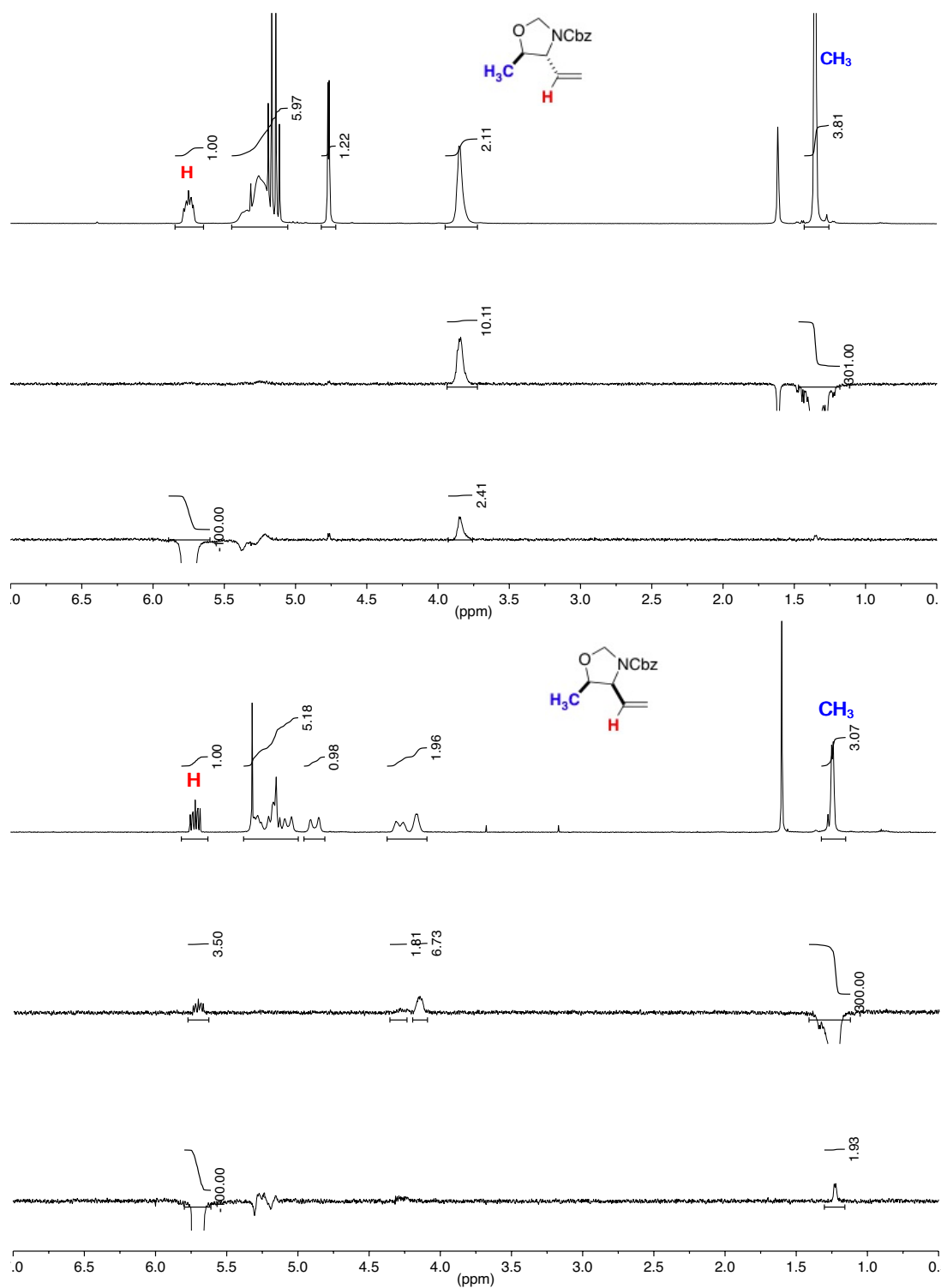
116.83, 67.05, 64.89, 55.11; HRMS (ESI) calculated for $[\text{C}_{12}\text{H}_{15}\text{NO}_3 + \text{H}]^+$ requires m/z 222.1125, found 222.1116.



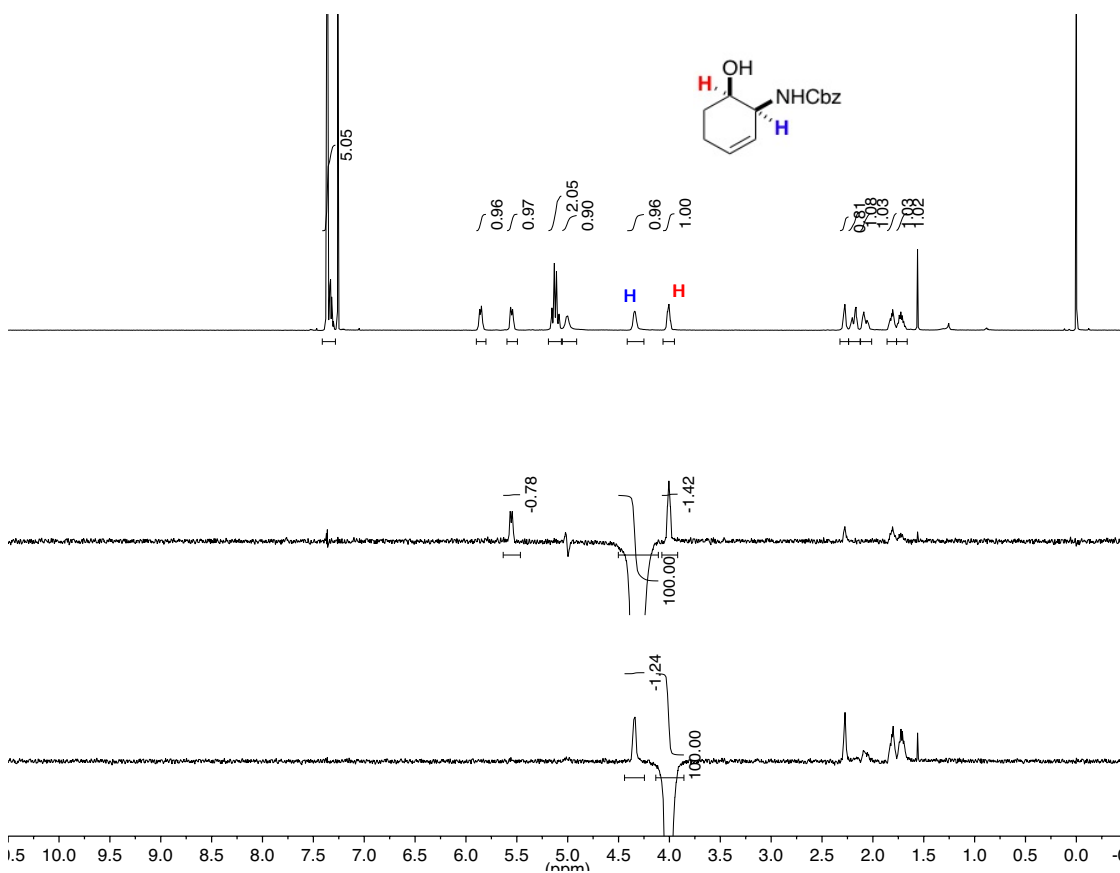
S6: Oxazolidine **6j** (1 equiv, 0.235 mmol, 61 mg) was weighed into a 25 ml round bottom flask and dissolved in 2.35 ml of ethanol (0.1M). HCl (5 M, 50 equiv, 11.8 mmol, 2.35 ml) was added, and the reaction vessel was equipped with a stir bar and reflux condenser and heated to 80-85 °C (reflux) for 1 hour. After cooling to room temperature, the reaction mixture was diluted with ethyl acetate and quenched with a saturated aqueous solution of sodium bicarbonate. The aqueous layer was extracted a total of 3x with ethyl acetate, and the combined organics were then washed with brine, dried over MgSO_4 and concentrated to oil. Purification on silica with a CombiFlash Rf automated chromatography system using a 0-100% EtOAc/hexanes solvent program afforded the product (31 mg, 53% yield) as a white solid and recovered starting material (13 mg, 21% yield). ^1H NMR (500 MHz, CDCl_3) δ 7.42 – 7.28 (m, 5H), 5.91 – 5.79 (m, 1H), 5.60 – 5.50 (m, 1H), 5.14 (d, $J = 12.1$ Hz, 1H), 5.09 (d, $J = 12.3$ Hz, 1H), 5.06 – 5.02 (m, 1H), 4.33 (m, 1H), 4.05 – 3.96 (m, 1H), 2.42 – 2.35 (m, 1H), 2.18 (dtdt, $J = 16.5, 6.0, 4.0, 2.0$ Hz, 1H), 2.07 (dtd, $J = 15.5, 6.4, 2.9$ Hz, 1H), 1.81 (ddt, $J = 14.7, 6.4, 3.1$ Hz, 1H), 1.71 (dq, $J = 13.9, 6.8$ Hz, 1H); ^{13}C NMR (126 MHz, CDCl_3) δ 157.11, 136.39, 131.00, 128.69, 128.34, 128.31, 125.19, 68.50, 67.19, 50.22, 26.44, 22.52; HRMS (ESI) calculated for $[\text{C}_{14}\text{H}_{17}\text{NO}_3 + \text{H}]^+$ requires m/z 248.1282, found 248.1282.

2.4.7. NOESY-1D analysis of **6a** and **6j**

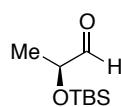
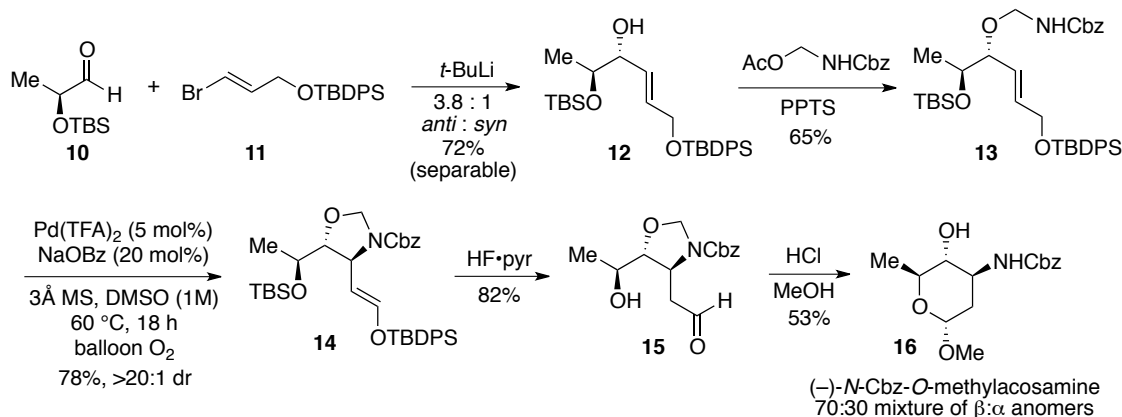
The following NOESY-1D analyses of oxazolidine **6a** (*major* and *minor* diastereomers) were performed on a Varian 600 MHz spectrometer with mix time set to 1.26 milliseconds:



Oxazolidine **6j** was deprotected to afford **S6** (see above) and subjected to NOESY-1D analysis using a Bruker 500 MHz spectrometer and mix time set to 0.6 milliseconds:

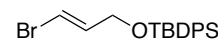


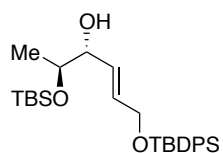
2.4.8. Synthesis of (–)-*N*-Cbz-*O*-methylacosamine, COSY analysis



10: Prepared from TBS-protected ethyl-*L*-lactate as reported previously. TBS-protected ethyl-*L*-lactate (1 equiv, 2.15 mmol, 500 mg) was weighed into a 100 ml round bottom flask equipped with a stir bar. The reaction vessel was evacuated and back-filled with N_2 , and dry diethyl ether (11 ml, 0.2M) was added via syringe. The reaction mixture was cooled to -78°C in a dry ice / acetone bath, and DIBAL-H (1.0M solution in hexanes, 1.2 equiv, 2.6 mmol, 2.6 ml) was added dropwise via syringe. After stirring for 1 hour at -78°C , the reaction mixture was diluted with an additional 11 ml of diethyl ether, warmed to 0°C and quenched with the cautious addition of a saturated aqueous Rochelle's salt (sodium potassium tartrate) solution (approximately 30 ml). The mixture was allowed to warm to room temperature and vigorous stirring was continued for 1 hour. The mixture was transferred to a separatory funnel and diluted further with ether and saturated aqueous Rochelle's salt solution. The ether layer was partitioned, and the aqueous layer was extracted 2x with additional ether. The combined organics were washed with brine, dried over MgSO_4 , and concentrated gently to a clear liquid. This material was immediately purified on silica, eluting 15:1 hexanes : ethyl acetate and concentrated gently (15 mbar at room temperature) to afford the product aldehyde (300 mg,

74% yield) as a clear liquid. This aldehyde is not bench stable and should be used immediately to avoid decomposition. Characterization data matched prior reports: ^1H NMR (300 MHz, CDCl_3) δ 9.62 (d, $J = 1.3$ Hz, 1H), 4.10 (qd, $J = 6.9, 1.3$ Hz, 1H), 1.28 (d, $J = 6.9$ Hz, 3H), 0.92 (s, 9H), 0.11 (s, 3H), 0.09 (s, 3H).

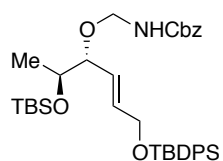
 **11**: 3-Bromo-2*E*-propenol (1 equiv, 4.26 mmol, 584 mg) was weighed into a 50 ml round bottom flask equipped with a stir bar, dissolved in DMF (4.3 ml, 1M) and imidazole (2.2 equiv, 9.38 mmol, 638 mg) was added. The reaction vessel was placed under nitrogen and *tert*-butyl(chloro)diphenylsilane (1.1 equiv, 4.69 mmol, 1.22 ml) was added via syringe. After stirring at room temperature for 3 h, TLC (4:1 hexanes : EtOAc) indicated complete consumption of the starting alcohol. The reaction mixture was transferred to a separatory funnel and partitioned between 50 ml hexanes and 50 ml saturated aqueous ammonium chloride solution. The aqueous layer was extracted 2x with additional hexanes, and the combined organics were washed with brine, dried over MgSO_4 and concentrated to oil. The oil was purified on silica, eluting 19:1 hexanes : EtOAc to afford the TBDPS-protected alcohol (1.58 g, 99% yield) as a clear oil, which solidified at reduced temperature. ^1H NMR (400 MHz, CDCl_3) δ 7.65 (dd, $J = 7.9, 1.6$ Hz, 4H), 7.49 – 7.34 (m, 6H), 6.34 (dt, $J = 13.4, 1.7$ Hz, 1H), 6.26 (dt, $J = 13.4, 4.4$ Hz, 1H), 4.13 (dd, $J = 4.4, 1.6$ Hz, 2H), 1.06 (s, 9H); ^{13}C NMR (101 MHz, CDCl_3) δ 136.42, 135.62, 133.24, 129.98, 127.92, 106.32, 64.12, 26.91, 19.37; HRMS (ESI) calculated for $[\text{C}_{19}\text{H}_{23}\text{BrOSi} - \text{C}(\text{CH}_3)_3]^+$ requires m/z 316.9992, found 316.9975.



12: Vinyl bromide **11** (1.2 equiv, 1.59 mmol, 569 mg) was weighed into a 50 ml round bottom flask equipped with a stir bar and evacuated / back-filled

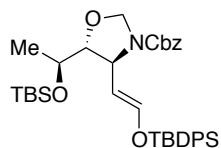
with N₂. TBS-protected *L*-lactaldehyde **10** (1 equiv, 1.33 mmol, 250 mg) was weighed into a separate 50 ml round bottom flask with a stir bar and purged with N₂. The vinyl bromide was dissolved in 8 ml of dry diethyl ether (0.2M) and the aldehyde was dissolved in 3.3 ml of dry diethyl ether (0.4M). The vinyl bromide was cooled to -78 °C in a dry ice / acetone bath, and *tert*-butyllithium (0.90M in pentanes, 1.2 equiv, 1.59 mmol, 1.77 ml) was added dropwise via syringe. The mixture was allowed to stir at -78 °C for 20 min, and then warmed to -60 °C in a dry ice / chloroform bath and allowed to stir an additional 10 min. Meanwhile, the aldehyde was cooled to -78 °C in a dry ice / acetone bath. The vinyl lithium solution was transferred dropwise to the reaction vessel containing the aldehyde via cannula at -78 °C. After stirring for 1 hour at -78 °C, the reaction mixture was warmed to 0 °C and quenched with addition of 20 ml saturated aqueous ammonium chloride solution. The mixture was transferred to a separatory funnel and diluted with additional ether and water. The ether layer was partitioned, washed with brine and dried over MgSO₄ and concentrated to clear oil. TLC on silica using 19:1 hexanes : EtOAc and an extra long plate (20 cm) showed clear separation of the *anti* and *syn* diastereomers. Purification with a CombiFlash Rf automated chromatography system using a 0-5% gradient / 5% isocratic EtOAc/hexanes solvent program on an over-sized silica column afforded the desired *anti* diastereomer (367 mg, 57% yield) and the *syn* diastereomer (98 mg, 15% yield). [Note: the mixture of diastereomers could also be carried forward through the synthesis to afford the final sugar in comparable overall yield and with only trace impurity (presumed to be the minor diastereomer).] *Anti* diastereomer: ¹H NMR (400 MHz, CDCl₃) δ 7.72 – 7.64 (m, 4H), 7.48 – 7.31 (m, 6H), 5.89 – 5.71 (m, 2H), 4.29 – 4.17 (m, 2H), 4.10 – 3.99 (m, 1H), 3.85 (qd, *J* = 6.2, 3.5 Hz, 1H), 2.25 (d, *J* = 4.3 Hz, 1H), 1.08 (d, *J* = 6.2 Hz, 3H), 1.06 (s, 9H), 0.90 (s, 9H), 0.09 (s, 6H); ¹³C NMR (101 MHz, CDCl₃) δ 135.66, 133.82, 133.79, 131.74, 129.77, 127.90, 127.79,

76.14, 71.54, 63.92, 26.95, 25.96, 19.39, 18.20, 17.92, -4.26, -4.67; HRMS (ESI) calculated for $[C_{28}H_{44}O_3Si_2 + NH_4]^+$ requires m/z 502.3168, found 502.3175. *Syn* diastereomer: 1H NMR (400 MHz, $CDCl_3$) δ 7.74 – 7.61 (m, 4H), 7.49 – 7.30 (m, 6H), 5.85 (dt, $J = 15.5, 4.0$ Hz, 1H), 5.76 (dd, $J = 15.5, 5.9$ Hz, 1H), 4.28 – 4.16 (m, 2H), 3.85 (q, $J = 5.5, 5.0$ Hz, 1H), 3.67 (p, $J = 6.1$ Hz, 1H), 2.57 (d, $J = 4.4$ Hz, 1H), 1.14 (d, $J = 6.2$ Hz, 3H), 1.06 (s, 9H), 0.90 (s, 9H), 0.10 (s, 3H), 0.09 (s, 3H); ^{13}C NMR (101 MHz, $CDCl_3$) δ 135.67, 135.65, 133.79, 133.75, 131.61, 129.77, 129.02, 127.79, 76.70, 72.14, 63.91, 26.95, 25.97, 20.15, 19.38, 18.18, -4.05, -4.61; HRMS (ESI) calculated for $[C_{28}H_{44}O_3Si_2 + NH_4]^+$ requires m/z 502.3168, found 502.3163.



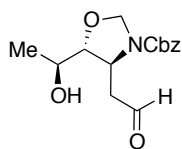
13: Prepared from allylic alcohol **12** (*anti* diastereomer, 1 equiv, 0.41 mmol, 200 mg) according to the general procedure described above (section III).

Purification on silica with a CombiFlash Rf automated chromatography system using a 0-15% EtOAc/hexanes solvent program afforded the product (173 mg, 65% yield) and recovered starting material (37 mg, 19% yield) as clear oils. 1H NMR (400 MHz, $CDCl_3$) δ 7.74 – 7.62 (m, 4H), 7.47 – 7.27 (m, 11H), 5.79 (dt, $J = 15.5, 3.9$ Hz, 1H), 5.70 (dd, $J = 15.6, 5.6$ Hz, 1H), 5.57 (t, $J = 7.1$ Hz, 1H), 5.18 – 5.04 (m, 2H), 4.78 – 4.58 (m, 2H), 4.29 – 4.07 (m, 2H), 3.76 (d, $J = 5.3$ Hz, 2H), 1.10 (d, $J = 5.6$ Hz, 3H), 1.05 (s, 9H), 0.87 (s, 9H), 0.05 (s, 3H), 0.04 (s, 3H); ^{13}C NMR (101 MHz, $CDCl_3$) δ 156.28, 136.45, 135.67, 135.66, 133.78, 133.33, 129.78, 128.63, 128.27, 128.24, 127.79, 127.14, 83.23, 71.25, 71.11, 66.94, 63.79, 26.96, 26.00, 19.42, 19.37, 18.26, -4.48, -4.51; HRMS (ESI) calculated for $[C_{37}H_{53}NO_5Si_2 + NH_4]^+$ requires m/z 665.3801, found 665.3817.



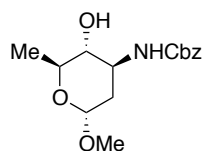
14: Prepared according to a modified version of general procedure **B** (section IV), in which the concentration in DMSO is increased to 1M and the reaction is stopped after 18 hours. A 25 ml Schlenk tube was charged with substrate **11**

(1 equiv, 0.238 mmol, 154 mg), pulverized sodium benzoate (0.2 equiv, 0.0475 mmol, 6.9 mg), powdered 3Å molecular sieves (95 mg, not activated³³) and a stir bar. A septum was used to seal the top of the tube and the apparatus was evacuated and back-filled with O₂ from a balloon. A 0.24 ml stock solution containing Pd(TFA)₂ (0.05 equiv, 0.0119 mmol, 3.95 mg) in DMSO was added via syringe. The reaction vessel was submerged in an oil bath held at 60 °C and stirred *vigorously* under a balloon of O₂ for 18 hrs. The reaction mixture was cooled to room temperature and then partitioned between ether and water (approximately 50 ml of each). The aqueous layer was re-extracted an additional 2x with ether. The combined organics were washed with brine, dried over MgSO₄ and concentrated *in vacuo*. The resulting oil was purified on silica using a CombiFlash Rf automated chromatography system with a 0-15% gradient of ethyl acetate in hexanes to afford the silyl enol ether product (120 mg, 78% yield) as a clear oil. ¹H NMR (400 MHz, CDCl₃) δ 7.83 – 7.57 (m, 4H), 7.50 – 7.13 (m, 11H), 6.67 – 6.37 (m, 1H), 5.21 – 4.84 (m, 4H), 4.67 (m, 1H), 4.35 (m, 1H), 3.90 – 3.76 (m, 1H), 3.56 (t, *J* = 4.4 Hz, 1H), 1.12 – 0.99 (m, 12H), 0.77 (s, 9H), 0.05 – -0.15 (m, 6H); ¹³C NMR (101 MHz, CDCl₃) δ 144.53, 136.60, 135.55, 134.94, 132.57, 130.11, 129.77, 128.53, 127.99, 127.93, 127.90, 127.85, 110.57, 88.79, 78.42, 68.10, 66.94, 54.60, 26.63, 25.83, 20.30, 19.38, 18.03, -4.39, -4.73; HRMS (ESI) calculated for [C₃₇H₅₁NO₅Si₂ + H]⁺ requires *m/z* 646.3379, found 646.3370.



15: Silyl enol ether **14** (1 equiv, 0.19 mmol, 120 mg) was transferred to a 30 ml polyethylene bottle in a total volume of 1.9 ml of THF (0.1M). Pyridine (7.8

equiv, 1.5 mmol, 0.12 ml) was added via syringe. Hydrogen fluoride pyridine (70%HF•30%pyridine, 24 equiv HF, 4.6 mmol, 0.12 ml) was added via syringe (*caution*: follow standard safety precautions for handling HF solutions; a needle was not used in connection with the syringe). The reaction vessel was capped to prevent evaporation of solvent and allowed to stir at room temperature. The progress of the reaction was monitored by TLC (1:1 hexanes:EtOAc on silica, visualization with UV and CAM). The silyl enol ether was rapidly cleaved to yield the aldehyde with the secondary TBS-ether intact ($R_f = 0.88$). This spot slowly converts to a more polar spot ($R_f = 0.30$), which corresponds to the desired product. After 44 hours, the reaction mixture was diluted with ethyl acetate and washed 2x with saturated aqueous sodium bicarbonate solution. The organic layer was further washed with brine, dried over $MgSO_4$, and concentrated to oil. Purification on silica using a CombiFlash Rf automated chromatography system with a 0-100% gradient of ethyl acetate in hexanes afforded the product aldehyde (45 mg, 82% yield) as a clear oil. 1H NMR (400 MHz, $CDCl_3$) δ 9.78 (bs, 1H), 7.45 – 7.28 (m, 5H), 5.32 – 5.02 (m, 3H), 4.80 (d, $J = 4.4$ Hz, 1H), 4.39 (q, $J = 5.6$ Hz, 1H), 3.97 – 3.85 (m, 1H), 3.74 (t, $J = 5.3$ Hz, 1H), 2.92 – 2.71 (m, 1H), 2.13 (bs, 1H), 1.25 (d, $J = 6.4$ Hz, 3H); ^{13}C NMR (101 MHz, $CDCl_3$) δ 200.36, 153.45, 136.01, 128.73, 128.48, 128.27, 86.72, 78.69, 68.11, 67.64, 52.66, 47.09, 19.62; HRMS (ESI) calculated for $[C_{15}H_{19}NO_5 + H]^+$ requires m/z 294.1336, found 294.1335.

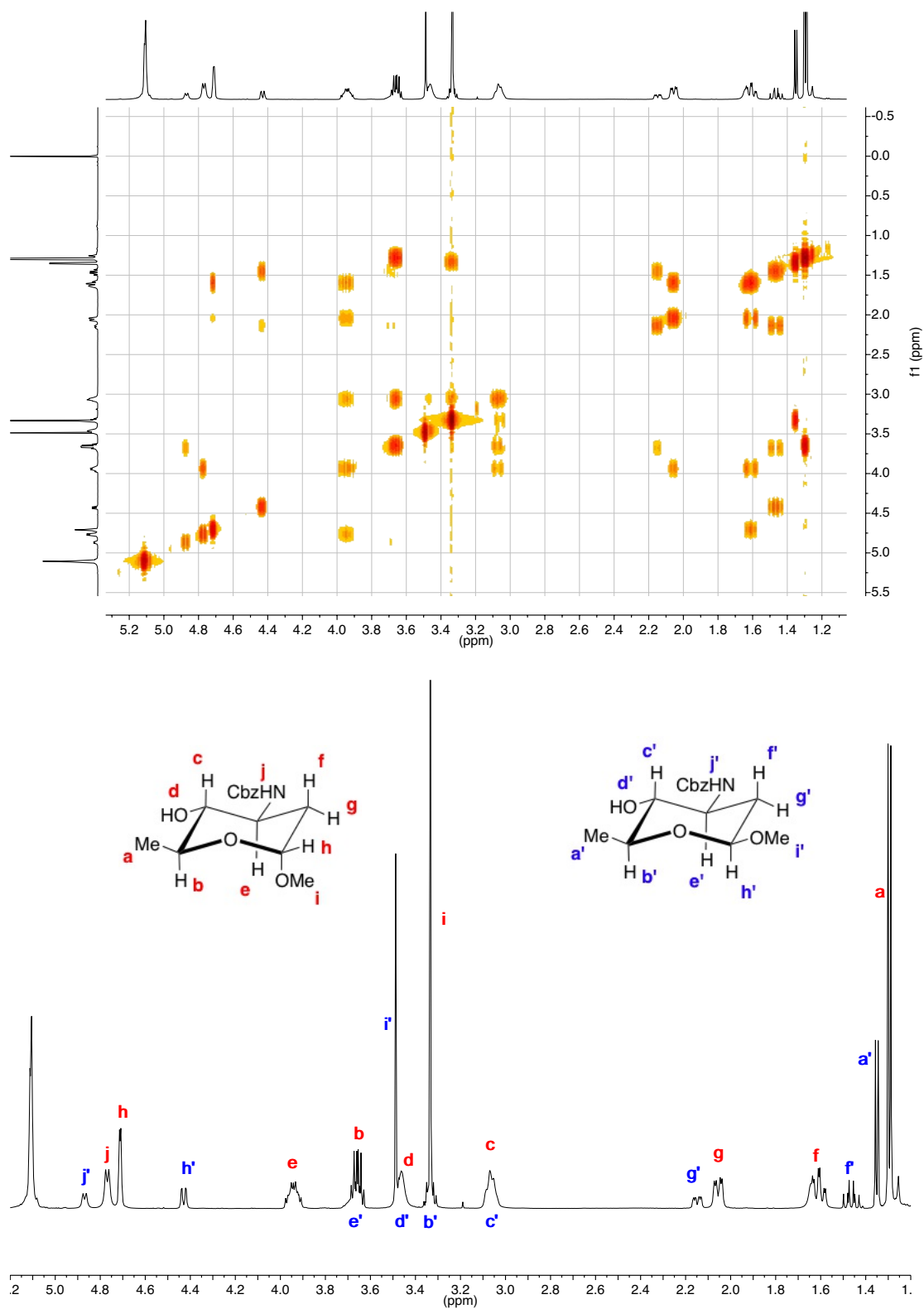


16: Aldehyde **15** (1 equiv, 0.147 mmol, 43 mg) was evaporated into a 24 ml glass vial and dissolved in 1.5 ml MeOH (0.1M). Hydrochloric acid (1M aqueous solution, 10 equiv, 1.5 mmol, 1.5 ml) was added. The vial was capped

and heated to 80-85°C for six hours. The reaction mixture was then cooled to room temperature, diluted with ethyl acetate and washed 2x with saturated aqueous sodium bicarbonate solution.

The organic layer was further washed with brine, dried over MgSO_4 , and concentrated. TLC (1:1 hexanes:EtOAc on silica, visualization with UV and CAM) indicated the desired product at $R_f = 0.33$. Purification on silica using a CombiFlash Rf automated chromatography system with a 0-100% gradient of ethyl acetate in hexanes afforded the product (23 mg, 53% yield) as a white solid (3:1 mixture of a:b anomers). ^1H NMR **a-anomer** (500 MHz, CDCl_3) δ 7.45 – 7.28 (m, 5H), 5.13 – 5.08 (m, 2H), 4.77 (d, $J = 7.3$ Hz, 1H), 4.71 (d, $J = 3.0$ Hz, 1H), 3.94 (dddd, $J = 12.0, 9.5, 7.23, 4.7$ Hz, 1H), 3.66 (dq, $J = 9.3, 6.2$ Hz, 1H), 3.46 (bs, 1H), 3.33 (s, 3H), 3.08 – 3.04 (m, 1H), 2.06 (dd, $J = 12.7, 4.9$ Hz, 1H), 1.61 (td, $J = 12.7, 3.5$ Hz, 1H), 1.29 (d, $J = 6.2$ Hz, 3H); ^1H NMR **b-anomer** (500 MHz, CDCl_3) δ 7.45 – 7.28 (m, 5H), 5.13 – 5.08 (m, 2H), 4.87 (d, $J = 7.3$ Hz, 1H), 4.43 (dd, $J = 9.4, 2.0$ Hz, 1H), 3.69 (m, 1H), 3.49 (s, 3H), 3.46 (bs, 1H), 3.08 – 3.04 (m, 1H), 2.15 (ddd, $J = 12.5, 4.9, 2.0$ Hz, 1H), 1.46 (td, $J = 12.5, 9.4$ Hz, 1H), 1.35 (d, $J = 6.2$ Hz, 3H); ^{13}C NMR **mix of anomers** (126 MHz, CDCl_3) δ 158.05, 157.90, 136.09, 135.96, 128.77, 128.74, 128.55, 128.49, 128.42, 100.66, 97.33, 77.93, 73.39, 68.38, 67.61, 67.50, 56.65, 54.65, 53.39, 50.64, 37.04, 35.86, 17.83; HRMS (ESI) calculated for $[\text{C}_{15}\text{H}_{21}\text{NO}_5 + \text{H}]^+$ requires m/z 296.1493, found 296.1488.

COSY analysis of aminosugar **16** assisted with the following assignment of peaks for the mixture of α - and β -anomers:



2.5 References and Notes

1. Bergmeier, S. C. *Tetrahedron* **2000**, *56*, 2561–2576.
2. For leading references, see: (a) Li, G. G.; Chang, H. T.; Sharpless, K. B. *Angew. Chem. Int. Ed.* **1996**, *35*, 451–454. (b) Reddy, K. L.; Sharpless, K. B. *J. Am. Chem. Soc.* **1998**, *120*, 1207–1217. (c) O'Brien, P. *Angew. Chem. Int. Ed.* **1999**, *38*, 326–329. (d) Donohoe, T.; Callens, C. K. A.; Flores, A.; Lacy, A. R.; Rath, A. H. *Chem. Eur. J.* **2011**, *17*, 58–76.
3. (a) Michaelis, D. J.; Ischay, M. A.; Yoon, T. P. *J. Am. Chem. Soc.* **2008**, *130*, 6610–6615. (b) Williamson, K. S.; Yoon, T. P. *J. Am. Chem. Soc.* **2012**, *134*, 12370–12373.
4. (a) Liu, G.; Stahl, S. S. *J. Am. Chem. Soc.* **2006**, *128*, 7179–7181. (b) Martínez, C.; Wu, Y.; Weinstein, A. B.; Stahl, S. S.; Liu, G.; Muñoz, K. *J. Org. Chem.* **2013**, *78*, 6309–6315.
5. For related examples of the use of detachable tethered nucleophiles in the synthesis of 1,2-aminoalcohol derivatives, see: (a) van Benthem, R. A. T. M.; Hiemstra, H.; Speckamp, W. N. *J. Org. Chem.* **1992**, *57*, 6083–6085. (b) van Benthem, R. A. T. M.; Hiemstra, H.; Longarela, G. R.; Speckamp, W. N. *Tetrahedron Lett.* **1994**, *35*, 9281–9284. (c) Espino, C. G.; Du Bois, J. *Angew. Chem. Int. Ed.* **2001**, *40*, 598–600. (d) Lei, A. W.; Liu, G.; Lu, X. *J. Org. Chem.* **2002**, *67*, 974–980. (e) Fraunhofer, K. J.; White, M. C. *J. Am. Chem. Soc.* **2007**, *129*, 7274–7176. (f) Joosten, A.; Persson, A. K. A.; Millet, R.; Johnson, M. T.; Bäckvall, J.-E. *Chem. Eur. J.* **2012**, *18*, 15151–15157.
6. For related work from our group on the synthesis of diamines, see: McDonald, R. I.; Stahl, S. S. *Angew. Chem. Int. Ed.* **2010**, *49*, 5529–5532.
7. For examples of intramolecular aminooxygenation reactions that generate heterocyclic products, see: (a) Donohoe, T. J.; Johnson, P. D.; Cowley, A.; Keenan, M. *J. Am. Chem. Soc.* **2002**, *124*, 12934–12935. (b) Alexanian, E. J.; Lee, C.; Sorensen, E. J. *J. Am. Chem. Soc.*

-
- 2005**, *127*, 7690–7691. (c) Desai, L. V.; Sanford, M. S. *Angew. Chem. Int. Ed.* **2007**, *46*, 5737–5740. (d) Fuller, P. H.; Kim, J. W.; Chemler, S. R. *J. Am. Chem. Soc.* **2008**, *130*, 17638–17639. (e) Lovick, H. M.; Michael, F. E. *J. Am. Chem. Soc.* **2010**, *132*, 1249–1251. (f) Schmidt, V. A.; Alexanian, E. J. *J. Am. Chem. Soc.* **2011**, *133*, 11402–11405. (g) Donohoe, T. J.; Callens, C. K. A.; Lacy, A. R.; Winter, C. *Eur. J. Org. Chem.* **2012**, 655–663. (h) Liu, G.; Zhang, Y.; Yuan, Y.; Xu, H. *J. Am. Chem. Soc.* **2013**, *135*, 3343–3346.
8. For leading references, see: (a) Arcamone, F.; Penco, S.; Vigevani, A.; Redaelli, S.; Franchi, G.; Dimarco, A.; Casazza, A. M.; Dasdia, T.; Formelli, F.; Necco, A.; Soranzo, C. *J. Med. Chem.* **1975**, *18*, 703–707. (b) Mallams, A. K. in *Carbohydrate Chemistry* (Ed. J. F. Kennedy), Clarendon Press, Oxford, **1988**, pp. 73–133. (c) Myers, A. G.; Kort, M. E.; Hammond, M. A. *J. Am. Chem. Soc.* **1997**, *119*, 2965–2972. (d) Croatt, M. P.; Carreira, E. M. *Org. Lett.* **2011**, *13*, 1390–1393. (e) Wilcock, B. C.; Endo, M. M.; Uno, B. E.; Burke, M. D. *J. Am. Chem. Soc.* **2013**, *135*, 8488–8491.
9. (a) Burns, N. Z.; Baran, P. S.; Hoffmann R. W. *Angew. Chem. Int. Ed.* **2009**, *48*, 2854–2876. (b) Werner, E. W.; Mei, T. S.; Burckle, A. J.; Sigman, M. S. *Science* **2012**, *338*, 1455–1458. (c) Mei, T. S.; Werner, E. W.; Burckle, A. J.; Sigman, M. S. *J. Am. Chem. Soc.* **2013**, *135*, 6830–6833.
10. See reference 6 and: (a) Larock, R. C.; Hightower, T. R. *J. Org. Chem.* **1993**, *58*, 5298–5300. (b) van Benthem, R. A. T. M.; Hiemstra, H.; Michels, J. J.; Speckamp, W. N. *J. Chem. Soc. Chem. Commun.* **1994**, 357–359. (c) Diao, T.; White, P.; Guzei, I.; Stahl, S. S. *Inorg. Chem.* **2012**, *51*, 11898–11909.
11. See reference 5f for a report that employs benzoquinone to promote the aza-Wacker cyclization of allylic *N*-tosyl carbamates.

-
12. These results are consistent with prior results reported in reference 5a by van Benthem et al.
13. Reversible β -hydride elimination can allow for alkene isomerization: Ye, X.; Liu, G.; Popp, B. V.; Stahl, S. S. *J. Org. Chem.* **2011**, *76*, 1031–1044.
14. For a recent review, see: Lumbroso, A.; Cooke, M. L.; Breit, B. *Angew. Chem. Int. Ed.* **2013**, *52*, 1890–1932.
15. (a) Evans, D. A.; Bartroli, J.; Shih, T. L. *J. Am. Chem. Soc.* **1981**, *103*, 2127–2129. (b) Gage, J. R.; Evans, D. A. *Org. Synth.* **1990**, *68*, 83–91.
16. For leading references on other syntheses of (–)-acosamine and related aminosugars, see references 5e, 8d, 8e and: (a) Trost, B. M.; Sudhakar, A. R. *J. Am. Chem. Soc.* **1987**, *109*, 3792–3794. (b) Hirama, M.; Shigemoto, T.; Ito, S. *J. Org. Chem.* **1987**, *52*, 3342–3346. (c) Ager, D. J.; East, M. B. *Tetrahedron* **1993**, *49*, 5683–5765. (d) Kirschning, A.; Jesberger, M.; Schoning, K. U. *Synthesis* **2001**, 507–540. (e) Sames, D.; Polt, R. *J. Org. Chem.* **1994**, *59*, 4596–4601. (f) Myers, A. G.; Liang, J.; Hammond, M.; Harrington, P. M.; Wu, Y.; Kuo, E. Y. *J. Am. Chem. Soc.* **1998**, *120*, 5319–5320. (g) Nicolaou, K. C.; Baran, P. S.; Zhong, Y.; Vega, J. A. *Angew. Chem. Int. Ed.* **2000**, *39*, 2525–2529. (h) Ginesta, X.; Pasto, M.; Pericas, M. A.; Riera, A. *Org. Lett.* **2003**, *5*, 3001–3004. (i) Levy, D. E.; Fugedi, P. *The Organic Chemistry of Sugars*, CRC Press, Florida, **2006**.
17. Optimization of the concentration and reaction time were necessary to minimize the slow decomposition of the silyl enol ether product under the reaction conditions.
18. Harding, K. E.; Marman, T. H.; Nam, D-H. *Tetrahedron* **1988**, *44*, 5606–5614.
19. Fustero, S.; Diego, J.; Moscardo, J.; Catalan, S.; del Pozo, C. *Org. Lett.* **2007**, *9*, 5283–5286.
20. Denmark, S. E.; Harmata, M. A.; White, K. S. *J. Org. Chem.* **1987**, *52*, 4031–4042.
21. Balduzzi, S.; Brook, M. A.; McGlinchey, M. J. *Organometallics* **2005**, *24*, 2617–2627.

-
22. Wang, L.; Thai, K.; Gravel, M. *Org. Lett.* **2009**, *11*, 891–893.
23. Gerusz, V.; Escaich, S.; Oxoby, M.; Denis, A. PCT Int. Appl., 2011061214, 26 May 2011.
24. Muri, D.; Carreira, E. M. *J. Org. Chem.* **2009**, *74*, 8695–8712.
25. Li, Z.; Parr, B. T.; Davies, H. M. L. *J. Am. Chem. Soc.* **2012**, *134*, 10942–10946.
26. Prepared from addition of benzyl magnesium bromide into crotonaldehyde analogously to the procedure found in reference 4. Characterization data matched literature precedence: Beckmann, E.; Desai, V.; Hoppe, D. *Synlett* **2004**, 2275–2280.
27. Becker, N.; Carreira, E. M. *Org. Lett.* **2007**, *9*, 3857–3858.
28. Raw, A. S.; Pedersen, S. F. *J. Org. Chem.* **1991**, *56*, 830–833.
29. Prepared from aldol addition of *N*-methoxy-*N*-methylacetamide to crotonaldehyde analogously to the procedure found in reference 7. Characterization data matched literature precedence: Smith, A. B.; Simov, V. *Org. Lett.* **2006**, 3315–3318.
30. Wang, Y.-G.; Takeyama, R.; Kobayashi, Y. *Angew. Chem. Int. Ed.* **2006**, *45*, 3320–3323.
31. Ichikawa, Y.; Miwa, T.; Narasaka, K. *Bull. Chem. Soc. Jpn.* **1985**, *58*, 3309–3311.
32. Evans, D. A.; Nagorny, P.; McRae, K. J.; Reynolds, D. J.; Sonntag, L.-S.; Vounatsos, F.; Xu, R. *Angew. Chem. Int. Ed.* **2007**, *46*, 537–540.
33. Steinhoff, B. A.; King, A. E.; Stahl, S. S. *J. Org. Chem.* **2006**, *71*, 1861–1868.
34. Steinhoff, B. A.; Stahl, S. S. *J. Am. Chem. Soc.* **2006**, *128*, 4348–4355.
35. Fraunhoffer, K. J.; White, M. C. *J. Am. Chem. Soc.* **2007**, *129*, 7274–7276.
36. Kimura, M.; Tanaka, S.; Tamaru, Y. *Bull. Chem. Soc. Jpn.* **1995**, *68*, 1689–1705.
37. van Benthem, R. A. T. M.; Heimstra, H.; Longarela, G. R.; Speckamp, W. N. *Tetrahedron Lett.* **1994**, *35*, 9281–9284.
38. van Benthem, R. A. T. M. Ph.D. Thesis, Universiteit van Amsterdam (NL), **1995**.

Chapter 3

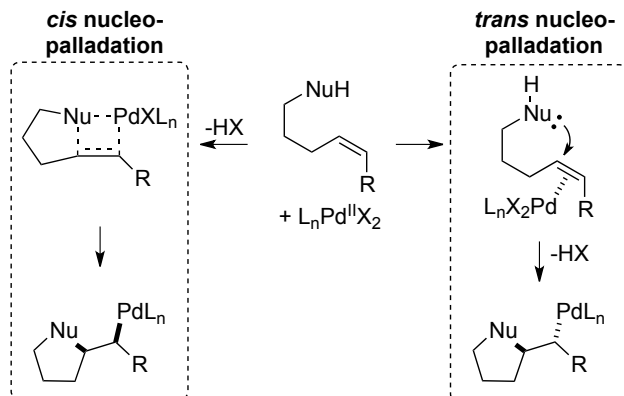
*Reconciling the Stereochemical Course of Nucleopalladation
with the Development of Enantioselective
Wacker-Type Cyclizations*

This work has been published: Weinstein, A. B.; Stahl, S. S. *Angew. Chem. Int. Ed.* **2012**, *51*, 11505–11509.

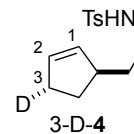
3.1 Introduction

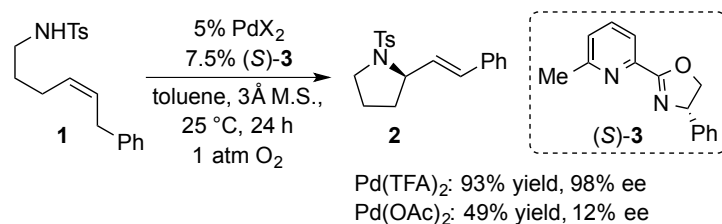
Palladium(II)-catalyzed oxidative functionalization of alkenes has been the focus of intense interest for decades, and Wacker-type cyclizations,¹ which enable synthesis of diverse heterocycles, are a prominent class of these reactions.² Substantial effort has been directed toward enantioselective applications, but successful examples (e.g., $\geq 90\%$ ee) remain rare and often exhibit limited substrate scope.^{3,4} A key challenge associated with these reactions is the possibility of *cis*- or *trans*-nucleopalladation (NP) of the alkene, because the formation of diastereomeric intermediates from these pathways could have significant consequences for the development of enantioselective transformations (Scheme 3.1).³ Examples of both *cis*- and *trans*-NP pathways in catalytic reactions have been documented,^{5,6} but only three enantioselective variants of these reactions have been characterized with respect to the stereochemical course of nucleopalladation. All three examples exhibited a preference for *cis*-NP.^{44f,k,n} The possible impact of the stereochemical course of nucleopalladation on the enantioselectivity of a given asymmetric Wacker-type reaction has not been established. Here, we present a mechanistic investigation of the factors that affect the stereochemical course of nucleopalladation in the context of a recently discovered catalyst system for the enantioselective cyclization of γ -alkenyl tosylamides. Implementation of a novel stereochemical probe demonstrates that both the chiral neutral donor ligand and the anionic ligands on the palladium center are capable of controlling the stereochemical pathway for amidopalladation (AP), but only the *trans*-AP pathway exhibits high enantioselectivity. These data provide the first direct correlation between nucleopalladation stereoselectivity and the enantioselectivity of the transformation in question. Such insights highlight valuable considerations for the development of enantioselective reactions that involve nucleopalladation of an alkene.

Scheme 3.1. Stereochemical pathways for alkene nucleopalladation.



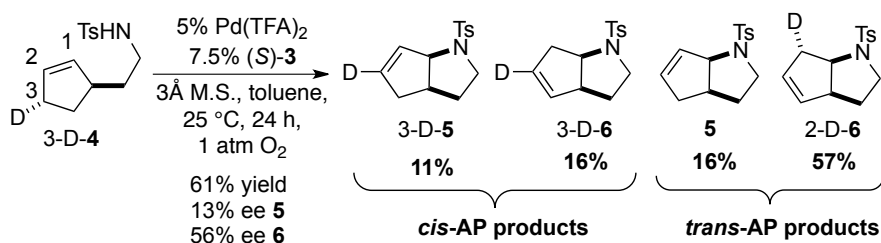
Recently, we showed that a Pd^{II} catalyst with a chiral pyridine-oxazoline (pyrox) ligand enables preparation of pyrrolidines in excellent yield and enantioselectivity (Scheme 3.2).^{4p,7} Based on several closely related precedents, we predicted that the Pd^{II} /pyrox catalyst system would favor a *cis*-amidopalladation (*cis*-AP) mechanism.^{8–11} For example, the isotopically labeled substrate 3-D-4 has been used to assess the mechanism of several different Pd^{II} catalyst systems for the aerobic, oxidative amidation of alkenes,^{5d} and $\text{Pd}(\text{OAc})_2/\text{pyridine}$ and $\text{Pd}(\text{TFA})_2/(-)\text{-sparteine}$ were among the catalyst systems shown to afford products exclusively arising from *cis*-AP of the alkene.¹² In the enantioselective cyclization of γ -alkenyl tosylamides, the identity of the anionic ligand was found to have a significant impact on the reaction outcome. Replacing $\text{Pd}(\text{pyrox})(\text{TFA})_2$ with $\text{Pd}(\text{pyrox})(\text{OAc})_2$ gave significantly diminished yield and enantioselectivity under otherwise identical conditions (Scheme 3.2). The disparity of these results raised the possibility that the reactions with these catalysts might involve different AP pathways.



Scheme 3.2. Pyrox-ligated palladium catalysts for enantioselective aza-Wacker cyclizations.

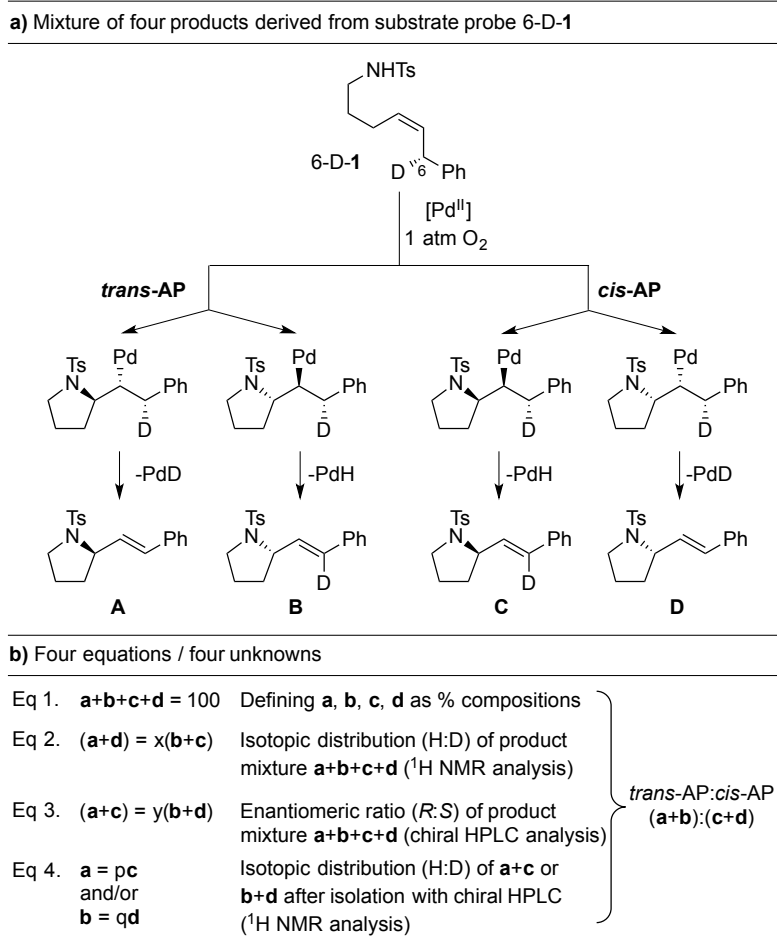
3.2 Results and Discussion

Our initial attempt to probe the AP pathway for the enantioselective reaction involved the use of substrate 3-D-4 under the previously optimized conditions. However, a mixture of all four of the possible bicyclic pyrrolidines was obtained in 61% yield, favoring the *trans*-AP products in approximately 3:1 ratio relative to *cis*-AP products (Scheme 3.3). This result was unexpected for two reasons: first, the *cis*-AP pathway was anticipated to be dominant for these conditions, and second, it seemed unlikely that a highly enantioselective reaction would involve simultaneous operation of both *cis*- and *trans*-AP pathways. Analysis of the product mixture by chiral HPLC revealed poor kinetic resolution; products 3-D-5 and 5 were formed in 13% ee, and products 3-D-6 and 2-D-6 were formed in 56% ee. The relevance of these results was not entirely clear, in part, because the cyclic alkene in 3-D-4 could influence the stereochemical course of the AP step and may not be a good model for acyclic alkenes that undergo highly enantioselective cyclization.^{4p}

Scheme 3.3. Cyclization of substrate 3-D-4 with chiral catalyst.

To circumvent the complications associated with the use of 3-D-4 as a mechanistic probe, we prepared a novel acyclic deuterated substrate probe, 6-D-1, which is a chiral analog of substrate **1** (Scheme 3.4).¹³ Analysis of the products formed by oxidative cyclization of 6-D-1 is more involved than the analysis of products derived from substrate 3-D-4 because both the absolute configuration of the product and the loss or retention of the deuterium atom must be accounted for (the four products **A-D** differ only in the absolute configuration of the stereogenic center and/or the presence or absence of the styrenyl deuterium atom at C6, Scheme 3.4a). Reliable results with 6-D-1 are possible because *trans*-styrenyl products are obtained with high selectivity over the *cis* isomers, and very little deuterium scrambling ($\leq 5\%$) occurs.¹⁴

Scheme 3.4. a) Mechanistic pathways for the reaction of 6-D-1 and b) mathematical relationships used to determine the yields of products **A-D**.

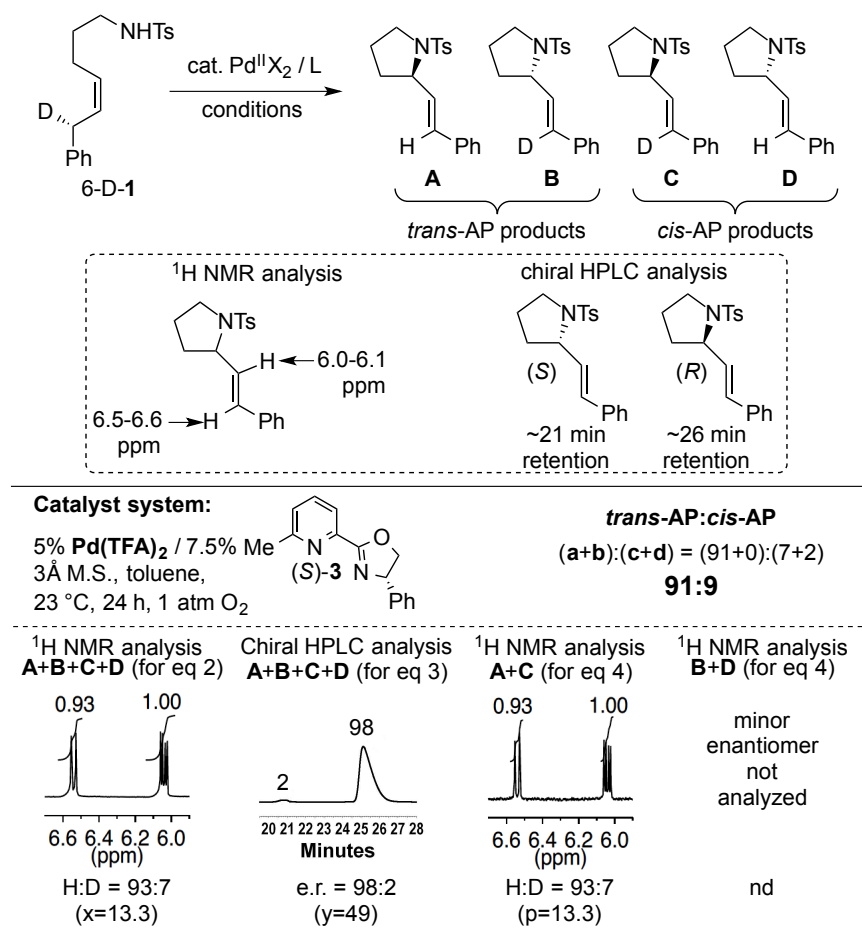


Three independent analytical measurements were used to establish the yield of products **A-D** from the reaction of 6-D-**1** under various conditions. First, the H/D ratio at C6 in the four styrenyl products was obtained by ^1H NMR spectroscopy. This quantity established the relationship $(\mathbf{a}+\mathbf{d}) = x(\mathbf{b}+\mathbf{c})$, where **a**, **b**, **c** and **d** represent the percent composition of the species **A-D**, and $x = \text{H/D at C6}$. Second, the enantiomeric ratio of the products was obtained by chiral HPLC analysis. This quantity established the relationship $(\mathbf{a}+\mathbf{c}) = y(\mathbf{b}+\mathbf{d})$, where $y = [(\textit{R})\text{-products}/(\textit{S})\text{-products}]$. Third, the two sets of enantiomeric products were separated by chiral HPLC, and the H/D ratio of the enantiomerically pure products was obtained by ^1H NMR spectroscopy.¹⁵ This quantity established the **a:c** and **b:d** ratios. With these data in hand and accounting for full mass balance ($\mathbf{a}+\mathbf{b}+\mathbf{c}+\mathbf{d} = 100$), it was possible to solve a system of four equations and four unknowns to determine the quantities **a**, **b**, **c**, and **d**, from which the *trans*-AP:*cis*-AP selectivity was obtained from the ratio $(\mathbf{a}+\mathbf{b}):(\mathbf{c}+\mathbf{d})$ (Scheme 3.4b).¹⁶

Substrate 6-D-**1** was subjected to the optimized chiral catalyst conditions, and the reaction proceeded in excellent yield and enantioselectivity (90% yield and 96% ee), consistent with the reactivity of **1** reported previously (cf. Scheme 3.1).^{4p} ^1H NMR spectroscopic analysis of the initial product mixture revealed a 93:7 preference for the protio products (Scheme 3.5). Because we had previously determined that the (*S*)-configuration of pyrox ligand **3** favors formation of the (*R*)-configuration of the pyrrolidine, the initial ^1H NMR and chiral HPLC analysis were enough to conclude that product **A** was the major species and the *trans*-AP pathway was heavily favored over the *cis* pathway. The product ratio was established more definitively with ^1H NMR analysis of the purified major enantiomer species **A** and **C**. The three measurements show that these reactions exhibit a very high selectivity for a *trans*-AP pathway (*trans*:*cis*-AP = 91:9). The correlation between the high enantioselectivity and high *trans*:*cis*-AP selectivity obtained from

substrate **6-D-1** may be contrasted to the poor enantioselectivity and poor *trans*:*cis*-AP selectivity observed with substrate **3-D-4** (cf. Scheme 3.3).^{17,18}

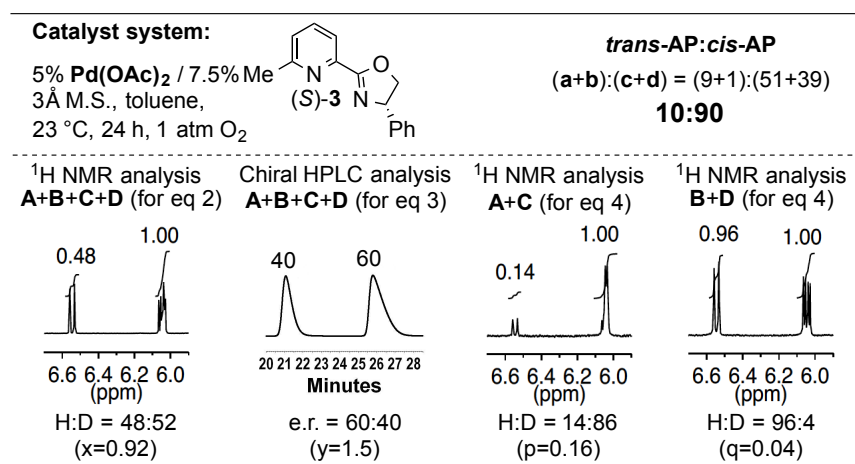
Scheme 3.5. Experimental data and *trans*:*cis*-AP selectivity obtained from oxidative cyclization of substrate **6-D-1** with the optimized chiral catalyst conditions.



These results established the utility of substrate probe **6-D-1** and the protocol for product analysis to correlate the enantioselectivity with the AP pathway of the oxidative cyclization reaction. We then turned our attention to the $\text{Pd}(\text{pyrox})(\text{OAc})_2$ -catalyzed reaction, which proceeds with much lower enantioselectivity under conditions identical to the $\text{Pd}(\text{pyrox})(\text{TFA})_2$ -catalyzed reaction. The reactivity of **6-D-1** with $\text{Pd}[(\text{S})\text{-3}](\text{OAc})_2$ as the catalyst was tested and, consistent with our prior results, the reaction proceeded in only 48% yield and 20% ee. ^1H NMR analysis of the initial product mixture revealed a 48:52 H:D ratio. Following separation of the

two enantiomeric products by chiral HPLC, analysis of the (*R*)-configured products revealed a 14:86 H:D ratio, while the purified (*S*)-configured products displayed a 96:4 H:D ratio (Scheme 3.6). Incorporation of the data from either of these two measurements into the system of four equations led to similar product ratios for species **A**, **B**, **C** and **D**, and the results show that the reaction strongly favored a *cis*-AP pathway (*trans*:*cis*-AP = 10:90), with a 9:1:51:39 ratio for **A**:**B**:**C**:**D**. While the overall reaction exhibited low enantioselectivity, consideration of the minor products **A** and **B**, which arose from *trans*-AP of the alkene, revealed that the *trans*-AP pathway was quite enantioselective (e.r. = 9:1). Thus, with this substrate and pyrox-Pd^{II} catalyst system, the *trans*-AP pathway proceeds with high enantioselectivity while the *cis*-AP pathway exhibits low enantioselectivity. These observations represent the first direct assessment of the enantioselectivity of two different NP pathways for otherwise identical reactions.

Scheme 3.6. Experimental data and *trans*:*cis*-AP selectivity obtained from oxidative cyclization of substrate 6-D-**1** with a Pd(pyrox)(OAc)₂ catalyst system (refer to Scheme 3.5 for depiction of the reaction).



The results of the reactions with the chiral ligands are summarized in Table 3.1, entries 1 and 2. In an effort to separate the influence of the neutral-donor and anionic ligands on the stereochemical course of the AP step, we investigated the oxidative cyclization of 6-D-**1** with Pd(OAc)₂ and Pd(TFA)₂ in the absence of an ancillary neutral-donor ligand. The results show

that both Pd^{II} sources favor *cis*-AP of the alkene (Table 3.1, entries 3 and 4; see also Schemes 3.8–3.14 in the supporting information). The selectivity is considerably higher with Pd(OAc)₂; only trace quantities of the *trans*-AP-derived product are detected by NMR/HPLC analysis. With Pd(TFA)₂, the *trans*:*cis*-AP selectivity is 1:6, suggesting that while the TFA ligand is intrinsically more compatible with the *trans*-AP mechanism, it still favors *cis*-AP. Taken together, the data in Table 3.1 demonstrate that the pyrox ligand plays an important role in enforcing the *trans*-AP pathway with Pd(TFA)₂ as the Pd^{II} source. Previous efforts to understand the factors that influence *trans* vs. *cis*-AP selectivity have implicated the carboxylate ligand as a Brønsted base to mediate Pd–amidate formation in the *cis*-AP pathway.^{5d,19} The present findings reveal that only with the combined presence of a trifluoroacetate anionic ligand and the pyrox neutral-donor ligand is a *trans*-AP pathway, initiated by substitution of TFA by the substrate alkene, favored over the *cis*-AP pathway involving formation of a Pd–amidate.

Table 3.1. Summary of amidopalladation studies with pyrox-ligated and ligand-free catalysts.

entry	Pd ^{II} (5%)	ligand (7.5%)	%yield ^[a]	%ee ^[b]	<i>trans</i> : <i>cis</i> -AP ^[c]
1	Pd(TFA) ₂	(<i>S</i>)- 3	90	96	>9 : 1
2	Pd(OAc) ₂	(<i>S</i>)- 3	48	20	1 : 9
3	Pd(TFA) ₂	None	55	0	1 : 6
4	Pd(OAc) ₂	None	15	0	<1 : 9

[a] Determined by ¹H NMR analysis of the crude reaction mixture. [b] Determined by HPLC analysis of the purified products [c] See the supporting information for full disclosure of the raw data.

In summary, the design, synthesis and implementation of a novel chiral substrate probe (6-D-1) has enabled key insights into the relationship between the NP pathway and the enantioselectivity of a catalytic transformation. The ability of an ancillary neutral-donor ligand to alter the stereochemical course of NP only when a suitable anionic ligand is present highlights the challenges associated with the discovery of efficient catalysts for the asymmetric Wacker-type oxidation of alkenes. Ideally, the factors that affect the NP stereochemistry should be considered in conjunction with the exploration of chiral ancillary ligands in the future development of enantioselective reactions.

3.3 Acknowledgements

We thank Dr. Richard I. McDonald and Chun Pong Tam for initiating the synthesis of substrate probe 6-D-1, and Paul B. White and Dr. Charlie G. Fry for assistance with NMR spectroscopic measurements. We thank the NIH (R01 GM67163) and Organic Syntheses (ACS Division of Organic Chemistry fellowship for A.B.W.) for financial support of this work. Spectroscopic instrumentation was partially funded by the NSF (CHE-0342998, CHE-9629688, CHE-9208463) and NIH (1 S10 RR13866-01).

3.4 Experimental Details and Supporting Information

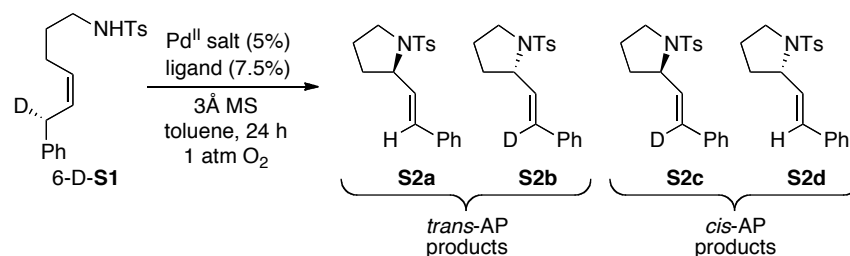
3.4.1. General Considerations

All commercially available compounds were purchased and used as received, unless otherwise noted. Solvents were dried over alumina columns prior to use; however, purification and drying of commercial solvents is not required for the catalytic reactions described here. ^1H and ^{13}C NMR spectra were recorded on Bruker or Varian 300 MHz spectrometers, or Varian 500 and 600 MHz spectrometers, and chemical shifts are given in parts per million relative to internal tetramethylsilane (0.00 ppm for ^1H) or CDCl_3 (77.23 ppm for ^{13}C). Chiral HPLC analysis and separations were carried out with a Shimadzu analytical HPLC system with a commercial Chiralcel column (OJ-H). Flash chromatography was performed using SiliaFlash® P60 (Silicycle, particle size 40-63 μm , 230-400 mesh) or activated basic aluminum oxide (Brockmann I, standard grade, particle size 58Å, ~150 mesh) from Sigma Aldrich. Some chromatography was carried out using a CombiFlash Rf® system with reusable high performance silica columns (RediSep® Rf Gold Silica, 20-40 μm spherical particles).

3.4.2. Experimental procedures and data for the determination of *trans*- vs. *cis*-AP

The catalytic aerobic oxidation reactions described in this report were carried out using a custom reaction apparatus that enabled several reactions to be performed simultaneously under a constant pressure of O_2 (approx 1 atm) with controlled temperature and orbital agitation. A control experiment demonstrated that similar results could be obtained using a standard round-bottom flask equipped with a stir bar and a balloon of O_2 (see previous publication^{4p}).

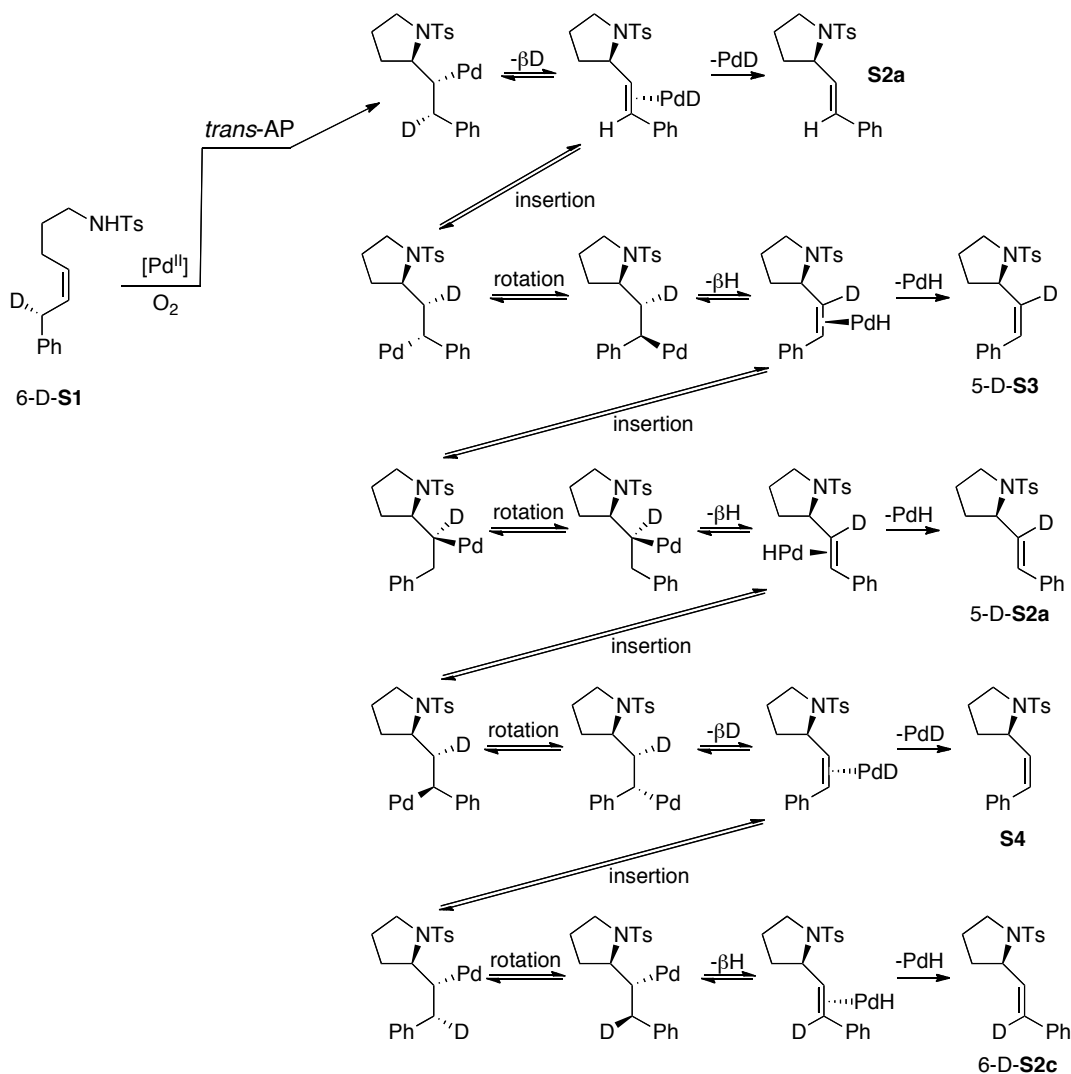
General procedure for catalytic aerobic oxidation reactions:



PdX_2 (0.00375 mmol, 0.05 equiv) and powdered 3Å molecular sieves (20 mg, 267 mg/mmol substrate) were weighed into a 10 ml glass vial (note: the powdered 3Å molecular sieves were stored on the benchtop; activation and glovebox storage was not required to achieve the beneficial effect²⁰). The vial was placed in a custom parallel reactor and the headspace was purged with O_2 for 10 min and temperature set to be maintained at 23 °C. A 0.35 ml solution of ligand in toluene was added by syringe (0.0056 mmol, 0.075 equiv) and the reaction apparatus was set to shake vigorously for 15 min. A 0.4 ml solution of substrate in toluene was added by syringe (0.075 mmol, 1 equiv) and the reaction apparatus was set to shake vigorously for 24 hrs. The resulting reaction mixture was filtered over a plug of basic alumina, eluting with EtOAc and then concentrated. The material was analyzed by ^1H NMR using CDCl_3 spiked with an internal standard to determine yields. The mixture of products and residual starting material was then purified over basic alumina using 3:1 hexanes:EtOAc. The purified mixture of isotopologue/enantiomeric products was analyzed by ^1H NMR, ^2H NMR and chiral HPLC. HPLC conditions were the same as described in our previous report^{4p} (Chiralcel OJ-H, 15% iPrOH, 1 ml/min, 230 nm). Enantiomers were separated using the analytical chiral HPLC set up: the two desired peaks were collected manually into distinct test tubes by diverting the material eluting from the detector. Each peak was collected over five HPLC runs in order to obtain tens of micrograms of material, which was analyzed in a Shigemi tube on a 600 MHz NMR and by ESI-MS. For a depiction of potential isomerization pathways that could complicate interpretation of

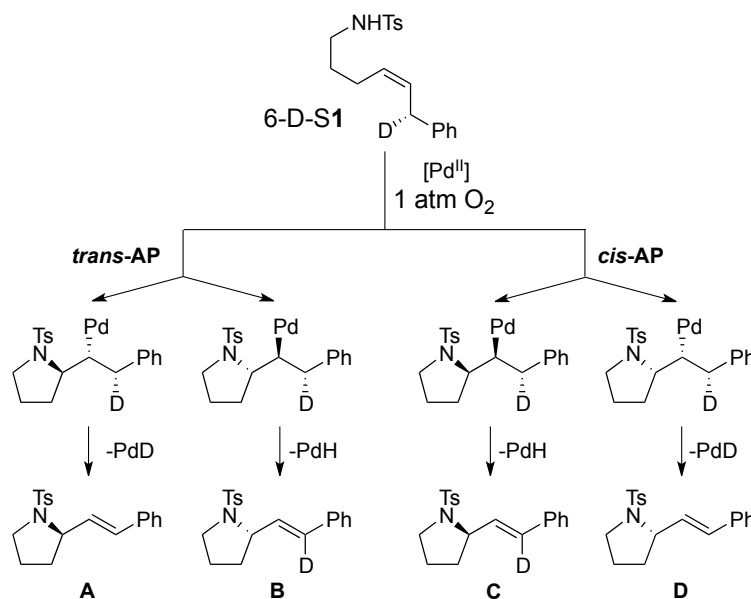
experimental results, see Scheme 3.7. The ^2H NMR analysis of the purified mixture of isotopologue/enantiomeric products was used as a measure of the extent of isomerization (only trace amounts of isomerization to 5-D-**S2a** was detected in each experiment presented in Table 3.1). For presentation of the raw data collected using substrate probe 6-D-**S1**, see Schemes 3.8-3.14.

Scheme 3.7. Potential isomerizations when using substrate probe 6-D-**S1**



Scheme 3.8. Application of novel deuterated substrate probe

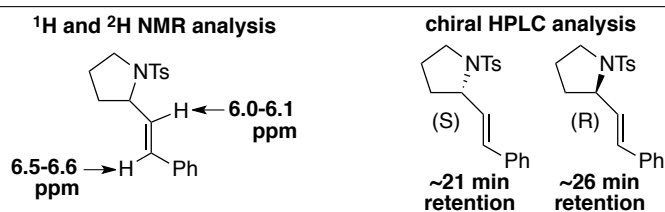
A. Mixture of four products derived from substrate probe 6-D-S1

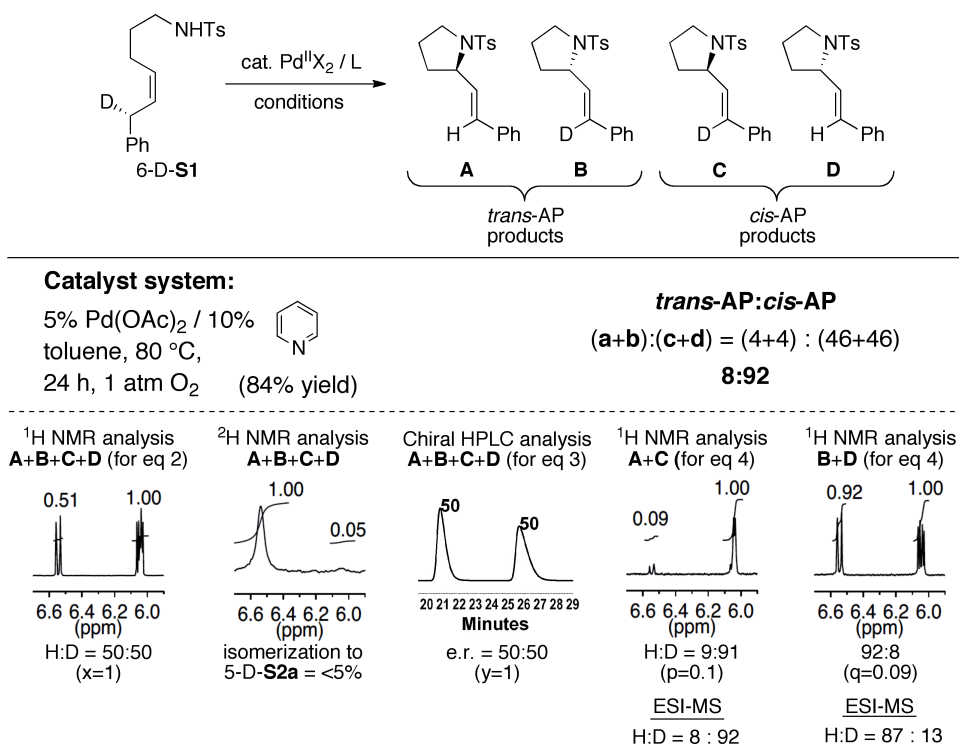


B. Four equations / four unknowns

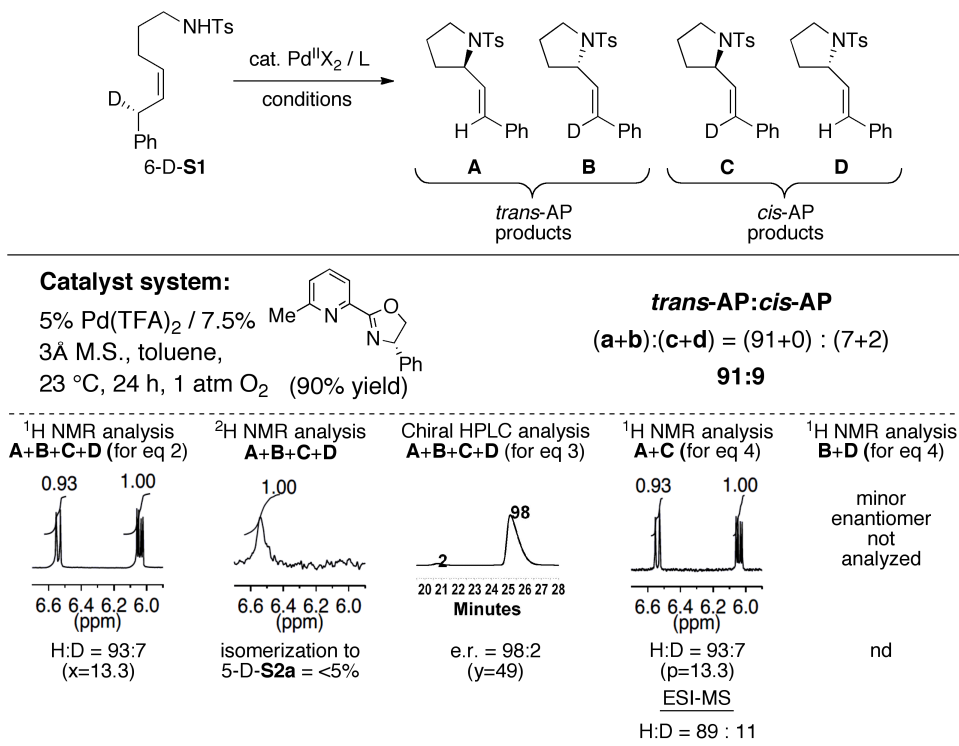
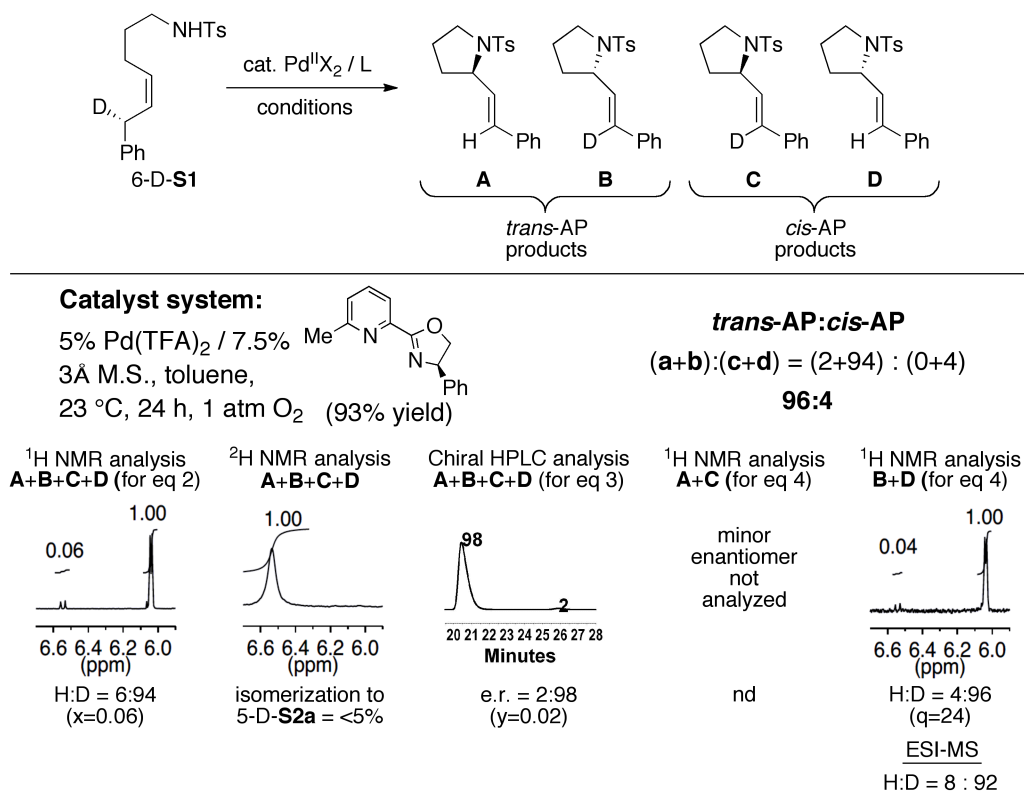
- | | | | |
|-------|--------------------------------|--|---|
| Eq 1. | $a+b+c+d = 100$ | Defining a, b, c, d as % compositions | } <i>trans</i> -AP: <i>cis</i> -AP
(a+b):(c+d) |
| Eq 2. | $(a+d) = x(b+c)$ | Isotopic distribution (H:D) of product mixture a+b+c+d (1H NMR analysis) | |
| Eq 3. | $(a+c) = y(b+d)$ | Enantiomeric ratio (<i>R</i> : <i>S</i>) of product mixture a+b+c+d (chiral HPLC analysis) | |
| Eq 4. | $a = pc$
and/or
$b = qd$ | Isotopic distribution (H:D) of a+c or b+d after isolation with chiral HPLC (1H NMR analysis) | |

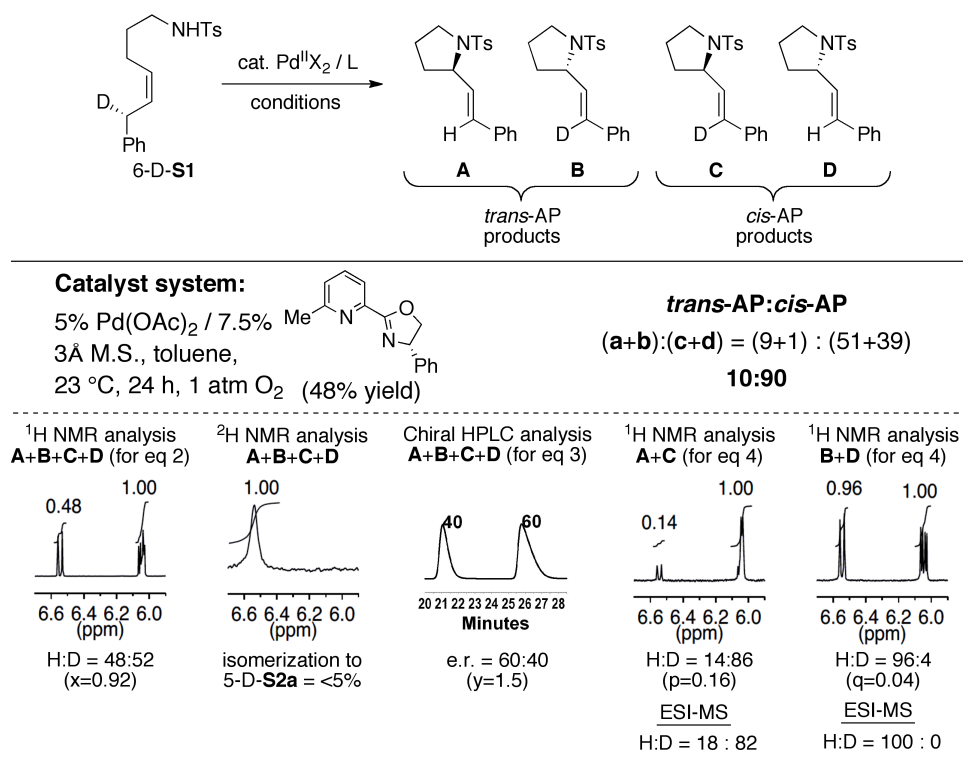
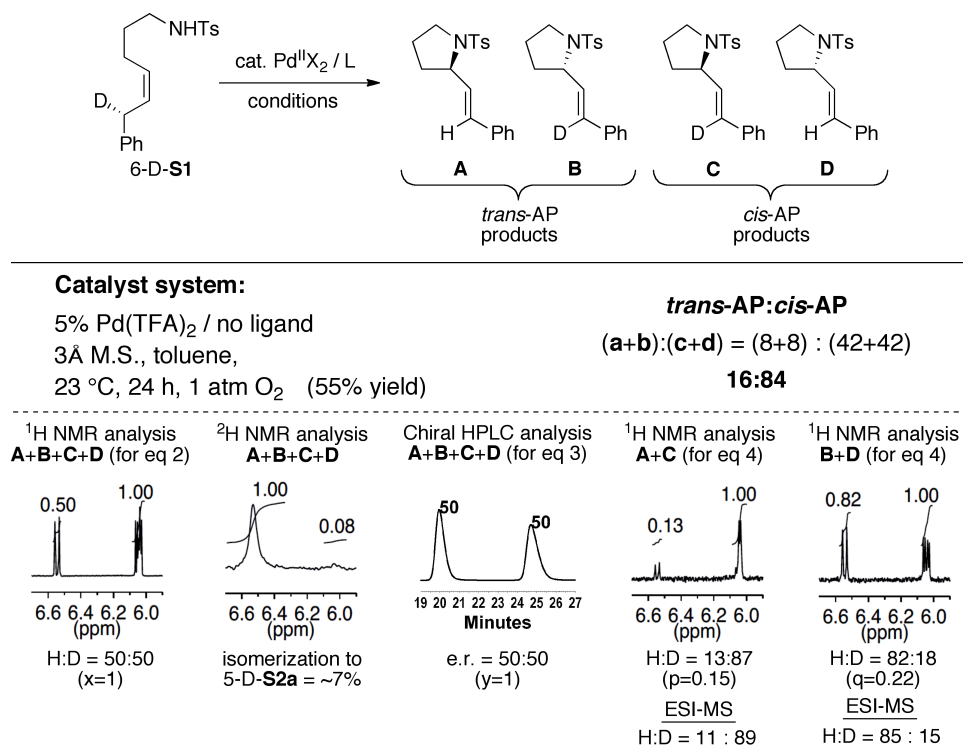
C. Analytical methods and key observables

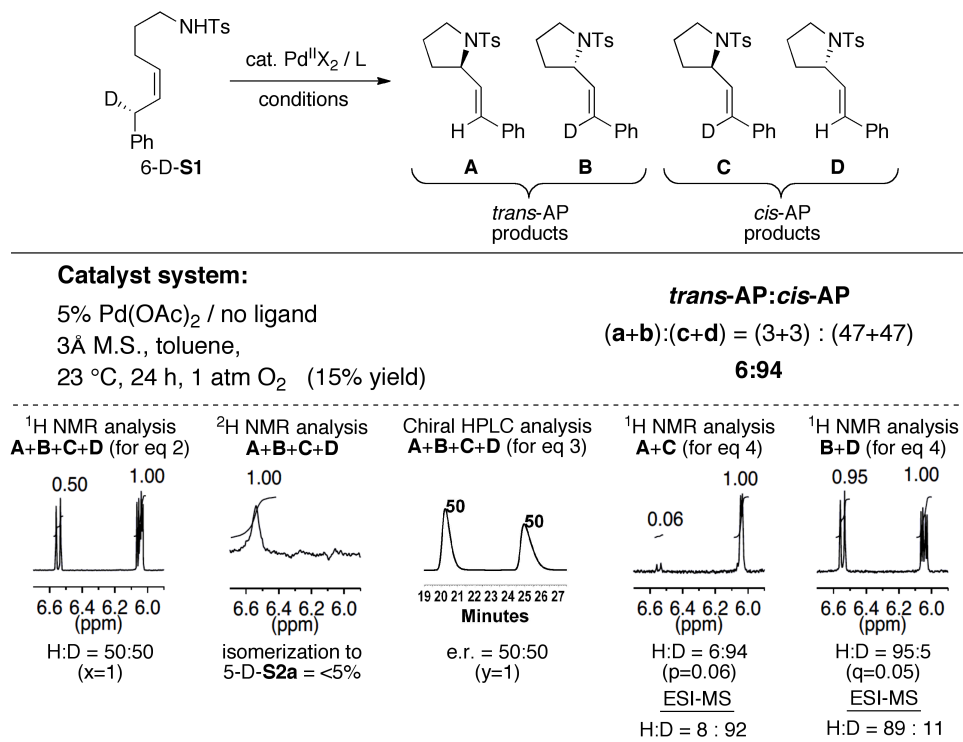


Scheme 3.9. Raw experimental data: Pd(OAc)₂ / pyridine catalyst system.

The above experiment demonstrates that the new substrate probe, 6-D-**S1**, and the protocol for product analysis, are capable of reproducing the previous conclusions obtained from the use of cyclopentenyl substrate probe 3-D-**4** (i.e., the *cis*-AP pathway is favored under these conditions).^{5d}

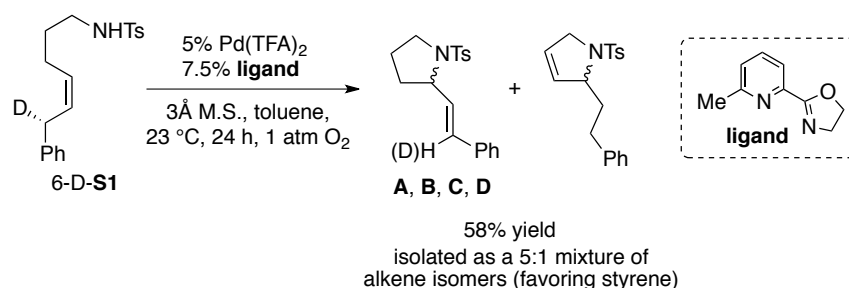
Scheme 3.10. Raw experimental data: Pd(TFA)₂ / (*S*)-pyrox catalyst system.**Scheme 3.11.** Raw experimental data: Pd(TFA)₂ / (*R*)-pyrox catalyst system.

Scheme 3.12. Raw experimental data: Pd(OAc)₂ / (*S*)-pyrox catalyst system.**Scheme 3.13.** Raw experimental data: Pd(TFA)₂ / no ligand catalyst system.

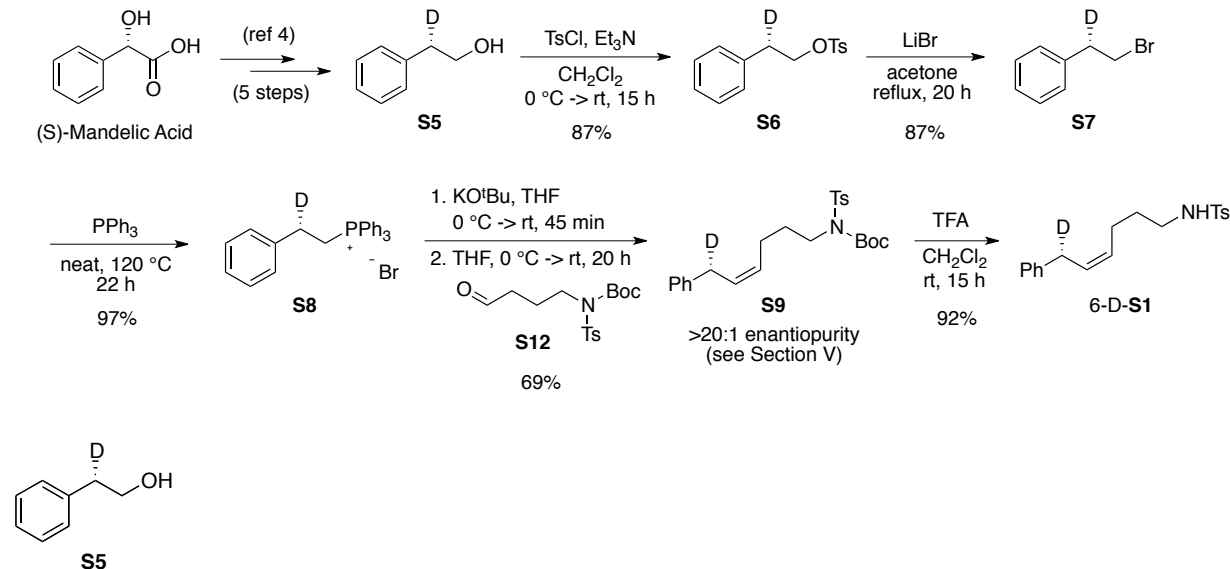
Scheme 3.14. Raw experimental data: Pd(OAc)₂ / no ligand catalyst system.

We were intrigued by the prospect of systematically studying the effect of the pyrox ligand structure on the amidopalladation pathway selectivity, and so an experiment in which the substrate probe was subjected to conditions with a pyrox ligand lacking a substituent on the oxazoline fragment was attempted (Scheme 3.15). Unfortunately, significant alkene isomerization associated with β -hydride elimination was observed (a 5:1 mixture of alkene isomers was isolated in 58% yield). This degree of isomerization prevents reliable interpretation of the result (cf. Scheme 3.7). This finding highlights the limitations of the experimental design presented in this work.

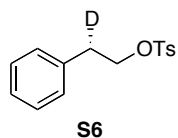
Scheme 3.15. Attempt to study reactivity with modified pyrox ligand.



3.4.3. Stereoselective synthesis of deuterium labeled substrate probe

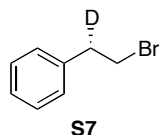


Stereoselectively deuterated phenethanol **S5** was synthesized in five steps from commercially available (*S*)-Mandelic acid using known procedures. Characterization data matched the literature report.¹³

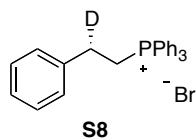


A 250 ml round-bottom flask was charged with a stir bar and alcohol **S5** (608 mg, 4.94 mmol, 1 equiv), and then taken up in 49 ml of dichloromethane (0.1 M). The reaction mixture was submerged in an ice bath. Triethylamine (2.56 ml, 18.3 mmol, 3.7 equiv) was added via syringe, followed by *p*-toluenesulfonyl chloride (1.505 g, 7.9 mmol, 1.6 equiv). The reaction mixture was allowed to warm to room temperature and stir for 15 h. The pale yellow solution was washed twice with 2M HCl, then with saturated sodium bicarbonate solution, and then with brine. The organic layer was dried over MgSO₄ and concentrated to orange-yellow oil. Purification on silica with 9:1 hexanes : ethyl acetate afforded 1.198 g of tosylate **S6** as a clear oil (87% yield), which

solidified at reduced temperature. ^1H NMR: (300 MHz, CDCl_3) δ 7.69 (d, $J = 8.4$ Hz, 2H), 7.33 – 7.18 (m, 5H), 7.14 – 7.06 (m, 2H), 4.20 (dt, $J = 7.1, 0.9$ Hz, 2H), 2.94 (ddd, $J = 7.2, 5.2, 2.0$ Hz, 1H), 2.43 (s, 3H); ^{13}C NMR: (75 MHz, CDCl_3) δ 144.83, 136.34, 133.15, 129.95, 129.06, 128.75, 127.99, 127.03, 70.73, 35.19 (t, $J_{\text{C-D}} = 19.5$ Hz), 21.79.

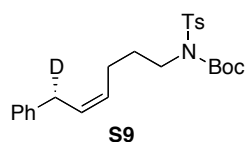


This procedure was adapted from literature precedence.²¹ A 50 ml round-bottom flask was charged with a stir bar and tosylate **S6** (1.198 g, 4.32 mmol, 1 equiv), and taken up in 11 ml of acetone (0.4 M). Lithium bromide (1.876 g, 21.6 mmol, 5 equiv) was added in one portion, and the reaction mixture was heated to reflux for 20 h. After allowing to cool to room temperature, the reaction mixture was partitioned between 150 ml dichloromethane and 150 ml water. The aqueous layer was extracted once with additional dichloromethane, and the combined organic layers were washed with brine, dried over MgSO_4 , and concentrated to a clear liquid. Purification on silica with hexanes afforded 700 mg of bromide **S7** as a clear liquid (87% yield). ^1H NMR: (300 MHz, CDCl_3) δ 7.40 – 7.09 (m, 5H), 3.56 (dt, $J = 7.6, 1.1$ Hz, 2H), 3.23 – 3.03 (m, 1H); ^{13}C NMR: (75 MHz, CDCl_3) δ 139.07, 128.86, 128.82, 127.13, 39.31 (t, $J_{\text{C-D}} = 19.5$ Hz), 33.04; HRMS (ESI) calculated for $\text{C}_8\text{H}_8\text{DBr}^+ [\text{M}]^+$ requires m/z 184.9945, found 184.9938.



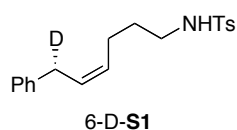
This procedure was adapted from literature precedence.²² A 5 ml thick walled pressure tube was charged with a stir bar and bromide **S7** (700 mg, 3.76 mmol, 1 equiv). Triphenylphosphine (987

mg, 3.76 mmol, 1 equiv) was added in one portion, and the vessel was sealed and heated to 120 °C behind a blast shield for 22 h. The resulting viscous oil was dried under vacuum at 105 °C for several hours, affording 1.635 g of a hard, glassy solid (97% yield). ^1H NMR: (300 MHz, CDCl_3) δ 7.94 – 7.74 (m, 10H), 7.74 – 7.62 (m, 5H), 7.36 – 7.12 (m, 5H), 4.28 – 4.16 (m, 2H), 3.06 (dt, $J = 14.5, 7.9$ Hz, 1H); ^{13}C NMR (75 MHz, CDCl_3) δ 138.23 (d, $J_{\text{C-P}} = 12.8$ Hz), 135.24, 133.68 (d, $J_{\text{C-P}} = 9$ Hz), 130.67 (d, $J_{\text{C-P}} = 12$ Hz), 128.84 (d, $J_{\text{C-P}} = 18.8$ Hz), 127.17, 118.69, 117.55, 28.12 (t, $J_{\text{C-D}} = 19.5$ Hz), 24.76 (d, $J_{\text{C-P}} = 48$ Hz); HRMS (ESI) calculated for $\text{C}_{26}\text{H}_{23}\text{DP}^+$ $[\text{M-Br}]^+$ requires m/z 368.1673, found 368.1682.



This procedure was adapted from literature precedence.^{4p} Wittig salt **S8** was scraped to a white powder and added to a dry 100 ml round bottom flask with a stir bar (776 mg, 1.73 mmol, 1 equiv) under an atmosphere of N_2 . Dry THF (10 ml) was added via syringe, and the reaction mixture was cooled to 0 °C. A solution of potassium *tert*-butoxide (2.0 ml of a 0.93 M solution in THF, 1.9 mmol, 1.1 equiv) was added dropwise via syringe. The mixture was allowed to stir at 0 °C for 15 min, then at room temperature for 45 min. The red-orange mixture was cooled back down to 0 °C, and a solution of aldehyde **S12** (886 mg, 2.6 mmol, 1.5 equiv) in 5 ml of dry THF was added dropwise via syringe (see below for synthesis of **S12**). The mixture was allowed to warm to room temperature and stir for 20 h. The pale yellow mixture was partitioned between 100 ml diethyl ether and 100 ml water. The aqueous layer was extracted an additional two times with diethyl ether, and the combined organics were washed with brine, dried over MgSO_4 , and concentrated to oil (~9:1 mixture of *cis:trans* alkene products present). Purification on silica

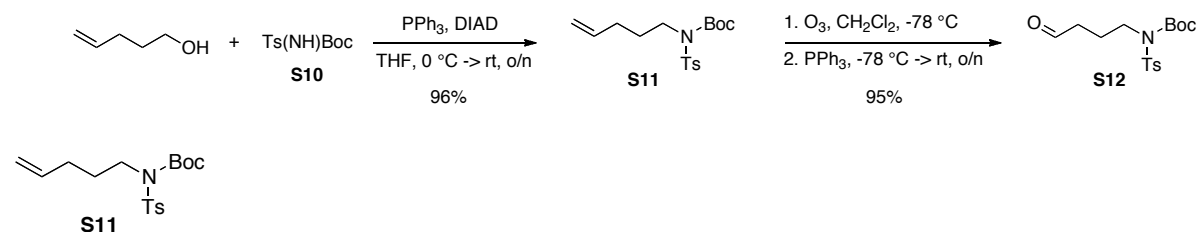
using 19:1 \rightarrow 9:1 hexanes : ethyl acetate as the solvent system afforded 518 mg of **S9** as a clear oil (69% yield). ^1H NMR: (300 MHz, CDCl_3) δ 7.77 (d, J = 8.3 Hz, 2H), 7.33 – 7.23 (m, 4H), 7.23 – 7.15 (m, 3H), 5.70 – 5.44 (m, 2H), 3.88 – 3.80 (m, 2H), 3.39 (d, J = 6.1 Hz, 1H), 2.44 (s, 3H), 2.23 (q, J = 7.3 Hz, 2H), 1.87 (p, J = 7.5 Hz, 2H), 1.33 (s, 9H); ^{13}C NMR: (75 MHz, CDCl_3) δ 151.16, 144.23, 141.08, 137.71, 129.54, 129.43, 129.24, 128.64, 128.53, 128.00, 126.08, 84.31, 47.03, 33.38 (t, $J_{\text{C-D}}$ = 19.5 Hz), 30.25, 28.09, 24.74, 21.81; HRMS (ESI) calculated for $\text{C}_{24}\text{H}_{30}\text{DNO}_4\text{SNa}^+$ $[\text{M}+\text{Na}]^+$ requires m/z 453.1929, found 452.1942.



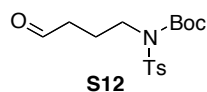
This procedure was adapted from literature precedence.²³ A 100 ml round bottom flask was charged with a stir bar, protected amine **S9** (515 mg, 1.2 mmol, 1 equiv) and 20 ml of dichloromethane (0.06 M). Trifluoroacetic acid (0.92 ml, 12 mmol, 10 equiv) was added cautiously via syringe. The mixture was allowed to stir for 15 h at room temperature. The mixture was quenched with saturated sodium bicarbonate solution and partitioned between 50 ml of dichloromethane and 50 ml saturated sodium bicarbonate solution. The organic layer was washed with an additional volume of saturated sodium bicarbonate solution, then brine, and then dried over MgSO_4 and concentrated to oil. Purification on silica with 4:1 hexanes : ethyl acetate afforded 364 mg of 6-D-**S1** as a clear oil (92% yield). ^1H NMR: (300 MHz, CDCl_3) δ 7.73 (d, J = 8.2 Hz, 2H), 7.33 – 7.23 (m, 4H), 7.23 – 7.10 (m, 3H), 5.59 (dd, J = 10.6, 7.7 Hz, 1H), 5.41 (dddd, J = 10.8, 8.8, 6.9, 1.5 Hz, 1H), 4.30 (t, J = 6.3 Hz, 1H), 3.32 (d, J = 6.9 Hz, 1H), 2.97 (q, J = 6.8 Hz, 2H), 2.42 (s, 3H), 2.14 (q, J = 6.9 Hz, 2H), 1.57 (p, J = 7.2 Hz, 2H); ^{13}C NMR: (75 MHz, CDCl_3) δ 143.56, 140.93, 137.18, 129.90, 129.52, 129.29, 128.66, 128.45, 127.28, 126.14,

43.05, 33.28 (t, $J_{C-D} = 19.5$ Hz), 29.72, 24.52, 21.72; HRMS (ESI) calculated for $C_{19}H_{22}DNO_2SNa^+ [M+Na]^+$ requires m/z 353.1405, found 353.1391.

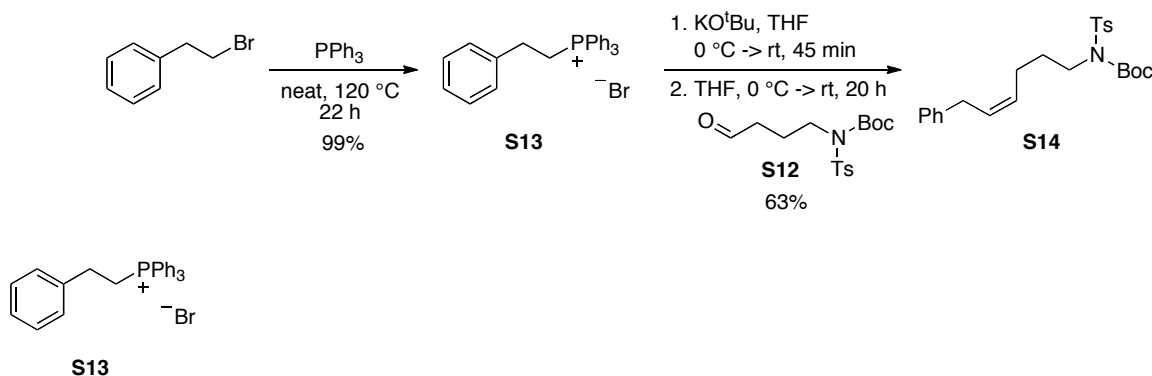
3.4.4. Synthesis of protio intermediates and analogues



Procedure adapted from literature precedence.²³ Triphenylphosphine (1.967 g, 7.5 mmol, 1.5 equiv) and **S10**²⁴ (1.899 g, 7 mmol, 1.4 equiv) were weighed into a 250 ml round bottom flask equipped with a stir bar and placed under an atmosphere of N_2 . Dry THF (29 ml, 0.17 M) was added via syringe, followed by 4-penten-1-ol (0.52 ml, 5 mmol, 1 equiv). The reaction mixture was cooled to 0 °C in an ice bath, and diisopropyl azodicarboxylate (1.23 ml, 6.25 mmol, 1.25 equiv) was added dropwise via syringe. The mixture was allowed to warm to room temperature and stirred for 20 h. The reaction mixture was concentrated to oil and purified on silica with 10:1 \rightarrow 8:1 hexanes : ethyl acetate to afford 1.634 g of **S11** as a clear oil that solidified at reduced temperature (96% yield). 1H NMR: (300 MHz, $CDCl_3$) δ 7.77 (d, $J = 8.4$ Hz, 2H), 7.30 (d, $J = 8.0$ Hz, 2H), 5.84 (ddt, $J = 16.8, 10.2, 6.6$ Hz, 1H), 5.07 (dq, $J = 17.1, 1.6$ Hz, 1H), 5.00 (ddd, $J = 10.2, 3.1, 1.2$ Hz, 1H), 3.86 – 3.78 (m, 2H), 2.44 (s, 3H), 2.13 (q, $J = 7.2$ Hz, 3H), 1.86 (p, $J = 7.5$ Hz, 2H), 1.33 (s, 8H); ^{13}C NMR: (75 MHz, $CDCl_3$) δ 151.12, 144.20, 137.64, 129.39, 127.94, 115.38, 84.26, 46.93, 31.04, 29.38, 28.05, 21.75; HRMS (ESI) calculated for $C_{17}H_{25}NO_4SNa^+ [M+Na]^+$ requires m/z 362.1397, found 362.1390.

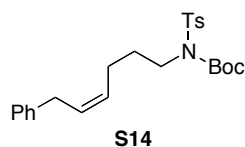


Starting alkene **S11** (1.162 g, 3.42 mmol, 1 equiv) was dissolved in 34 ml of dichloromethane in a 250 ml 3-neck flask equipped with a stir bar. The solution was cooled to -78 °C in a dry ice / acetone bath. An ozone generator was used to bubble ozone through the reaction mixture. After 10 min, the solution took on a characteristic lavender color. The ozone generator was turned off and O₂ was bubbled through the reaction mixture until the color disappeared (about 5 minutes). Triphenylphosphine (1.35 g, 5.13 mmol, 1.5 equiv) was added slowly and the reaction mixture was allowed to slowly warm to room temperature overnight, 15 h. The reaction mixture was concentrated to oil and purified on silica with 3:1 hexanes : ethyl acetate, affording 1.109 g of aldehyde **S12** as a clear oil. ¹H NMR: (300 MHz, CDCl₃) δ 9.82 (t, J = 1.2 Hz, 1H), 7.77 (d, J = 8.4 Hz, 2H), 7.30 (d, J = 8.0 Hz, 2H), 3.98 – 3.80 (m, 2H), 2.58 (td, J = 7.2, 1.1 Hz, 2H), 2.09 (p, J = 7.3 Hz, 2H), 1.34 (s, 10H); ¹³C NMR: (75 MHz, CDCl₃) δ 201.43, 177.92, 151.16, 144.47, 137.44, 129.50, 127.99, 84.68, 46.48, 40.95, 31.08, 28.08, 25.27, 22.79, 21.82; HRMS (ESI) calculated for C₁₆H₂₃NO₅SNa⁺ [M+Na]⁺ requires *m/z* 364.1190, found 364.1183.



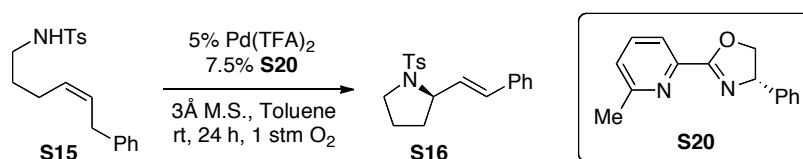
This procedure was reproduced from literature precedence.²² A 5 ml thick walled pressure tube was charged with a stir bar and (2-bromoethyl)benzene (1.371 g, 7.41 mmol, 1 equiv).

Triphenylphosphine (1.943 mg, 7.41 mmol, 1 equiv) was added in one portion, and the vessel was sealed and heated to 120 °C behind a blast shield for 22 h. The resulting viscous oil was dried under vacuum at 105 °C for several hours, affording 3.286 g of a hard, glassy solid (99% yield). Characterization data matched literature precedence. ^1H NMR: (300 MHz, CDCl_3) δ 7.96 – 7.83 (m, 6H), 7.83 – 7.74 (m, 3H), 7.74 – 7.62 (m, 6H), 7.50 – 7.38 (m, 1H), 7.34 – 7.12 (m, 4H), 4.27 (ddd, $J = 12.6, 8.3, 7.2$ Hz, 2H), 3.08 (dt, $J = 13.1, 7.8$ Hz, 2H); ^{13}C NMR (75 MHz, CDCl_3) δ 138.33 (d, $J_{\text{C-P}} = 12.8$ Hz), 135.24 (d, $J_{\text{C-P}} = 3$ Hz), 133.94 (d, $J_{\text{C-P}} = 9.75$ Hz), 130.66 (d, $J_{\text{C-P}} = 12.8$ Hz), 128.9 (d, $J_{\text{C-P}} = 17.3$ Hz), 127.20, 118.83, 117.69, 28.54, 28.50, 24.89 (d, $J_{\text{C-P}} = 48$ Hz); HRMS (ESI) calculated for $\text{C}_{26}\text{H}_{24}\text{P}^+ [\text{M-Br}]^+$ requires m/z 367.1611, found 367.1606.



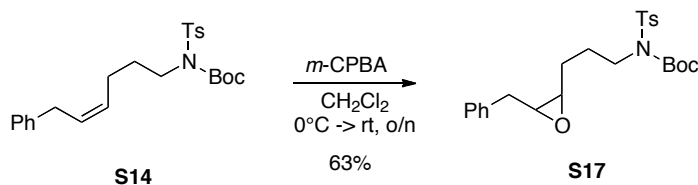
This procedure was adapted from literature precedence.^{4p} Wittig salt **S13** was scraped to a white powder and added to a dry 100 ml round bottom flask with a stir bar (502 mg, 1.12 mmol, 1 equiv) under an atmosphere of N_2 . Dry THF (8 ml) was added via syringe, and the reaction mixture was cooled to 0 °C. A solution of potassium *tert*-butoxide (1.28 ml of a 0.96 M solution in THF, 1.23 mmol, 1.1 equiv) was added dropwise via syringe. The mixture was allowed to stir at 0 °C for 15 min, then at room temperature for 45 min. The red-orange mixture was cooled back down to 0 °C, and a solution of aldehyde **S12** (575 mg, 1.68 mmol, 1.5 equiv) in 3 ml of dry THF was added dropwise via syringe. The mixture was allowed to warm to room temperature and stir for 20 h. The pale yellow mixture was partitioned between 100 ml diethyl ether and 100 ml water. The aqueous layer was extracted an additional two times with diethyl ether, and the combined organics were washed with brine, dried over MgSO_4 , and concentrated

to oil (~9:1 mixture of *cis:trans* alkene products present). Purification on silica using 19:1 → 9:1 hexanes : ethyl acetate as the solvent system afforded 301 mg of **S14** as a clear oil (63% yield). ¹H NMR: (300 MHz, CDCl₃) δ 7.77 (d, J = 8.3 Hz, 2H), 7.34 – 7.24 (m, 4H), 7.22 – 7.16 (m, 3H), 5.69 – 5.47 (m, 2H), 3.89 – 3.80 (m, 2H), 3.41 (d, J = 6.7 Hz, 2H), 2.43 (s, 3H), 2.23 (q, J = 7.0 Hz, 2H), 1.87 (p, J = 7.5 Hz, 2H), 1.33 (s, 9H); ¹³C NMR: (75 MHz, CDCl₃) δ 151.16, 144.23, 141.12, 137.73, 129.53, 129.43, 129.28, 128.63, 128.53, 128.00, 126.07, 84.30, 47.04, 33.70, 30.25, 28.09, 24.74, 21.80; HRMS (ESI) calculated for C₂₄H₃₅N₂O₄S⁺ [M+NH₄]⁺ requires *m/z* 447.2313, found 447.2311.



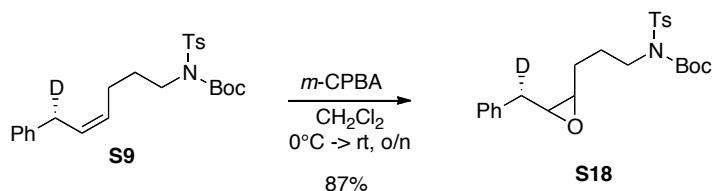
Substrate **S15** and pyrrolidine **S16** could be synthesized as previously described. Characterization data matched previous reports.^{4p}

3.4.5. Characterization of stereochemical purity of the deuterated substrate probe



This procedure was adapted from literature precedence.²⁵ A 25 ml round bottom flask was charged with a stir bar and **S14** (61 mg, 0.142 mmol, 1 equiv) and dissolved in 1 ml of dichloromethane. The reaction vessel was submerged in an ice bath and 3-chloroperbenzoic acid (40 wt%) (122 mg, 0.283 mmol, 2 equiv) was added in one portion. The heterogeneous reaction mixture was allowed to warm to room temperature and stirred for 18 h. The dichloromethane

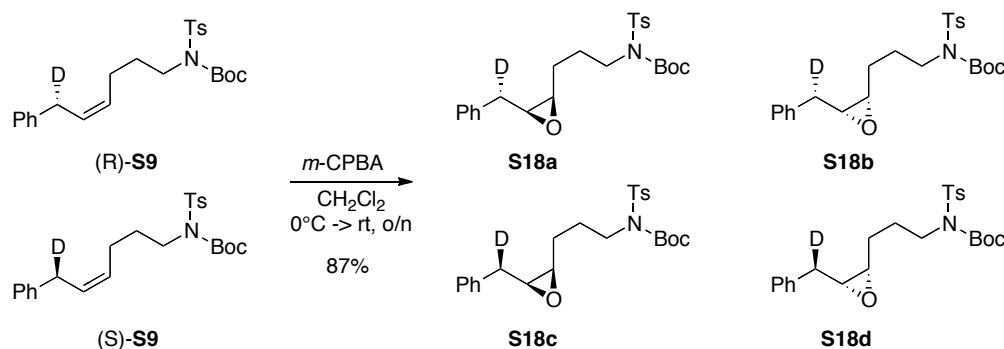
was removed and the reaction mixture was dissolved in ethyl acetate and washed with 1M sodium bisulfite solution, saturated sodium bicarbonate solution, and then brine. The organic layer was dried over MgSO_4 and concentrated to an oil, which was purified on silica with 3:1 hexanes : ethyl acetate to afford 40 mg of epoxide **S17** as a clear oil (63% yield). HPLC analysis (Chiralcel, OJ-H, 10% iPrOH, 1 ml, min, 230 nm) achieved separation of enantiomers. ^1H NMR: (300 MHz, CDCl_3) δ 7.85 – 7.70 (m, 1H), 7.43 – 7.17 (m, 4H), 4.04 – 3.80 (m, 2H), 3.20 (td, J = 6.3, 4.1 Hz, 1H), 3.12 – 2.99 (m, 1H), 2.93 (dd, J = 14.7, 6.4 Hz, 1H), 2.81 (dd, J = 14.7, 6.2 Hz, 1H), 2.44 (s, 3H), 1.99 (dddd, J = 17.2, 10.8, 6.9, 4.0 Hz, 1H), 1.88 – 1.59 (m, 1H), 1.34 (s, 4H); ^{13}C NMR: (75 MHz, CDCl_3) δ 151.14, 144.31, 137.96, 137.61, 129.45, 128.99, 128.83, 127.99, 126.74, 84.45, 57.54, 56.95, 46.95, 34.47, 28.07, 27.64, 25.54, 21.79; HRMS (ESI) calculated for $\text{C}_{24}\text{H}_{35}\text{N}_2\text{O}_5\text{S}^+$ $[\text{M}+\text{NH}_4]^+$ requires m/z 463.2262, found 463.2258.



This procedure was adapted from literature precedence.²⁵ A 25 ml round bottom flask was charged with a stir bar and **S9** (52 mg, 0.12 mmol, 1 equiv) and dissolved in 1 ml of dichloromethane. The reaction vessel was submerged in an ice bath and 3-chloroperbenzoic acid (40 wt%) (104 mg, 0.24 mmol, 2 equiv) was added in one portion. The heterogeneous reaction mixture was allowed to warm to room temperature and stirred for 18 h. The dichloromethane was removed and the reaction mixture was dissolved in ethyl acetate and washed with 1M sodium bisulfite solution, saturated sodium bicarbonate solution, and then brine. The organic layer was dried over MgSO_4 and concentrated to an oil, which was purified on silica with 3:1

hexanes : ethyl acetate to afford 47 mg of epoxide **S18** as a clear oil (87% yield). HPLC analysis (Chiralcel, OJ-H, 10% iPrOH, 1 ml, min, 230 nm) achieved separation of enantiomers. ^1H NMR: (300 MHz, CDCl_3) δ 7.78 (d, J = 8.4 Hz, 2H), 7.40 – 7.17 (m, 7H), 4.07 – 3.76 (m, 2H), 3.19 (dd, J = 6.2, 4.1 Hz, 1H), 3.05 (dt, J = 7.4, 4.6 Hz, 1H), 2.91 (d, J = 6.4 Hz, 0.5H), 2.80 (d, J = 6.0 Hz, 0.5H), 2.44 (s, 3H), 2.11 – 1.87 (m, 2H), 1.86 – 1.60 (m, 2H), 1.34 (s, 9H); ^{13}C NMR: (75 MHz, CDCl_3) δ 151.15, 144.32, 137.93, 137.63, 129.46, 129.00, 128.84, 128.00, 126.75, 84.45, 57.48, 56.93, 46.96, 34.15 (t, $J_{\text{C-D}}$ = 19.5 Hz), 28.08, 27.65, 25.56, 21.80; HRMS (ESI) calculated for $\text{C}_{24}\text{H}_{34}\text{DN}_2\text{O}_5\text{S}^+ [\text{M}+\text{NH}_4]^+$ requires m/z 464.2324, found 464.2325.

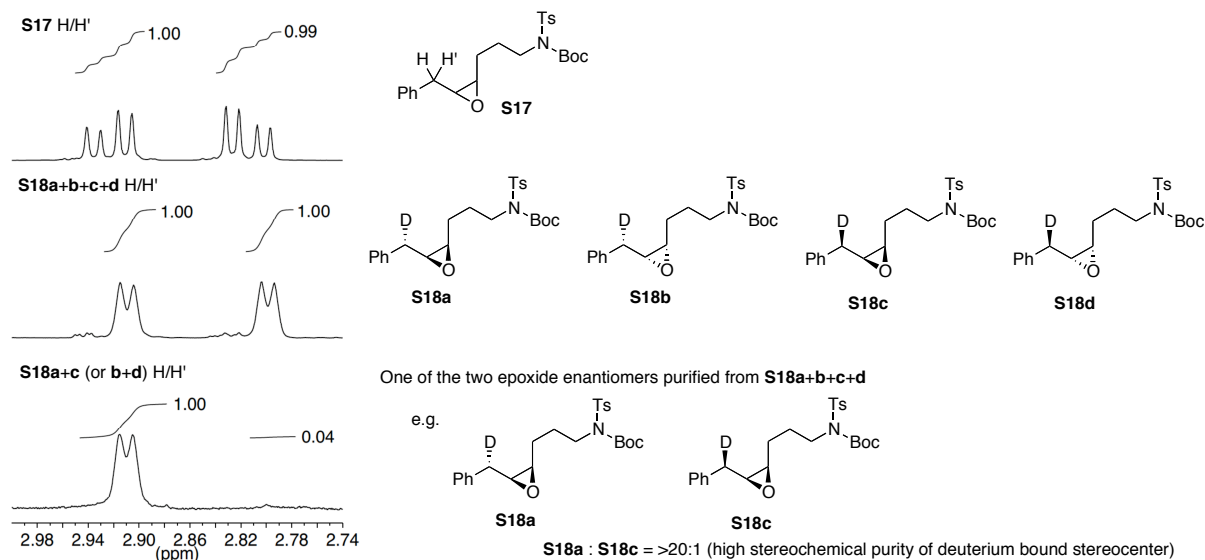
Supposing the deuterium label in **S9** is not perfectly stereopure, four stereoisomeric products are possible from the epoxidation:



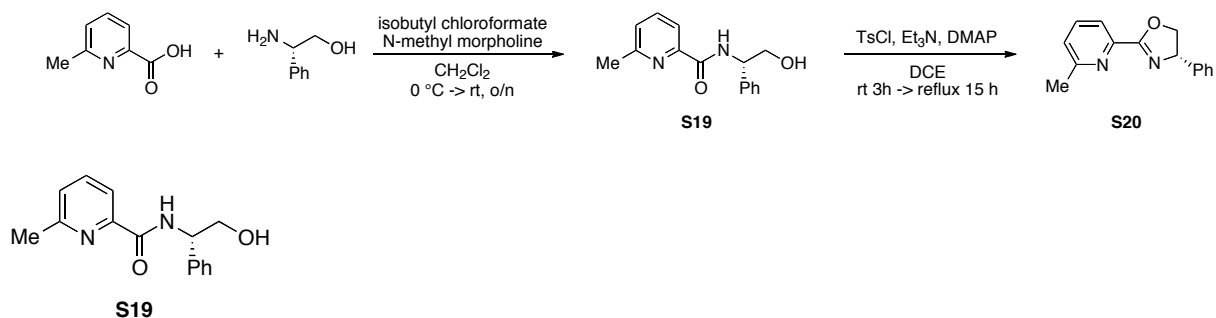
Epoxide enantiomers **S18a+c** and **S18b+d** were separated using the analytical chiral HPLC set up. One of the two enantiomers was collected manually into a test tube by diverting the material eluting from the detector. Material was collected over five HPLC runs in order to obtain tens of micrograms of material, which was analyzed in a Shigemi tube on a 600 MHz NMR. Below, this resulting spectrum is presented, zoomed in on the methylene proton(s) of interest and compared to spectra taken of protio compound **S17** and the mixture of **S18** products prior to separation of

enantiomers. Note: the absolute configuration of the epoxide was not determined, so the configuration of the purified enantiomer that was analyzed is ambiguous. The results indicate that the substrate probe has a high degree of stereochemical purity (>20:1 desired stereochemistry, Scheme 3.16).

Scheme 3.16. Characterization of stereochemical purity of probe 6-D-S1.

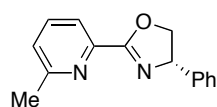


3.4.6. Synthesis of pyridine-oxazoline ligand



This procedure was adapted from literature precedence.^{4p} A dry 250 ml round bottom flask was charged with a stir bar and 6-methylpicolinic acid (700 mg, 5.1 mmol, 1 equiv) and put under an atmosphere of N₂. Dry dichloromethane (50 ml, 0.1M) was added and the reaction vessel was submerged in a brine ice bath. 4-Methylmorpholine (0.84 ml, 7.65 mmol, 1.5 equiv) was added

slowly by syringe and the mixture was stirred for 15 min. Isobutylchloroformate (0.77 ml, 5.87 mmol, 1.15 equiv) was added dropwise by syringe and stirred for 30 min. A solution of (S)-phenylglycinol (840 mg, 6.13 mmol, 1.2 equiv) in 10 ml of dichloromethane and with additional 4-methylmorpholine (0.64 ml, 5.87 mmol, 1.15 equiv) was added dropwise and stirred at reduced temperature for 1 h and then allowed to warm to room temperature and stir overnight (18 h). The reaction mixture was diluted with dichloromethane and washed twice with saturated ammonium chloride solution, then water, then brine. The organic layer was dried over MgSO_4 and concentrated to yellow-pink oil. The oil was purified on silica with a 25% ethyl acetate / 40% hexanes / 5% methanol / 30% dichloromethane solvent system to afford 1.253 g of amide **S19** as a clear oil (96% yield). Characterization data matched previous report. ^1H NMR: (300 MHz, CDCl_3) δ 8.74 (d, $J = 5.7$ Hz, 1H), 8.01 (d, $J = 7.7$ Hz, 1H), 7.73 (t, $J = 7.7$ Hz, 1H), 7.51 – 7.17 (m, 6H), 5.26 (ddd, $J = 7.4, 6.1, 4.3$ Hz, 1H), 4.13 – 3.93 (m, 2H), 2.80 (dd, $J = 7.1, 5.3$ Hz, 1H), 2.58 (s, 3H); ^{13}C NMR: (75 MHz, CDCl_3) δ 165.24, 157.52, 149.03, 139.22, 137.69, 129.11, 128.07, 127.08, 126.31, 119.66, 67.04, 56.50, 24.49; HRMS (ESI) calculated for $\text{C}_{15}\text{H}_{17}\text{N}_2\text{O}_2^+$ $[\text{M}+\text{H}]^+$ requires m/z 257.1285, found 257.1280.

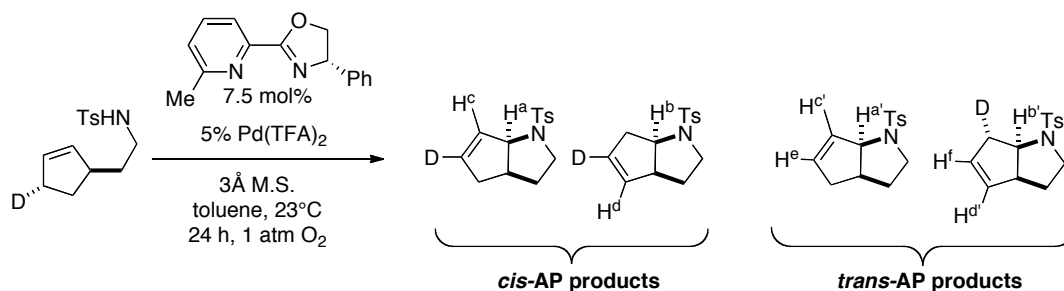
**S20**

This procedure was adapted from literature precedence.^{4p} A dry 50 ml 2-neck round bottom flask equipped with a stir bar and reflux condenser was placed under N_2 . 4-Dimethylaminopyridine (15 mg, 0.12 mmol, 0.1 equiv) and *p*-toluenesulfonylchloride (350 mg, 1.84 mmol, 1.5 equiv) were added to the reaction vessel under a positive pressure of N_2 . Amide **S19** (314 mg, 1.23 mmol, 1 equiv) was added in a solution of 12 ml of dry 1,2-dichloroethane (0.1 M) to the

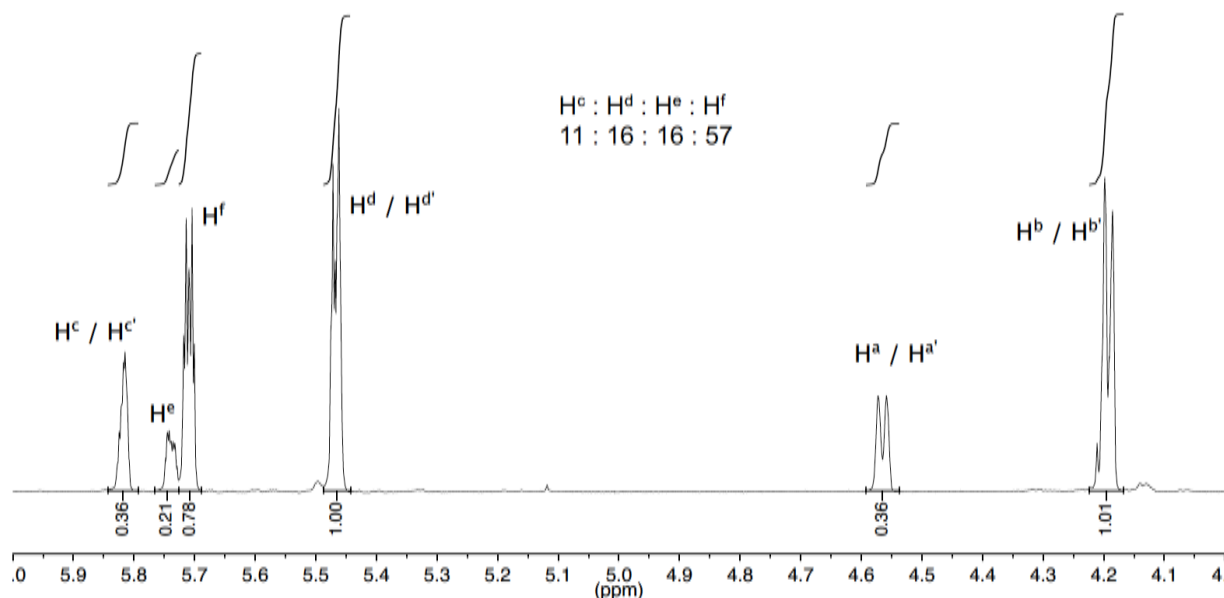
reaction vessel by syringe. Triethylamine (0.98 ml, 7.04 mmol, 4 equiv) was added to the reaction mixture by syringe. The reaction mixture was stirred at room temperature for 3 h and then heated to reflux for 17 h. The deep red solution was cooled to room temperature, diluted with dichloromethane and washed twice with saturated sodium bicarbonate, then water, then brine. The organic layer was dried over MgSO_4 and concentrated to red oil. Purification on a CombiFlash Rf purification system using a high performance basic alumina column (Teledyne-Isco RediSep) and 5 \rightarrow 35% ethyl acetate in hexanes gradient afforded 147 mg of **S20** as a pale red oil (50% yield). Note: this reaction proceeds with nearly complete conversion to product, but purification results in problematic decomposition. Use of activated basic alumina and dry-loading the crude mixture (pre-adsorb onto small amount of alumina for purification) are recommended for purification of this ligand. Characterization data matched the previous report. ^1H NMR: (300 MHz, CDCl_3) δ 7.99 (d, J = 7.8 Hz, 1H), 7.68 (t, J = 7.8 Hz, 1H), 7.47 – 7.15 (m, 6H), 5.44 (dd, J = 10.3, 8.5 Hz, 1H), 4.96 – 4.82 (m, 1H), 4.39 (t, J = 8.5 Hz, 1H), 2.66 (s, 3H); ^{13}C NMR: (75 MHz, CDCl_3) δ 164.21, 159.02, 146.30, 142.10, 136.99, 128.94, 127.88, 127.04, 125.74, 121.66, 75.56, 70.49, 24.87; HRMS (ESI) calculated for $\text{C}_{15}\text{H}_{15}\text{N}_2\text{O}^+$ $[\text{M}+\text{H}]^+$ requires m/z 239.1179, found 239.1175.

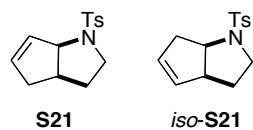
3.4.7. Use of cyclopentenyl deuterated substrate probe

For the synthesis and characterization of the cyclopentenyl substrate probe, please see our previous publication. The catalytic reaction of the cyclopentenyl substrate probe was carried out as described in section II. The products and starting material were isolated using silica chromatography (hexanes/ethyl acetate solvent system). The product mixture was analyzed on a 600 MHz NMR spectrometer to obtain a ratio of the four products (see below).



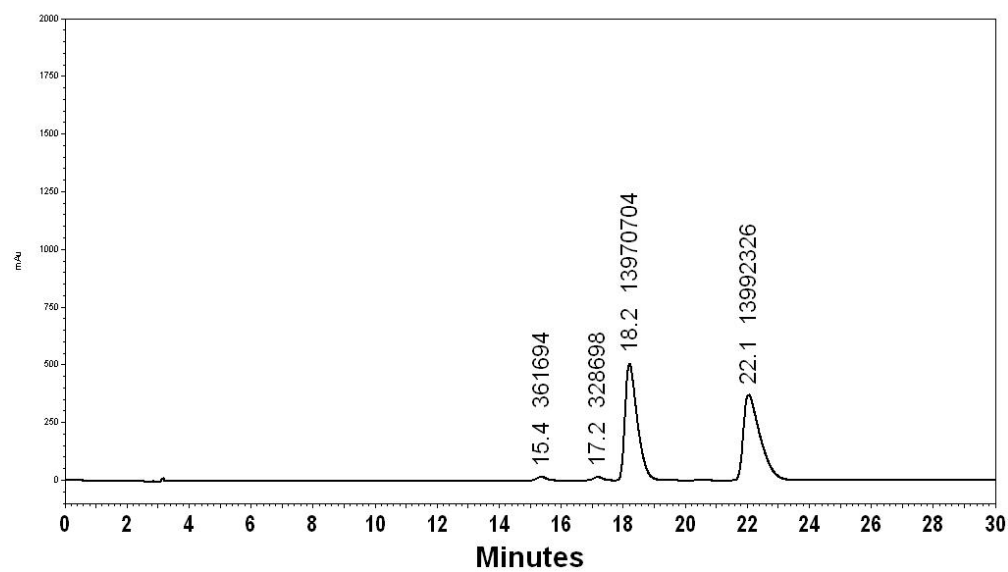
61% yield (¹H NMR yield, 0.075 mmol scale), 27% remaining starting material.





Racemic sample of predominantly **S21** with minor amount of iso-**S21**

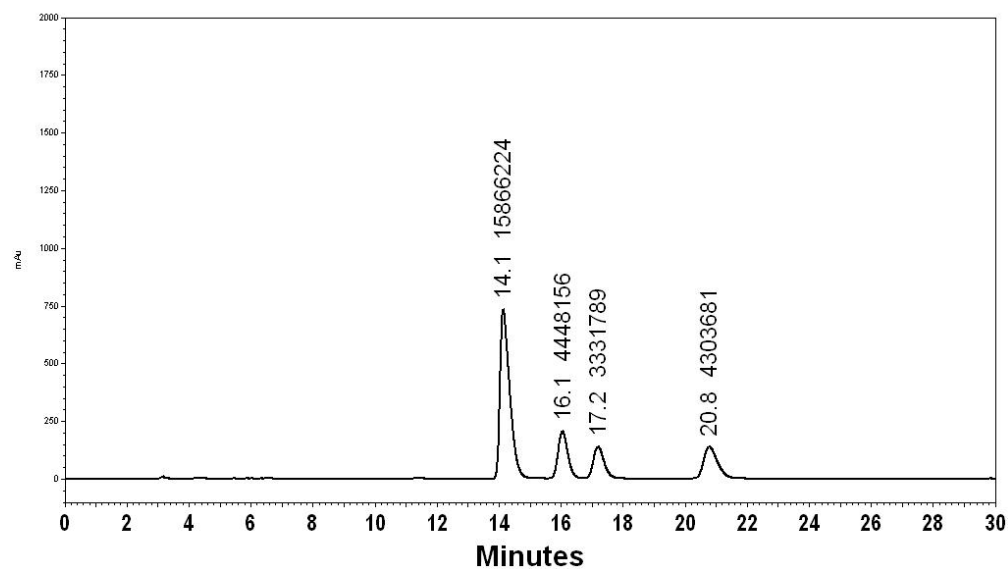
Chiralcel *OJ-H*, 10% iPrOH, 1 ml/min, 230 nm



Product mixture from Scheme 3.3:

13% ee of partially deuterated **S21**, 56% ee of partially deuterated iso-**S21**

Chiralcel *OJ-H*, 10% iPrOH, 1 ml/min, 230 nm



3.5 References and Notes

1. Henry, P. M. in *Palladium Catalyzed Oxidation of Hydrocarbons*, Vol. 2, D. Reidel Publishing Co., Dordrecht, The Netherlands, **1980**.
2. (a) Zeni, G.; Larock, R. C. *Chem. Rev.* **2004**, *104*, 2285–2309. (b) Beccalli, E. M.; Broggini, G.; Martinelli, M.; Sottocornola, S. *Chem. Rev.* **2007**, *107*, 5318–5365. (c) Minatti, A.; Muñiz, K. *Chem. Soc. Rev.* **2007**, *36*, 1142–1152. (d) Kotov, V.; Scarborough, C. C.; Stahl, S. S. *Inorg. Chem.* **2007**, *46*, 1910–1923. (e) Jensen, K. H.; Sigman, M. S. *Org. Biomol. Chem.* **2008**, *6*, 4083–4088.
3. McDonald, R. I.; Liu, G. S.; Stahl, S. S. *Chem. Rev.* **2011**, *111*, 2981–3019.
4. For leading primary references, see: (a) Hosokawa, T.; Uno, T.; Inui, S.; Murahashi, S.-I. *J. Am. Chem. Soc.* **1981**, *103*, 2318–2323. (b) Uozumi, Y.; Kato, K.; Hayashi, T. *J. Am. Chem. Soc.* **1997**, *119*, 5063–5064. (c) Uozumi, Y.; Kato, K.; Hayashi, T. *J. Org. Chem.* **1998**, *63*, 5071–5075. (d) Arai, M. A.; Kuraishi, M.; Arai, T.; Sasai, H. *J. Am. Chem. Soc.* **2001**, *123*, 2907–2908. (e) Trend, R. M.; Ramtohul, Y. K.; Ferreira, E. M.; Stoltz, B. M. *Angew. Chem. Int. Ed.* **2003**, *42*, 2892–2895. (f) Hayashi, T.; Yamasaki, K.; Mimura, M.; Uozumi, Y. *J. Am. Chem. Soc.* **2004**, *126*, 3036–3037. (g) Trend, R. M.; Ramtohul, Y. K.; Stoltz, B. M. *J. Am. Chem. Soc.* **2005**, *127*, 17778–17788. (h) Yip, K.-T.; Yang, M.; Law, K.-L.; Zhu, N.-Y.; Yang, D. *J. Am. Chem. Soc.* **2006**, *128*, 3130–3131. (i) Zhang, Y. J.; Wang, F.; Zhang, W. *J. Org. Chem.* **2007**, *72*, 9208–9213. (j) Tsujihara, T.; Shinohara, T.; Takenaka, K.; Takizawa, S.; Onitsuka, K.; Hatanaka, M.; Sasai, H. *J. Org. Chem.* **2009**, *74*, 9274–9279. (k) He, W.; Yip, K. T.; Zhu, N. Y.; Yang, D. *Org. Lett.* **2009**, *11*, 5626–5628. (l) Scarborough, C. C.; Bergant, A.; Sazama, G. T.; Guzei, I. A.; Spencer, L. C.; Stahl, S. S. *Tetrahedron* **2009**, *65*, 5084–5092. (m) Jiang, F.; Wu, Z.; Zhang, W. *Tetrahedron Lett.* **2010**, *51*, 5124–5126. (n)

-
- Mai, D. N.; Wolfe, J. P. *J. Am. Chem. Soc.* **2010**, *132*, 12157–12159. (o) Jensen, K. H.; Webb, J. D.; Sigman, M. S. *J. Am. Chem. Soc.* **2010**, *132*, 17471–17482. (p) McDonald, R. I.; White, P. B.; Weinstein, A. B.; Tam, C. P.; Stahl, S. S. *Org. Lett.* **2011**, *13*, 2830–2833. (q) Yang, G.; Shen, C.; Zhang, W. *Angew. Chem. Int. Ed.* **2012**, *51*, 9141–9145.
5. For examples of *cis*-nucleopalladation, see the following leading references: 4f,g,k,n and (a) Ney, J. E.; Wolfe, J. P. *Angew. Chem. Int. Ed.* **2004**, *43*, 3605–3608. (b) Hay, M. B.; Wolfe, J. P. *J. Am. Chem. Soc.* **2005**, *127*, 16468–16476. (c) Nakhla, J. S.; Kampf, J. W.; Wolfe, J. P. *J. Am. Chem. Soc.* **2006**, *128*, 2893–2901. (d) Liu, G.; Stahl, S. S. *J. Am. Chem. Soc.* **2007**, *129*, 6328–6335. (e) Muñiz, K.; Hovelmann, C. H.; Streuff, J. *J. Am. Chem. Soc.* **2008**, *130*, 763–773. (f) Michel, B. W.; Steffens, L. D.; Sigman, M. S. *J. Am. Chem. Soc.* **2011**, *133*, 8317–8325.
6. For examples of *trans*-nucleopalladation, see the following leading references: 4g,o, 5c,d and (a) Watson, M. P.; Overman, L. E.; Bergman, R. G. *J. Am. Chem. Soc.* **2007**, *129*, 5031–5044. (b) Cochran, B. M.; Michael, F. E. *J. Am. Chem. Soc.* **2008**, *130*, 2786–2792. (c) Sibbald, P. A.; Rosewall, C. F.; Swartz, R. D.; Michael, F. E. *J. Am. Chem. Soc.* **2009**, *131*, 15945–15951.
7. Quinox and pyrox ligands have emerged as a versatile class of chiral ligands for Pd^{II}-catalyzed reactions with alkenes. For examples other than those described in references 4k,m,o,p and 11, see: (a) Perch, N. S.; Widenhoefer, R. A. *J. Am. Chem. Soc.* **1999**, *121*, 6960–6961. (b) Perch, N. S.; Pei, T.; Widenhoefer, R. A. *J. Org. Chem.* **2000**, *65*, 3836–3845. (c) Zhang, Y.; Sigman, M. S. *J. Am. Chem. Soc.* **2007**, *129*, 3076–3077. (d) Pathak, T. P.; Gligorich, K. M.; Welm, B. E.; Sigman, M. S. *J. Am. Chem. Soc.* **2010**, *132*, 7870–7871. (e) Jana, R.; Pathak, T. P.; Jensen, K. H.; Sigman, M. S. *Org. Lett.* **2012**, *14*, 4074–4077.

-
8. See reference 5d and: Ye, X.; Liu, G.; Popp, B. V.; Stahl, S. S. *J. Org. Chem.* **2011**, *76*, 1031–1044.
 9. Investigation of a well-defined (bipyridine)Pd^{II}–tosylamidate complex provided fundamental insights into alkene insertion into a Pd–N(R)Ts bond (i.e., the *cis*-AP step); see (a) White, P. B.; Stahl, S. S. *J. Am. Chem. Soc.* **2011**, *133*, 18594–18597. For other studies of alkene insertion into Pd–N bonds, see the following leading references: (b) Hanley, P. S.; Hartwig, J. F. *J. Am. Chem. Soc.* **2011**, *133*, 15661–15673. (c) Neukom, J. D.; Perch, N. S.; Wolfe, J. P. *Organometallics* **2011**, *30*, 1269–1277.
 10. Yang and co-workers recently reported a Pd^{II}/quinoline-oxazoline (quinox) catalyst system for enantioselective oxidative cyclization of anilides bearing tethered alkenes, and stereochemical analysis of the products revealed that the reaction involves *cis*-AP of the alkene (see reference 4k).
 11. Further circumstantial evidence supporting a *cis*-AP mechanism comes from the use of quinox and pyrox ligands in other Pd^{II}-catalyzed reactions, such as oxidative Heck reactions, which involve *cis* addition of Pd^{II} and an aryl group across an alkene C=C bond. For *cis*-nucleopalladation reactions employing pyrox/quinox ligands, see reference 4k, 5f, and: Yoo, K. S.; Park, C. P.; Yoon, C. H.; Sakaguchi, S.; O’Neil, J.; Jung, K. W. *Org. Lett.* **2007**, *9*, 3933–3935.
 12. See reference 5d. (–)-Sparteine is a chiral diamine (bidentate) ligand.
 13. Substrate 6-D-1 was synthesized from (*S*)-Mandelic acid in ten steps, with the first five steps having direct precedent in the literature: Alberti, M. N.; Vassilikogiannakis, G.; Orfanopoulos, M. *Org. Lett.* **2008**, *10*, 3997–4000. Derivatization and analysis of an

advanced intermediate established the stereochemical purity of the substrate probe to be very high (>20:1, see Supp. Info. for details).

14. A detailed consideration of how alkene isomerization and deuterium scrambling could complicate our results is provided in the Supp. Info. (Scheme 3.7). However, under all catalyst conditions tested in this study, the *trans*-styrenyl products are obtained in >20:1 selectivity, and it was possible to remove trace quantities of the *cis*-styrenyl products by chromatography prior to further analysis. The extent of deuterium scrambling was characterized by ^2H NMR analysis of the mixture of four products **A-D** (Schemes 3.9-3.14), and only trace quantities ($\leq 5\%$) of deuterium at the C5 position were observed in our experiments.
15. This quantity was corroborated by ESI-MS analysis of the enantiomerically pure products (Schemes 3.9-3.14).
16. The validity of this protocol was tested by subjecting **6-D-1** to the previously reported $\text{Pd}(\text{OAc})_2/\text{pyridine}$ oxidative cyclization conditions. The data arising from this experiment show that the reaction proceeds with very high selectivity for *cis*-AP of the alkene (*trans:cis* = 8:92; see supporting information Scheme 3.9), supporting the previously reported conclusions derived from the use of substrate **3-D-4** as the mechanistic probe (see reference 5d).
17. Cyclization of substrate **6-D-1** with the opposite antipode of the ligand, (*R*)-**3**, resulted in 93% yield, 96% ee, and a 96:4 *trans:cis*-AP ratio (see the supporting information Scheme 3.11). The similar *trans:cis*-AP ratios obtained with ligands (*S*)-**3** and (*R*)-**3** in the reactions of **6-D-1** show that any kinetic isotope effect associated with β -hydride elimination from the C6 position has minimal impact on the AP pathway.

-
18. We previously reported DFT calculations that implicated high enantioselectivity for a *cis*-AP pathway (see ref. 4p). The present results suggest that at least one other *cis*-AP pathway exists that is lower in energy than the one presented in ref. 4p. DFT calculations to explore this issue and to analyze the *trans*-AP mechanism are currently under investigation.
19. For other discussion of factors contributing to *cis*- vs, *trans*-nucleopalladation, see refs. 3, 4g, 5c and the following: Keith, J. A.; Henry, P. M. *Angew. Chem. Int. Ed.* **2009**, *48*, 9038–9049.
20. Steinhoff, B. A.; King, A. E.; Stahl, S. S. *J. Org. Chem.* **2006**, *71*, 1861–1868.
21. Novak, J.; Linhart, I.; Dvorakova, H.; Kubelka, V. *Org. Lett.* **2003**, *5*, 637–639.
22. Angelis, Y. S.; Orfanopoulos, M. *J. Org. Chem.* **1997**, *62*, 6083–6085.
23. Brenzovich, W. E.; Benitez, D.; Lackner, A. D.; Shunatona, H. P.; Tkatchouk, E.; Goddard, W. A.; Toste, D. F. *Angew. Chem. Int. Ed.* **2010**, *49*, 5519–5522.
24. Neustadt, B. R. *Tetrahedron. Lett.* **1994**, *25*, 379–380.
25. Denton, R. M.; Tang, X.; Przeslak, A. *Org. Lett.* **2010**, *12*, 4678–4681.

Chapter 4

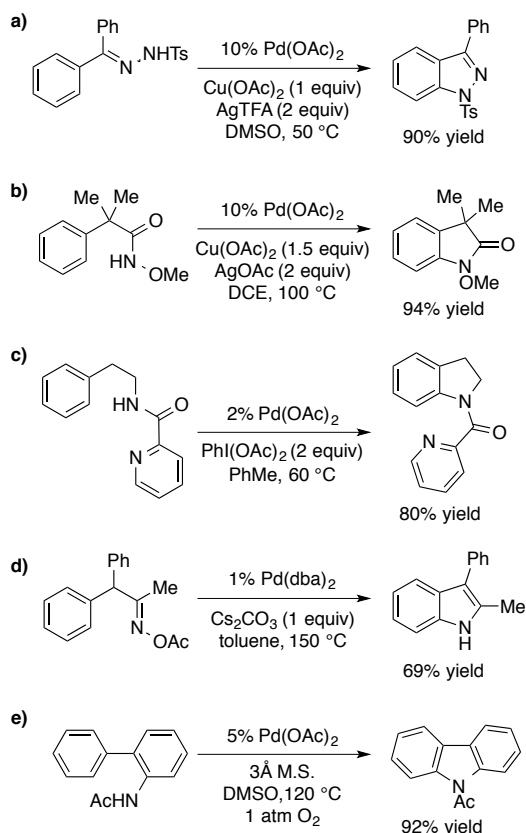
Synthesis of Indole-2-carboxylates via Palladium-Catalyzed Aryl C–H Amination Reactions

This work was done in collaboration with Dr. Stefan Koenig of Genentech

4.1 Introduction

The construction of aryl C–N bonds is of fundamental importance in the synthesis of biologically active organic molecules. Cross coupling reactions between aryl halides and nitrogen nucleophiles in the presence of palladium catalysts (Buchwald-Hartwig coupling) provide an effective means for generating aryl C–N bonds.^{1,2} In the interest of streamlining the synthesis of complex molecules, significant effort has been placed on the development of palladium catalyzed methods for the generation of aryl C–N bonds by the direct, oxidative functionalization of aryl C–H bonds.^{3,4} We have targeted palladium catalyzed intramolecular aryl C–H aminations for the synthesis of nitrogen-containing heterocyclic pharmacophores. A challenge with these reactions is the ability to couple the palladium mediated oxidative transformation of the substrate with molecular oxygen as the clean terminal oxidant.

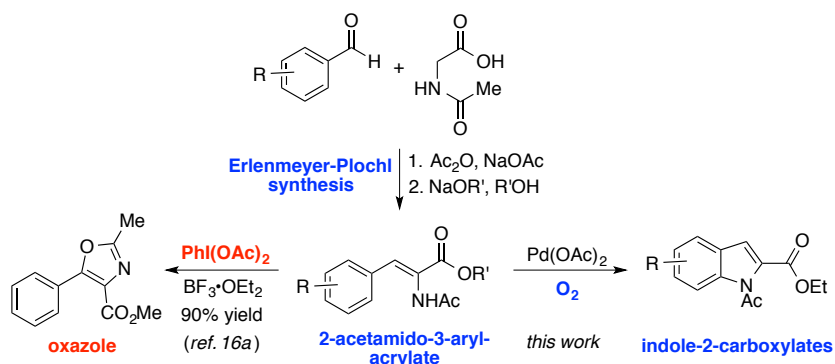
Prior studies in the development of palladium-catalyzed intramolecular aryl C–H aminations⁵ have uncovered methods for the synthesis of indazoles from aryl hydrazones (Scheme 4.1a),⁶ lactams from α -aryl-*N*-methoxyamides (Scheme 4.1b),⁷ indolines from β -arylethylamines (e.g., Scheme 4.1c),^{8,9} indoles from α -aryl oxime acetates (Scheme 4.1d),¹⁰ and carbazoles from 2-aminobiphenyls (e.g., Scheme 4.1e).^{11,12} Notably, the only example in which molecular oxygen was used as the terminal oxidant is for carbazole synthesis, and a limited substrate scope was demonstrated under these conditions (alternative catalyst systems that employ hypervalent iodine^{12b} or oxone^{12c} as the terminal oxidant have also been reported for carbazole synthesis).

Scheme 4.1. Prior examples of intramolecular palladium catalyzed aryl C–H aminations.

Here, we report the discovery of a palladium-catalyzed aerobic amination of aryl C–H bonds for the synthesis of indole-2-carboxylate derivatives. We envisioned that indole-2-carboxylates, which are useful building blocks in the synthesis of indole-containing bioactive molecules,¹³ could be derived from the intramolecular aryl C–H amination of 2-acetamido-3-aryl-acrylates. These substrates are particularly attractive because they are readily accessible from benzaldehyde derivatives and *N*-acetyl glycine via the Erlenmeyer-Plöchl synthesis (Scheme 4.2).¹⁴ The Erlenmeyer-Plöchl synthesis has been used extensively in the synthesis of unnatural amino acids and is amenable to large-scale processes.¹⁵ However, prior reports employing 2-acetamido-3-aryl-acrylate substrates under oxidative coupling conditions have yielded oxazoles from alkene functionalization rather than indoles from aryl C–H amination (e.g., Scheme 4.2, left pathway).¹⁶ We hypothesized that sufficiently mild and selective conditions could be found for

the desired aryl C–H amination by taking advantage of palladium(II) catalysts and molecular oxygen as the oxidant (Scheme 4.2, right pathway).

Scheme 4.2. An aerobic aryl C–H amination reaction for the synthesis of indole-2-carboxylates from readily accessible 2-acetamido-3-aryl-acrylates.

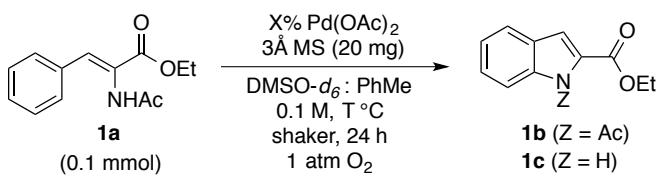


4.2 Results and Discussion

We initiated our study by testing 2-acetamido-3-phenyl-ethylacrylate (substrate **1a**) under the aerobic oxidation conditions reported by Buchwald for carbazole synthesis (Table 4.1, entry 1). This catalyst system employs dimethylsulfoxide as the solvent, which has been shown to lead to stable, catalytically competent nanoclusters of palladium in aerobic oxidation reactions.¹⁷ As a result, carbazole synthesis could be carried out at high temperatures (120 °C). Under these same conditions, substrate **1a** reacts to give a mixture of indole product **1b** and deacetylated indole product **1c** in 45% yield. Control experiments revealed that Brønsted base or acid additives were detrimental to the reaction (not shown), suggesting that hydrolysis of the acetyl group would need to be minimized in order to improve the efficiency of the catalytic C–H amination. Thus, lowering of the temperature and introduction of dry toluene co-solvent was found to improve the yield of indole product **1b** (Table 4.1, entries 2-7). Lowering the loading of palladium catalyst from 10 mol% to 7 mol% was tolerated, but the yield of indole began to drop at 5 mol% of catalyst (Table 4.1, entries 8-9). As expected, introduction of diacetoxyiodobenzene [PhI(OAc)₂], a strong oxidant commonly employed to access Pd^{IV} species,¹⁸ resulted in complete

decomposition of the substrate without formation of the desired indole product (Table 4.1, entry 11).

Table 4.1. Investigation of dimethylsulfoxide-based palladium catalyst systems for intramolecular aerobic C–H amination of 2-acetamido-3-phenyl-ethylacrylate.

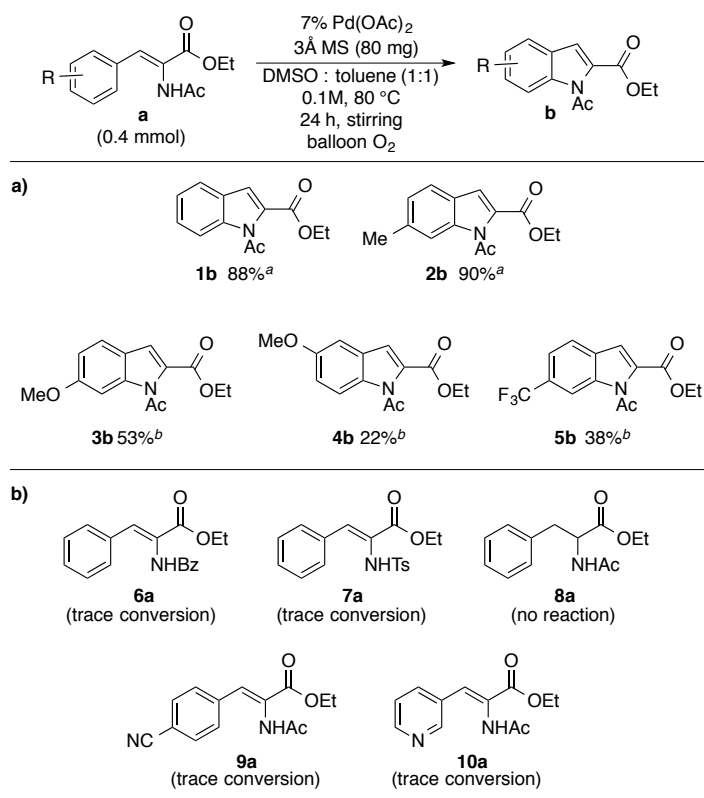
						
entry	mol% Pd(OAc) ₂	DMSO : PhMe	T °C	¹ H NMR Yield ^a		
				% 1a	% 1b	% 1c
1	10	1 : 0	120	45	23	22
2	10	1 : 0	80	16	61	23
3	10	3 : 1	80	10	69	21
4	10	1 : 1	80	2	77	15
5	10	1 : 3	80	2	80	12
6	10	1 : 9	80	31	50	13
7	10	0 : 1	80	80	1	0
8	7	1 : 1	80	5	85	10
9	5	1 : 1	80	35	60	5
10 ^b	7	1 : 1	80	49	36	12
11 ^c	7	1 : 1	80	0	0	0

^a ¹H NMR yields relative to phenyltrimethylsilane added at the end of the reaction time. ^b without 3Å M.S. ^c with 2 equiv PhI(OAc)₂.

With catalyst conditions for the aerobic intramolecular aryl C–H amination of substrate **1a** in hand, we began our efforts toward establishing the scope of the reaction (Table 4.2a). Parent substrate **1a** and methylated substrate **2a** cyclized efficiently using a bench scale setup (round bottomed flask, balloon of O₂). Unfortunately, the catalytic reaction was found to be remarkably sensitive to electronic perturbations on the aromatic ring. Inductive withdrawing groups *meta* to the site of C–H functionalization (substrates **3a** and **5a**) were poorly tolerated, and a donating methoxy-group *para* to the site of C–H functionalization was also poorly tolerated (substrate **4a**). The reason for the sensitivity of this transformation under these conditions is not presently understood, though it is consistent with observations made by Buchwald and coworkers when

lower temperatures were tested for carbazole synthesis.¹¹ Completely ineffective substrates are shown in Table 4.2b.

Table 4.2. a) Preliminary investigation of the scope of intramolecular aerobic C–H amination of 2-acetamido-3-aryl-ethylacrylates. b) Ineffective substrates.



^a Isolated yield. ^b ¹H NMR yield relative to phenyltrimethylsilane added at the end of the reaction time.

To conclude, an aerobic palladium-catalyzed aryl C–H amination strategy for the synthesis of indole-2-carboxylates from 2-acetamido-3-aryl-acrylates was developed, but the transformation was found to be exceptionally sensitive to deviations from the parent substrate. Alternative approaches to aerobic palladium-catalyzed aryl C–H amination reactions will be discussed in chapters 5 and 6.

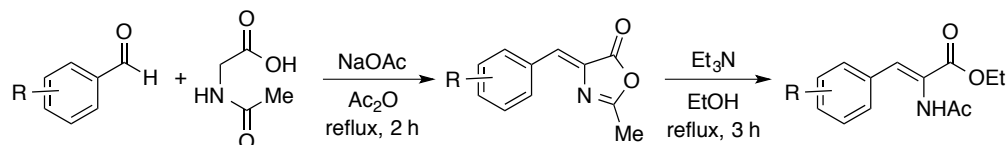
4.3 Experimental Details and Supporting Information

4.3.1. General considerations

All commercially available compounds were purchased and used as received, unless otherwise noted. Toluene was dried over an alumina column prior to use. Dimethylsulfoxide (DMSO) was purchased from Aldrich and stored over molecular sieves. ^1H and ^{13}C NMR spectra were recorded on Bruker 300 MHz, 400 MHz or 500 MHz spectrometers and chemical shifts are given in parts per million relative to internal tetramethylsilane (0.00 ppm for ^1H) or CDCl_3 (77.16 ppm for ^{13}C). Flash chromatography was carried out with SiliaFlash® P60 (Silicycle, particle size 40-63 μm , 230-400 mesh) or by using a CombiFlash Rf® automated chromatography system with reusable high performance silica columns (RediSep® Rf Gold Silica, 20-40 μm spherical particles).

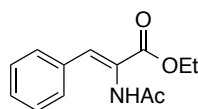
4.3.2. Preparation of 2-acetamido-3-aryl-ethylacrylate substrates

General procedure adapted from literature precedent.^{14,16a}

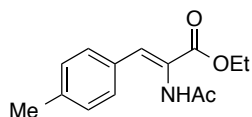


Aldehyde (1 equiv), *N*-acetyl glycine (1 equiv), and sodium acetate (1 equiv) were combined in a round-bottomed flask equipped with a stir bar. Acetic anhydride (5.3 equiv, 2 M) was added and a reflux condenser was equipped. The reaction mixture was heated to reflux for 2 hours and then cooled to room temperature and allowed to stand over night. The solids were broken up with a spatula, washed with water and collected and dried over a Buchner funnel. The solids were transferred to a large round-bottomed flask, suspended in ethanol and concentrated on a rotovap to remove residual water. The solid residue was then suspended in ethanol (0.5 M) and triethylamine (2 equiv) was added via syringe. A reflux condenser and stir bar were equipped,

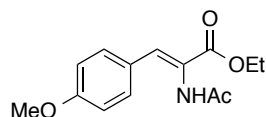
and the reaction mixture was heated to reflux for 3 hours. The reaction mixture was allowed to cool to room temperature and was concentrated to oil on a rotovap. Purification on silica with a hexanes / ethyl acetate solvent system afforded the product as a solid, which could be recrystallized from a minimal amount of hot ethyl acetate and hexanes to afford pale yellow or white needles.



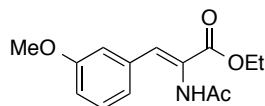
1a: Started with 42.7 mmol of benzaldehyde; obtained 4.1 g of **1a** (41% over two steps). ^1H NMR (400 MHz, CDCl_3) δ 7.70 – 7.29 (m, 6H), 7.03 (s, 1H), 4.31 (q, J = 7.1 Hz, 2H), 2.13 (s, 3H), 1.36 (t, J = 7.1 Hz, 3H).



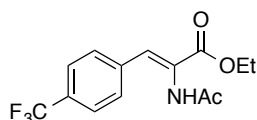
2a: Started with 8.32 mmol of *p*-tolualdehyde; obtained 895 mg of **2a** (44% over two steps). ^1H NMR (400 MHz, CDCl_3) δ 7.55 (m, 1H), 7.37 (d, J = 8.9 Hz, 2H), 7.22 – 7.14 (m, 2H), 6.94 (s, 1H), 4.30 (q, J = 7.1 Hz, 2H), 2.36 (s, 3H), 2.15 (s, 3H), 1.35 (t, J = 7.1 Hz, 3H).



3a: Started with 7.34 mmol of *p*-anisaldehyde; obtained 757 mg of **3a** (39% over two steps). ^1H NMR (400 MHz, CDCl_3) δ 7.64 (m, 1H), 7.49 – 7.37 (m, 2H), 6.98 – 6.81 (m, 3H), 4.29 (q, J = 7.1 Hz, 2H), 3.83 (s, 3H), 2.17 (s, 3H), 1.35 (t, J = 7.1 Hz, 3H).



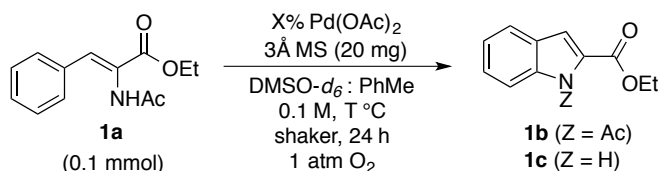
4a: Started with 7.34 mmol of 3-methoxybenzaldehyde; obtained 754 mg of **4a** (39% over two steps). ^1H NMR (400 MHz, CDCl_3) δ 7.41 – 7.28 (m, 2H), 7.12 – 6.82 (m, 3H), 4.31 (q, $J = 7.1$ Hz, 2H), 3.80 (s, 3H), 2.14 (s, 3H), 1.36 (t, $J = 7.1$ Hz, 3H).



5a: Started with 5.74 mmol of 4-(trifluoromethyl)benzaldehyde; obtained 1.187 g of **5a** (69% over two steps). ^1H NMR (500 MHz, CDCl_3) δ 7.61 (d, $J = 8.0$ Hz, 2H), 7.53 (d, $J = 8.6$ Hz, 2H), 7.39 (s, 1H), 7.17 (s, 1H), 4.34 (q, $J = 7.1$ Hz, 2H), 2.14 (s, 3H), 1.37 (t, $J = 7.1$ Hz, 3H).

4.3.3. Preparation of indole-2-carboxylates

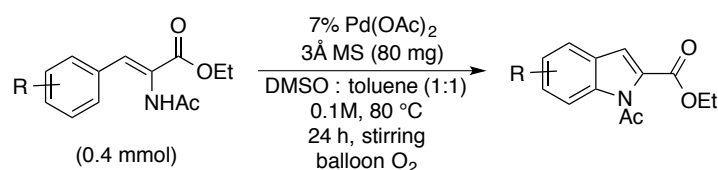
General procedure for screening results obtained in a custom shaker apparatus:



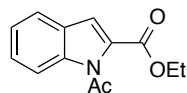
A heavy wall 13x100 mm culture tube was charged with 2-acetamido-3-aryl-ethylacrylate substrate (0.1 mmol) and 20 mg 3Å molecular sieves (note: the molecular sieves were stored on the benchtop). The culture tube was loaded onto a custom 48-well parallel reactor that allowed for heating under a reflux condenser and 1 atm of O_2 with orbital shaking. The reaction vessel was purged with O_2 after being loaded onto the shaker apparatus. A stock solution of $\text{Pd}(\text{OAc})_2$ in $\text{DMSO}-d_6$ (from freshly cracked ampules) was prepared such that the desired amount of

$\text{Pd}(\text{OAc})_2$ and DMSO could be added via syringe. Toluene was added via syringe. The concentration of substrate was 0.1 M in the final volume. The reaction mixtures were heated to the desired temperature and allowed to shake vigorously for 24 hours. The reaction mixtures were allowed to cool to room temperature, removed from the parallel reactor and then diluted with additional $\text{DMSO-}d_6$ spiked with phenyltrimethylsilane. The mixtures were analyzed by ^1H NMR spectroscopy.

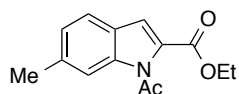
General procedure for yields obtained with a standard bench-top set up:



A 100 ml Schlenk tube was charged with a stir bar and 80 mg of 3Å molecular sieves and flame dried. As the vessel cooled partially, 2-acetamido-3-aryl-ethylacrylate substrate (0.4 mmol) was added in one portion, and the reaction vessel was evacuated and back-filled with O_2 from a balloon three times. Toluene (2 ml) was added via syringe. $\text{Pd}(\text{OAc})_2$ (0.07 equiv, 0.028 mmol, 6.3 mg) was added in a solution of DMSO (2 ml) via syringe. The reaction vessel was submerged in an oil-bath pre-heated to 80 $^\circ\text{C}$ and the mixture was allowed to stir vigorously for 24 hours. The reaction vessel was cooled to room temperature and partitioned between ether and water in a separatory funnel. The aqueous layer was re-extracted with ether two times, and the combined organics were washed with brine, dried over MgSO_4 , concentrated to oil and analyzed by ^1H NMR spectroscopy. Purification on silica using a hexanes : ethyl acetate solvent system afforded the isolated product.



1b: Isolated 81 mg (88%) as a clear oil. ^1H NMR (400 MHz, CDCl_3) δ 8.18 – 8.10 (m, 1H), 7.63 (dt, $J = 8.0, 1.0$ Hz, 1H), 7.45 (ddd, $J = 8.6, 7.2, 1.3$ Hz, 1H), 7.38 – 7.31 (m, 1H), 7.32 – 7.27 (m, 1H), 4.41 (q, $J = 7.1$ Hz, 2H), 2.62 (s, 3H), 1.42 (t, $J = 7.1$ Hz, 3H).



2b: Isolated 89 mg (90%) as a clear oil. ^1H NMR (400 MHz, CDCl_3) δ 7.97 (d, $J = 0.8$ Hz, 1H), 7.50 (d, $J = 8.0$ Hz, 1H), 7.30 (d, $J = 0.9$ Hz, 1H), 7.12 (dd, $J = 8.1, 0.7$ Hz, 1H), 4.39 (q, $J = 7.1$ Hz, 2H), 2.60 (s, 3H), 2.49 (s, 3H), 1.41 (t, $J = 7.1$ Hz, 3H).

4.4 References and Notes

1. (a) Guram, A. S.; Buchwald, S. L. *J. Am. Chem. Soc.* **1994**, *116*, 7901. (b) Paul, F.; Patt, J.; Hartwig, J. F. *J. Am. Chem. Soc.* **1994**, *116*, 5969. (c) Hartwig, J. F. *Angew. Chem. Int. Ed.* **1998**, *37*, 2047. (d) Hartwig, J. F. *Acc. Chem. Res.* **2008**, *41*, 1534. (e) Surry, D. S.; Buchwald, S. L. *Angew. Chem. Int. Ed.* **2008**, *47*, 6338.
2. Copper catalyzed (Goldberg) cross coupling reactions are also prominent. For reviews, see: (a) Kunz, K.; Scholz, U.; Ganzer, D. *Synlett* **2003**, 2428. (b) Chemler, S. R.; Fuller, P. H. *Chem. Soc. Rev.* **2007**, *36*, 1153. (c) Evano, G.; Blanchard, N.; Toumi, M. *Chem. Rev.* **2008**, *108*, 3054. (d) Ma, D. W.; Cai, Q. A. *Acc. Chem. Res.* **2008**, *41*, 1450.
3. For examples of palladium catalyzed intermolecular aryl C-H aminations, see: (a) Thu, H. Y.; Yu, W. Y.; Che, C. M. *J. Am. Chem. Soc.* **2006**, *128*, 9048. (b) Ng, K. H.; Chan, A. S. C.; Yu, W. Y. *J. Am. Chem. Soc.* **2010**, *132*, 12862. (c) Sun, K.; Li, Y.; Xiong, T.; Zhang, J. P.; Zhang, Q. A. *J. Am. Chem. Soc.* **2011**, *133*, 1694. (d) Xiao, B.; Gong, T. J.; Xu, J.; Liu, Z. J.; Liu, L. *J. Am. Chem. Soc.* **2011**, *133*, 1466. (e) Yoo, E. J.; Ma, S.; Mei, T. S.; Chan, K. S. L.; Yu, J. Q. *J. Am. Chem. Soc.* **2011**, *133*, 7652. (f) Shrestha, R.; Mukherjee, P.; Tan, Y. C.; Litman, Z. C.; Hartwig, J. F. *J. Am. Chem. Soc.* **2013**, *135*, 8480. (g) Boursalian, G. B.; Ngai, M. Y.; Hojczyk, K. N.; Ritter, T. *J. Am. Chem. Soc.* **2013**, *135*, 13278.
4. Copper catalyzed aryl C–H amination reactions are also prominent. For leading references, see: (a) Wendlandt, A. E.; Suess, A. M.; Stahl, S. S. *Angew. Chem. Int. Ed.* **2011**, *50*, 11062. (b) Tran, L. D.; Roane, J.; Daugulis, O. *Angew. Chem. Int. Ed.* **2013**, *52*, 6043. (c) Shang, M.; Sun, S. Z.; Dai, H. X.; Yu, J. Q. *J. Am. Chem. Soc.* **2014**, *136*, 3354.

-
5. For a review, see: Mei, T. S.; Kou, L.; Ma, S.; Engle, K. M.; Yu, J. Q. *Synthesis* **2012**, *44*, 1778.
 6. Inamoto, K.; Saito, T.; Katsuno, M.; Sakamoto, T.; Hiroya, K. *Org. Lett.* **2007**, *9*, 2931.
 7. Wasa, M.; Yu, J. Q. *J. Am. Chem. Soc.* **2008**, *130*, 14058.
 8. He, G.; Lu, C. X.; Zhao, Y. S.; Nack, W. A.; Chen, G. *Org. Lett.* **2012**, *14*, 2944.
 9. (a) Mei, T. S.; Wang, X. S.; Yu, J. Q. *J. Am. Chem. Soc.* **2009**, *131*, 10806. (b) Nadres, E. T.; Daugulis, O. *J. Am. Chem. Soc.* **2012**, *134*, 7. (c) Haffemayer, B.; Gulias, M.; Gaunt, M. J. *Chem. Sci.* **2011**, *2*, 312. (d) He, G.; Zhao, Y. S.; Zhang, S. Y.; Lu, C. X.; Chen, G. *J. Am. Chem. Soc.* **2012**, *134*, 3. (e) Mei, T. S.; Leow, D.; Xiao, H.; Laforteza, B. N.; Yu, J. Q. *Org. Lett.* **2013**, *15*, 3058.
 10. Tan, Y. C.; Hartwig, J. F. *J. Am. Chem. Soc.* **2010**, *132*, 3676.
 11. Tsang, W. C. P.; Munday, R. H.; Brasche, G.; Zheng, N.; Buchwald, S. L. *J. Org. Chem.* **2008**, *73*, 7603.
 12. (a) Tsang, W. C. P.; Zheng, N.; Buchwald, S. L. *J. Am. Chem. Soc.* **2005**, *127*, 14560. (b) Jordan-Hore, J. A.; Johansson, C. C. C.; Gulias, M.; Beck, E. M.; Gaunt, M. J. *J. Am. Chem. Soc.* **2008**, *130*, 16184. (c) Youn, S. W.; Bihn, J. H.; Kim, B. S. *Org. Lett.* **2011**, *13*, 3738.
 13. For example, see: (a) Perrault, W. R.; Shephard, K. P.; LaPean, L. A.; Krook, M. A.; Dobrowolski, P. J.; Lyster, M. A.; McMillan, M. W.; Knoechel, D. J.; Evenson, G. N.; Watt, W.; Pearlman, B. A. *Org. Process Res. Dev.* **1997**, *1*, 106. (b) Gan, T.; Liu, R. Y.; Yu, P.; Zhao, S.; Cook, J. M. *J. Org. Chem.* **1997**, *62*, 9298.
 14. Herbst, R. M.; Shemin, D. *Org. Synth.* **1939**, *19*, 1.
 15. (a) Humphrey, C. E.; Furegati, M.; Laumen, K.; La Vecchia, L.; Leutert, T.; Constanze, J.; Muller-Hartwig, D.; Vogtle, M. *Org. Process. Res. Dev.* **2007**, *11*, 1069. (b) Alimardanov,

-
- A.; Nikitenko, A.; Connolly, T. J.; Feigelson, G.; Chan, A. W.; Ding, Z. X.; Ghosh, M.; Shi, X. X.; Ren, J. X.; Hansen, E.; Farr, R.; MacEwan, M.; Tadayon, S.; Springer, D. M.; Kreft, A. F.; Ho, D. M.; Potoski, J. R. *Org. Process. Res. Dev.* **2009**, *13*, 1161. (c) Zhao, H.; Koenig, S. G.; Dankwardt, J. W.; Singh, S. P. *Org. Process. Res. Dev.* **2014**, *18*, 198.
16. (a) Zheng, Y. H.; Li, X. M.; Ren, C. F.; Zhang-Negrerie, D.; Du, Y. F.; Zhao, K. *J. Org. Chem.* **2012**, *77*, 10353. (b) Wendlandt, A. E.; Stahl, S. S. *Org. Biomol. Chem.* **2012**, *10*, 3866.
17. van Benthem, R. A. T. M.; Hiemstra, H.; Vanleeuwen, P. W. N. M.; Geus, J. W.; Speckamp, W. N. *Angew. Chem. Int. Ed.* **1995**, *34*, 457.
18. For a review, see: Deprez, N. R.; Sanford, M. S. *Inorg. Chem.* **2007**, *46*, 1924.

Chapter 5

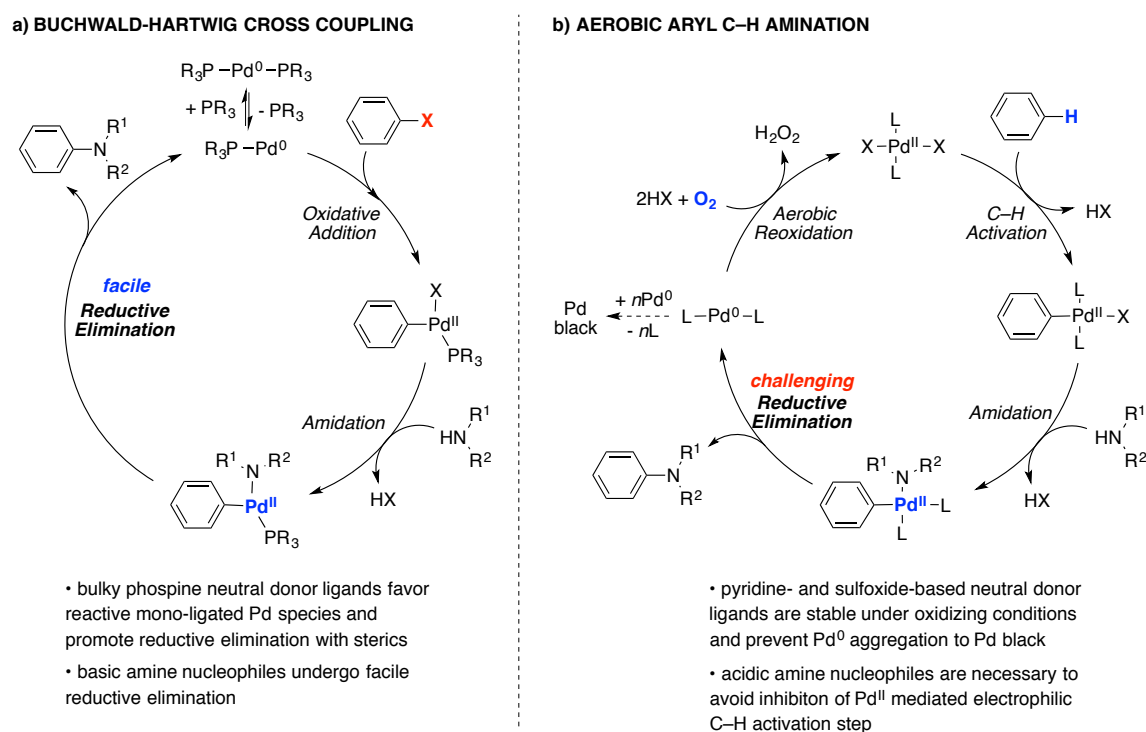
Design of 8-Aryl Quinoline Ligands for Palladium-Catalyzed Aryl C–H Amination Reactions

This work was done in collaboration with undergraduate chemistry student David P. Schuman

5.1 Introduction

Buchwald-Hartwig cross coupling has enjoyed widespread utility in the synthesis of aryl C–N bonds from aryl halides and amines.¹ A major factor in the development of highly efficient palladium catalyst systems has been the identification of bulky phosphine ligands that promote oxidative addition of mono-ligated Pd⁰ species into aryl–halide bonds and reductive elimination of aniline derivatives from L₁Pd^{II}(Ar)(amido) species (Scheme 5.1a).² The desired aerobic, oxidative variations of these amination reactions pose unique challenges (Scheme 5.1b).³

Scheme 5.1. Mechanistic manifolds for Pd^{II}/Pd⁰-catalyzed construction of aryl C–N bonds.



In an oxidative process, the palladium catalyst must effect an aryl C–H activation event in order to generate the requisite Pd–aryl species. This process typically involves an electrophilic Pd^{II} species and a cyclometalation-deprotonation mechanism.⁴ The electron rich, basic amine nucleophiles that are readily employed in Buchwald-Hartwig couplings are not expected to be compatible with electrophilic Pd^{II} mediated C–H activation, as these amines bind strongly to the

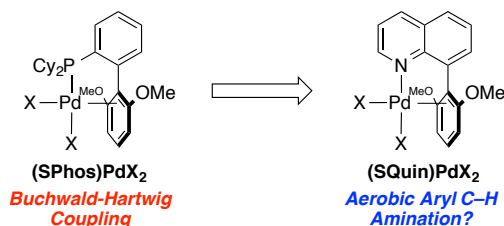
metal and inhibit reactivity.⁵ The electron poor, acidic nitrogen nucleophiles that are expected to be compatible with the C–H activation process will exhibit reduced efficiency in the reductive elimination step, where a more nucleophilic amido ligand facilitates bond formation.⁶ For this reason, we speculate that the dearth in oxidative aryl C–H amination reactions that proceed via Pd^{II}/Pd⁰ catalysis⁷ can be attributed to the difficulty of the reductive elimination step (for a discussion of oxidative aryl C–H amination processes that proceed via high valent Pd^{IV} or Pd^{III} catalysis in the presence of strong terminal oxidant additives, see chapter 6).

An additional challenge in the desired aerobic process is that the reductive elimination step yields a Pd⁰ intermediate that must be stabilized from aggregation to inactive Pd-black prior to reoxidation by molecular oxygen.³ Pyridine- and sulfoxide-based neutral donor ligands are typically used to stabilize Pd⁰ and retain the electrophilic reactivity of Pd^{II}. Unlike strongly donating phosphine ligands, pyridine- and sulfoxide-based neutral donor ligands are stable under aerobic oxidation conditions.

Although the C–H activation and reoxidation events impose important restrictions on the design of catalytic aryl C–H amination reactions, it is noteworthy that reductive elimination from an L_nPd^{II}(Ar)(amido) species is an analogous process in the established Buchwald-Hartwig coupling reactions and the oxidative reactions under development. We propose here that certain design principles used for the development of highly effective phosphine ligands in cross coupling reactions could inspire the design of oxidatively stable (pyridine-based) ligands that promote analogous reductive elimination steps (Scheme 5.2). In particular, bulky biaryl phosphines developed by Buchwald and coworkers have been adopted as practical and effective ligands for the Pd-catalyzed amination of aryl halides (as well as a variety of other traditional cross coupling reactions).⁸ These ligands have been proposed to promote reductive elimination

from $L_1Pd^{II}(Ar)(amido)$ species due to (1) a stabilizing arene-Pd interaction that enforces a *cis* relationship between the aryl and amido ligands,⁹ and (2) steric bulk associated with the biaryl ring and the two alkyl groups on phosphorus.¹⁰ The steric bulk of these ligands pushes the aryl and amido ligands closer together, which lowers the transition state energy of C–N bond formation and leads to a relief in steric strain upon reduction of the palladium coordination number. An exploration of aerobic aryl C–H amination reactivity in the presence of new 8-aryl quinoline ligands that mimic the architecture of biaryl phosphines is presented below.

Scheme 5.2. Design of oxidatively stable 8-aryl-quinoline ligands that mimic the architecture of biaryl phosphine ligands.

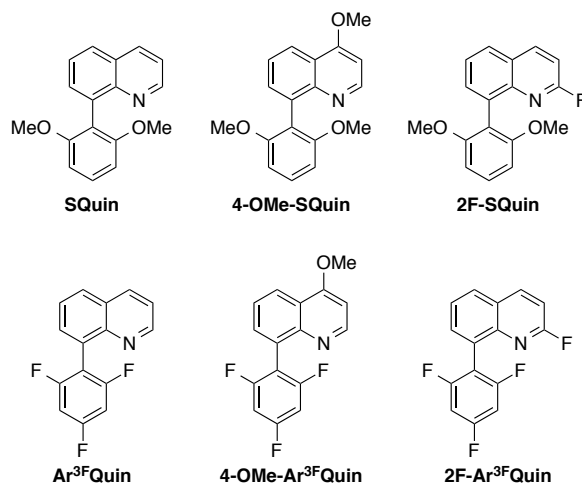


5.2 Results and Discussion

We initiated our studies by synthesizing an electronically diverse array of 8-aryl-quinoline ligand derivatives (Scheme 5.3). To our knowledge, only SQuin (named for its analogy to the popular Buchwald ligand, SPhos) is a previously known molecule, and none of these structures have been utilized as ligands in metal catalyzed processes.¹¹ The SQuin ligand series could be synthesized with Suzuki reactions between the corresponding 8-bromoquinoline and 2,6-dimethoxyphenylboronic acid. The $Ar^{3F}Quin$ ligand series, which features an electron deficient orthoganol aryl ring, was synthesized with Suzuki reactions between the corresponding 8-quinolineboronic acid derivatives and 1-bromo-2,4,6-trifluorobenzene. All of the 8-aryl-quinoline ligands are obtained in good yields and as tractable solids. The 4-methoxy and 2-fluoro substituents on the quinoline ring were chosen to assess a range of neutral donating ability of the

quinoline nitrogen in the catalytic reactions to be tested. This is a critical variable with respect to stabilization of the Pd^0 intermediate or activation of the Pd^{II} species for electrophilic C–H activation and reductive elimination.¹² The electron rich and electron deficient arene rings were chosen to assess the preferred nature of the interaction of the orthogonal arene with the palladium center in the catalytic reactions to be tested.

Scheme 5.3. Palette of electronically diverse 8-aryl-quinoline ligands.



Benzenesulfonyl-protected 2-aminobiphenyl substrate was subjected to a ligand screen under mild conditions (1 mol% $\text{Pd}(\text{OAc})_2$ / in benzene / 60 °C / 1 atm O_2) for carbazole synthesis (Figure 5.1). This substrate was selected based on its established reactivity in the sole example of aerobic aryl C–N bond formation (with 5 mol% $\text{Pd}(\text{OAc})_2$ / in dimethylsulfoxide / 120 °C / 1 atm O_2),^{7a} as well as for the ease of analysis of the product/starting material reaction mixture. Control experiments using no ligand additive, quinoline, 4-methoxypyridine, and 2-fluoropyridine were included to distinguish the potential benefit of the 8-aryl-quinoline architecture in catalysis. 4,5-Diazafluorenone was also included due to its precedent in enabling aerobic allylic acetoxylation reactions¹³ and its intriguing coordination chemistry that is currently under study in our group. The initial screening effort demonstrated that the SQuin and 4-methoxy-SQuin ligands were beneficial to the aerobic aryl C–N bond formation in the synthesis of the benzenesulfonyl-

protected carbazole. Palladium black was not formed under these reactions conditions, so we hypothesized that an increase in temperature might be tolerated. We further speculated the

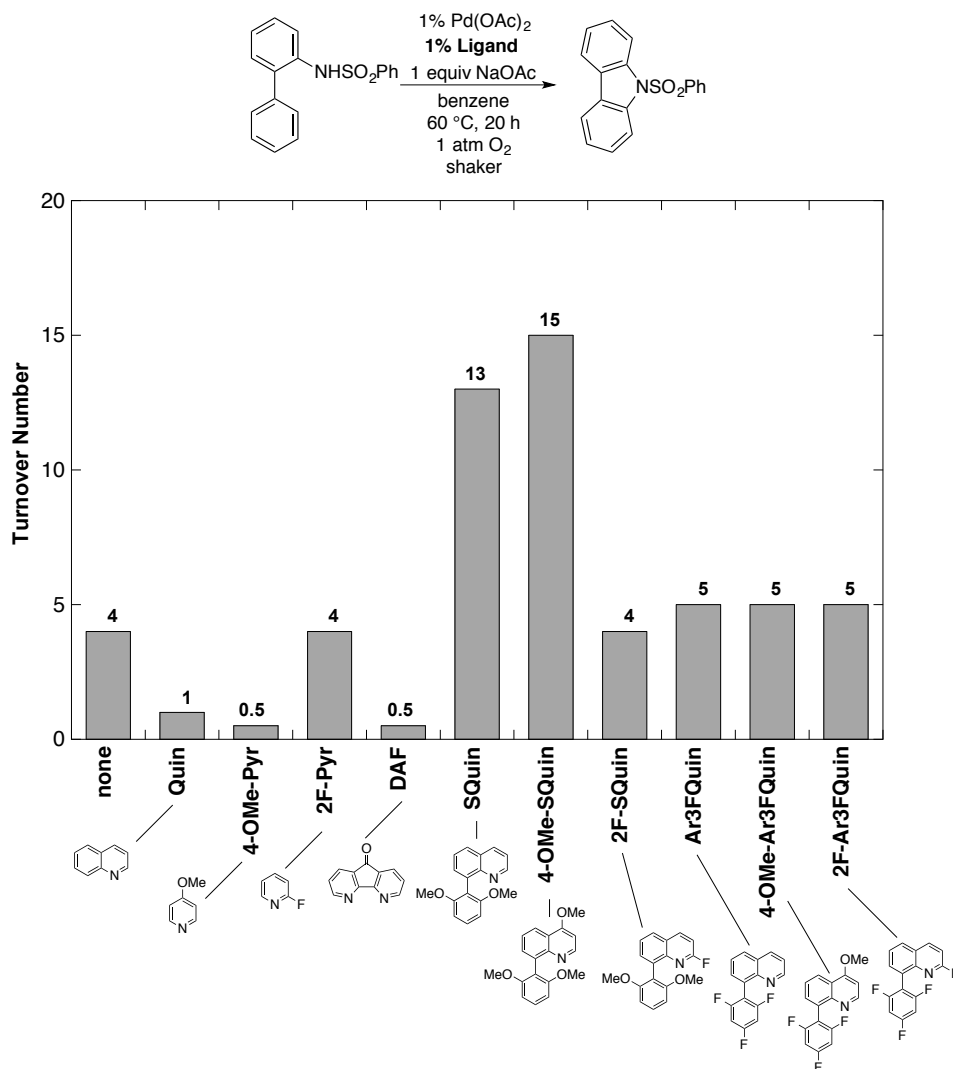


Figure 5.1. Ligand screen for carbazole synthesis (solvent = benzene; temperature = 60 °C). Yield of product was determined by ^1H NMR spectroscopic analysis of the reaction mixture using phenyltrimethylsilane as the internal standard.

proposed interaction between the arene ring on the ligand and the Pd center might be more pronounced in a non-aromatic solvent, so dioxane was selected as a high boiling alternative that has good oxygen solubility. The benzenesulfonyl-protected 2-aminobiphenyl substrate was again subjected to a ligand screen under such conditions (1 mol% Pd(OAc)₂ / in dioxane / 80 °C / 1

atm O₂) for carbazole synthesis (Figure 5.2). The SQuin and 4-methoxy-SQuin ligands had a larger promoting effect under these conditions, and Pd black was noted at the end of the reaction. The presence of inactive Pd black in these catalytic aerobic oxidation reactions is indicative of productive substrate oxidation steps (i.e., C–H activation and reductive elimination) followed by catalyst death associated with inefficient reoxidation of Pd⁰ by molecular oxygen.

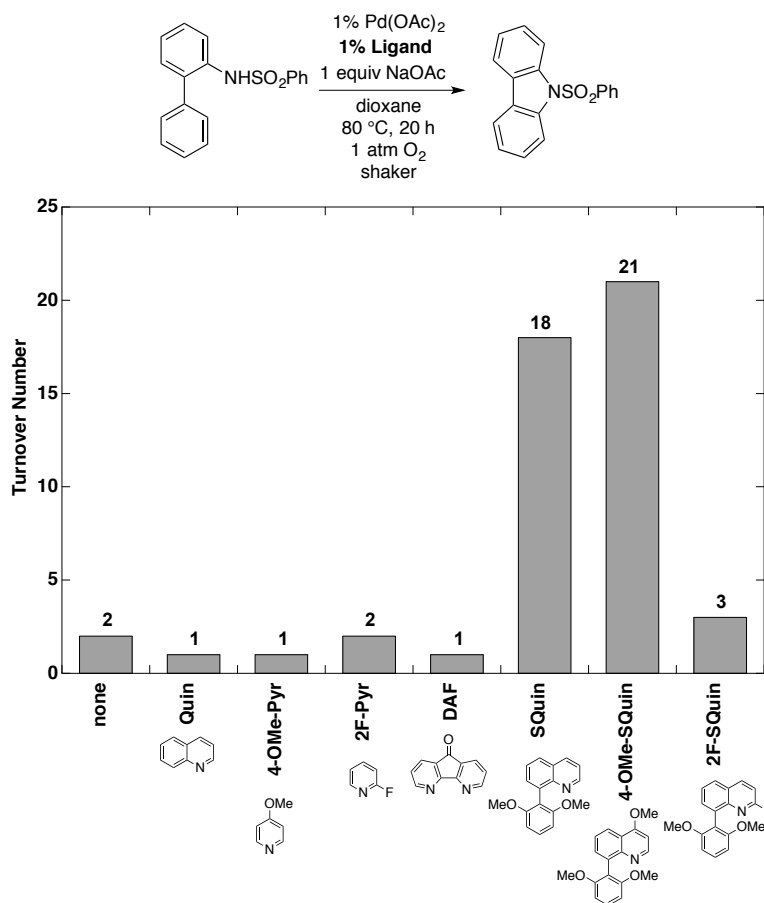
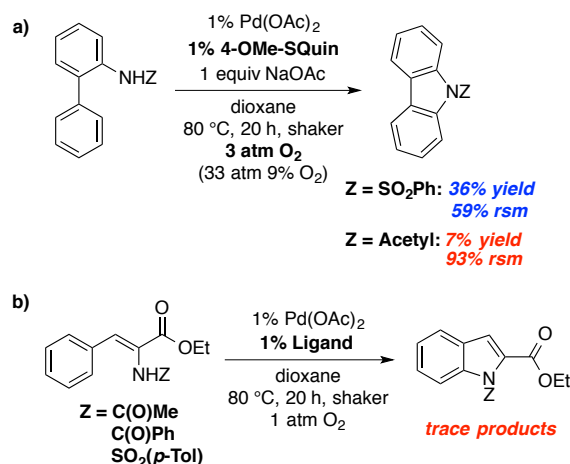


Figure 5.2. Ligand screen for carbazole synthesis (solvent = dioxane; temperature = 80 °C). Yield of product was determined by ¹H NMR spectroscopic analysis of the reaction mixture using phenyltrimethylsilane as the internal standard.

A straightforward solution to this problem, in some cases, is to run the reactions at increased O₂ pressure, which will increase the concentration of O₂ in solution and thus increase the rate of reaction between Pd⁰ and O₂.¹⁴ Although this is not ideal in terms of bench-friendly methods

development, implementation of aerobic oxidation reactions in flow reactors enables highly efficient gas-liquid mixing at elevated O₂ pressure.¹⁵ When the reaction was carried out at approximately 3 atm of O₂ (using 33 atm of 9% O₂ diluted in N₂ to avoid explosion hazards) on a custom shaker apparatus, no palladium black was observed and 36% yield of carbazole was obtained (Scheme 5.4a). This level of efficiency could be maintained with an increase in Pd/ligand loading to 2 mol%, which gave 70% yield of carbazole (not shown). However, changing the protecting group from benzenesulfonyl to acetyl was quite detrimental to the reaction, leading to carbazole product with only seven turnovers of the catalyst. Furthermore, our attempts to apply the 8-aryl-quinoline ligands in the synthesis of indoles from *N*-protected 2-amino-3-phenyl-ethylacrylate substrates (cf. Chapter 4) were met with no success (Scheme 5.4b).

Scheme 5.4. a) Carbazole synthesis with 4-OMe-SQuin ligated Pd^{II} catalyst at elevated oxygen pressure. b) Attempted extension to substrates for indole synthesis failed.



Finally, our attempts to apply these ligands in diverse other reactions, including indole arylation,¹⁶ benzene to biphenyl homocoupling,¹⁷ and allylic amination,¹⁸ were met with limited success (not shown).

To conclude, novel 8-aryl-quinolines were synthesized and tested as ligands in aerobic palladium catalyzed oxidative coupling reactions. The SQuin ligand architecture promoted aryl

C–H amination reaction for the synthesis of carbazoles from benzenesulfonyl-protected 2-aminobiphenyl, but this reactivity did not extend to other substrates for aryl C–H amination. A significant challenge in the discovery of new ligands that promote catalytic reactions is the ability to screen multiple ligands against varied reaction conditions (i.e., metal precursor, solvent, temperature, etc.). Further screening efforts will be necessary in order to determine whether 8-aryl-quinoline ligands might find utility in oxidative coupling reactions.

5.3 Experimental Details and Supporting Information

5.3.1. General considerations

All commercially available compounds were purchased and used as received, unless otherwise noted. Tetrakis(triphenylphosphine)palladium(0) was purchased from Aldrich and stored in a glovebox freezer. ^1H and ^{13}C NMR spectra were recorded on Bruker 400 MHz or 500 MHz spectrometers and chemical shifts are given in parts per million relative to internal tetramethylsilane (0.00 ppm for ^1H) or CDCl_3 (77.16 ppm for ^{13}C). Flash chromatography was carried out with SiliaFlash® P60 (Silicycle, particle size 40-63 μm , 230-400 mesh) or by using a CombiFlash Rf® automated chromatography system with reusable high performance silica columns (RediSep® Rf Gold Silica, 20-40 μm spherical particles).

5.3.2. General procedures for reaction screening

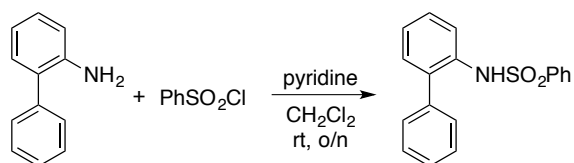
Reactions carried out at 1 atm of O_2 in a custom shaker apparatus:

A heavy wall 13x100 mm culture tube was charged with substrate (0.05 mmol) and other solid additives, such as sodium acetate, as desired. Separate stock solutions of $\text{Pd}(\text{OAc})_2$ and ligand were prepared such that the correct quantity of each (1-5 mol%) could be delivered and the total volume would reach 0.5 ml (0.1 M). The culture tube was loaded onto a custom 48-well parallel reactor that allowed for heating under a reflux condenser and 1 atm of O_2 with orbital shaking. The reaction vessel was purged with O_2 after being loaded onto the shaker apparatus. The reaction mixtures were heated to the desired temperature and allowed to shake vigorously. At the desired time point, the reaction mixtures were allowed to cool to room temperature, removed from the parallel reactor and concentrated to oil. The mixtures were analyzed by ^1H NMR spectroscopy using CDCl_3 spiked with phenyltrimethylsilane as the internal standard.

Reactions carried out at elevated O₂ pressure in a custom shaker apparatus (CAT-24):

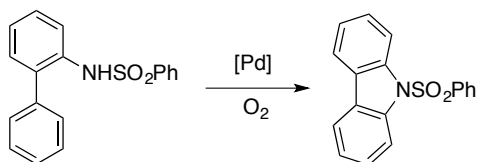
A heavy wall 10x75 mm culture tube was charged with substrate (0.05 mmol) and other solid additives, such as sodium acetate, as desired. Separate stock solutions of Pd(OAc)₂ and ligand were prepared such that the correct quantity of each (1-5 mol%) could be delivered and the total volume would reach 0.5 ml (0.1 M). The culture tube was loaded into a 24-well Parr bomb equipped with cold fingers on the roof of the reactor and sealed. The bomb was secured on a shaker apparatus that allowed for heating and orbital agitation. The bomb was pressurized with 9% O₂ diluted in N₂ such that the desired partial pressure of O₂ was established (*note: the use of diluted O₂ is a critical safety precaution for high pressure aerobic oxidation reactions*). The bomb was heated to the desired temperature with shaking. At the desired time point, the bomb was allowed to cool to room temperature, vented carefully, and reaction tubes were removed from the bomb. The reaction mixtures were concentrated to oil and analyzed by ¹H NMR spectroscopy using CDCl₃ spiked with phenyltrimethylsilane as the internal standard.

5.3.3. Benzenesulfonyl-protected 2-aminobiphenyl and carbazole



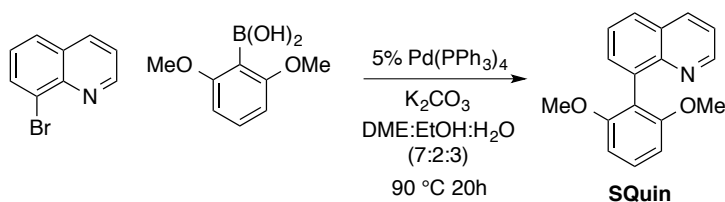
N-Benzenesulfonyl-2-aminobiphenyl: A 250 ml round-bottomed flask was charged with 2-aminobiphenyl (1.5 g, 8.86 mmol, 1 equiv) and dissolved in 88 ml of dichloromethane (0.1 M). Pyridine (3.58 ml, 44.3 mmol, 5 equiv) and benzenesulfonyl chloride (1.71 ml, 13.3 mmol, 1.5 equiv) were added via syringe. The reaction mixture was allowed to stir under air for 16 hours. The reaction mixture was diluted with dichloromethane, washed 3x with water, dried over MgSO₄ and concentrated. Purification on silica with hexanes : ethyl acetate (4:1) afforded the

product (2.51 g, 93%) as an off-white solid. ^1H NMR (400 MHz, CDCl_3) δ 7.73 (dd, $J = 8.3, 1.2$ Hz, 1H), 7.61 – 7.51 (m, 3H), 7.45 – 7.29 (m, 6H), 7.16 (td, $J = 7.5, 1.2$ Hz, 1H), 7.09 (dd, $J = 7.6, 1.7$ Hz, 1H), 6.81 (dd, $J = 7.7, 1.8$ Hz, 2H), 6.58 (s, 1H).



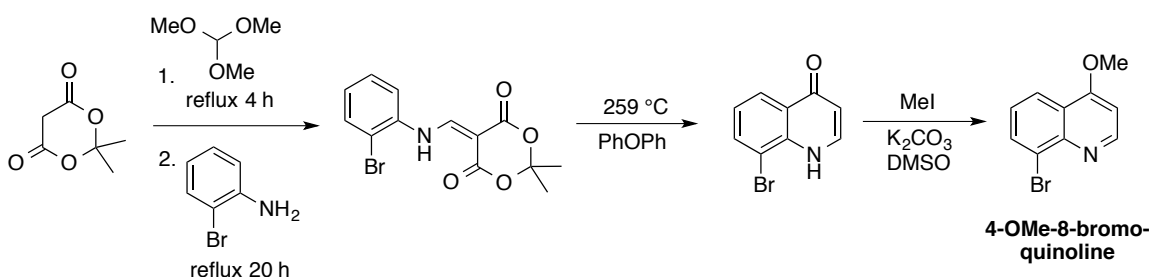
N-Benzenesulfonyl-carbazole: The carbazole was obtained from the palladium catalyzed aerobic oxidation reactions and was isolated as a white solid with purification on silica using a hexanes : ethyl acetate solvent system (5:1). ^1H NMR (400 MHz, CDCl_3) δ 8.34 (dt, $J = 8.5, 0.8$ Hz, 2H), 7.91 (dt, $J = 7.7, 1.0$ Hz, 2H), 7.82 (dd, $J = 8.4, 1.3$ Hz, 2H), 7.50 (ddd, $J = 8.6, 7.4, 1.3$ Hz, 2H), 7.47 – 7.42 (m, 1H), 7.37 (td, $J = 7.5, 1.0$ Hz, 2H), 7.32 (t, $J = 7.9$ Hz, 2H).

5.3.4. Synthesis of 8-aryl-quinoline ligands



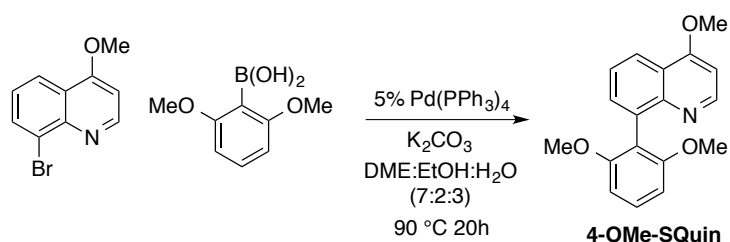
SQuin: A 100 ml Schlenk tube was charged with a stir bar, 2,6-dimethoxyphenylboronic acid (983 mg, 5.4 mmol, 1.5 equiv), tetrakis(triphenylphosphine)palladium(0) (208 mg, 0.18 mmol, 0.05 equiv), and potassium carbonate (1.49 g, 10.8 mmol, 3 equiv). The reaction vessel was evacuated and back-filled with N_2 three times. 8-Bromoquinoline (750 mg, 3.6 mmol, 1 equiv) was added in a solution of 7 ml of 1,2-dimethoxyethane via syringe. Ethanol (2 ml) and water (3 ml) were added via syringe. The reaction vessel was heated to 90 °C and stirred for 22 hours.

The reaction vessel was allowed to cool to room temperature and was diluted with chloroform and washed with water in a separatory funnel. The organic layer was dried over MgSO_4 and concentrated to solid. Purification over silica with a hexanes : ethyl acetate solvent system (10-60% ethyl acetate gradient) afforded the product (904 mg, 95%) as a white crystalline solid. ^1H NMR (400 MHz, CDCl_3) δ 8.87 (dd, $J = 4.2, 1.8$ Hz, 1H), 8.16 (dd, $J = 8.3, 1.8$ Hz, 1H), 7.82 (dd, $J = 6.9, 2.7$ Hz, 1H), 7.68 – 7.53 (m, 2H), 7.43 – 7.29 (m, 2H), 6.73 (d, $J = 8.4$ Hz, 2H), 3.65 (s, 6H).



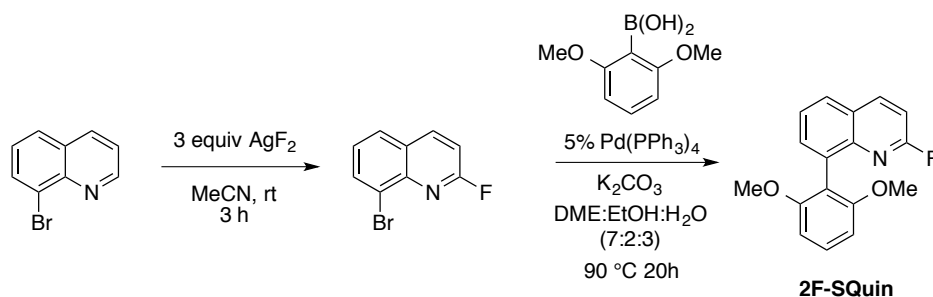
4-OMe-8-bromoquinoline: A 200 ml pear-shaped flask was charged with a stir bar and Meldrum's acid (5.77 g, 40 mmol, 1.6 equiv). Trimethylorthoformate (76 ml, 695 mmol, 27.8 equiv, 0.33 M) was added and a reflux condenser was equipped. The reaction mixture was heated to reflux for 4 hours, and then 2-bromoaniline (2.83 ml, 25 mmol, 1 equiv) was added via syringe and reflux was continued for 20 hours. The reaction mixture was cooled to room temperature and concentrated to dark oil. The oil was triturated in ether and the green solids were collected over a Buchner funnel and rinsed with ether. The crude solid (4.994 g, 61%) was carried on to the next reaction in a 200 ml pear-shaped round-bottomed flask equipped with a stir bar. Diphenyl ether (35 ml, 0.43 M) was added and a reflux condenser was equipped. The reaction vessel was heated to 259 °C (reflux) in a sand bath for 4 hours with stirring. The reaction vessel was allowed to cool to room temperature, and diethyl ether was added to

precipitate the product. The majority of the liquids were decanted and then the solids were collected over a Buchner funnel. The product (2.13 g, 73 weight % in PhOPh, 62%) was carried on to the next reaction in a 500 ml 3-neck round-bottomed flask equipped with a stir bar. Potassium carbonate (1.97 g, 14.3 mmol, 1.5 equiv) was added followed by dimethylsulfoxide (150 ml, 0.06 M). A reflux condenser was equipped and the reaction vessel was heated to 70 °C for 1 hour under nitrogen. The reaction vessel was cooled to 35 °C and methyl iodide (1.2 ml, 19 mmol, 2 equiv) was added via syringe and allowed to stir for 2 hours. The reaction mixture was allowed to cool to room temperature and then poured into 1 L of water. The aqueous mixture was extracted 2x with ether and 2x with dichloromethane. The combined organics were concentrated partially, washed with brine, dried over MgSO₄ and then concentrated to oil. Purification on silica using a hexanes : ethyl acetate solvent system (20-100% ethyl acetate gradient) gave the product (1.677 g, 74%) as a yellow solid. The yield was 28% over 3 steps from 8-bromoquinoline. ¹H NMR (500 MHz, CDCl₃) δ 8.89 (d, *J* = 5.1 Hz, 1H), 8.20 (dd, *J* = 8.3, 1.3 Hz, 1H), 8.04 (dd, *J* = 7.4, 1.4 Hz, 1H), 7.35 (dd, *J* = 8.4, 7.4 Hz, 1H), 6.81 (d, *J* = 5.2 Hz, 1H), 4.07 (s, 3H).



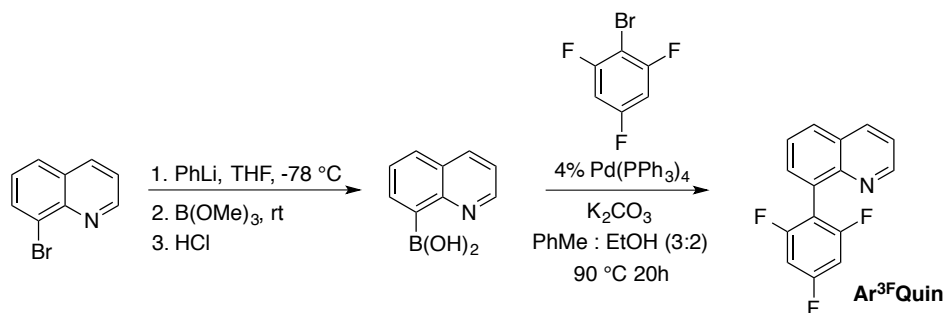
4-OMe-SQuin: A 50 ml Schlenk tube was charged with a stir bar, 4-methoxy-8-bromoquinoline (500 mg, 2.1 mmol, 1 equiv), 2,6-dimethoxyphenylboronic acid (573 mg, 3.15 mmol, 1.5 equiv), tetrakis(triphenylphosphine)palladium(0) (121 mg, 0.105 mmol, 0.05 equiv), and potassium carbonate (871 mg, 6.3 mmol, 3 equiv). The reaction vessel was evacuated and back-filled with

nitrogen. 1,2-Dimethoxyethane (4.1 ml), ethanol (1.2 ml) and water (1.8 ml) were added via syringe and the reaction mixture was heated to 90 °C with stirring for 22 hours. The reaction vessel was allowed to cool to room temperature and was diluted with chloroform and washed with water in a separatory funnel. The organic layer was dried over MgSO_4 and concentrated to solid. Purification over silica with a hexanes : ethyl acetate solvent system (10-70% ethyl acetate gradient) afforded the product (498 mg, 80%) as a white crystalline solid. ^1H NMR (400 MHz, CDCl_3) δ 8.71 (d, J = 5.1 Hz, 1H), 8.23 (dd, J = 7.8, 2.1 Hz, 1H), 7.64 – 7.49 (m, 2H), 7.35 (t, J = 8.4 Hz, 1H), 6.78 – 6.64 (m, 3H), 4.04 (s, 3H), 3.65 (s, 6H).



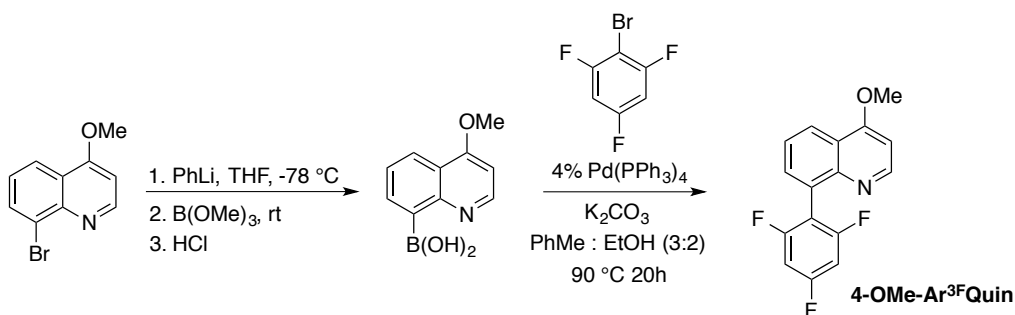
2F-Squin: The procedure for fluorination of 8-bromoquinoline was adapted from literature precedence.¹⁹ A 250 ml round-bottomed flask was charged with a stir bar and 8-bromoquinoline (416 mg, 2 mmol, 1 equiv). Acetonitrile (80 ml, 0.025 M) was added, followed by silver(II)difluoride (875 mg, 6 mmol, 3 equiv) in one portion. The reaction mixture was stirred at room temperature under nitrogen for 3 hours, and then was partitioned between ether and saturated aqueous sodium bicarbonate. The ether layer was washed with brine, dried over MgSO_4 , and concentrated. Purification on silica with a hexanes : ethyl acetate solvent system (9:1) afforded the product (187 mg, 41%) as a white crystalline solid. Characterization data matched the literature precedent, and the material was carried forward. A 25 ml Schlenk tube was charged with a stir bar, 2-fluoro-8-bromoquinoline (187 mg, 0.827 mmol, 1 equiv), 2,6-

dimethoxyphenylboronic acid (226 mg, 1.24 mmol, 1.5 equiv), tetrakis(triphenylphosphine) palladium(0) (48 mg, 0.041 mmol, 0.05 equiv), and potassium carbonate (343 mg, 2.48 mmol, 3 equiv). The reaction vessel was evacuated and back-filled with nitrogen. 1,2-Dimethoxyethane (1.75 ml), ethanol (0.5 ml) and water (0.75 ml) were added via syringe and the reaction mixture was heated to 90 °C with stirring for 22 hours. The reaction vessel was allowed to cool to room temperature and was diluted with chloroform and washed with water in a separatory funnel. The organic layer was dried over MgSO₄ and concentrated to solid. Purification over silica with a hexanes : ethyl acetate solvent system (5-25% ethyl acetate gradient) afforded the product (211 mg, 90%) as a white crystalline solid. ¹H NMR (400 MHz, CDCl₃) δ 8.25 (t, *J* = 8.5 Hz, 1H), 7.83 (dd, *J* = 8.1, 1.6 Hz, 1H), 7.66 (dd, *J* = 7.0, 1.4 Hz, 1H), 7.59 (t, *J* = 7.6 Hz, 1H), 7.36 (t, *J* = 8.4 Hz, 1H), 7.02 (dd, *J* = 8.7, 3.1 Hz, 1H), 6.72 (d, *J* = 8.4 Hz, 2H), 3.67 (s, 6H).

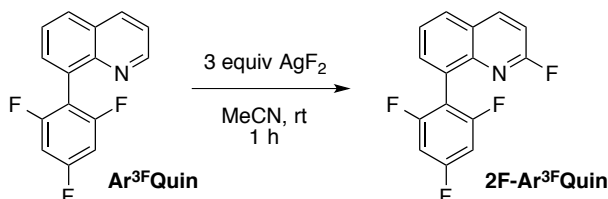


Ar^{3F}Quin: A 100 ml round-bottomed flask was charged with a stir bar and 8-bromoquinoline (2 g, 9.61 mmol, 1 equiv). The reaction vessel was evacuated and back-filled with nitrogen, and dry THF (38 ml, 0.25 M) was added via syringe. The reaction vessel was cooled to -78 °C and phenyllithium (1.2 M in di-*n*-butyl ether, 8.41 ml, 10.1 mmol, 1.05 equiv) was added dropwise over 5 minutes via syringe. The reaction mixture was stirred for 1 hour at -78 °C, and then trimethylborate (4.29 ml, 38.4 mmol, 4 equiv) was added slowly via syringe. The reaction mixture was allowed to stir for 15 minutes at -78 °C, and then for 3.5 hours at room temperature.

Approximately 45 ml of 3M HCl were added, and then the aqueous layer was transferred to a separatory funnel and washed with approximately 90 ml of ether. The aqueous layer was collected in an Erlenmeyer and neutralized with approximately 45 ml of 10% NaOH. The crude precipitate was allowed to stand over night, and then the solids were collected over a Buchner funnel, taken up in hot acetone and precipitated with hexanes. An off-white powder (1.33 g, 80%) was obtained and carried on to the Suzuki reaction. A 100 ml Schlenk tube was charged with a stir bar, 8-quinolineboronic acid (400 mg, 2.31 mmol, 1 equiv), tetrakis(triphenylphosphine)palladium(0) (107 mg, 0.924 mmol, 0.04 equiv), and potassium carbonate (1.6 g, 11.6 mmol, 5 equiv). The reaction vessel was evacuated and back-filled with nitrogen. Toluene (7.5 ml, 0.3 M), ethanol (5 ml, 0.45 M) and 1-bromo-2,4,6-trifluorobenzene (0.41 ml, 3.47 mmol, 1.5 equiv) were added via syringe. The reaction vessel was heated to reflux (80-90 °C) for 22 hours. The reaction mixture was cooled to room temperature, filtered over celite (eluting ethyl acetate), and concentrated to oil. Purification over silica using a hexanes : ethyl acetate solvent system (0-20% ethyl acetate in hexanes) gave the product (420 mg, 70%) as a solid. ¹H NMR (400 MHz, CDCl₃) δ 8.92 (dd, *J* = 4.2, 1.7 Hz, 1H), 8.22 (dd, *J* = 8.3, 1.8 Hz, 1H), 7.93 (dd, *J* = 8.1, 1.5 Hz, 1H), 7.75 – 7.68 (m, 1H), 7.64 (dd, *J* = 8.1, 7.1 Hz, 1H), 7.44 (dd, *J* = 8.3, 4.2 Hz, 1H), 6.82 (dd, *J* = 8.9, 7.2 Hz, 2H).



4-OMe-Ar^{3F}Quin: A 100 ml round-bottomed flask was charged with a stir bar and 4-methoxy-8-bromoquinoline (686 mg, 2.88 mmol, 1 equiv). The reaction vessel was evacuated and back-filled with nitrogen, and dry THF (11.5 ml, 0.25 M) was added via syringe. The reaction vessel was cooled to -78 °C and phenyllithium (1.2 M in di-*n*-butyl ether, 2.53 ml, 3.03 mmol, 1.05 equiv) was added dropwise over 5 minutes via syringe. The reaction mixture was stirred for 1 hour at -78 °C, and then trimethylborate (1.28 ml, 11.5 mmol, 4 equiv) was added slowly via syringe. The reaction mixture was allowed to stir for 15 minutes at -78 °C, and then for 3.5 hours at room temperature. Approximately 15 ml of 3M HCl were added, and then the aqueous layer was transferred to a separatory funnel and washed with approximately 30 ml of ether. The aqueous layer was collected in an Erlenmeyer and neutralized with approximately 15 ml of 10% NaOH. The crude precipitate was allowed to stand over night, and then the solids were collected over a Buchner funnel, taken up in hot acetone and precipitated with hexanes. A pink powder was obtained and carried on to the Suzuki reaction. A 100 ml Schlenk tube was charged with a stir bar, 4-methoxy-8-quinolineboronic acid (378 mg, 1.86 mmol, 1 equiv), tetrakis(triphenylphosphine)palladium(0) (86 mg, 0.074 mmol, 0.04 equiv), and potassium carbonate (1.29 g, 9.3 mmol, 5 equiv). The reaction vessel was evacuated and back-filled with nitrogen. Toluene (6 ml, 0.3 M), ethanol (4 ml, 0.45 M) and 1-bromo-2,4,6-trifluorobenzene (0.33 ml, 2.79 mmol, 1.5 equiv) were added via syringe. The reaction vessel was heated to reflux (80-90 °C) for 22 hours. The reaction mixture was cooled to room temperature, filtered over



2F-Ar^{3F}Quin: The procedure was based on related literature precedence.¹⁹ A 100 ml round-bottomed flask was charged with a stir bar and Ar^{3F}Quin (52 mg, 0.2 mmol, 1 equiv) Acetonitrile (8 ml, 0.025 M) was added, followed by silver(II)difluoride (88 mg, 0.6 mmol, 3 equiv) in one portion. The reaction mixture was stirred at room temperature under nitrogen for 1 hour, and then was partitioned between ether and saturated aqueous sodium bicarbonate. The ether layer was washed with brine, dried over MgSO₄, and concentrated. Purification on silica with a hexanes : ethyl acetate solvent system afforded the product (19 mg, 34%) as a white solid.

¹H NMR (400 MHz, CDCl₃) δ 8.31 (t, *J* = 8.4 Hz, 1H), 7.94 (dd, *J* = 8.2, 1.5 Hz, 1H), 7.74 (dd, *J* = 6.9, 1.4 Hz, 1H), 7.63 (t, *J* = 7.7 Hz, 1H), 7.11 (dd, *J* = 8.8, 3.0 Hz, 1H), 6.90 – 6.74 (m, 2H).

5.4 References and Notes

1. (a) Guram, A. S.; Buchwald, S. L. *J. Am. Chem. Soc.* **1994**, *116*, 7901. (b) Paul, F.; Patt, J.; Hartwig, J. F. *J. Am. Chem. Soc.* **1994**, *116*, 5969. (c) Hartwig, J. F. *Angew. Chem. Int. Ed.* **1998**, *37*, 2047.
2. (a) Surry, D. S.; Buchwald, S. L. *Angew. Chem. Int. Ed.* **2008**, *47*, 6338. (b) Hartwig, J. F. *Acc. Chem. Res.* **2008**, *41*, 1534.
3. (a) Campbell, A. N.; Stahl, S. S. *Acc. Chem. Res.* **2012**, *45*, 851. (b) Gligorich, K. M.; Sigman, M. S. *Chem. Commun.* **2009**, 3854. (c) Stahl, S. S. *Angew. Chem. Int. Ed.* **2004**, *43*, 3400.
4. (a) Davies, D. L.; Donald, S. M. A.; Macgregor, S. A. *J. Am. Chem. Soc.* **2005**, *127*, 13754. (b) Lafrance, M.; Gorelsky, S. I.; Fagnou, K. *J. Am. Chem. Soc.* **2007**, *129*, 14570. (c) Gorelsky, S. I.; Lapointe, D.; Fagnou, K. *J. Am. Chem. Soc.* **2008**, *130*, 10848.
5. Engle, K. M.; Mei, T. S.; Wasa, M.; Yu, J. Q. *Acc. Chem. Res.* **2012**, *45*, 788.
6. (a) Driver, M. S.; Hartwig, J. F. *J. Am. Chem. Soc.* **1995**, *117*, 4708. (b) Driver, M. S.; Hartwig, J. F. *J. Am. Chem. Soc.* **1997**, *119*, 8232. (c) Yamashita, M.; Vicario, J. V. C.; Hartwig, J. F. *J. Am. Chem. Soc.* **2003**, *125*, 16347. (e) Hartwig, J. F. *Inorg. Chem.* **2007**, *46*, 1936.
7. To our knowledge, only two examples exist: (a) Tsang, W. C. P.; Munday, R. H.; Brasche, G.; Zheng, N.; Buchwald, S. L. *J. Org. Chem.* **2008**, *73*, 7603. (b) Tan, Y. C.; Hartwig, J. F. *J. Am. Chem. Soc.* **2010**, *132*, 3676.
8. See ref. 2a and: Martin, R.; Buchwald, S. L. *Acc. Chem. Res.* **2008**, *41*, 1461.
9. Barder, T. E.; Buchwald, S. L. *J. Am. Chem. Soc.* **2007**, *129*, 12003.

-
10. See ref. 9 and: (a) Yamashita, M.; Hartwig, J. F. *J. Am. Chem. Soc.* **2004**, *126*, 5344. (b) Fujita, K.; Yamashita, M.; Puschmann, F.; Alvarez-Falcon, M. M.; Incarvito, C. D.; Hartwig, J. F. *J. Am. Chem. Soc.* **2006**, *128*, 9044.
11. For thought provoking studies on the coordination chemistry and reactivity of platinum(II) with 1,2,4,5-tetrakis(quinolin-8-yl)benzene ligands, see: Tan, R.; Jia, P.; Rao, Y.; Jia, W.; Hadzovic, A.; Yu, Q.; Li, X.; Song, D. *Organometallics* **2008**, *27*, 6614.
12. For example, see: Izawa, Y.; Stahl, S. S. *Adv. Synth. Catal.* **2010**, *352*, 3223.
13. Campbell, A. N.; White, P. B.; Guzei, I. A.; Stahl, S. S. *J. Am. Chem. Soc.* **2010**, *132*, 15116.
14. Steinhoff, B. A.; Stahl, S. S. *J. Am. Chem. Soc.* **2006**, *128*, 4348.
15. For example, see: Ye, X. A.; Johnson, M. D.; Diao, T. N.; Yates, M. H.; Stahl, S. S. *Green Chem.* **2010**, *12*, 1180.
16. (a) Stuart, D. R.; Fagnou, K. *Science* **2007**, *316*, 1172. (b) Campbell, A. N.; Meyer, E. B.; Stahl, S. S. *Chem. Commun.* **2011**, *47*, 10257.
17. (a) Mukhopadhyay, S.; Rothenberg, G.; Lando, G.; Agbaria, K.; Kazanci, M.; Sasson, Y. *Adv. Synth. Catal.* **2001**, *343*, 455. (b) Yokota, T.; Sakaguchi, S.; Ishii, Y. *Adv. Synth. Catal.* **2002**, *344*, 849.
18. (a) Liu, G.; Yin, G.; Wu, L. *Angew. Chem. Int. Ed.* **2008**, *47*, 4733. (b) Reed, S. A.; Mazzotti, A. R.; White, M. C. *J. Am. Chem. Soc.* **2009**, *131*, 11701.
19. Fier, P. S.; Hartwig, J. F. *Science* **2013**, *342*, 956.

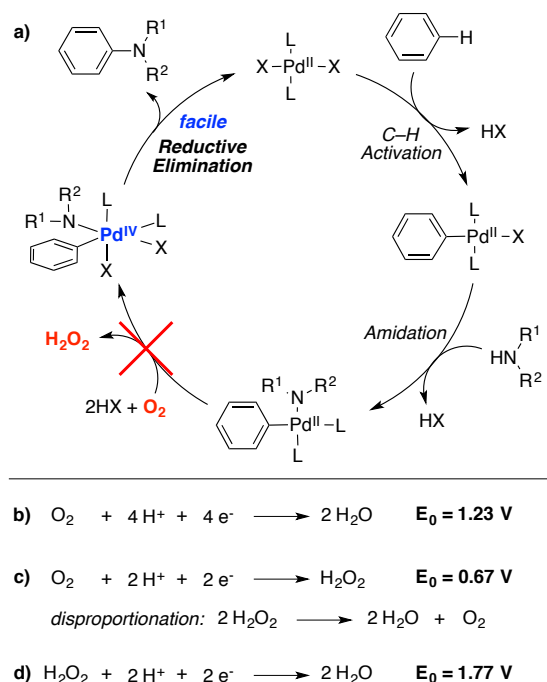
Chapter 6

*Powerful Peroxide Oxidants Derived from Molecular Oxygen
for Palladium-Catalyzed Aryl C–H Amination Reactions*

6.1 Introduction

The discovery of palladium catalyzed oxidative methods for the construction of aryl C–N bonds from aryl C–H bonds and amines is an important goal for reaction development, as such transformations could replace widely utilized Buchwald-Hartwig cross coupling reactions in the streamlined synthesis of complex target molecules.¹ Palladium catalyzed methods for aryl C–H amination predominantly require the stoichiometric addition of a strong oxidant, such as diacetoxyiodobenzene,² oxone,³ or $[F^+]$ sources.^{4,5,6,7} A salient feature of the mechanism of these reactions is oxidation of a Pd^{II} species to a high-valent Pd^{III} or Pd^{IV} species,⁸ which facilitates reductive elimination of the C–N bond and circumvents the intermediacy of an unstable Pd^0 species (Scheme 6.1a) (for a discussion of the factors that effect reductive elimination of C–N bonds from Pd^{II} species, see chapter 5).

Scheme 6.1. The oxidant problem in Pd^{II}/Pd^{IV} catalysis of aryl C–H amination reactions.



The requirement for stoichiometric strong oxidant additives limits the utility of the presently available palladium catalyzed aryl C–H amination reactions, as the advantage of direct C–H

functionalization in terms of step economy are partially counterbalanced by reduced atom economy. To address this deficiency, we are interested in developing aryl C–H amination methods that employ molecular oxygen as the oxidant. Molecular oxygen contains substantial oxidizing power, as is evident from the standard reduction potential of molecular oxygen to water (Scheme 6.1b).⁹ However, aerobic palladium oxidation catalysis does not typically take advantage of the majority of this oxidizing power, because the oxidative organic transformations of interest are two electron processes, and the standard reduction potential of O₂ to H₂O₂ is relatively low (Scheme 6.1c). The two-electron oxidizing power of O₂ is sufficient for catalytic processes that take advantage of a Pd^{II}/Pd⁰ cycle, in which Pd^{II} mediates the two-electron oxidative transformation of a substrate while O₂ reoxidizes the ensuing Pd⁰ species to Pd^{II}.¹⁰ This process yields hydrogen peroxide as the byproduct,¹¹ which does not typically build up over the course of the reaction, as it has been observed to undergo rapid disproportionation under the reaction conditions¹² or to participate in unproductive decomposition pathways.¹³ Thus, a significant portion of the oxidizing power of O₂ is not harnessed in Pd^{II}/Pd⁰ catalysis, as the two-electron reduction of H₂O₂ to water releases the majority of the potential (Scheme 6.1d).⁹ With regards to our goal of developing aryl C–H amination reactions, the ability to couple the oxidative transformation to the two-electron reduction of hydrogen peroxide rather than molecular oxygen would provide access to high-valent Pd^{IV} or Pd^{III} intermediates that can perform the desired reductive elimination of C–N bonds.^{14,15,16}

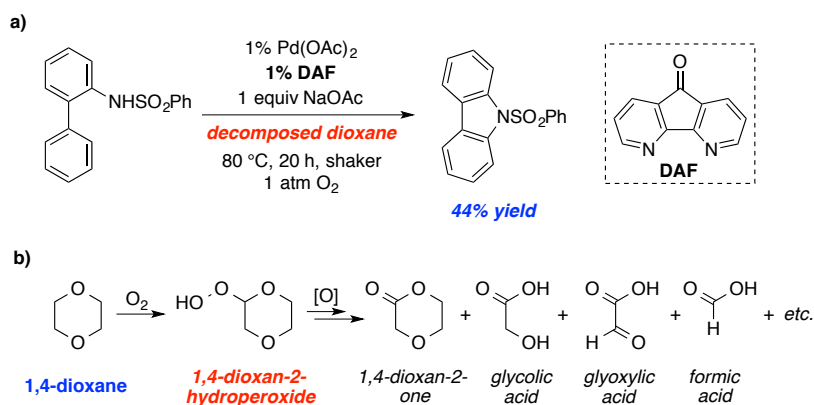
Here, we report the discovery of aerobic catalyst conditions that make use of a sacrificial reductant for the *in situ* generation of a peroxide species that serves as the active oxidant in an aryl C–H amination reaction. These findings have important implications for the development of

efficient palladium catalyzed C–H functionalization methods that harness the substantial oxidizing power of molecular oxygen.¹⁷

6.2 Results and Discussion

As part of our ongoing efforts to discover mild conditions for aryl C–H amination reactions, we evaluated the ability of a variety of neutral donor ligands to promote the transformation of 2-aminobiphenyl derivatives into carbazoles with molecular oxygen as the sole oxidant (cf. Chapter 5). This model transformation was selected as a starting point based on the ease of analysis of the product as well as its precedence as the sole substrate that undergoes aerobic aryl C–H amination, albeit only at high temperature (120 °C) and with limited scope.^{6a,b} During the course of our screening efforts, we were somewhat surprised to observe 44 turnovers with a Pd(OAc)₂ / 4,5-diazafluorenone (DAF) / in dioxane / 80 °C / 1 atm O₂ catalyst system (Scheme 6.2a). Inspection of the crude ¹H NMR spectrum of the reaction mixture revealed the presence of a number of byproducts, and it was determined that an aging bottle of dioxane had been used in this experiment. Significant quantities of 1,4-dioxan-2-hydroperoxide and associated oxidative fragmentation products were present during the reaction (Scheme 6.2b).

Scheme 6.2. a) Discovery of a positive effect of peroxide species in carbazole synthesis. b) Dioxane decomposition by autoxidation.

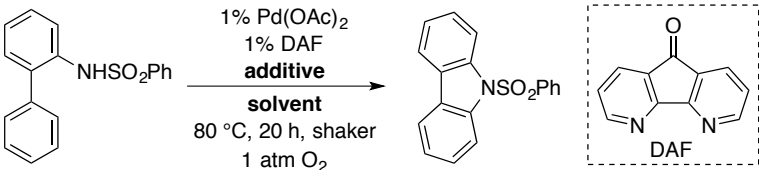


Unsure of the implications of this finding, we repeated the experiment using a fresh bottle of dioxane and found that there is no reaction under these conditions (Table 6.1, entry 1). Changing the solvent to toluene and adding *tert*-butylhydroperoxide (TBHP) gave a comparable yield to what was obtained with the decomposed dioxane (entry 2), suggesting that 1,4-dioxan-2-hydroperoxide is capable of promoting the reaction. Addition of a more activated peroxide oxidant, *tert*-butylperoxybenzoate (TBPB), provided substantially higher yields of carbazole (entry 3). These results resemble findings in past work by Alper¹⁸ and Sigman¹⁹ on Wacker oxidations of alkenes in tetrahydrofuran (THF), where it was noted that productive catalysis occurred with concomitant oxidative decomposition of THF, and TBHP could be used directly as the oxidant.

The results discussed above appear to explain the surprising reactivity that was discovered from the experiment conducted with contaminated dioxane solvent; however, another unexpected result was obtained when control experiments to assess the potential impact of non-peroxide contaminants on the reaction were performed. Glycolic acid, glyoxylic acid, and oxalic acid were each tested as additives (Table 6.1, entries 4-9), and glycolic acid was found to promote the reaction to 80% yield of carbazole when two equivalents were used (entry 6). We noted that the production of carbazole in good yield correlated with the consumption of glycolic acid and observation of oxidative decomposition products of dioxane.²⁰ Specifically, 1,4-dioxan-2-hydroperoxide and 1,4-dioxan-2-one could be isolated, and a mixture of unidentified formate species was observable in the ¹H NMR spectrum of the crude reaction mixture (see the supporting information for details). When glycolic acid was included and the reaction carried out in toluene as the solvent, no carbazole product was observed (entry 7). We hypothesized that the activated primary alcohol of glycolic acid was being oxidized under the reaction conditions and

was triggering the decomposition of dioxane (see mechanistic discussion below), and so we tested other additives with oxidizable functional groups. We found that *N*-acetyl glycine, which has a similarly activated primary amine functional group, also promoted the reaction, though less

Table 6.1. Investigation of additive effects on carbazole synthesis with a Pd(OAc)₂ / DAF / 1 atm O₂ catalyst system.



entry	additive (equiv)	solvent (0.1M)	% Yield	observed dioxane decomposition? ^a
1	none	dioxane	0	no
2	<i>t</i> -butylhydroperoxide (1.1)	toluene	45	n/a
3	<i>t</i> -butylperoxybenzoate (1.1)	toluene	82 ^b	n/a
4	glycolic acid (0.1)	dioxane	10	trace
5	glycolic acid (1)	dioxane	43	yes
6	glycolic acid (2)	dioxane	80	yes
7	glycolic acid (2)	toluene	0	n/a
8	glyoxylic acid (2)	dioxane	0	no
9	oxalic acid (2)	dioxane	0	no
10	<i>N</i> -acetyl glycine (2)	dioxane	38	yes
11	methyl glycolate (2)	dioxane	4	trace
12	ethylene glycol (2) ^c	dioxane	0	no
13	1-propanol (2) ^c	dioxane	0	no

^a 1,4-Dioxan-2-hydroperoxide and 1,4-dioxan-2-one could be isolated from the reaction mixtures. Unidentified formate species were also observed in the crude ¹H NMR spectra. ^b A comparable yield was obtained under these conditions in the absence of 4,5-diazafluorenone (DAF). ^c Co-solvent quantities (4:1 dioxane: alcohol) were also ineffective.

effectively than glycolic acid (entry 10). Methyl glycolate provided trace reactivity (entry 11), while ethylene glycol and propanol were completely ineffective (entries 12-13). Last, we were interested in assessing the importance of 4,5-diazafluorenone (DAF) as the neutral donor ligand. A screen of common bipyridyl ligand derivatives in the presence of glycolic acid revealed that DAF plays a crucial role in promoting reactivity (Figure 6.1).²¹ Alternative diazafluorene derivatives and 6,6'-dimethylbipyridine also promoted the reaction, but not as effectively as DAF

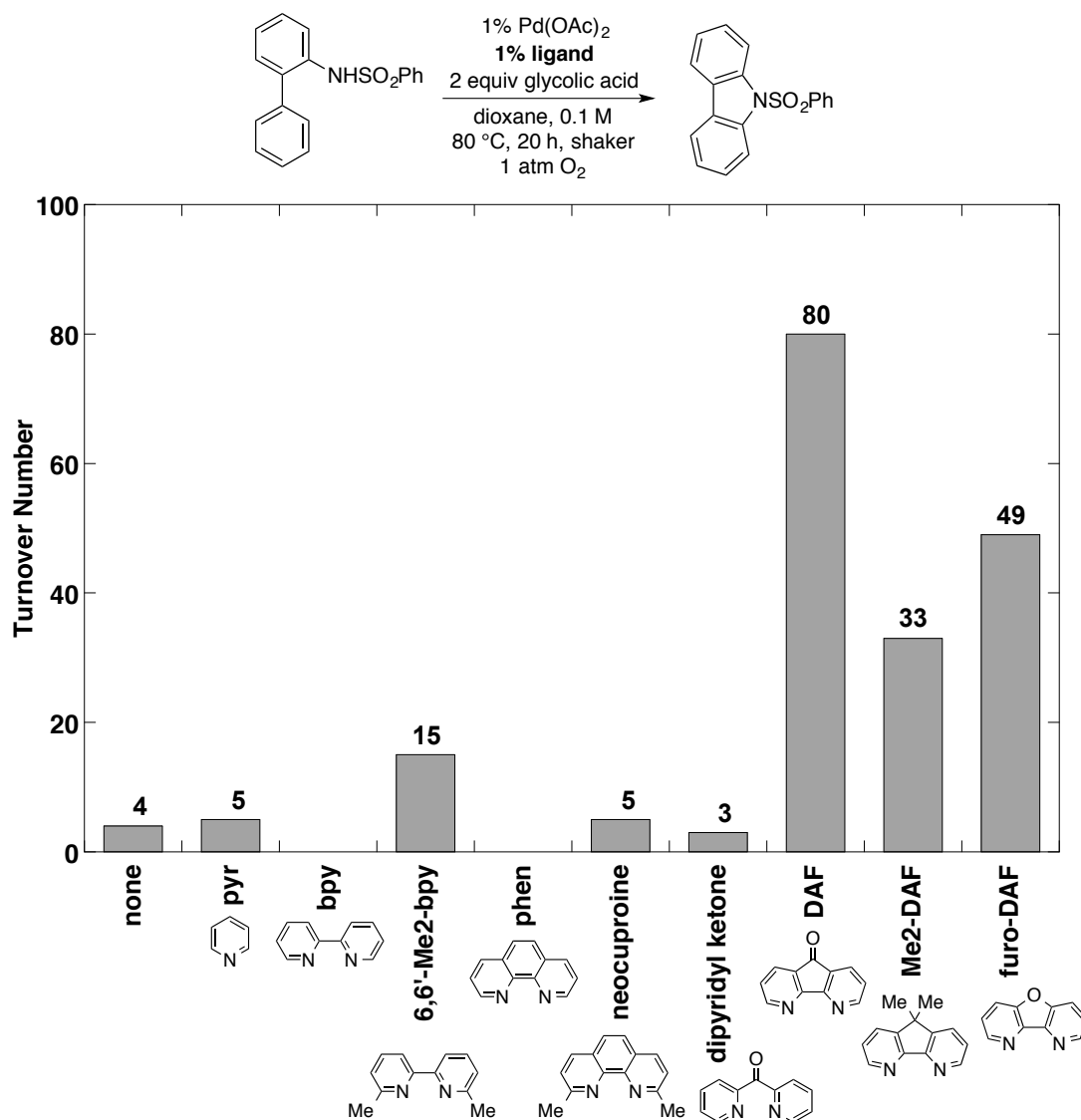


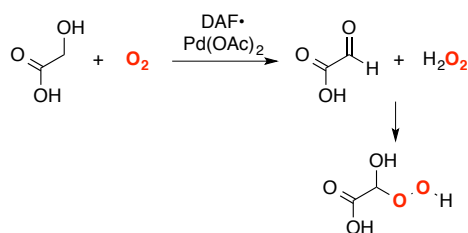
Figure 6.1. Ligand screen for carbazole synthesis in the presence of glycolic acid and dioxane solvent. Yield of product was determined by ^1H NMR spectroscopic analysis of the reaction mixture using phenyltrimethylsilane as the internal standard.

Simple pyridine, bipyridine, and phenanthroline derivatives did not promote the reaction, and a control experiment in which no ligand was added gave only trace carbazole product.

A plausible reaction mechanism that accounts for the results presented above is presented in Schemes 6.3, 6.4 and 6.5. First, glycolic acid is oxidized to glyoxylic acid by the $\text{Pd}(\text{OAc})_2/\text{DAF}/\text{O}_2$ catalyst system in a traditional $\text{Pd}^{\text{II}}/\text{Pd}^0$ cycle, which produces an equivalent of hydrogen peroxide (Scheme 6.3a).¹⁰ The glyoxylic acid then serves as an excellent electrophile for nucleophilic attack by the hydrogen peroxide, effectively trapping and activating the peroxide. Significant quantities of hydrogen peroxide are unlikely to be trapped in the early stages of the reaction, though it is conceivable that the presence of an activated peroxide species initiates the autoxidation of dioxane (Scheme 6.3b). Homolysis of the activated peroxide O–O bond in the presence of dioxane as the solvent will abstract a hydrogen atom from dioxane. The

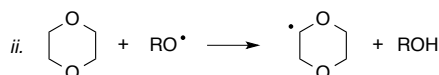
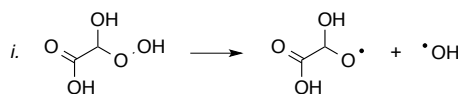
Scheme 6.3. a) Generation of activated peroxide by reduction of O_2 and *in situ* trapping. b) Autoxidation of dioxane initiated by activated trapped peroxide.

a) Alcohol oxidation, O_2 reduction, and H_2O_2 trapping

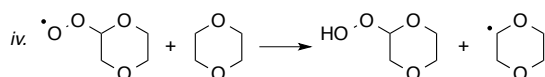
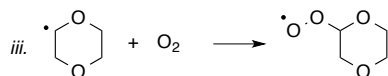


b) Dioxane autoxidation

Initiation by trapped peroxide



Propagation with O_2

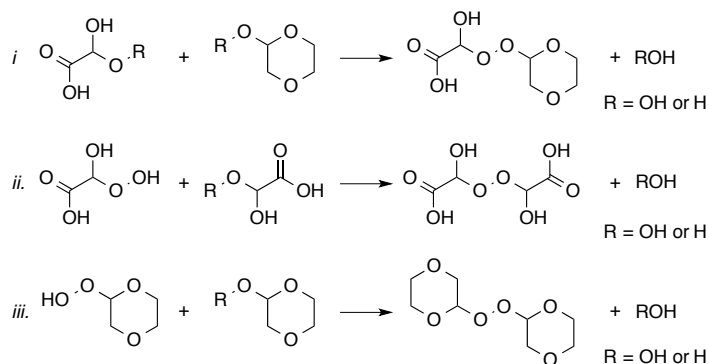


resulting carbon-centered radical is rapidly trapped by molecular oxygen, yielding a peroxo-based radical that propagates the oxidation of dioxane to give 1,4-dioxan-2-hydroperoxide.

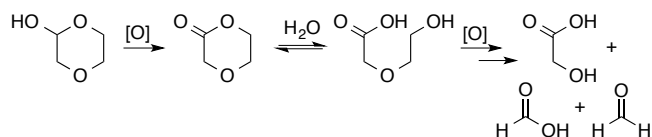
Our results suggested that 1,4-dioxan-2-hydroperoxide and TBHP are capable of promoting the aryl C–H amination reaction, but we also found that more activated TBPB gives a higher yield that is comparable to what is obtained when glycolic acid is used in dioxane (cf. Table 6.1). The 1,4-dioxan-2-hydroperoxide species that is generated from the autoxidation of dioxane is likely to build up to appreciable quantities over the course of the reaction, and a variety of further trapping processes become available to provide species with more activated O–O bonds (Scheme 6.4a). Any one of these peroxide species could contribute to the catalytic aryl C–H amination reaction. These oxidizing species are also likely to be partially consumed in oxidative decomposition pathways for dioxane (Scheme 6.4b) and glycolic acid (Scheme 6.5c). At the end of the reaction, a significant quantity of 1,4-dioxan-2-one is detected (52% by ^1H NMR spectroscopic analysis, relative to aminobiphenyl starting material). Glycolic acid is consumed during the reaction, but glyoxylic acid and oxalic acid are not detected as products. Further experiments will be necessary to better determine the fate of glycolic acid oxidation products – presently, we presume that the powerful oxidizing conditions generated as the reaction progresses are capable of rapidly degrading glyoxylic and oxalic acid to low molecular weight formate species and/or carbon dioxide.

Scheme 6.4. Mechanistic pathways for a) further peroxide activation b) decomposition of dioxane and c) decomposition of glycolic acid.

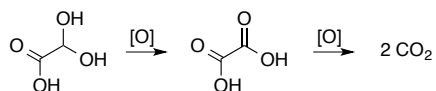
a) Further peroxide activation processes



b) Oxidative decomposition of dioxane

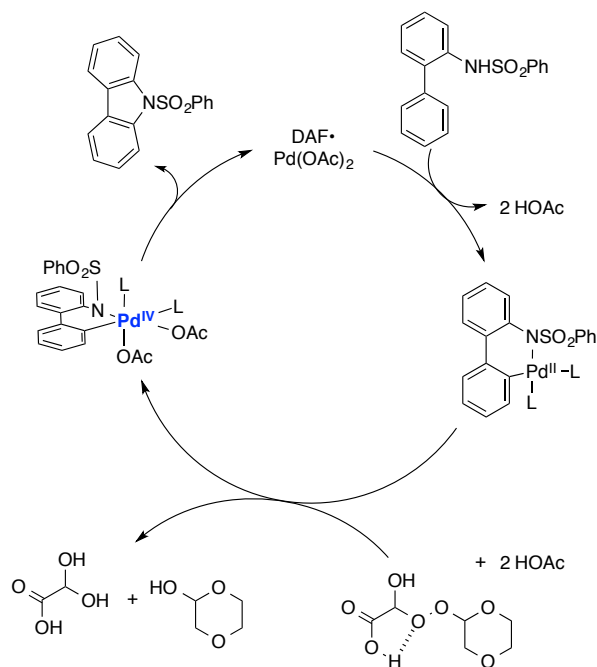


c) Oxidative decomposition of glycolic acid



The mechanistic discussion presented above provides a rationale for the generation of strong peroxide oxidants from the aerobic oxidation of glycolic acid with a DAF•Pd(OAc)₂ catalyst in dioxane. We propose that the presence of these peroxide oxidants enables a Pd^{IV}/Pd^{II} catalytic cycle in the intramolecular aryl C–H amination reaction of benzenesulfonyl-protected 2-aminobiphenyl substrate to the corresponding carbazole product (Scheme 6.5).

Scheme 6.5. Proposed mechanism for substrate oxidation via Pd^{IV}/Pd^{II} catalysis with an *in situ* generated peroxide as the oxidant.



The ability to perform this challenging oxidation reaction with relatively high turnover numbers and with molecular oxygen as the terminal oxidant is an intriguing discovery; however, there are drawbacks to this system. The addition of glycolic acid and decomposition of dioxane complicates the system and generates organic waste in much the same manner as the addition of alternative strong oxidants, such as *t*-butylperoxybenzoate (cf. Table 6.1, entry 3). Second, the involvement of reactive radical species to initiate the autoxidation and peroxide trapping processes may limit the scope of substrates that are amenable to these conditions (for example, the 2-acetamido-3-aryl-acrylate substrates for indole synthesis discussed in Chapter 4 did not respond to these conditions). A reasonable goal in light of the present study will be to discover catalyst conditions that could take advantage of controlled hydrogen peroxide production and trapping events. This strategy could become an enabling technology in scenarios where addition of a peroxide oxidant in a large scale single batch presents hazards, or when a particularly strong peroxide oxidant that cannot be isolated is necessary for the reaction. For now, we advise that

oxidation reactions that are carried out in ethereal solvents are analyzed for possible simultaneous autoxidation processes that could have significant impact on the mechanism of the transformation under study.

6.3 Experimental Details and Supporting Information

6.3.1. General considerations

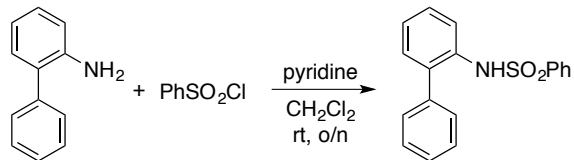
All commercially available compounds were purchased and used as received, unless otherwise noted. 1,4-Dioxane was purchased from Aldrich and in 100 ml sure-seal bottles. ^1H and ^{13}C NMR spectra were recorded on Bruker 400 MHz or 500 MHz spectrometers and chemical shifts are given in parts per million relative to internal tetramethylsilane (0.00 ppm for ^1H) or CDCl_3 (77.16 ppm for ^{13}C). Flash chromatography was carried out with SiliaFlash® P60 (Silicycle, particle size 40-63 μm , 230-400 mesh) or by using a CombiFlash Rf® automated chromatography system with reusable high performance silica columns (RediSep® Rf Gold Silica, 20-40 μm spherical particles).

6.3.2. General procedure for reaction set up

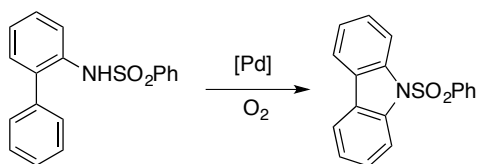
Reactions carried out at 1 atm of O_2 in a custom shaker apparatus:

A heavy wall 13x100 mm culture tube was charged with substrate (0.05 mmol) and other solid additives, such as glycolic acid, as desired. Separate stock solutions of $\text{Pd}(\text{OAc})_2$ and ligand were prepared such that the correct quantity of each (1 mol%) could be delivered and the total volume would reach 0.5 ml (0.1 M). The culture tube was loaded onto a custom 48-well parallel reactor that allowed for heating under a reflux condenser and 1 atm of O_2 with orbital shaking. The reaction vessel was purged with O_2 after being loaded onto the shaker apparatus. The reaction mixtures were heated to the desired temperature and allowed to shake vigorously. At the desired time point, the reaction mixtures were allowed to cool to room temperature, removed from the parallel reactor and concentrated to oil. The mixtures were analyzed by ^1H NMR spectroscopy using CDCl_3 spiked with phenyltrimethylsilane as the internal standard.

6.3.3. Benzenesulfonyl-protected 2-aminobiphenyl and carbazole



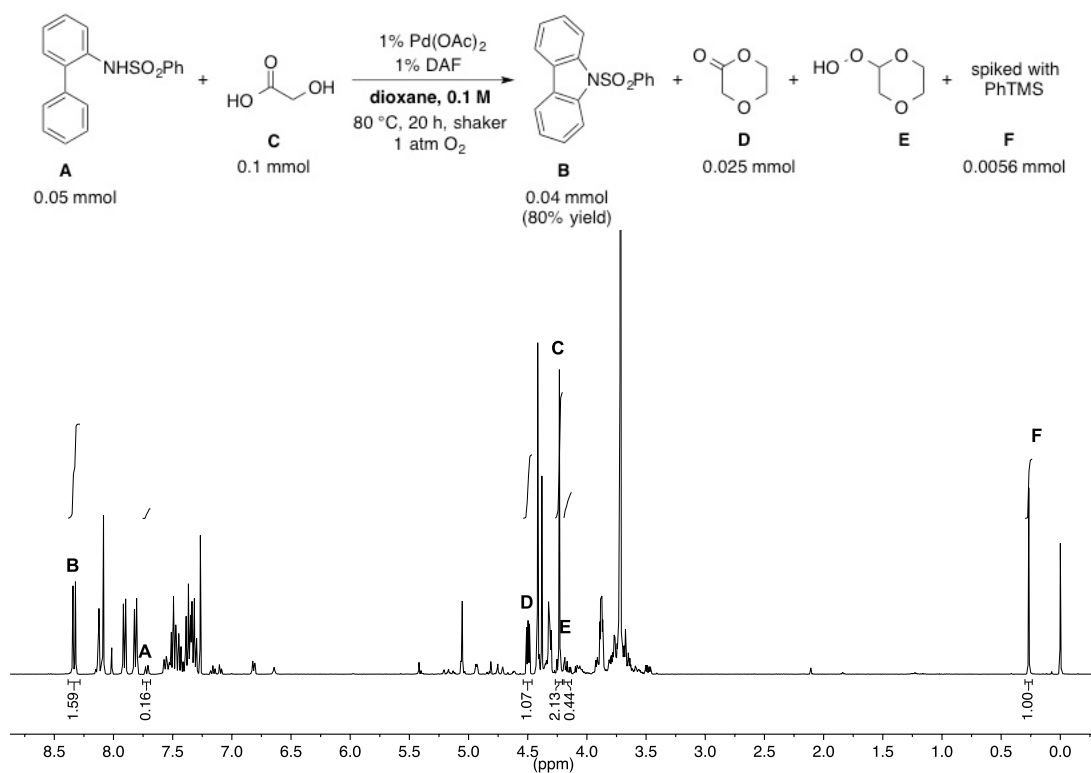
***N*-Benzenesulfonyl-2-aminobiphenyl:** A 250 ml round-bottomed flask was charged with 2-aminobiphenyl (1.5 g, 8.86 mmol, 1 equiv) and dissolved in 88 ml of dichloromethane (0.1 M). Pyridine (3.58 ml, 44.3 mmol, 5 equiv) and benzenesulfonyl chloride (1.71 ml, 13.3 mmol, 1.5 equiv) were added via syringe. The reaction mixture was allowed to stir under air for 16 hours. The reaction mixture was diluted with dichloromethane, washed 3x with water, dried over MgSO_4 and concentrated. Purification on silica with hexanes : ethyl acetate (4:1) afforded the product (2.51 g, 93%) as an off-white solid. ^1H NMR (400 MHz, CDCl_3) δ 7.73 (dd, $J = 8.3, 1.2$ Hz, 1H), 7.61 – 7.51 (m, 3H), 7.45 – 7.29 (m, 6H), 7.16 (td, $J = 7.5, 1.2$ Hz, 1H), 7.09 (dd, $J = 7.6, 1.7$ Hz, 1H), 6.81 (dd, $J = 7.7, 1.8$ Hz, 2H), 6.58 (s, 1H).



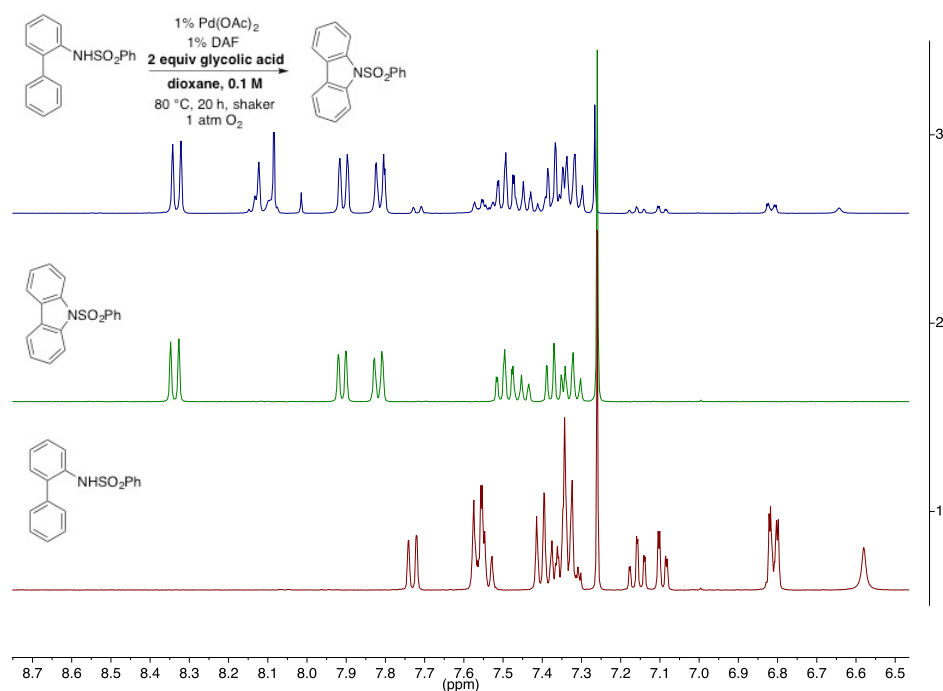
***N*-Benzenesulfonyl-carbazole:** The carbazole was obtained from the palladium catalyzed aerobic oxidation reactions and was isolated as a white solid with purification on silica using a hexanes : ethyl acetate solvent system (5:1). ^1H NMR (400 MHz, CDCl_3) δ 8.34 (dt, $J = 8.5, 0.8$ Hz, 2H), 7.91 (dt, $J = 7.7, 1.0$ Hz, 2H), 7.82 (dd, $J = 8.4, 1.3$ Hz, 2H), 7.50 (ddd, $J = 8.6, 7.4, 1.3$ Hz, 2H), 7.47 – 7.42 (m, 1H), 7.37 (td, $J = 7.5, 1.0$ Hz, 2H), 7.32 (t, $J = 7.9$ Hz, 2H).

6.3.4. Typical crude ^1H NMR spectrum and isolation of autoxidation byproducts

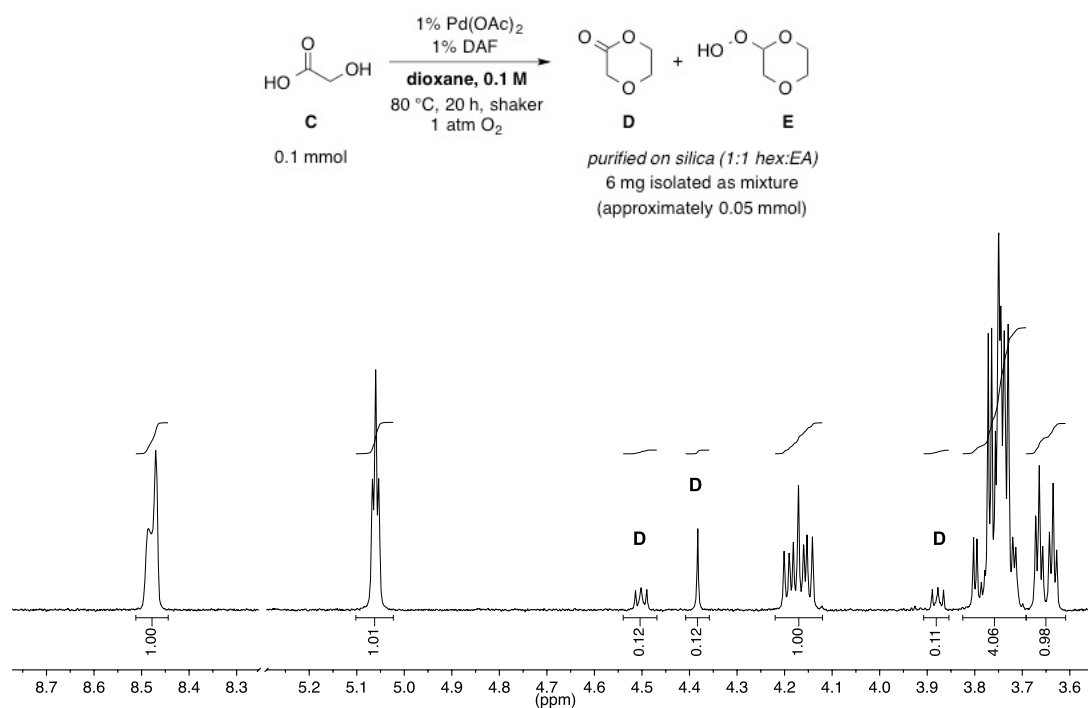
Crude ^1H NMR after the reaction was carried out according to the general procedure above:



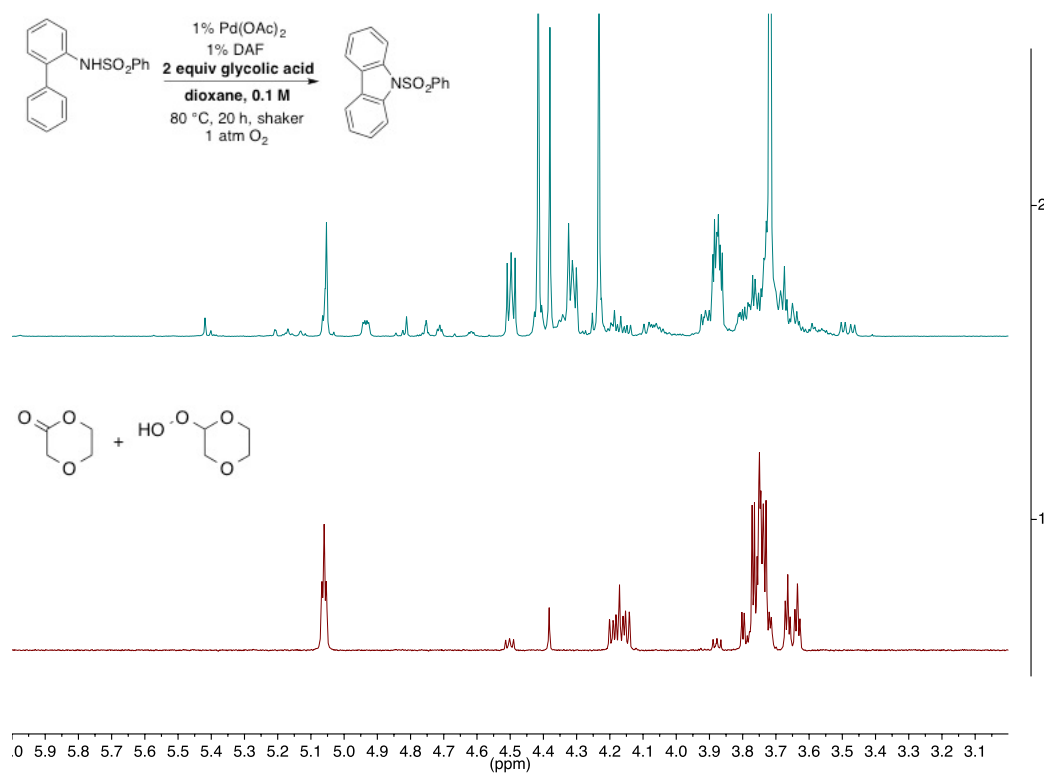
Crude ^1H NMR spectrum with comparison to product and starting material spectra:



Isolated 1,4-dioxan-2-hydroperoxide and 1,4-dioxan-2-one:



Crude ¹H NMR spectrum with comparison to 1,4-dioxan-2-hydroperoxide and 1,4-dioxan-2-one:



6.4 References and Notes

1. (a) Guram, A. S.; Buchwald, S. L. *J. Am. Chem. Soc.* **1994**, *116*, 7901. (b) Paul, F.; Patt, J.; Hartwig, J. F. *J. Am. Chem. Soc.* **1994**, *116*, 5969. (c) Hartwig, J. F. *Angew. Chem. Int. Ed.* **1998**, *37*, 2047. (d) Surry, D. S.; Buchwald, S. L. *Angew. Chem. Int. Ed.* **2008**, *47*, 6338. (e) Hartwig, J. F. *Acc. Chem. Res.* **2008**, *41*, 1534.
2. (a) Jordan-Hore, J. A.; Johansson, C. C. C.; Gulias, M.; Beck, E. M.; Gaunt, M. J. *J. Am. Chem. Soc.* **2008**, *130*, 16184. (b) He, G.; Zhao, Y. S.; Zhang, S. Y.; Lu, C. X.; Chen, G. *J. Am. Chem. Soc.* **2012**, *134*, 3. (c) He, G.; Lu, C. X.; Zhao, Y. S.; Nack, W. A.; Chen, G. *Org. Lett.* **2012**, *14*, 2944. (e) Nadres, E. T.; Daugulis, O. *J. Am. Chem. Soc.* **2012**, *134*, 7. (f) Mei, T. S.; Leow, D.; Xiao, H.; Laforteza, B. N.; Yu, J. Q. *Org. Lett.* **2013**, *15*, 3058. (g) Shrestha, R.; Mukherjee, P.; Tan, Y. C.; Litman, Z. C.; Hartwig, J. F. *J. Am. Chem. Soc.* **2013**, *135*, 8480.
3. (a) Thu, H. Y.; Yu, W. Y.; Che, C. M. *J. Am. Chem. Soc.* **2006**, *128*, 9048. (b) Youn, S. W.; Bihn, J. H.; Kim, B. S. *Org. Lett.* **2011**, *13*, 3738.
4. (a) Mei, T. S.; Wang, X. S.; Yu, J. Q. *J. Am. Chem. Soc.* **2009**, *131*, 10806. (b) Sun, K.; Li, Y.; Xiong, T.; Zhang, J. P.; Zhang, Q. A. *J. Am. Chem. Soc.* **2011**, *133*, 1694. (c) Xiao, B.; Gong, T. J.; Xu, J.; Liu, Z. J.; Liu, L. *J. Am. Chem. Soc.* **2011**, *133*, 1466. (d) Boursalian, G. B.; Ngai, M. Y.; Hojczyk, K. N.; Ritter, T. *J. Am. Chem. Soc.* **2013**, *135*, 13278.
5. For examples of palladium catalyzed that aryl C–H amination that are less likely to involve high-valent palladium intermediates, but are likely to involve heterobimetallic species based on the requirement of stoichiometric silver or copper oxidants, see: (a) Inamoto, K.; Saito, T.; Katsuno, M.; Sakamoto, T.; Hiroya, K. *Org. Lett.* **2007**, *9*, 2931. (b) Yoo, E. J.; Ma, S.; Mei, T. S.; Chan, K. S. L.; Yu, J. Q. *J. Am. Chem. Soc.* **2011**, *133*, 7652. (c) Wasa, M.; Yu, J. Q. *J.*

-
- Am. Chem. Soc.* **2008**, *130*, 14058.
6. For two examples of aryl C–H amination that use Pd^{II}/Pd⁰ catalysis, see: (a) Tsang, W. C. P.; Zheng, N.; Buchwald, S. L. *J. Am. Chem. Soc.* **2005**, *127*, 14560. (b) Tsang, W. C. P.; Munday, R. H.; Brasche, G.; Zheng, N.; Buchwald, S. L. *J. Org. Chem.* **2008**, *73*, 7603. (c) Tan, Y. C.; Hartwig, J. F. *J. Am. Chem. Soc.* **2010**, *132*, 3676.
 7. For an example of aryl C–H amination that may involve nitrene insertion into a Pd–aryl bond, see: (a) Ng, K. H.; Chan, A. S. C.; Yu, W. Y. *J. Am. Chem. Soc.* **2010**, *132*, 12862. (b) Dick, A. R.; Remy, M. S.; Kampf, J. W.; Sanford, M. S. *Organometallics* **2007**, *26*, 1365.
 8. For leading references, see: (a) Canty, A. J.; Denney, M. C.; Skelton, B. W.; White, A. H. *Organometallics* **2004**, *23*, 1122. (b) Dick, A. R.; Kampf, J. W.; Sanford, M. S. *J. Am. Chem. Soc.* **2005**, *127*, 12790. (c) Deprez, N. R.; Sanford, M. S. *Inorg. Chem.* **2007**, *46*, 1924. (d) Powers, D. C.; Ritter, T. *Nat. Chem.* **2009**, *1*, 302. (e) Deprez, N. R.; Sanford, M. S. *J. Am. Chem. Soc.* **2009**, *131*, 11234. (f) Muñiz, K. *Angew. Chem. Int. Ed.* **2009**, *48*, 9412. (g) Powers, D. C.; Lee, E.; Ariafield, A.; Sanford, M. S.; Yates, B. F.; Canty, A. J.; Ritter, T. *J. Am. Chem. Soc.* **2012**, *134*, 12002. (h) Powers, D. C.; Ritter, T. *Acc. Chem. Res.* **2012**, *45*, 840. (i) Hickman, A. J.; Sanford, M. S. *Nature* **2012**, *484*, 177.
 9. Yeager, E. *J. Mol. Catal.* **1986**, *38*, 5.
 10. (a) Stahl, S. S.; Thorman, J. L.; Nelson, R. C.; Kozee, M. A. *J. Am. Chem. Soc.* **2001**, *123*, 7188. (b) Stahl, S. S. *Angew. Chem. Int. Ed.* **2004**, *43*, 3400. (c) Gligorich, K. M.; Sigman, M. S. *Chem. Commun.* **2009**, 3854.
 11. For an alternative mechanism, see: Ingram, A. J.; Solis-Ibarra, D.; Zare, R. N.; Waymouth, R. M. *Angew. Chem. Int. Ed.* **2014**, DOI: 10.1002/anie.201400134.

-
12. (a) Steinhoff, B. A.; Fix, S. R.; Stahl, S. S. *J. Am. Chem. Soc.* **2002**, *124*, 766. (b) Nishimura, T.; Onoue, T.; Ohe, K.; Uemura, S. *J. Org. Chem.* **1999**, *64*, 6750.
13. Conley, N. R.; Labios, L. A.; Pearson, D. M.; McCrory, C. C. L.; Waymouth, R. M. *Organometallics* **2007**, *26*, 5447.
14. For well defined studies of the ability to access high-valent Pd complexes in catalytically relevant systems using hydrogen peroxide as the oxidant, see: (a) Oloo, W.; Zavalij, P. Y.; Zhang, J.; Khaskin, E.; Vedernikov, A. N. *J. Am. Chem. Soc.* **2010**, *132*, 14400. (b) Vedernikov, A. N. *Acc. Chem. Res.* **2012**, *45*, 803.
15. For well defined studies in which high-valent Pd complexes are accessed with molecular oxygen as the oxidant, see: (a) Khusnutdinova, J. R.; Rath, N. P.; Mirica, L. M. *J. Am. Chem. Soc.* **2012**, *134*, 2414. (b) Khusnutdinova, J. R.; Qu, F. R.; Zhang, Y.; Rath, N. P.; Mirica, L. M. *Organometallics* **2012**, *31*, 4627. (c) Mirica, L. M.; Khusnutdinova, J. R. *Coord. Chem. Rev.* **2013**, *257*, 299. (d) Qu, F. R.; Khusnutdinova, J. R.; Rath, N. P.; Mirica, L. M. *Chem. Commun.* **2014**, *50*, 3036.
16. For examples of palladium-catalyzed C–H oxidations to C–O bonds using strong peroxide oxidants, see: (a) Giri, R.; Liang, J.; Lei, J. G.; Li, J. J.; Wang, D. H.; Chen, X.; Naggar, I. C.; Guo, C. Y.; Foxman, B. M.; Yu, J. Q. *Angew. Chem. Int. Ed.* **2005**, *44*, 7420. (b) Vickers, C. J.; Mei, T. S.; Yu, J. Q. *Org. Lett.* **2010**, *12*, 2511. (c) Wei, Y.; Yoshikai, N. *Org. Lett.* **2011**, *13*, 5504. (d) Shan, G.; Yang, X. L.; Ma, L. L.; Rao, Y. *Angew. Chem. Int. Ed.* **2012**, *51*, 13070. (e) Sharma, A.; Hartwig, J. F. *J. Am. Chem. Soc.* **2013**, *135*, 17983 (f) Zhu, H. T.; Chen, P. H.; Liu, G. S. *J. Am. Chem. Soc.* **2014**, *136*, 1766.
17. For examples of the exploitation of this concept, see refs 18, 19 and: (a) Yan, Y. P.; Feng, P.; Zheng, Q. Z.; Liang, Y. F.; Lu, J. F.; Cui, Y. X.; Jiao, N. *Angew. Chem. Int. Ed.* **2013**, *52*,

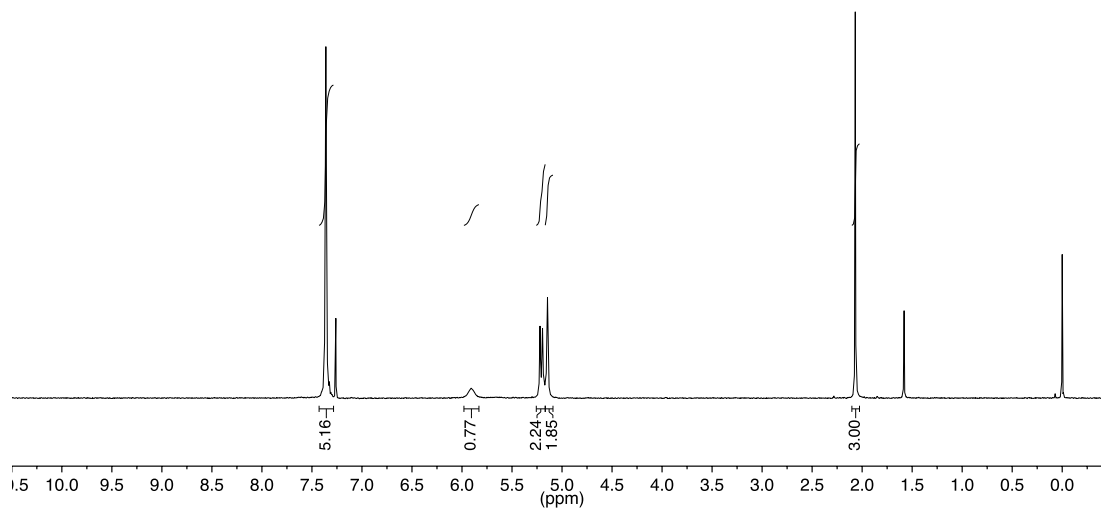
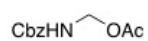
-
5827. (b) Murahashi, S. I.; Oda, Y.; Naota, T. *J. Am. Chem. Soc.* **1992**, *114*, 7913. (c) Clerici, M. G.; Ingallina, P. *Catal. Today* **1998**, *41*, 351. (d) Mukaiyama, T.; Yamada, T. *Bull. Chem. Soc. Jpn.* **1995**, *68*, 17.
18. Sommovigo, M.; Alper, H. *J. Mol. Catal.* **1994**, *88*, 151.
19. Cornell, C. N.; Sigman, M. S. *J. Am. Chem. Soc.* **2005**, *127*, 2796.
20. A detailed reaction timecourse would be compelling here. Qualitatively, a substantial induction period in the appearance of carbazole product was observed by TLC analysis.
21. For examples of 4,5-diazafluorenone promoting allylic C–H oxidation, see ref 16e and: Campbell, A. N.; White, P. B.; Guzei, I. A.; Stahl, S. S. *J. Am. Chem. Soc.* **2010**, *132*, 15116.

Appendix 1

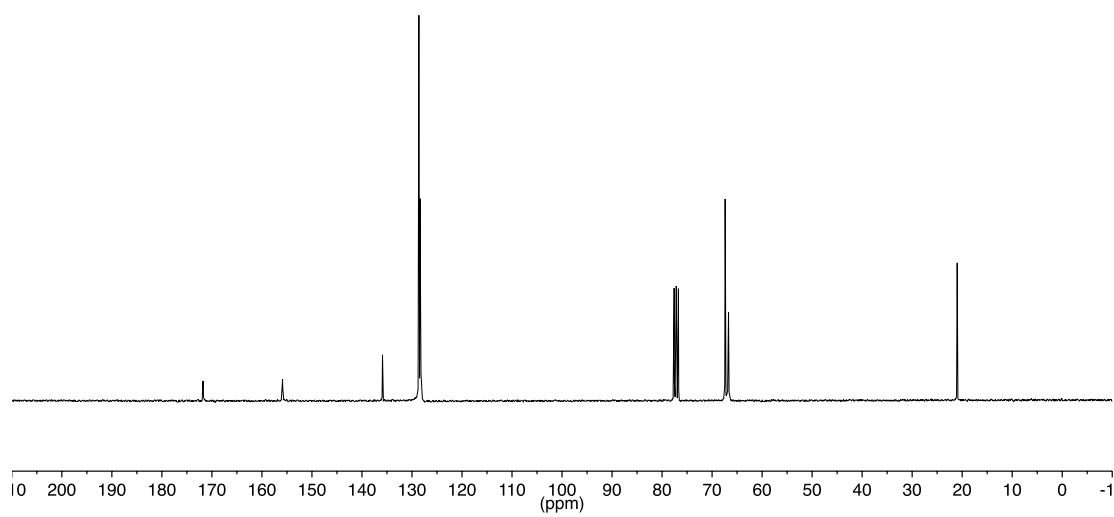
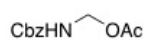
NMR Spectra for Chapter 2

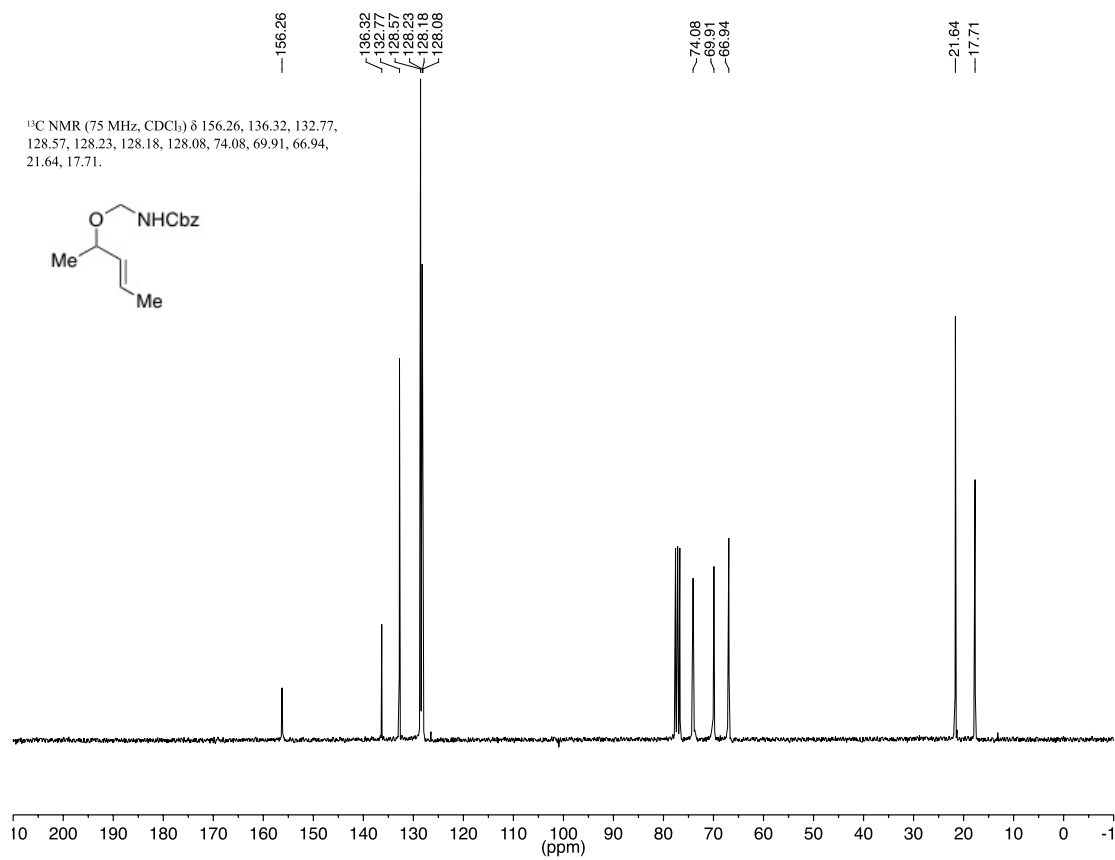
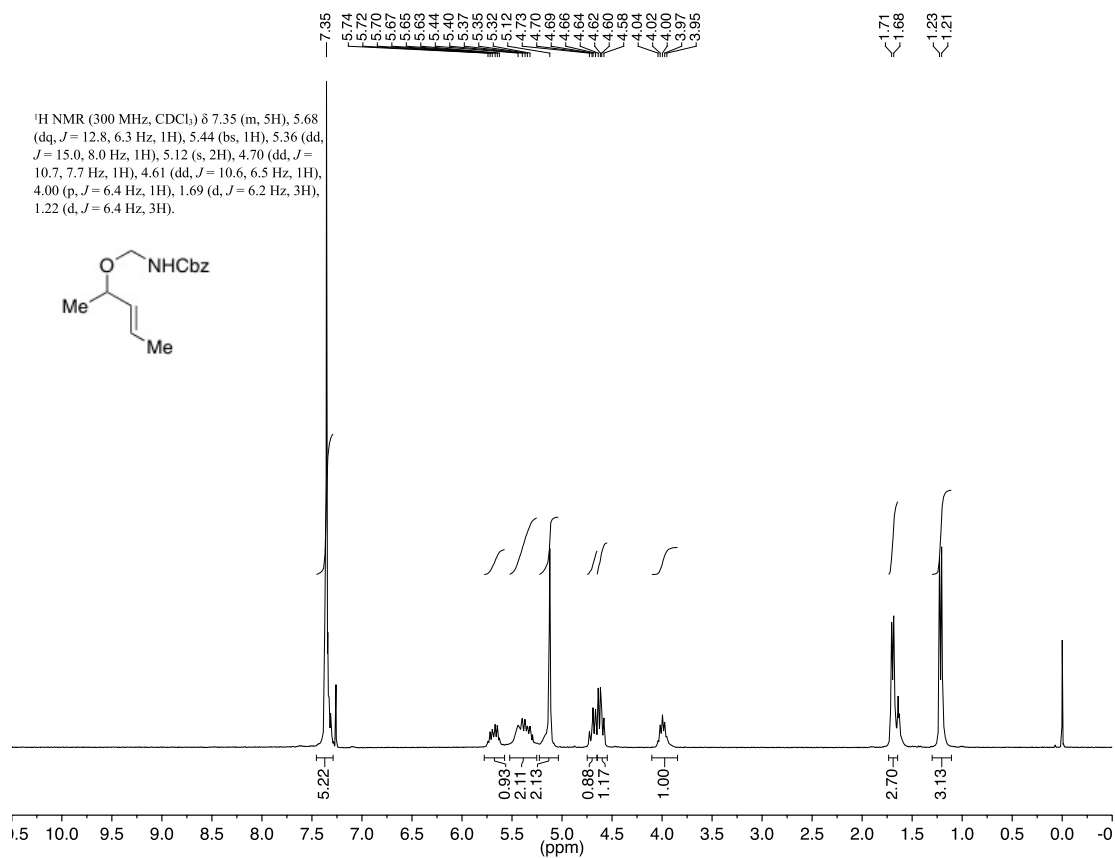
This work has been published: Weinstein, A. B.; Schuman, D. P.; Tan, Z. X.; Stahl, S. S. *Angew. Chem. Int. Ed.* **2013**, 52, 11867–11870.

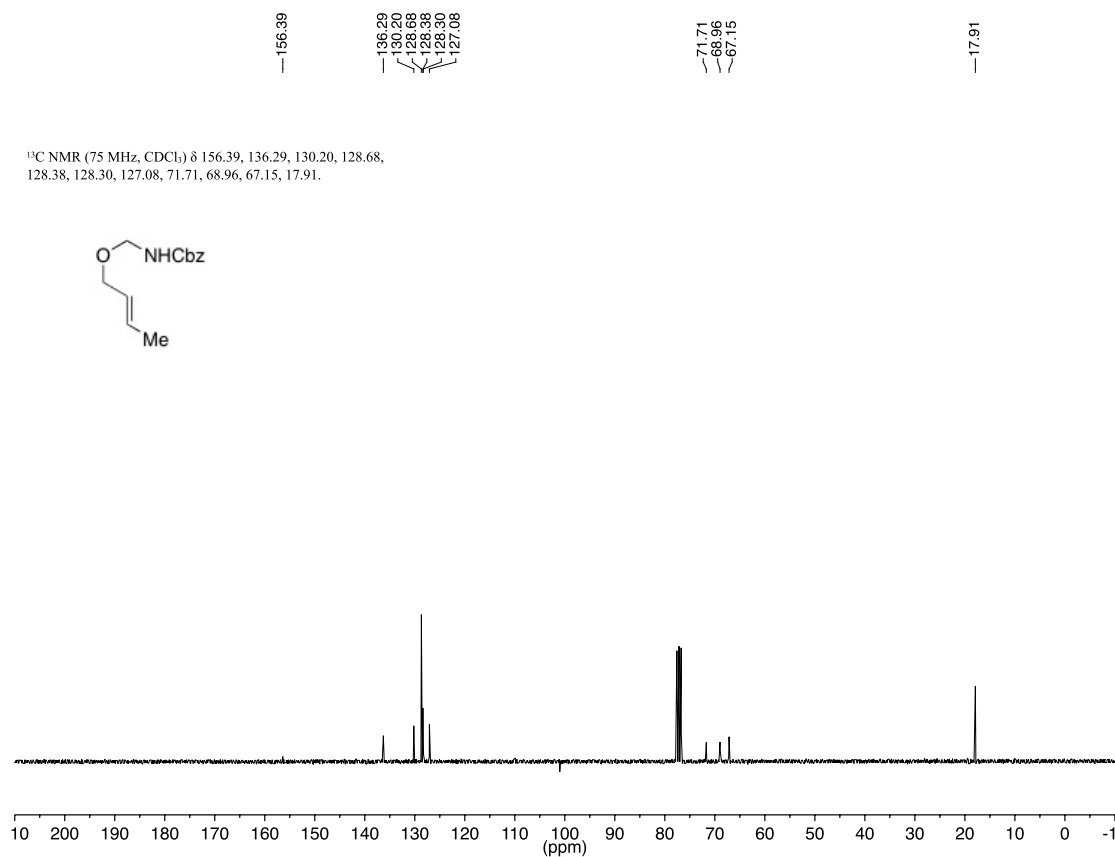
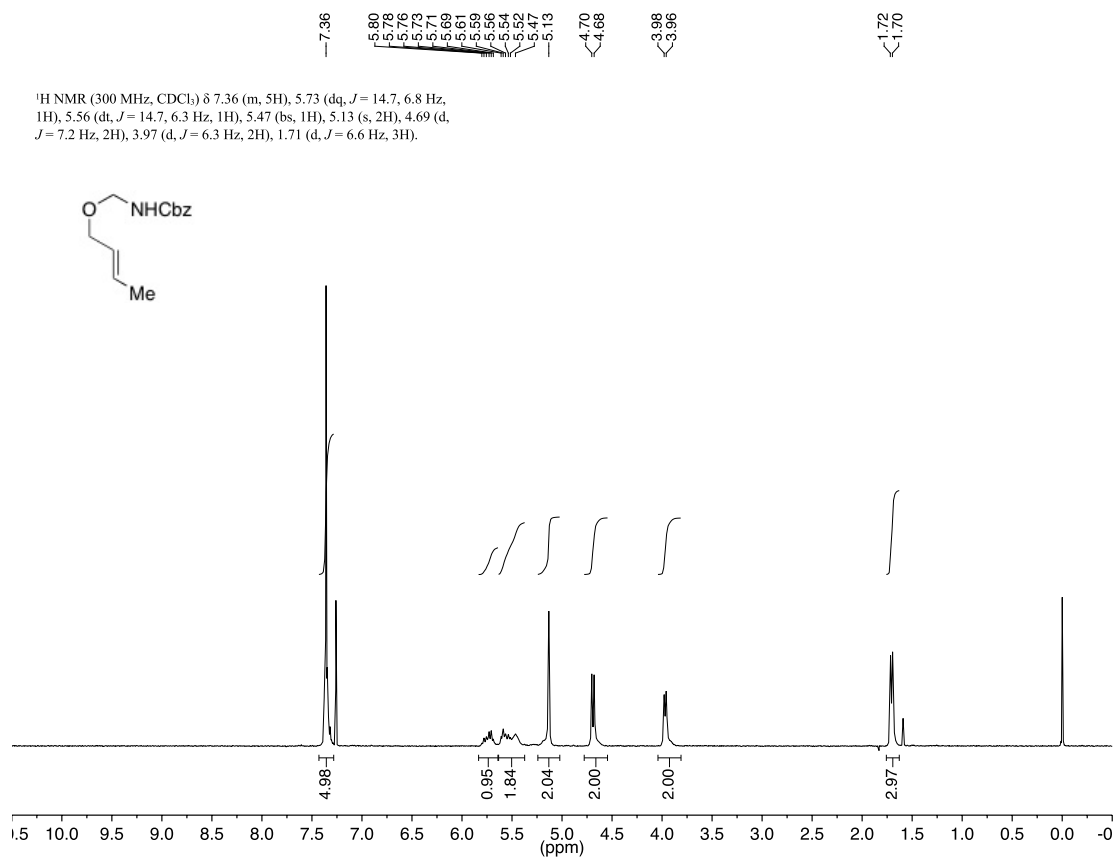
¹H NMR (300 MHz, CDCl₃) δ 7.36 (m, 5H), 5.91 (bs, 1H), 5.21 (d, *J* = 7.5 Hz, 2H), 5.15 (s, 2H), 2.07 (s, 3H).

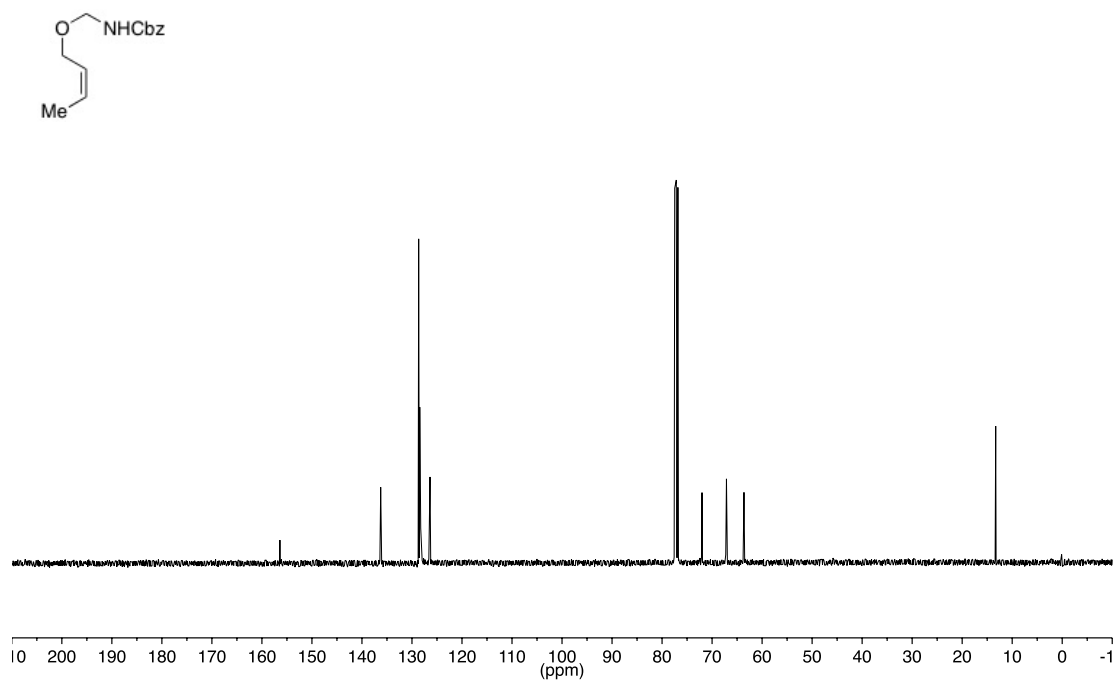
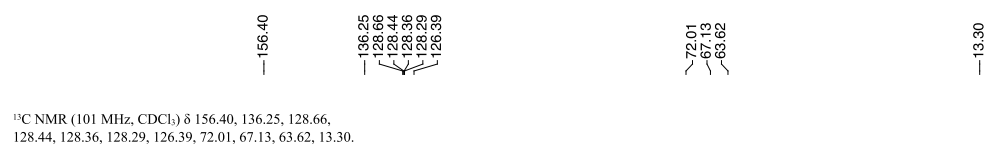
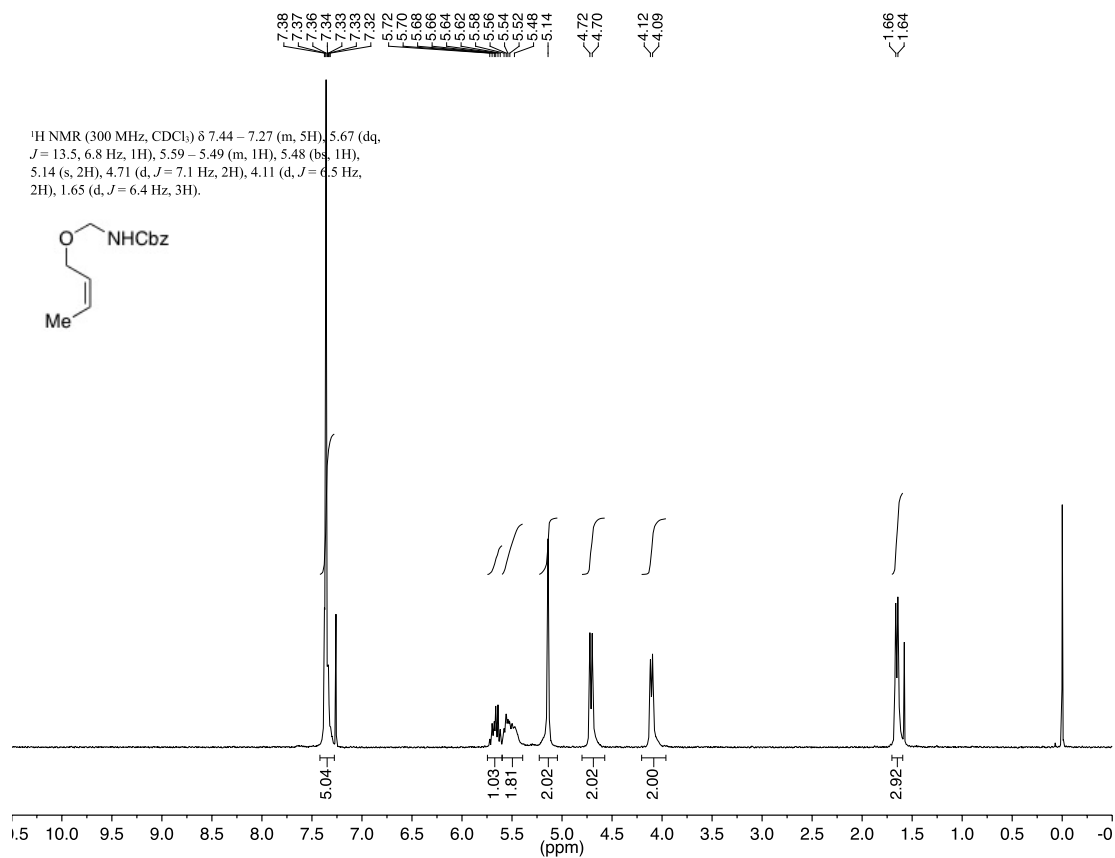


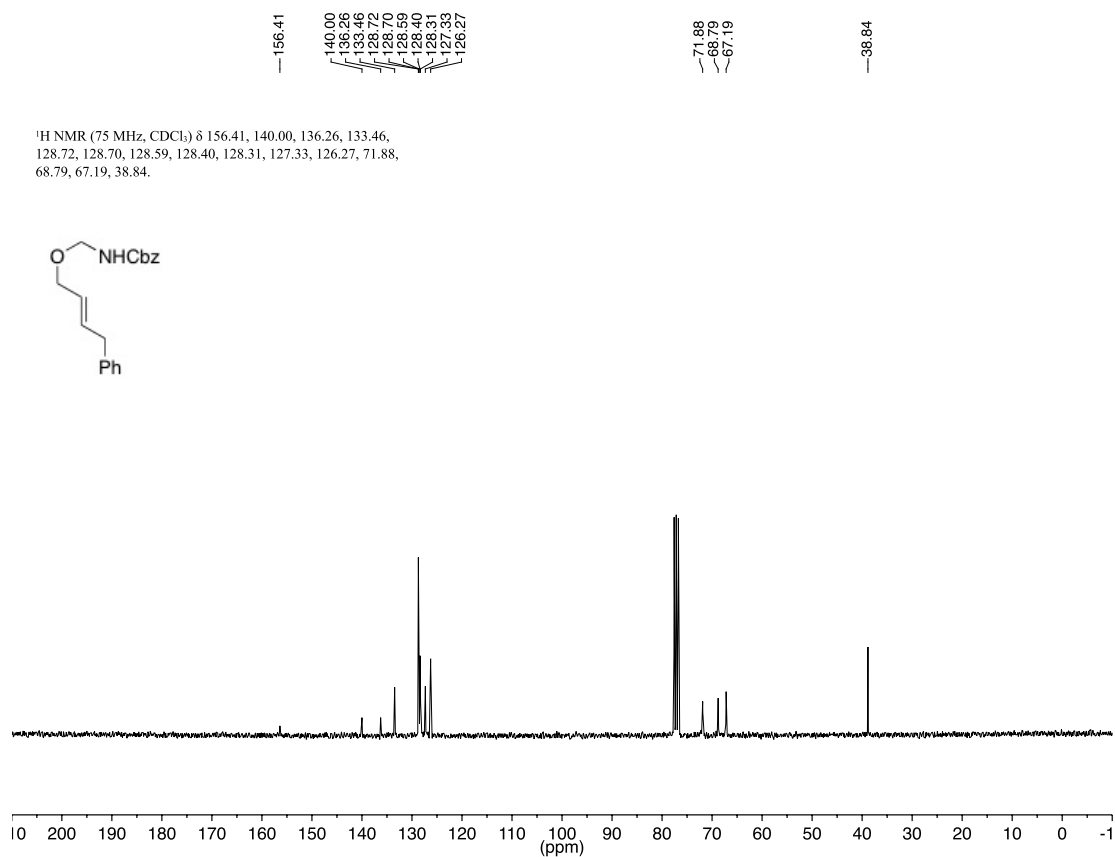
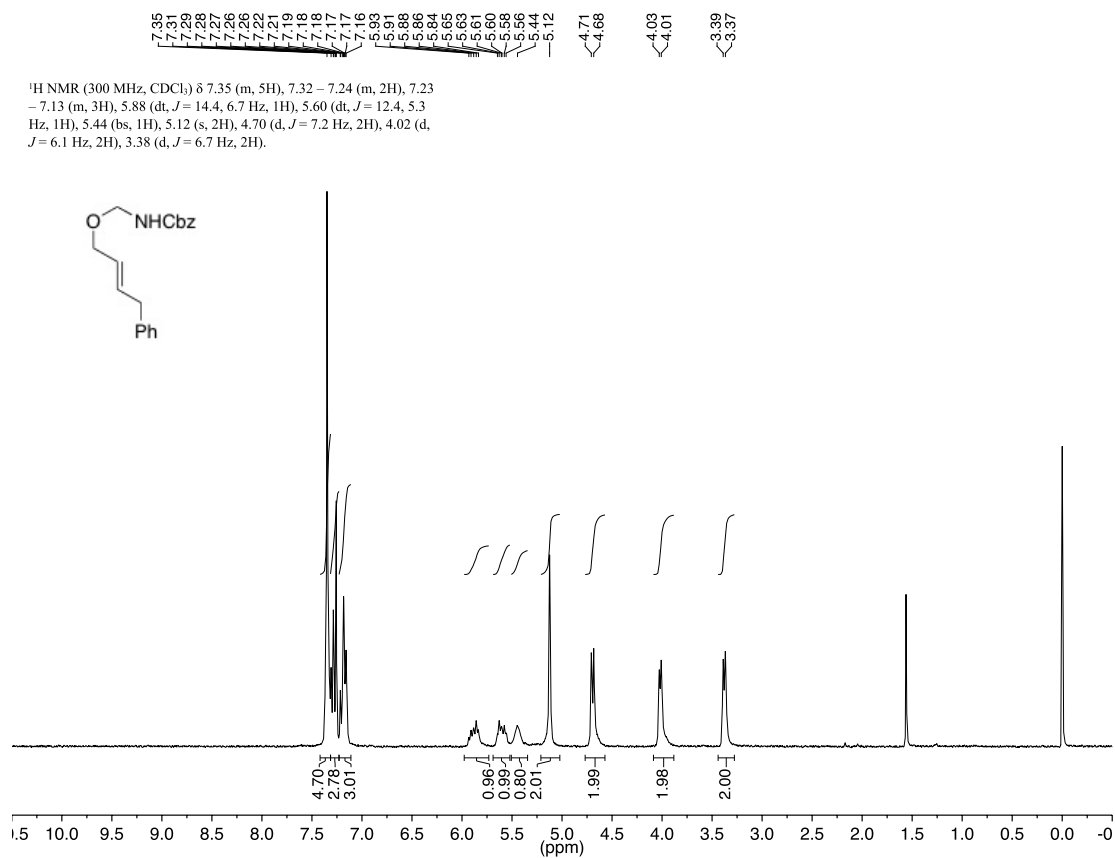
¹³C NMR (75 MHz, CDCl₃) δ 171.77, 155.87, 135.89, 128.62, 128.40, 128.30, 67.39, 66.71, 21.00.

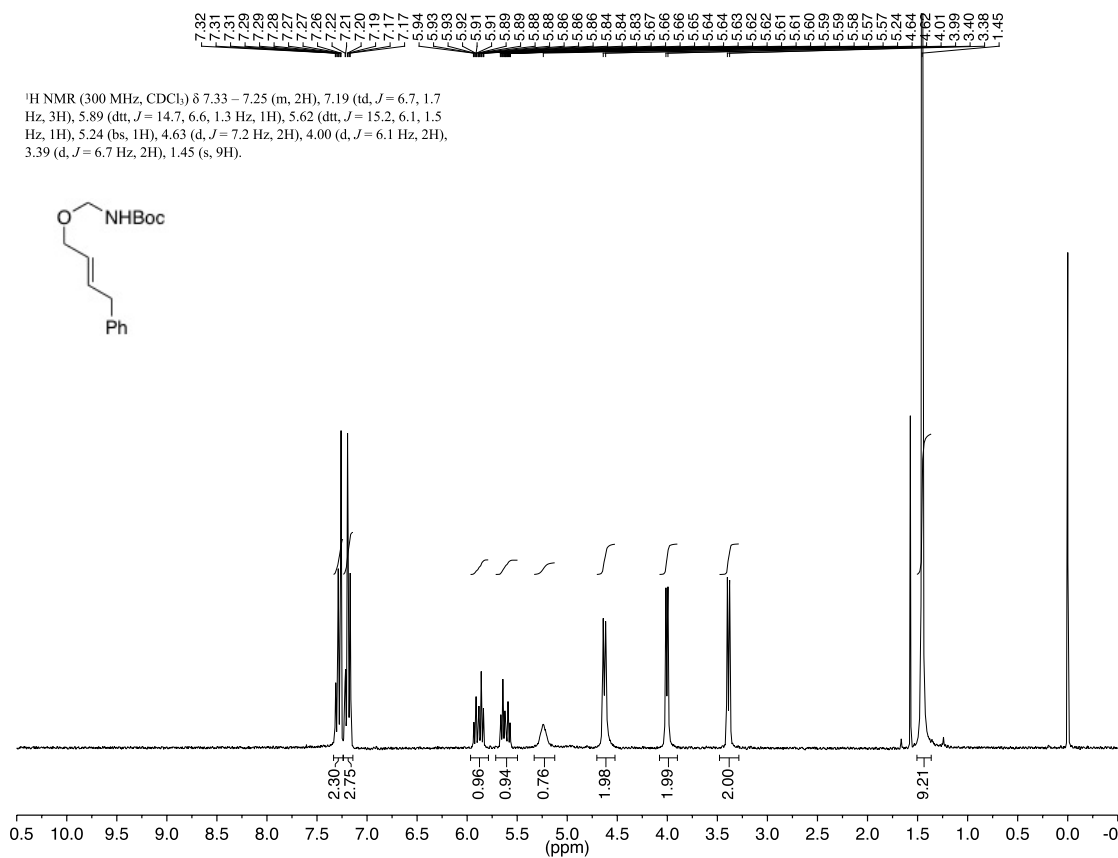




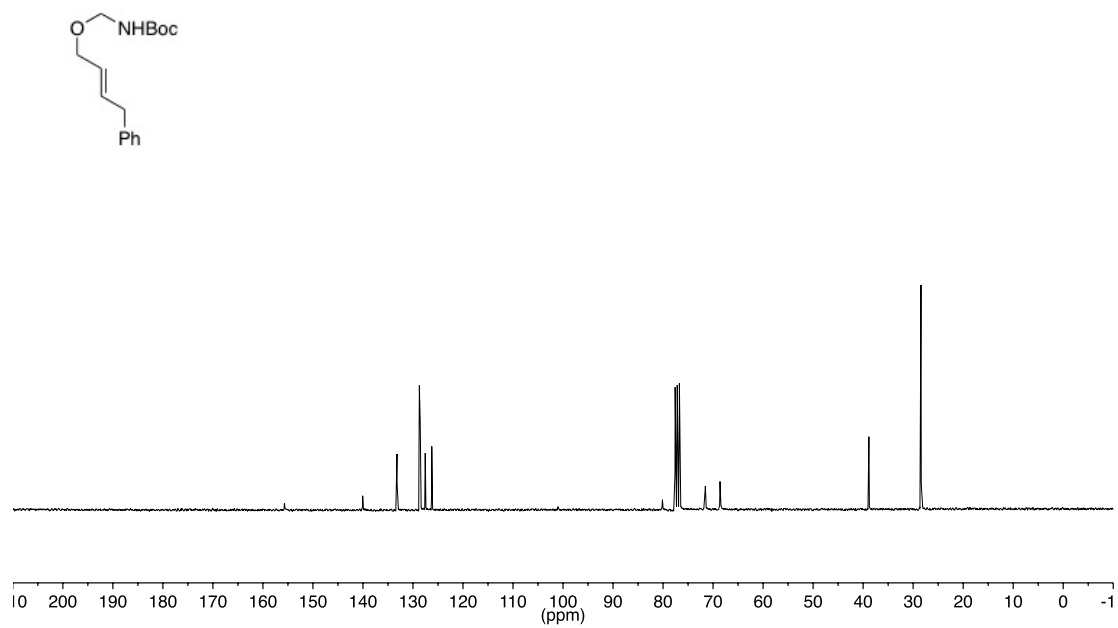


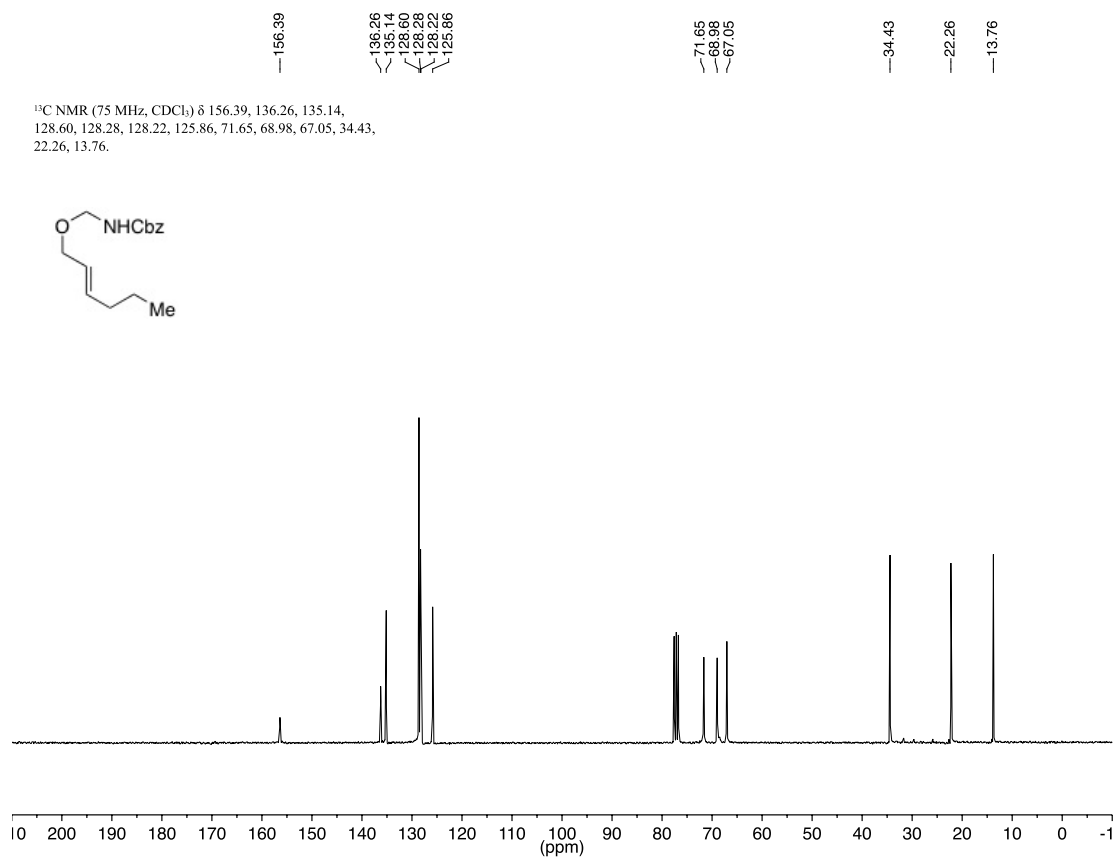
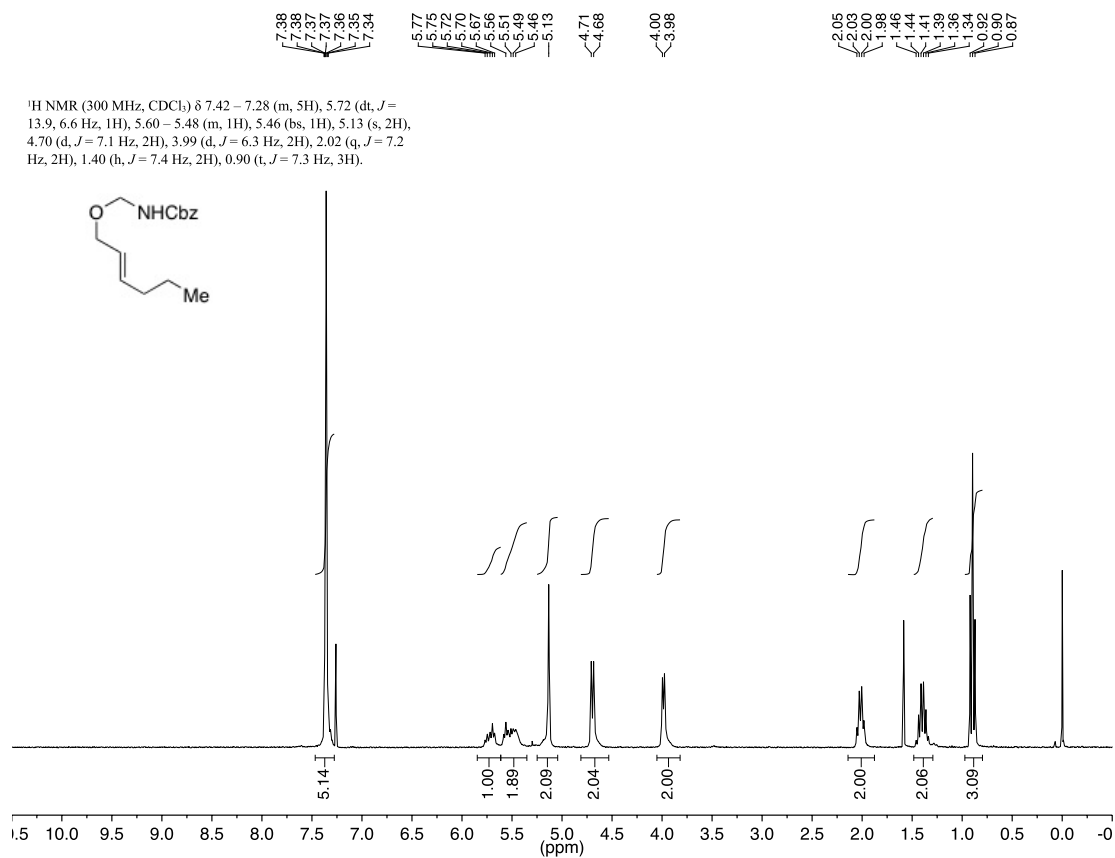


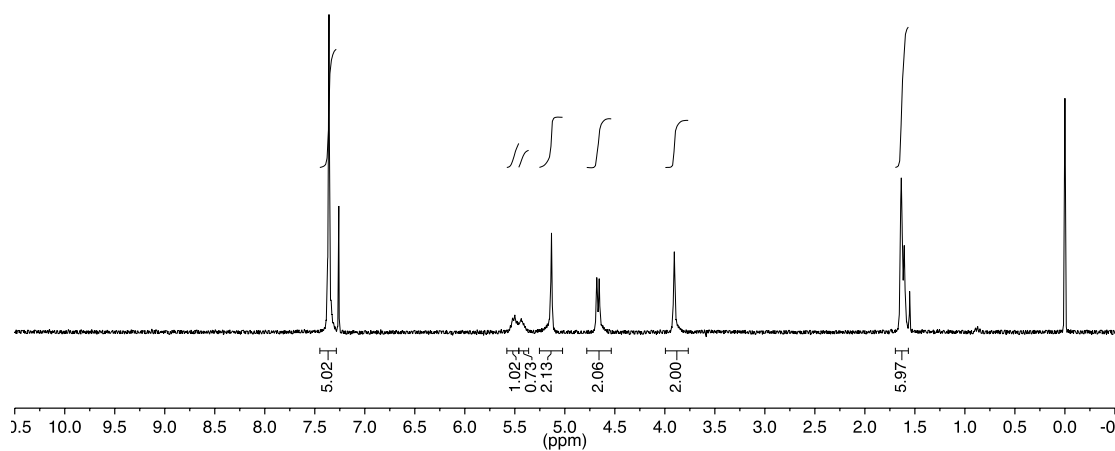
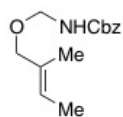
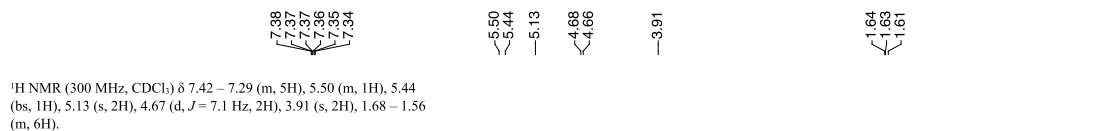




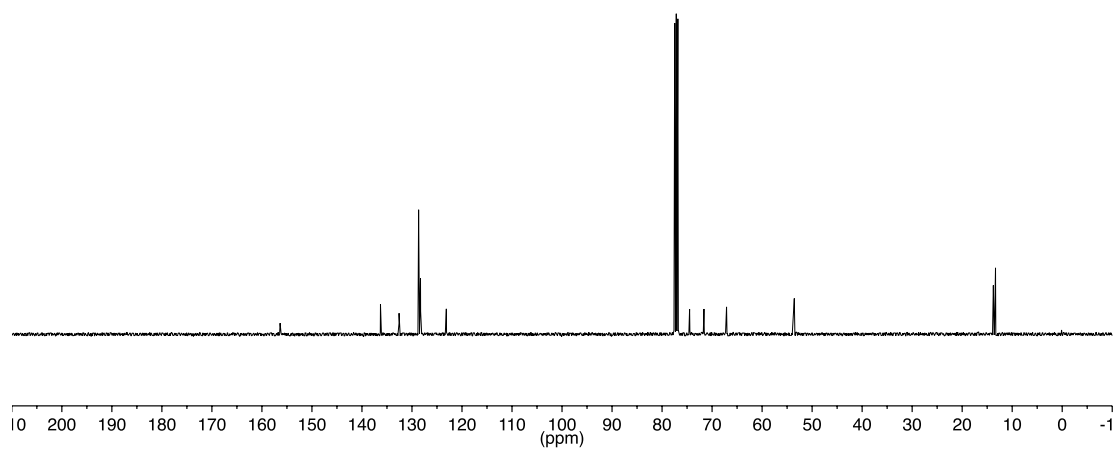
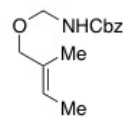
¹³C NMR (75 MHz, CDCl₃) δ 155.68, 140.05, 133.19, 128.72, 128.57, 127.55, 126.24, 80.12, 71.55, 68.61, 38.85, 28.44.

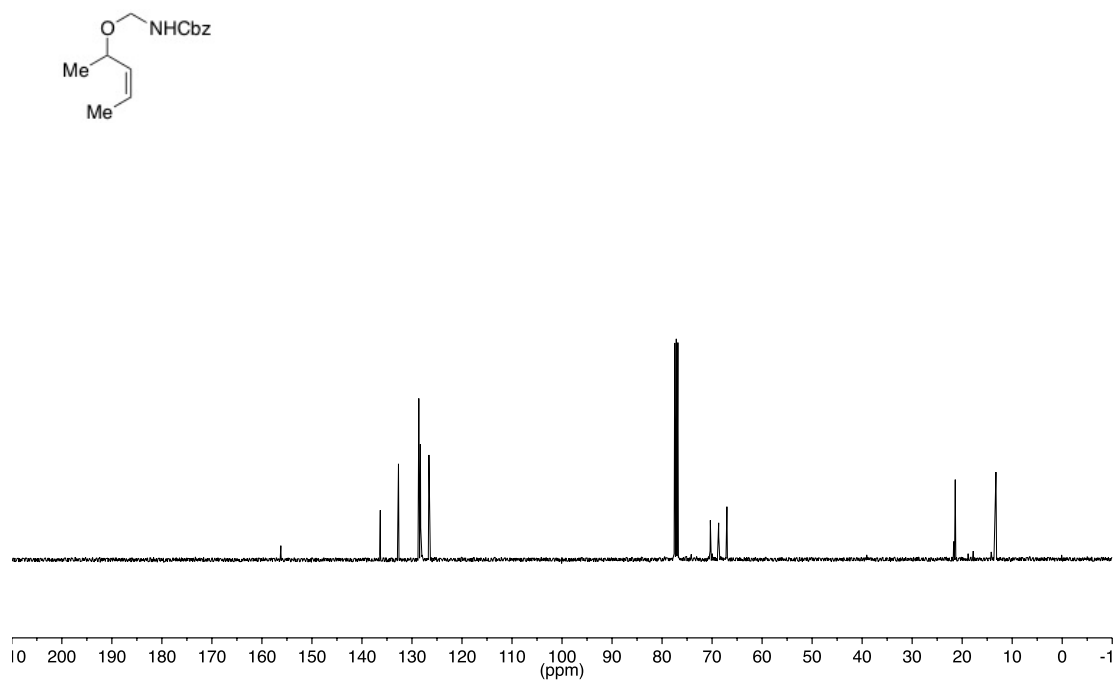
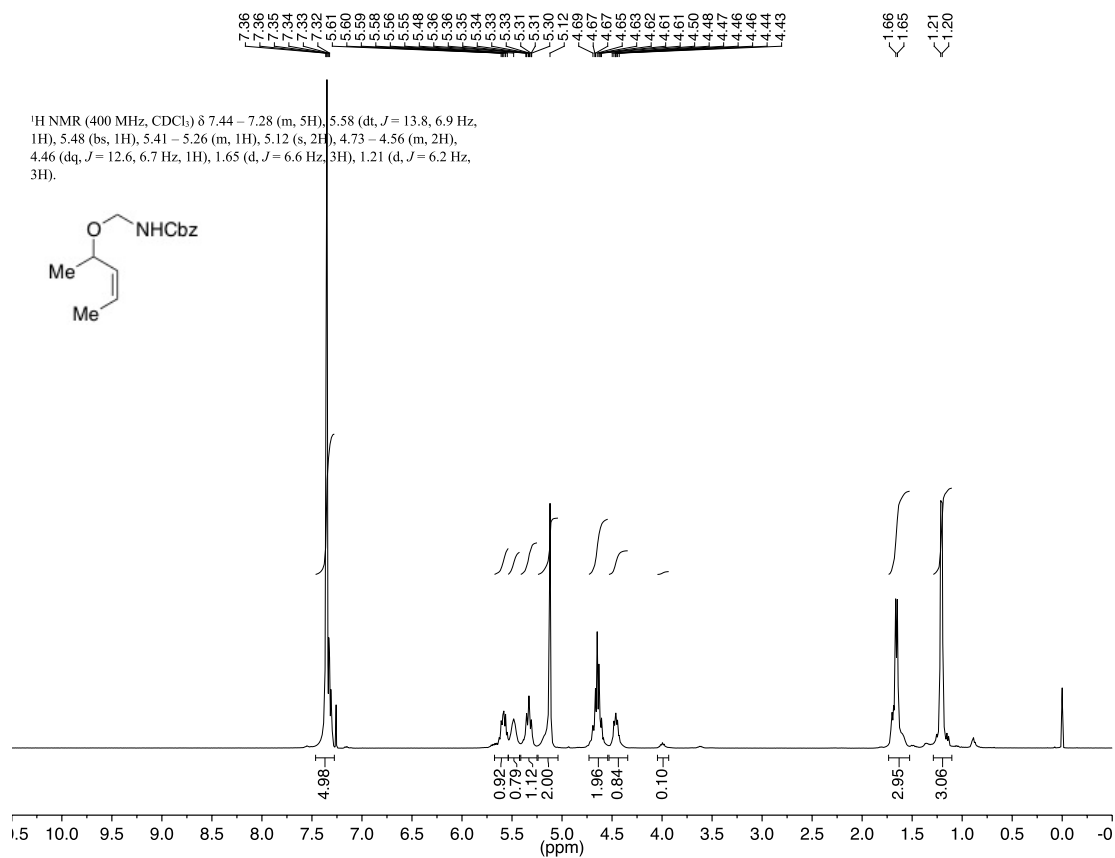


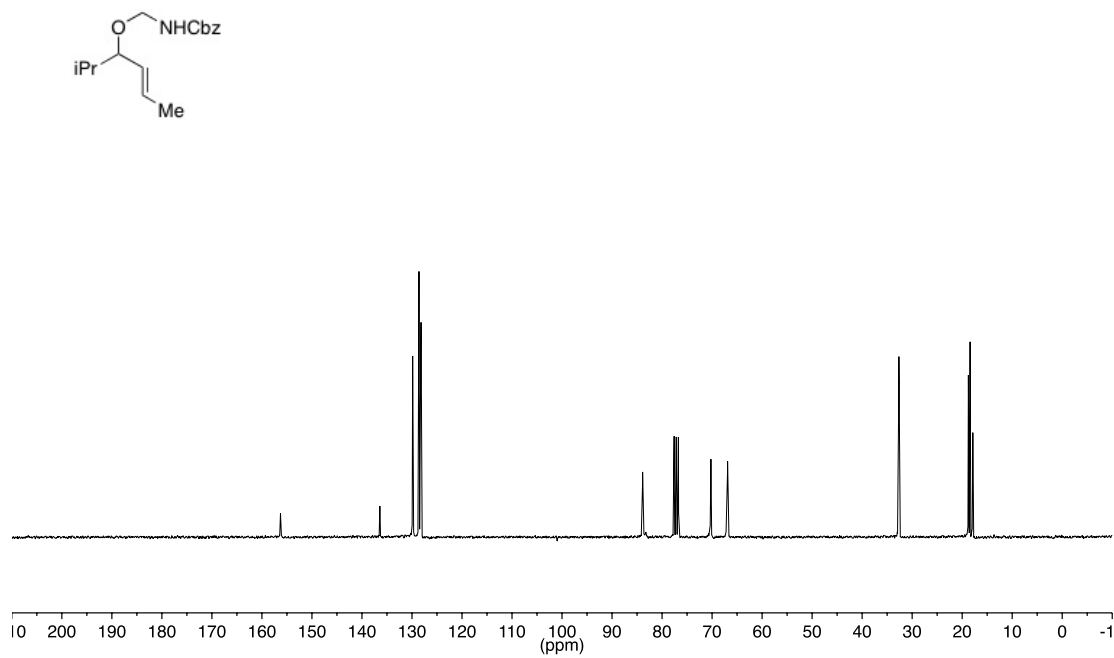
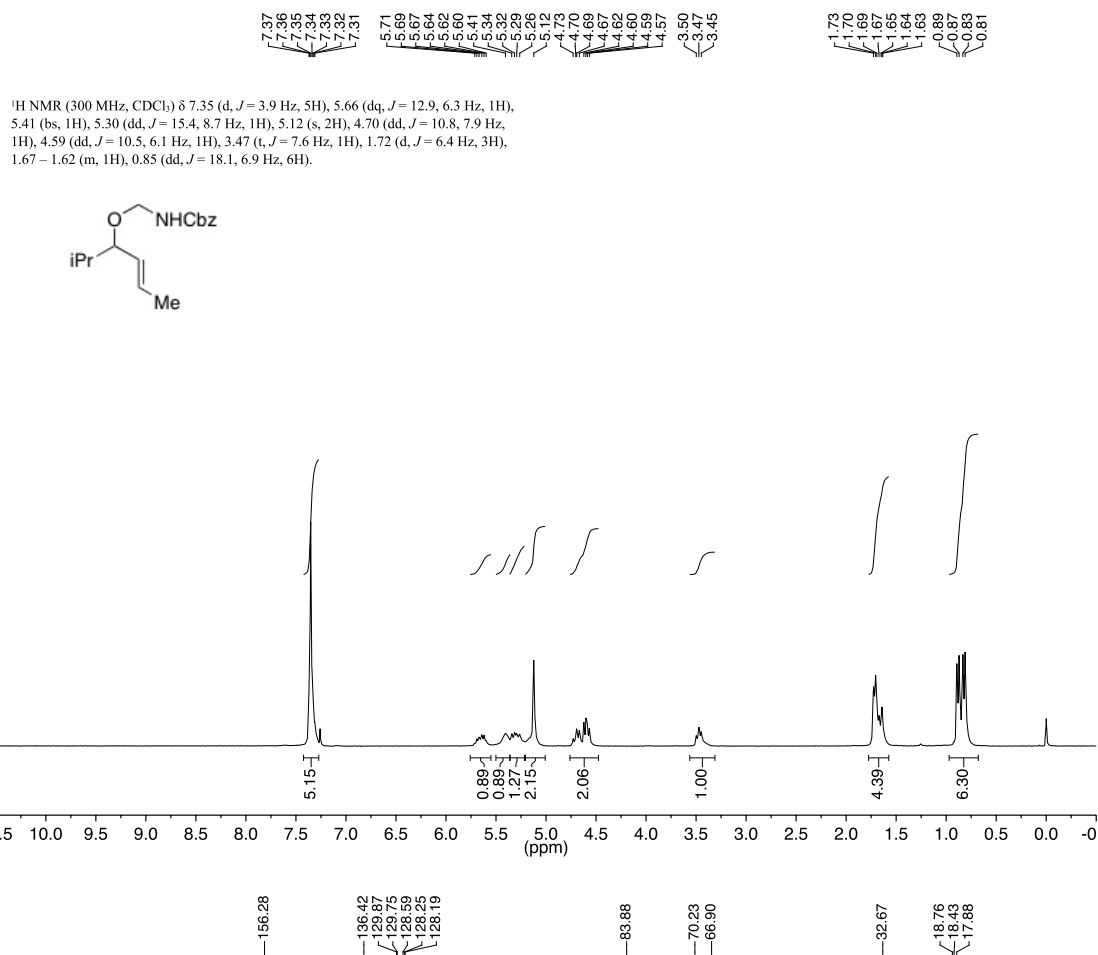


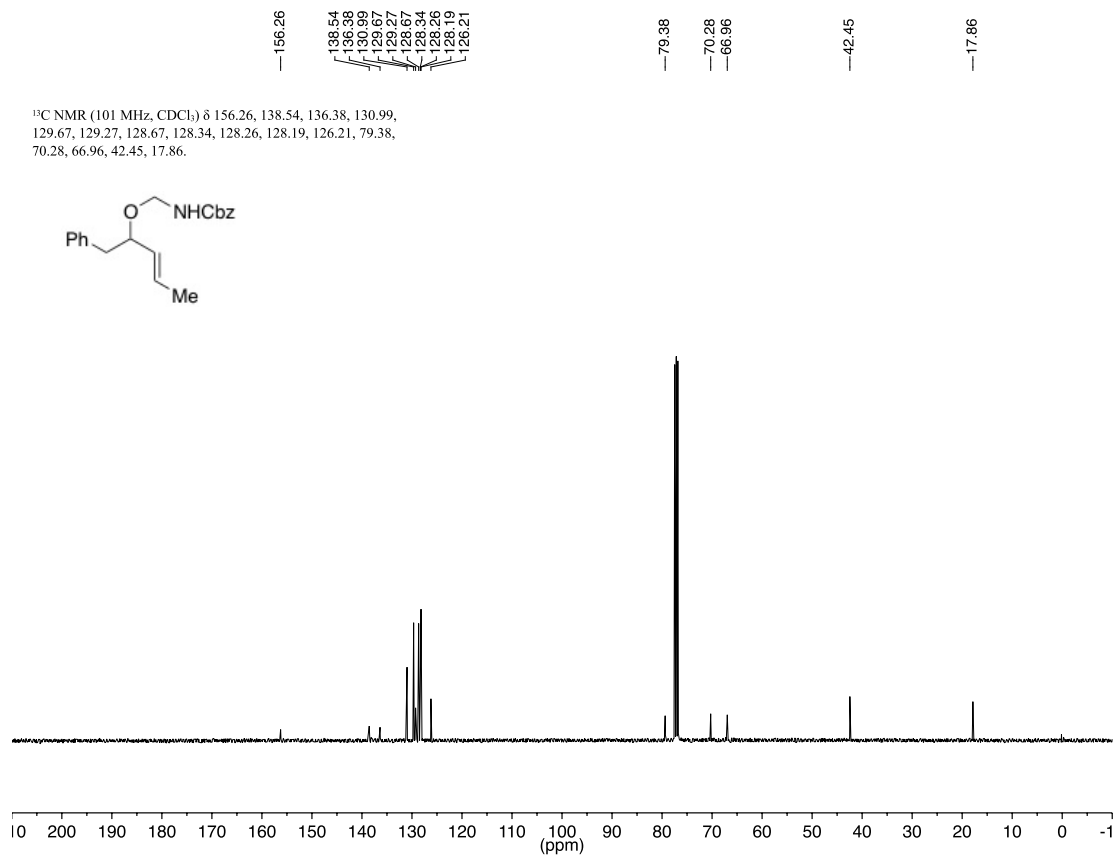
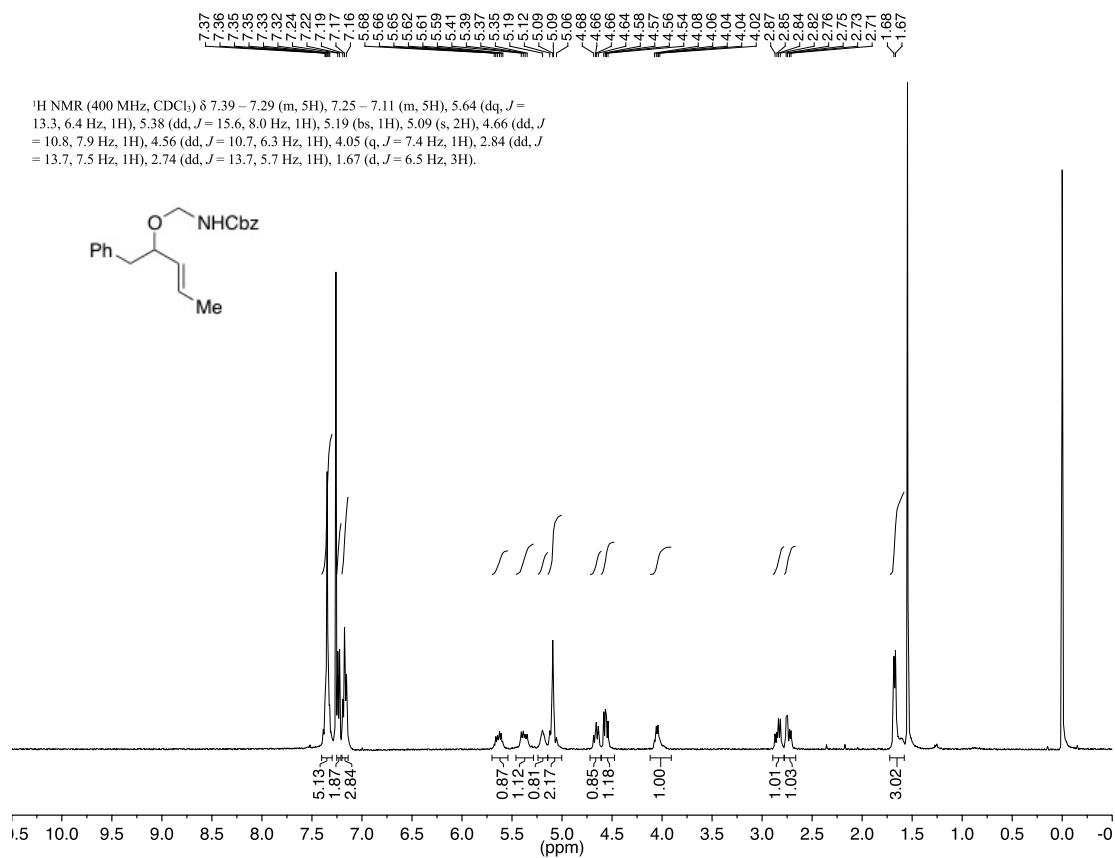


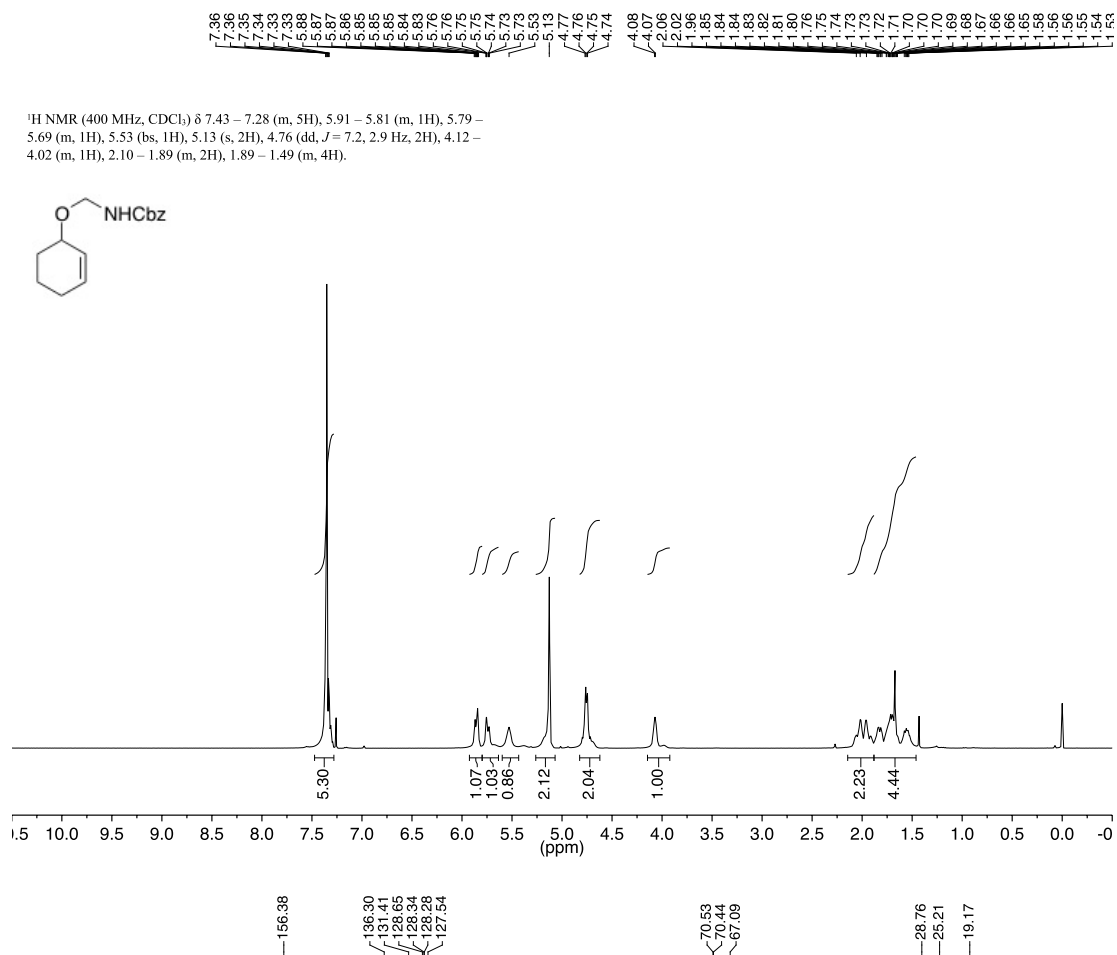
¹³C NMR (101 MHz, CDCl₃) δ 156.37, 136.29, 132.58, 128.67, 128.36, 128.29, 123.13, 74.50, 71.63, 67.11, 53.56, 13.77, 13.33.



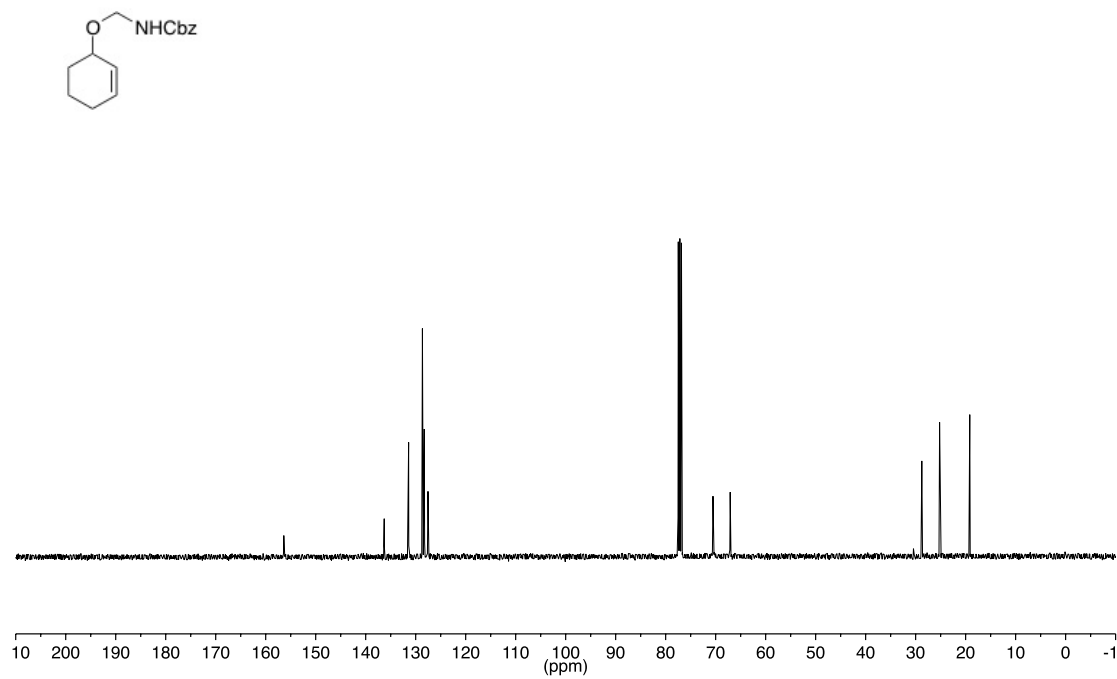


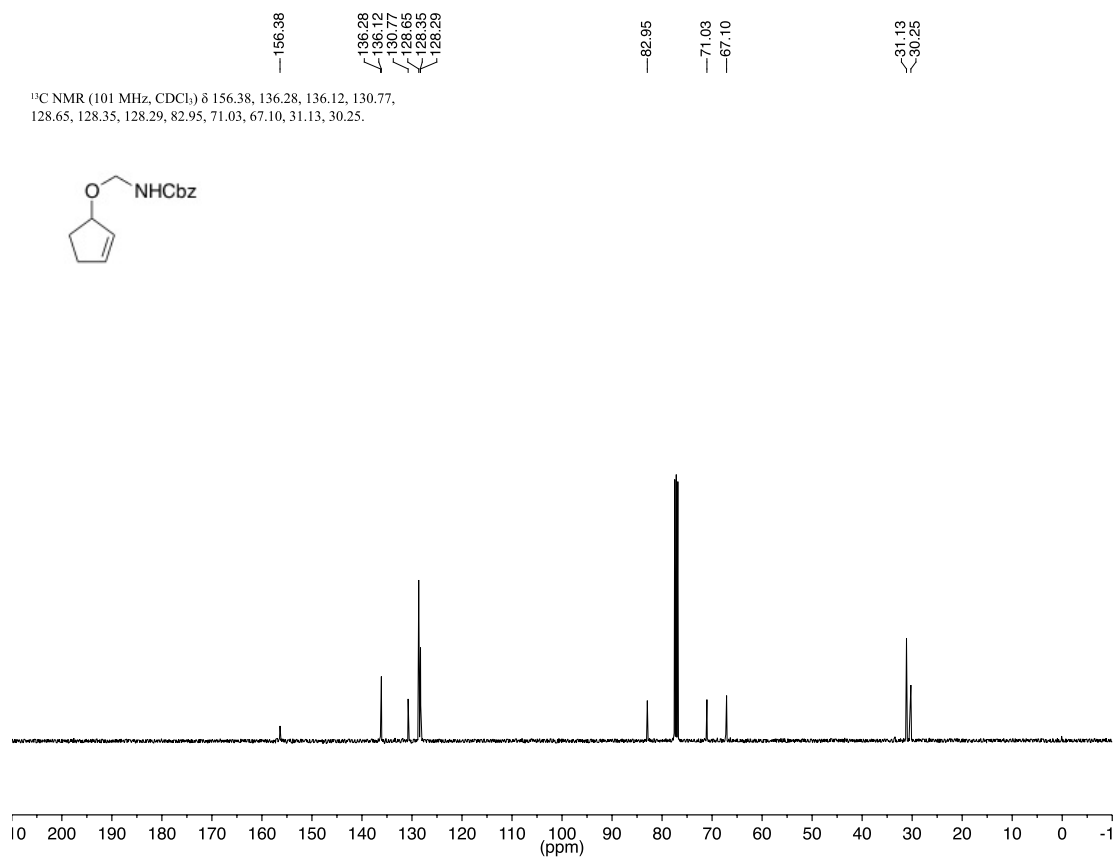
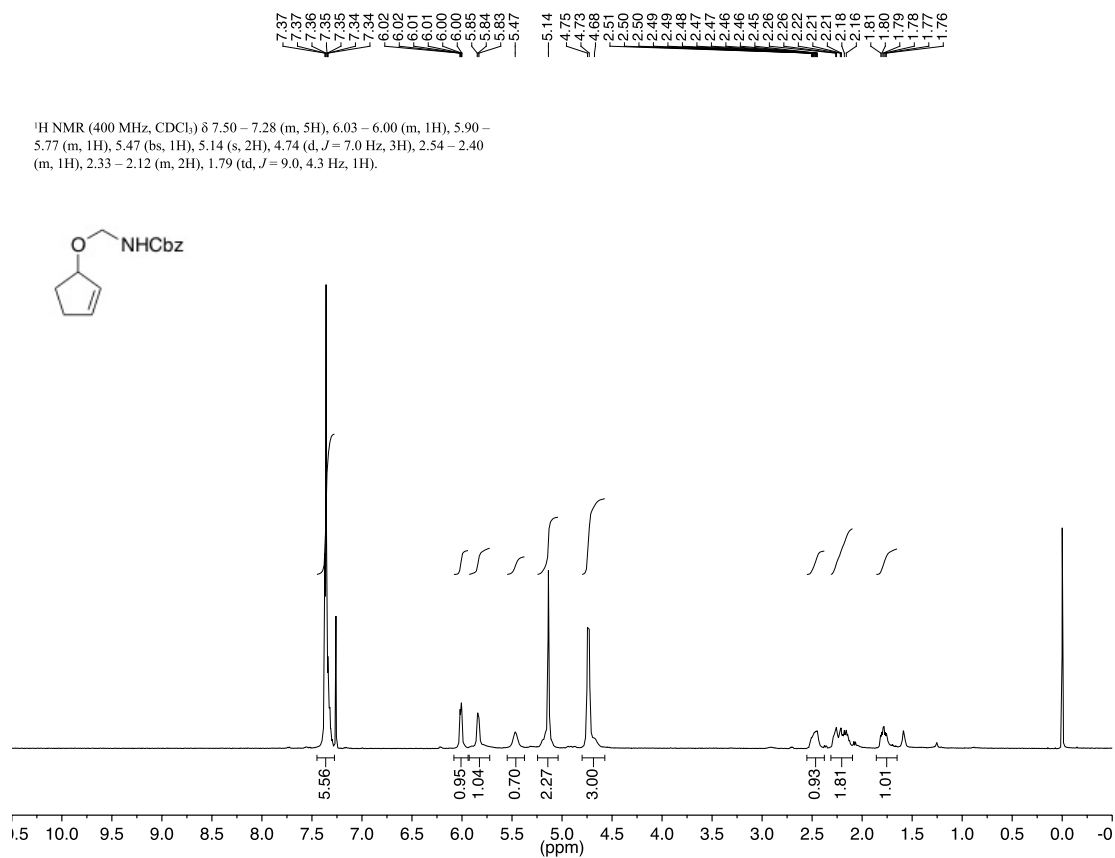


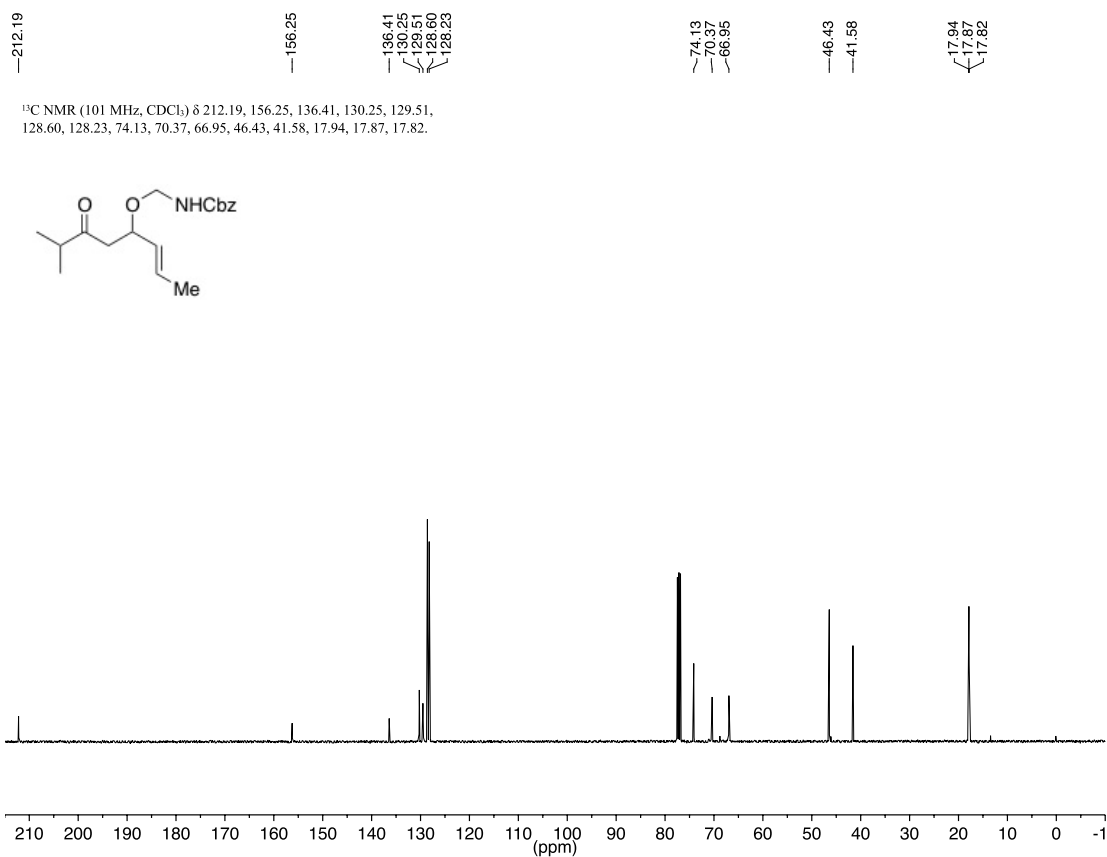
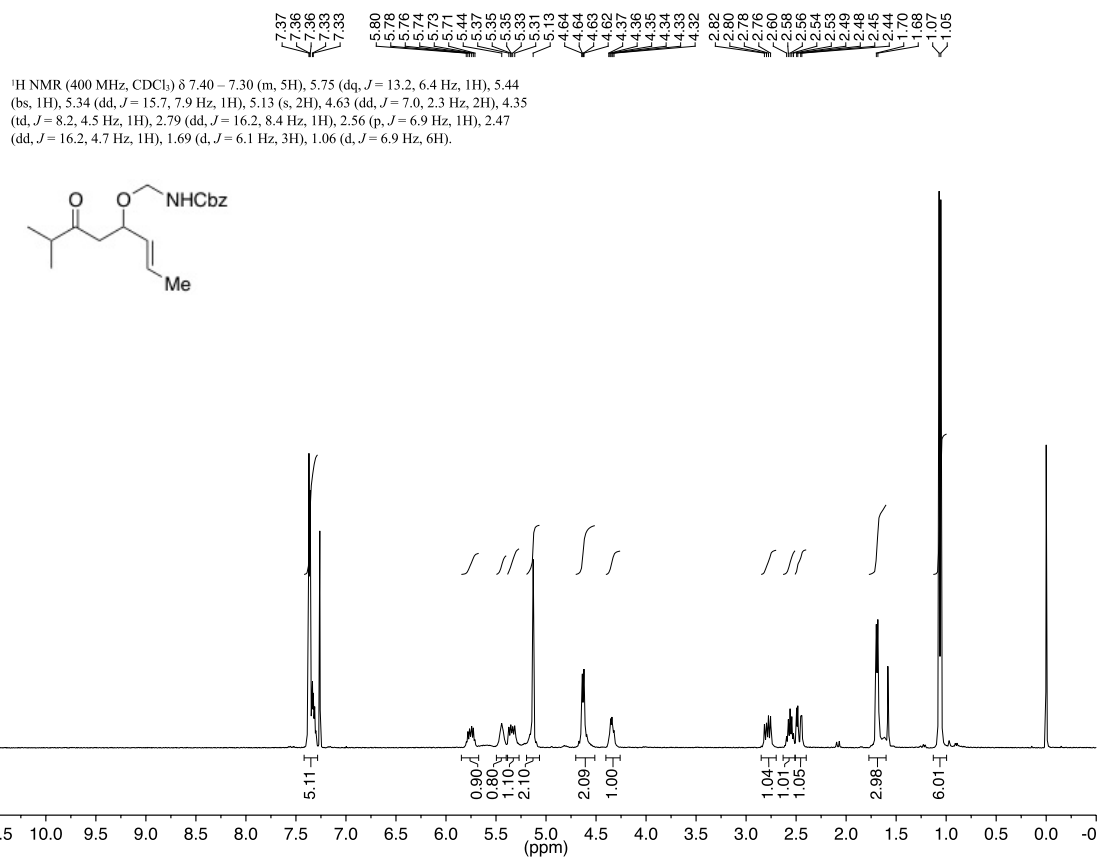




¹³C NMR (101 MHz, CDCl₃) δ 156.38, 136.30, 131.41, 128.65, 128.34, 128.28, 127.54, 70.53, 70.44, 67.09, 28.76, 25.21, 19.17.

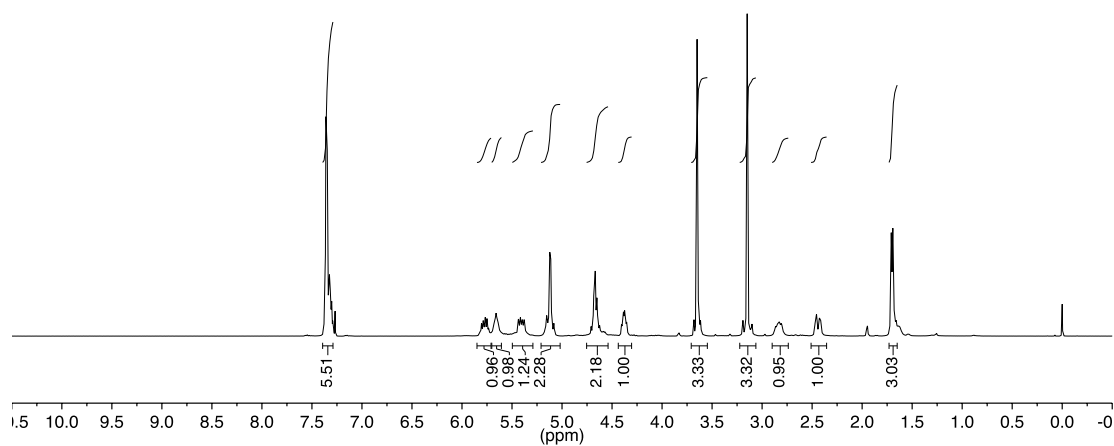
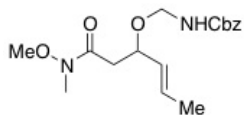




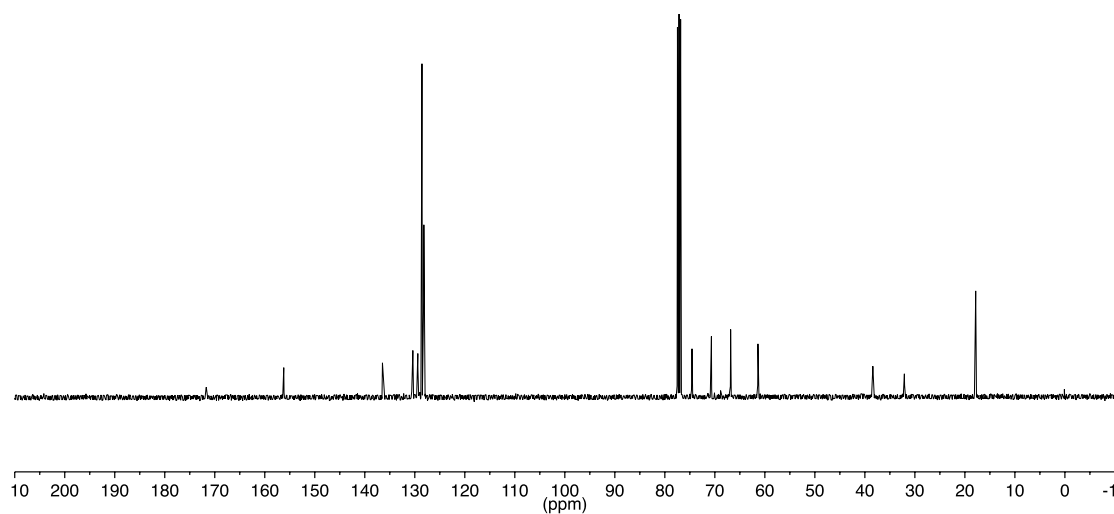
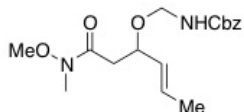




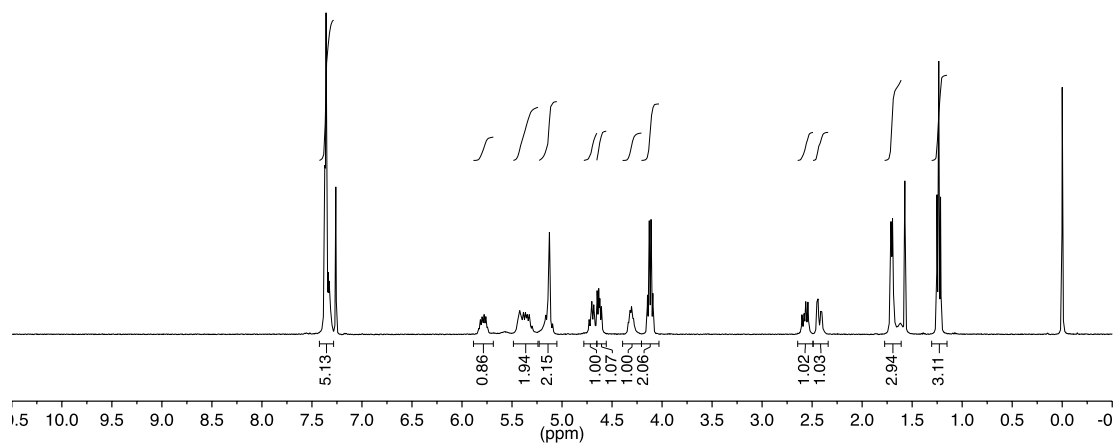
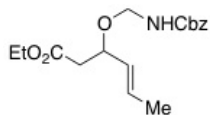
^1H NMR (400 MHz, CDCl_3) δ 7.47 – 7.28 (m, 5H), 5.78 (dq, J = 13.3, 6.5 Hz, 1H), 5.66 (bs, 1H), 5.41 (dd, J = 15.5, 7.9 Hz, 1H), 5.12 (d, J = 4.3 Hz, 2H), 4.66 (q, J = 10.7, 8.4 Hz, 2H), 4.38 (td, J = 8.3, 4.5 Hz, 1H), 3.65 (s, 3H), 3.15 (s, 3H), 2.84 (dd, J = 15.7, 8.6 Hz, 1H), 2.44 (dd, J = 15.5, 4.5 Hz, 1H), 1.70 (d, J = 6.6 Hz, 3H).



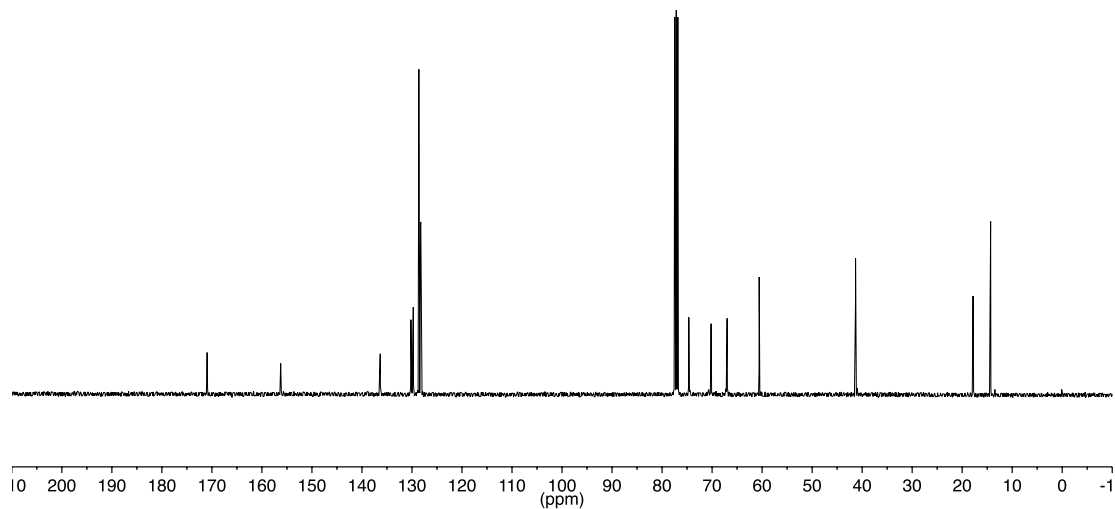
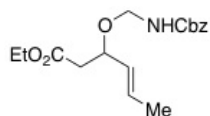
^{13}C NMR (101 MHz, CDCl_3) δ 171.70, 156.20, 136.47, 130.39, 129.39, 128.57, 128.22, 128.19, 74.57, 70.68, 66.84, 61.38, 38.40, 32.10, 17.84.

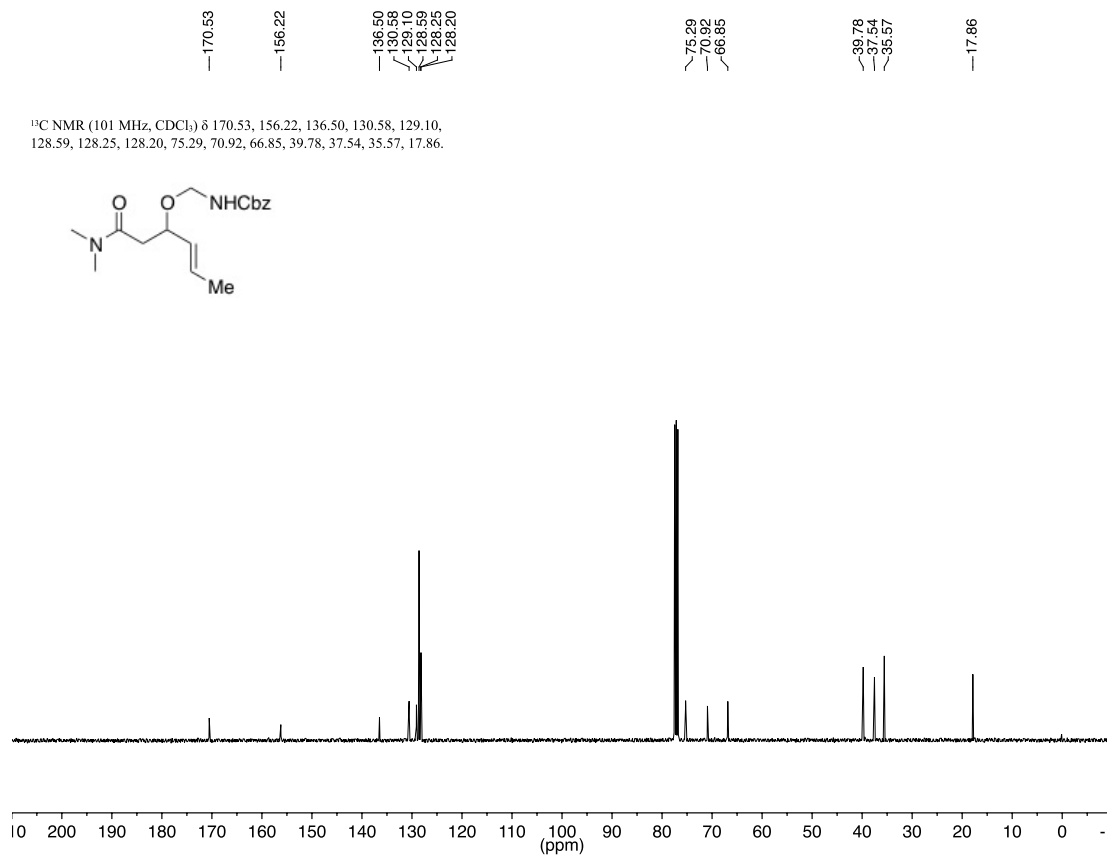
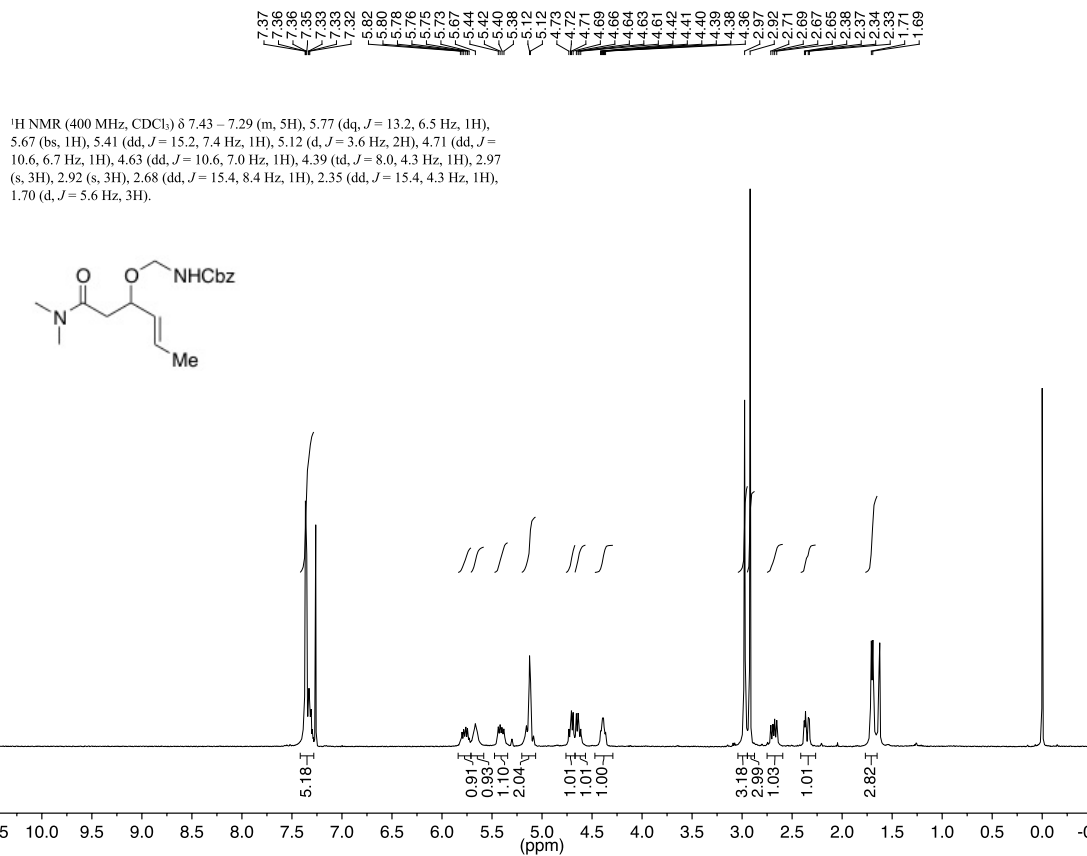


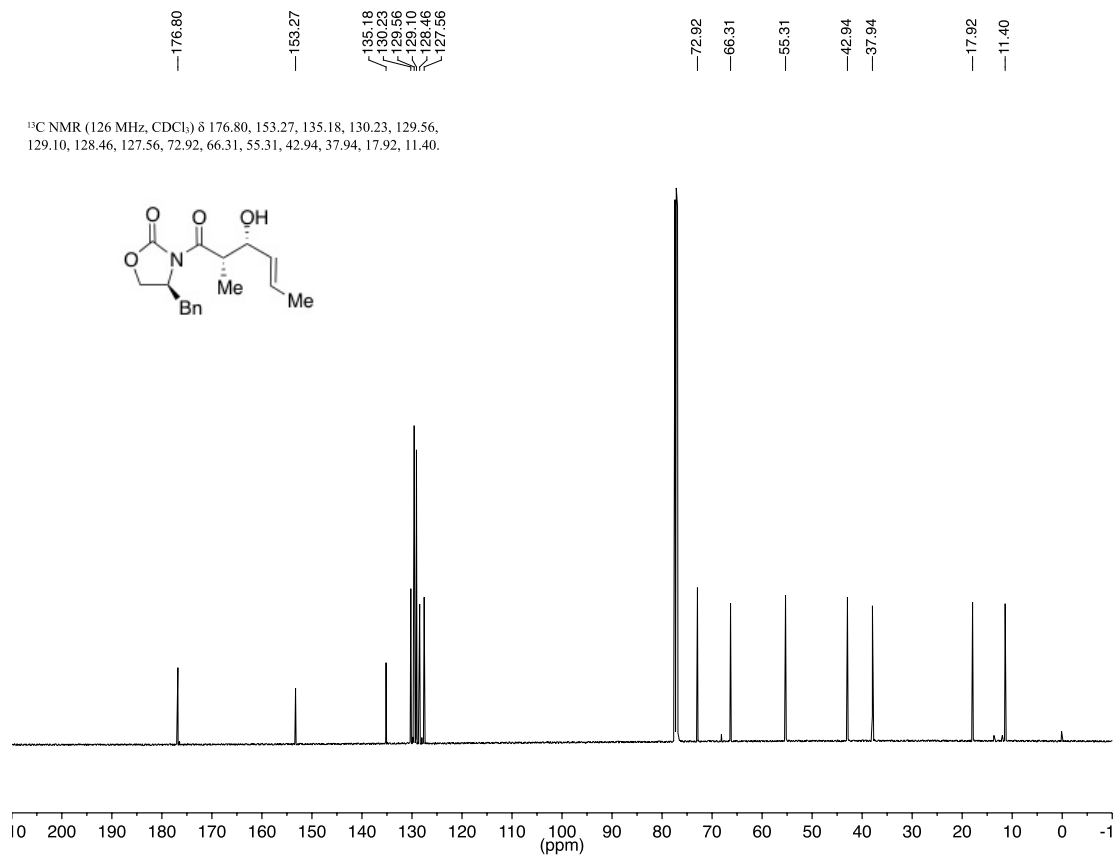
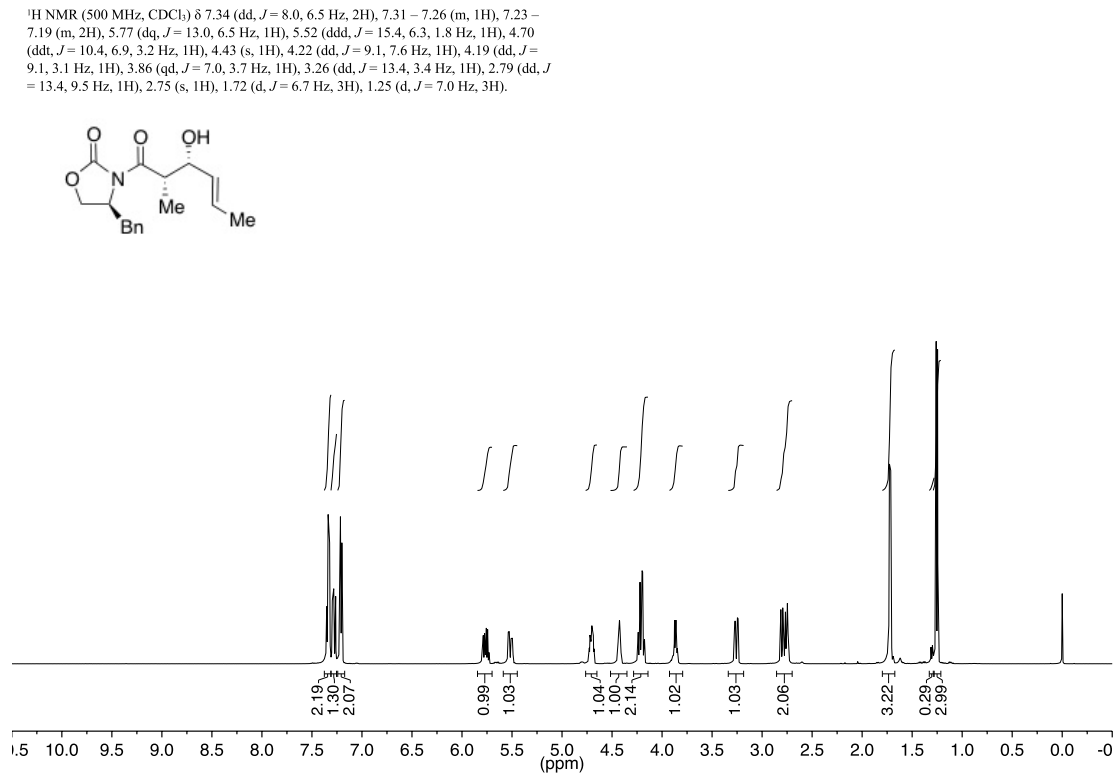
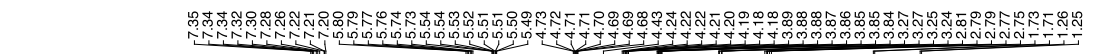
¹H NMR (400 MHz, CDCl₃) δ 7.46 – 7.29 (m, 5H), 5.79 (dq, *J* = 13.2, 6.4 Hz, 1H), 5.42 (bs, 1H), 5.40 – 5.27 (m, 1H), 5.13 (d, *J* = 3.1 Hz, 2H), 4.71 (dd, *J* = 10.8, 7.7 Hz, 1H), 4.63 (dd, *J* = 10.7, 6.3 Hz, 1H), 4.31 (td, *J* = 8.3, 4.9 Hz, 1H), 4.12 (q, *J* = 7.1 Hz, 2H), 2.57 (dd, *J* = 15.3, 8.5 Hz, 1H), 2.43 (dd, *J* = 15.1, 5.0 Hz, 1H), 1.70 (d, *J* = 6.5 Hz, 3H), 1.23 (t, *J* = 7.1 Hz, 3H).

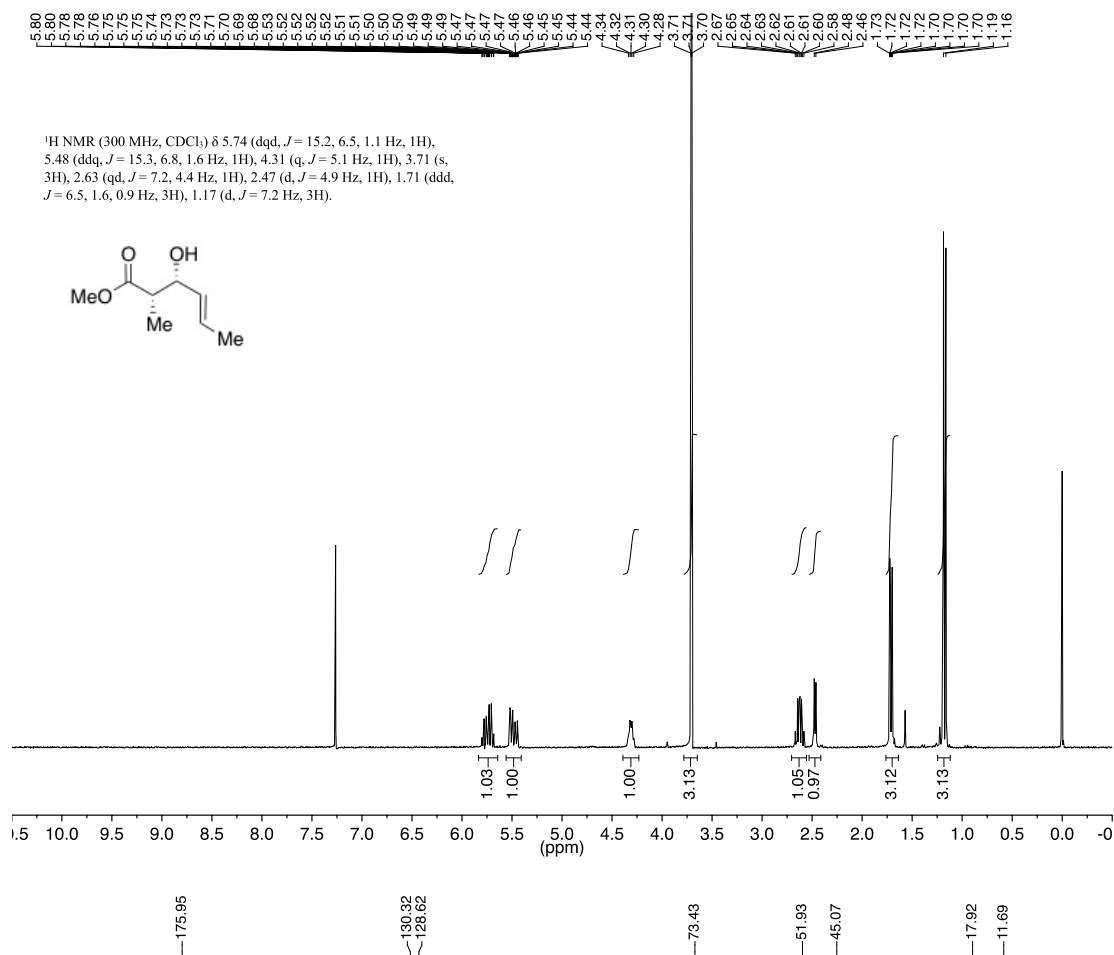


¹³C NMR (101 MHz, CDCl₃) δ 170.96, 156.25, 136.35, 130.21, 129.74, 128.62, 128.28, 128.24, 74.65, 70.20, 66.99, 60.58, 41.31, 17.83, 14.31.

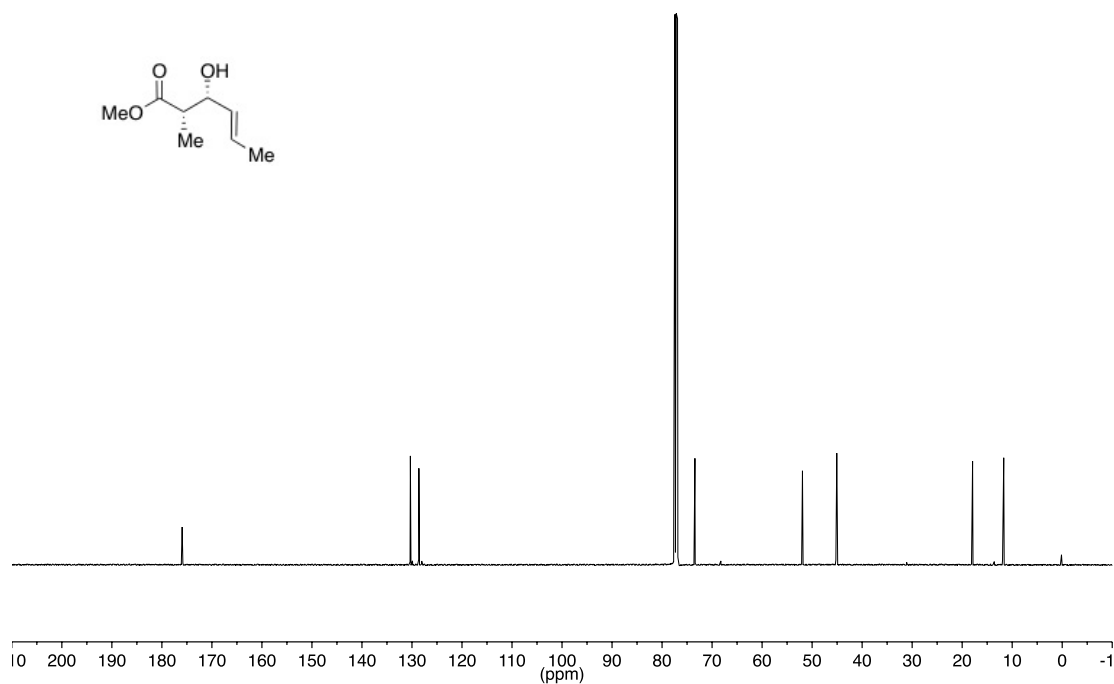


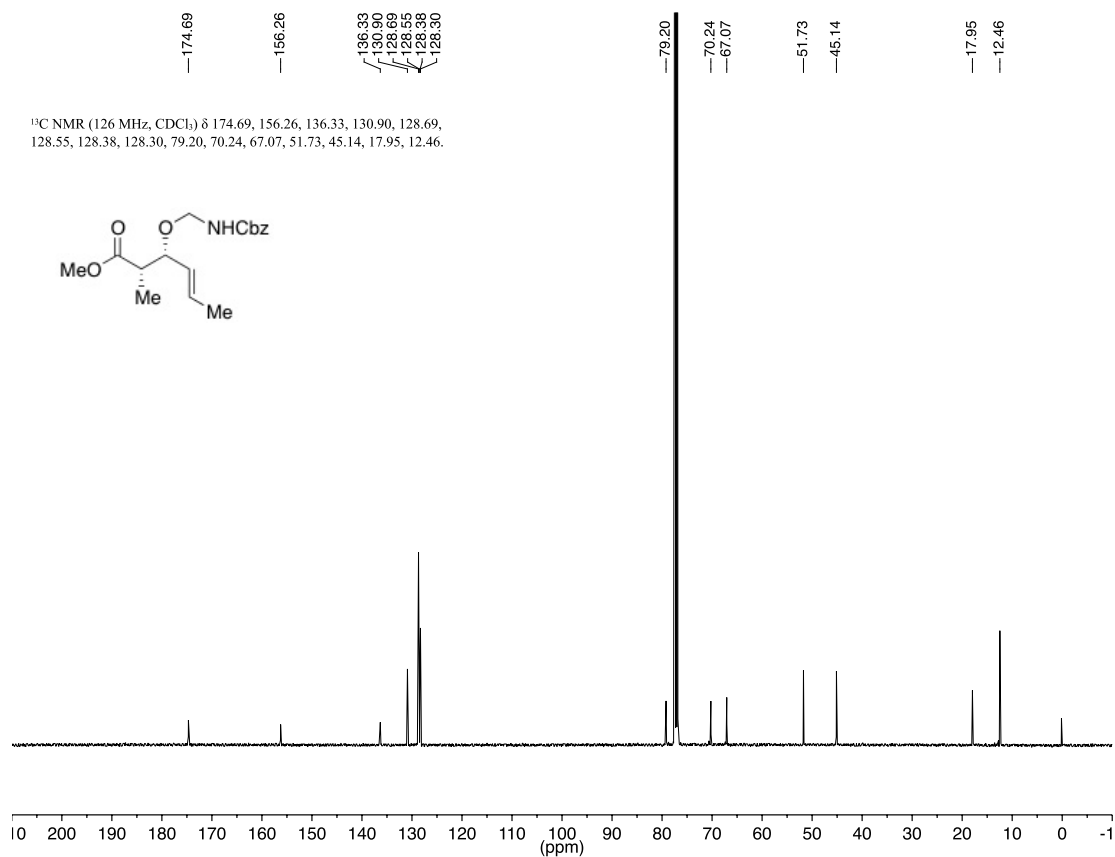
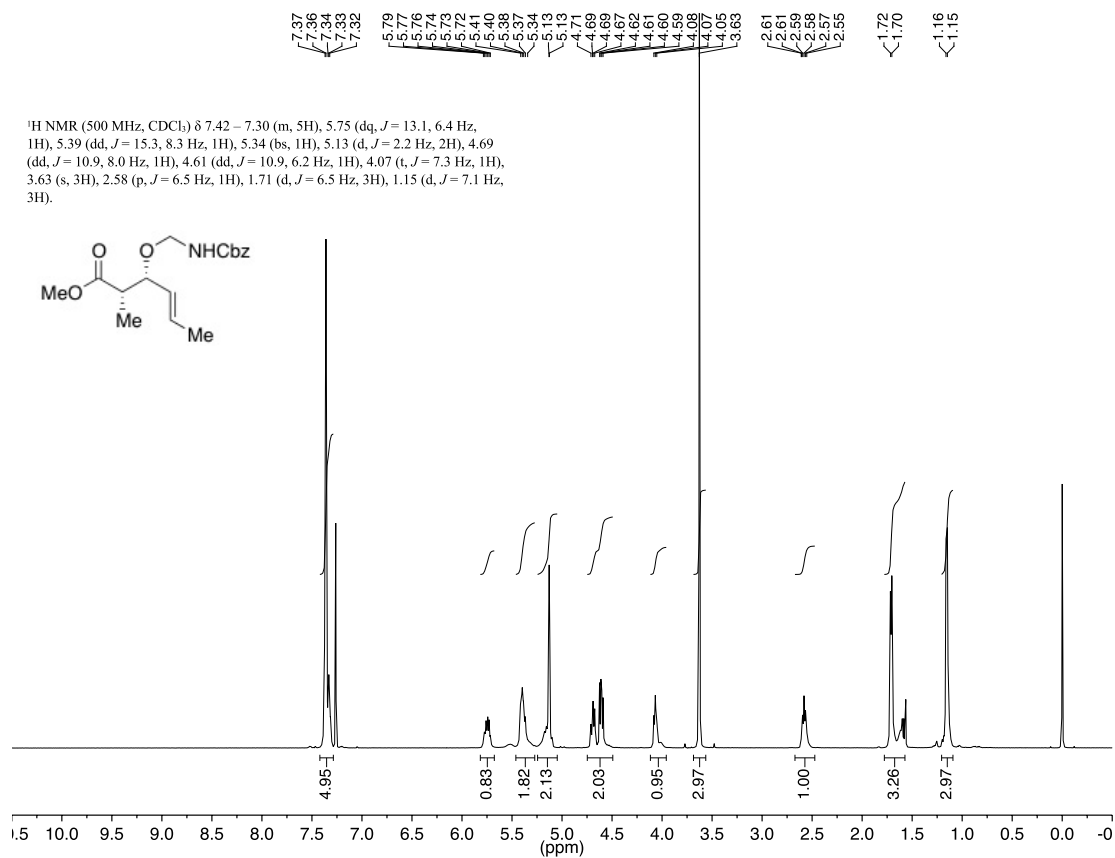






¹³C NMR (126 MHz, CDCl₃) δ 175.95, 130.32, 128.62, 73.43, 51.93, 45.07, 17.92, 11.69.



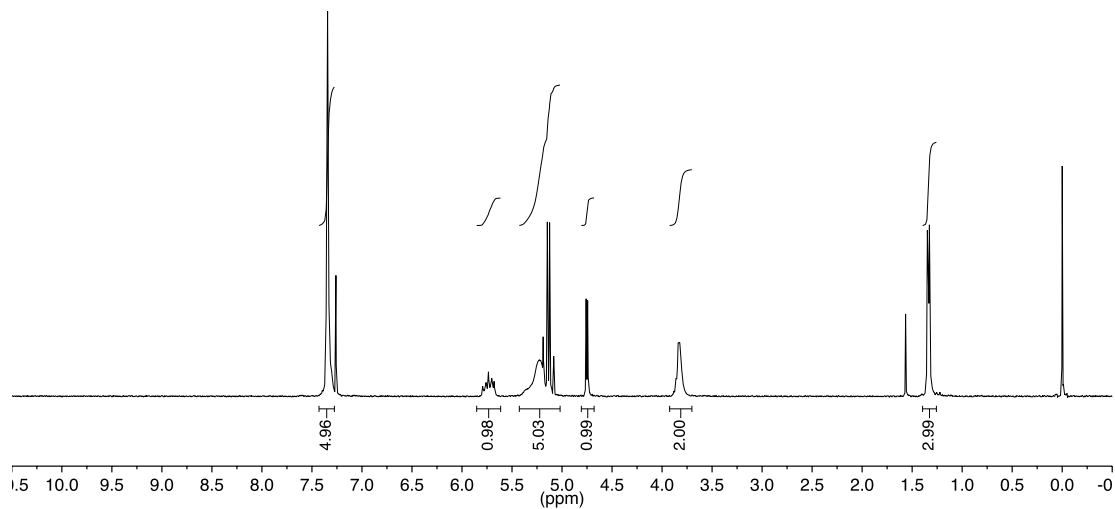
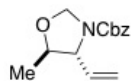


7.37
7.36
7.34
7.33
7.32
7.30
5.79
5.77
5.76
5.74
5.71
5.70
5.68
5.35
5.19
5.15
5.12
5.08
4.76
4.74

3.86
3.82

1.35
1.33

¹H NMR (300 MHz, CDCl₃) δ 7.43 – 7.28 (m, 5H), 5.74 (ddd, *J* = 17.0, 10.0, 6.9 Hz, 1H), 5.35 (m, 1H), 5.23 (m, 2H), 5.17 (d, *J* = 12.4 Hz, 1H), 5.10 (d, *J* = 12.4 Hz, 1H), 4.75 (d, *J* = 4.6 Hz, 1H), 3.86 (m, 1H), 3.82 (m, 1H), 1.34 (d, *J* = 6.0 Hz, 3H).



154.16

136.47

135.19

128.58

128.17

128.07

118.07

80.37

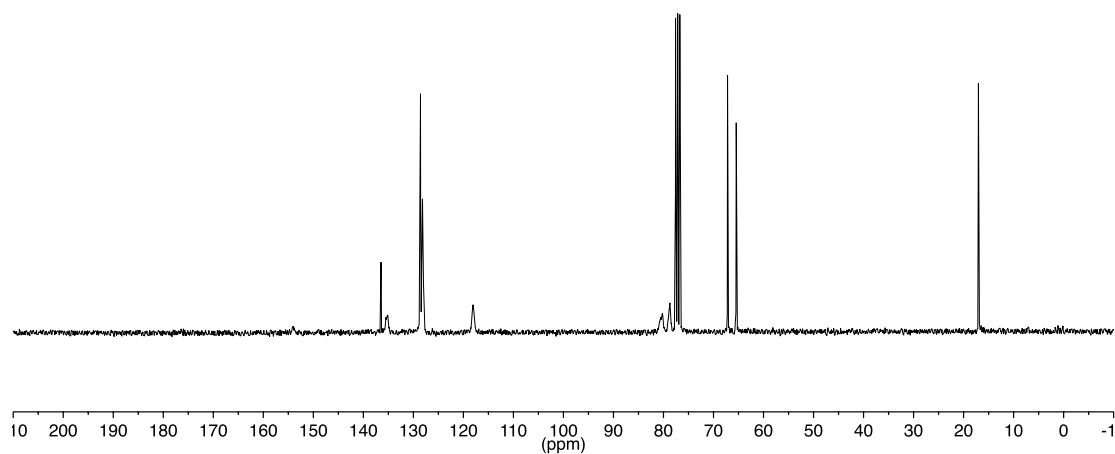
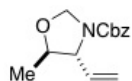
78.71

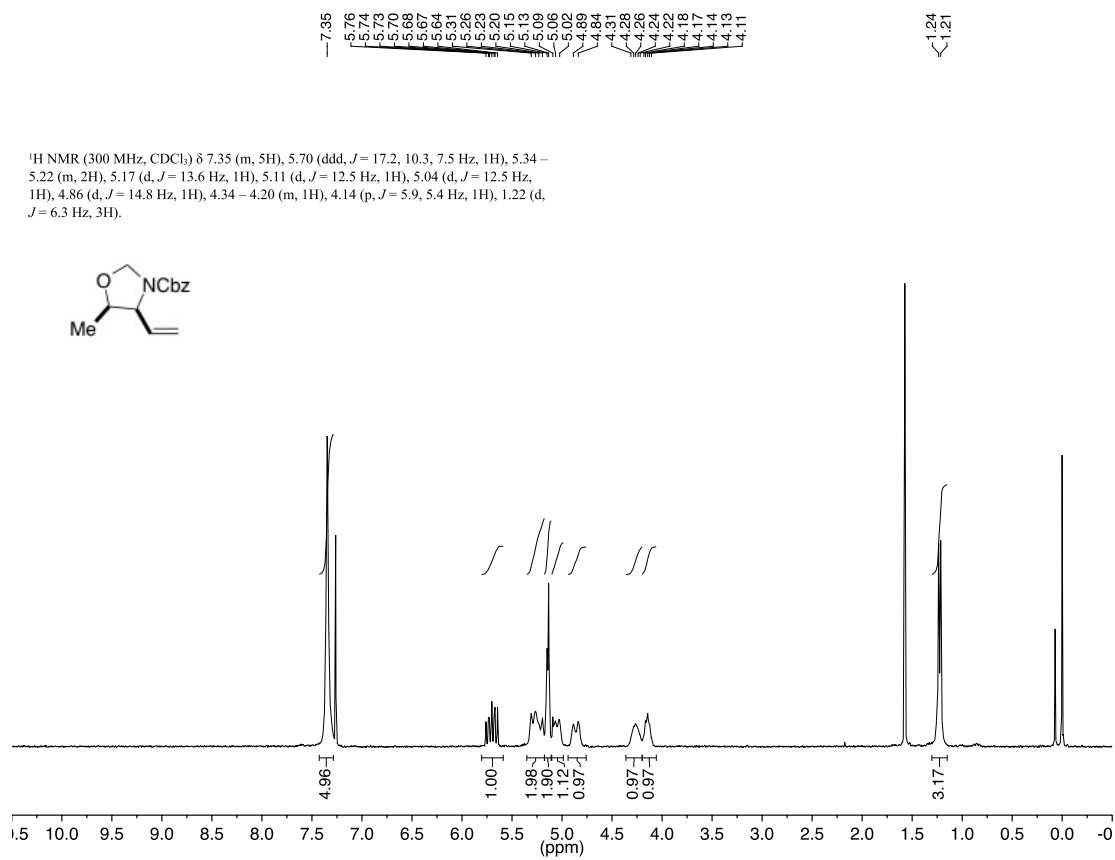
67.19

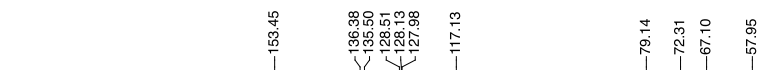
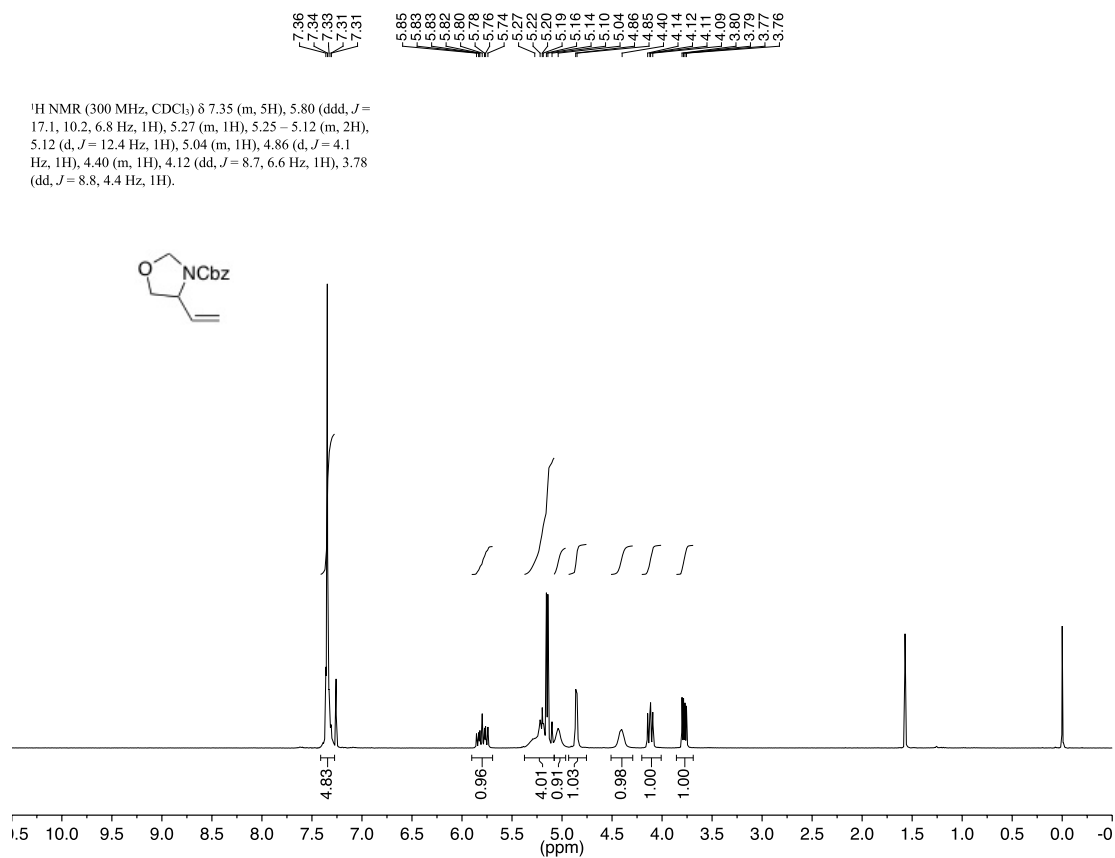
65.45

17.04

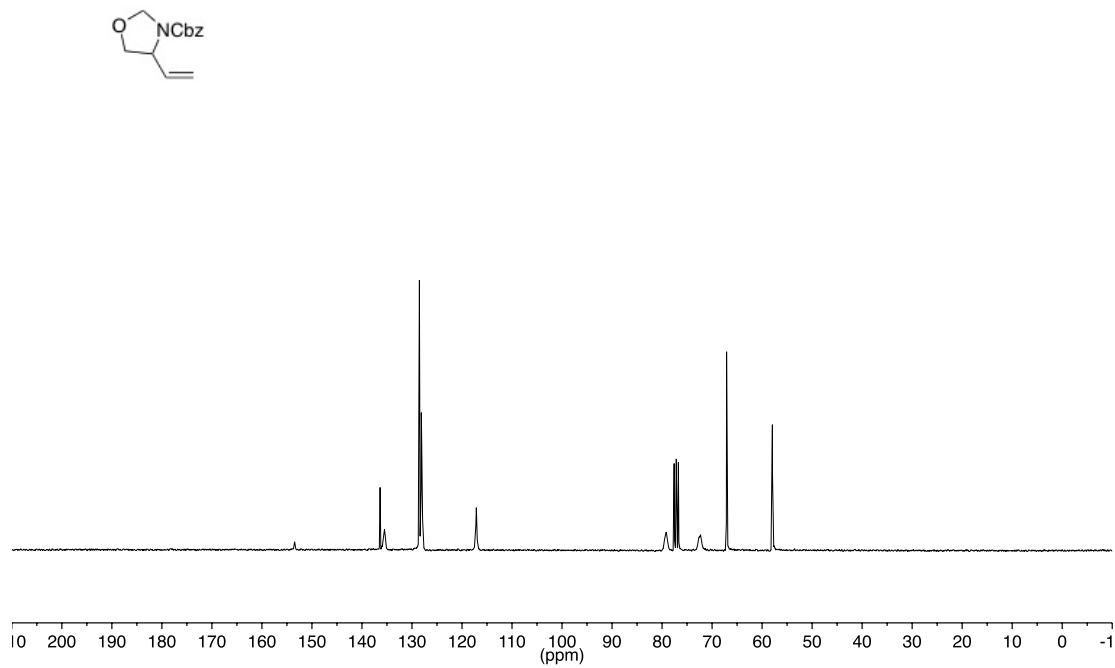
¹³C NMR (75 MHz, CDCl₃) δ 154.16, 136.47, 135.19, 128.58, 128.17, 128.07, 118.07, 80.37, 78.71, 67.19, 65.45, 17.04.





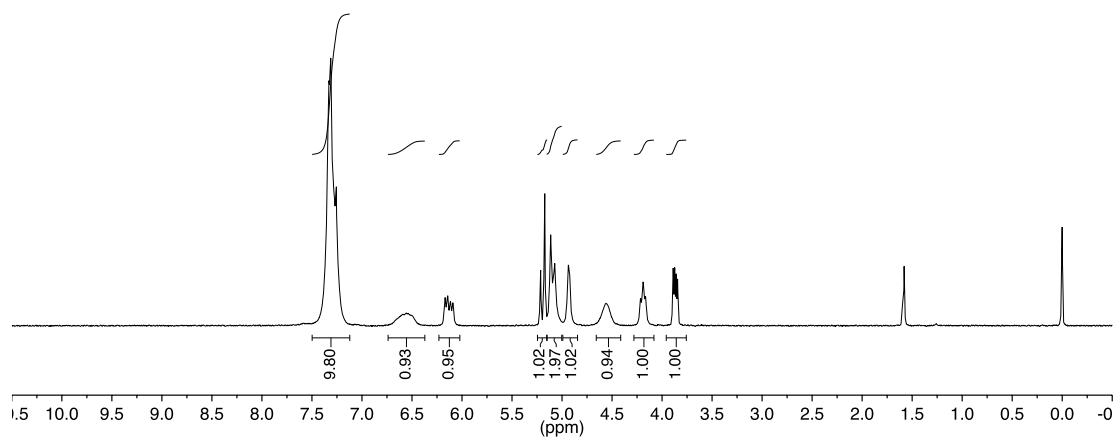
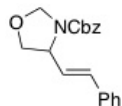


¹³C NMR (75 MHz, CDCl₃) δ 153.45, 136.38, 135.50, 128.51, 128.13, 127.98, 117.13, 79.14, 72.31, 67.10, 57.95.



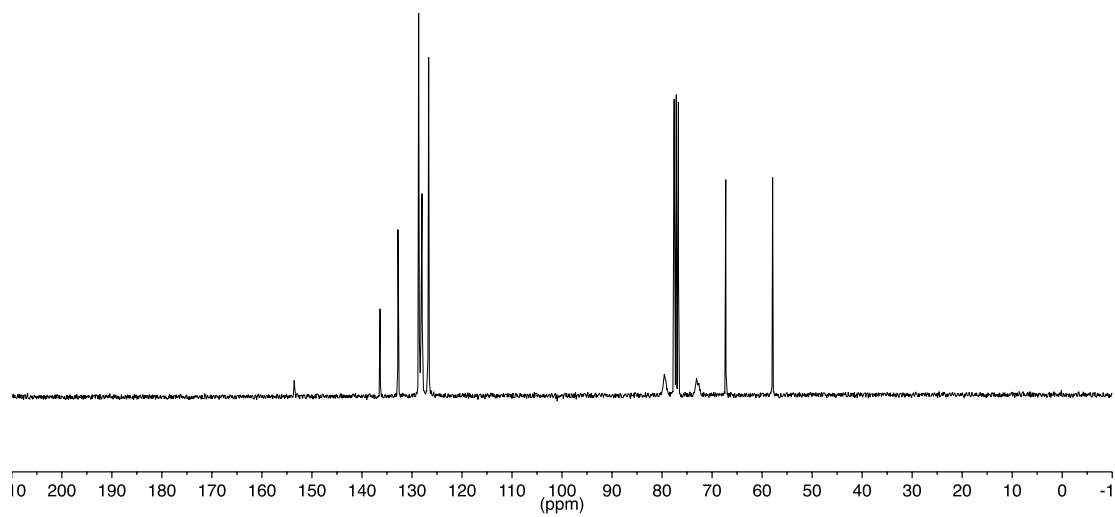
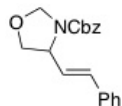
7.33
7.31
6.55
6.17
6.14
6.11
6.09
5.21
5.17
5.11
5.07
4.94
4.55
4.21
4.19
4.17
3.89
3.87
3.86
3.84

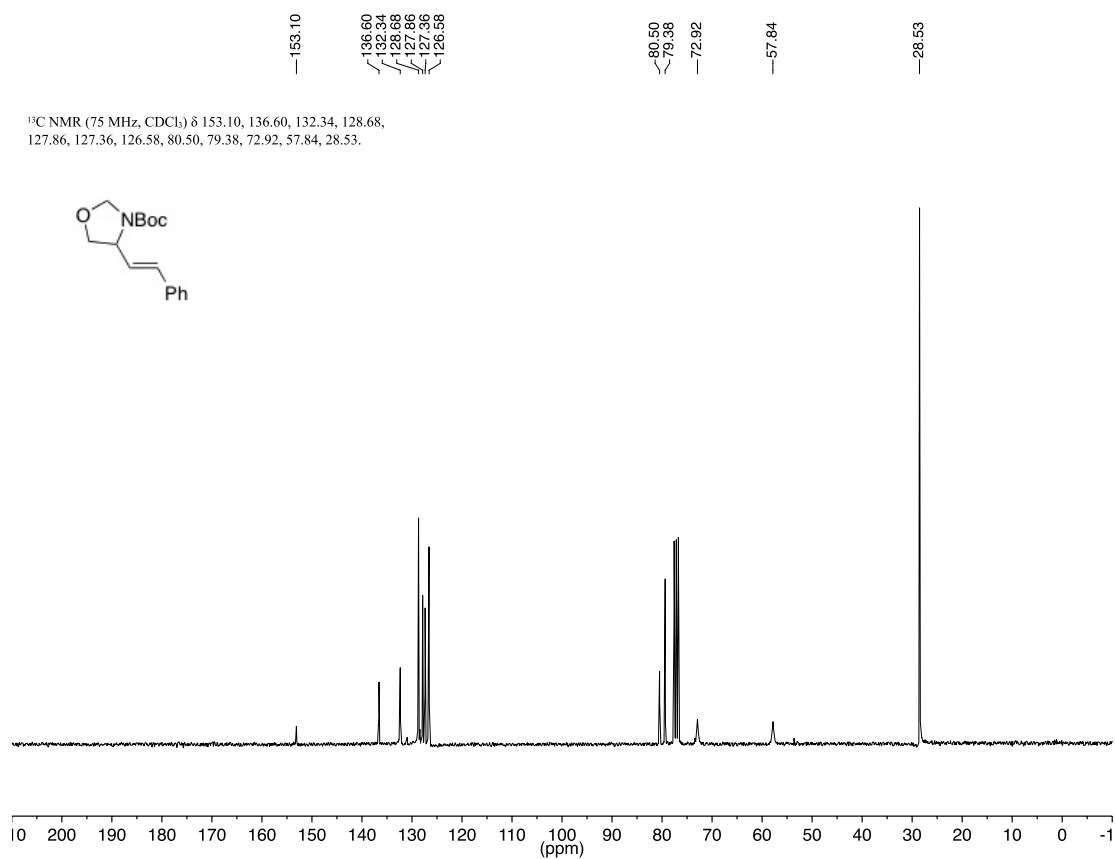
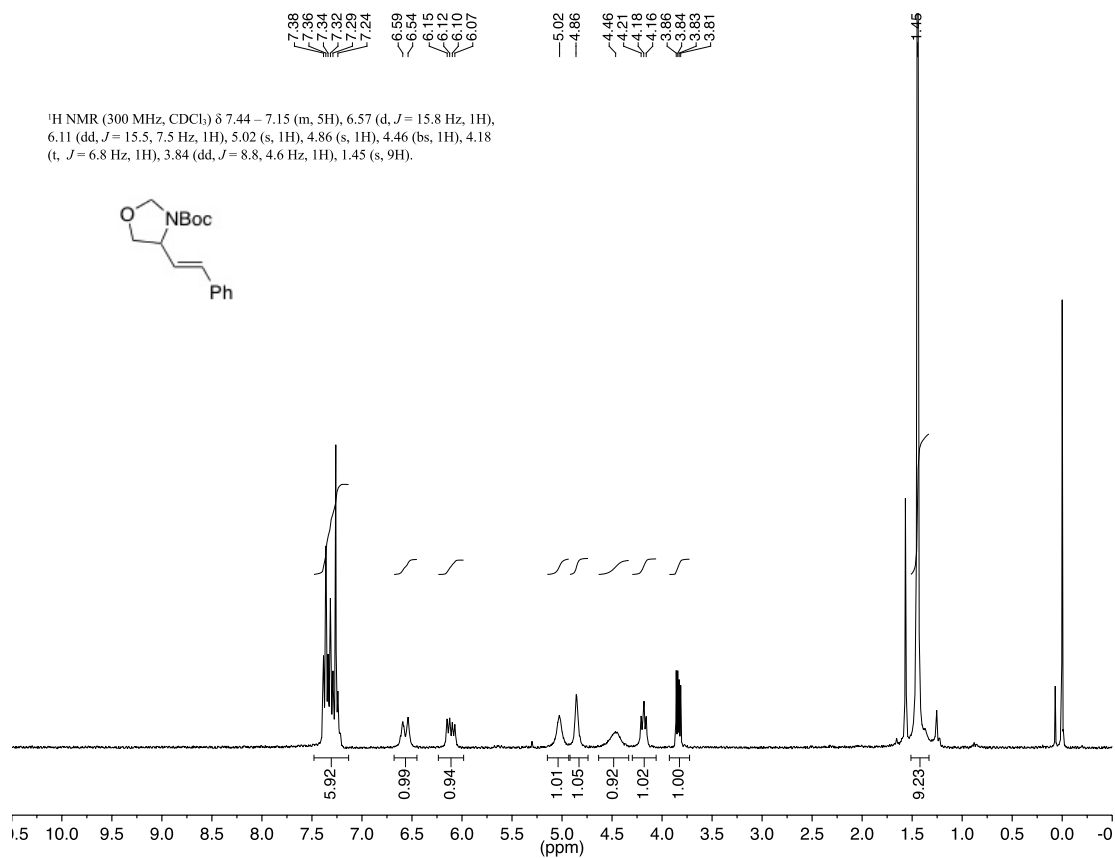
^1H NMR (300 MHz, CDCl_3) δ 7.43 – 7.20 (m, 10H), 6.55 (m, 1H), 6.13 (dd, J = 15.7, 7.3 Hz, 1H), 5.19 (d, J = 12.3 Hz, 1H), 5.09 (m, 2H), 4.94 (m, 1H), 4.55 (m, 1H), 4.19 (t, J = 7.4 Hz, 1H), 3.87 (dd, J = 8.8, 4.5 Hz, 1H).

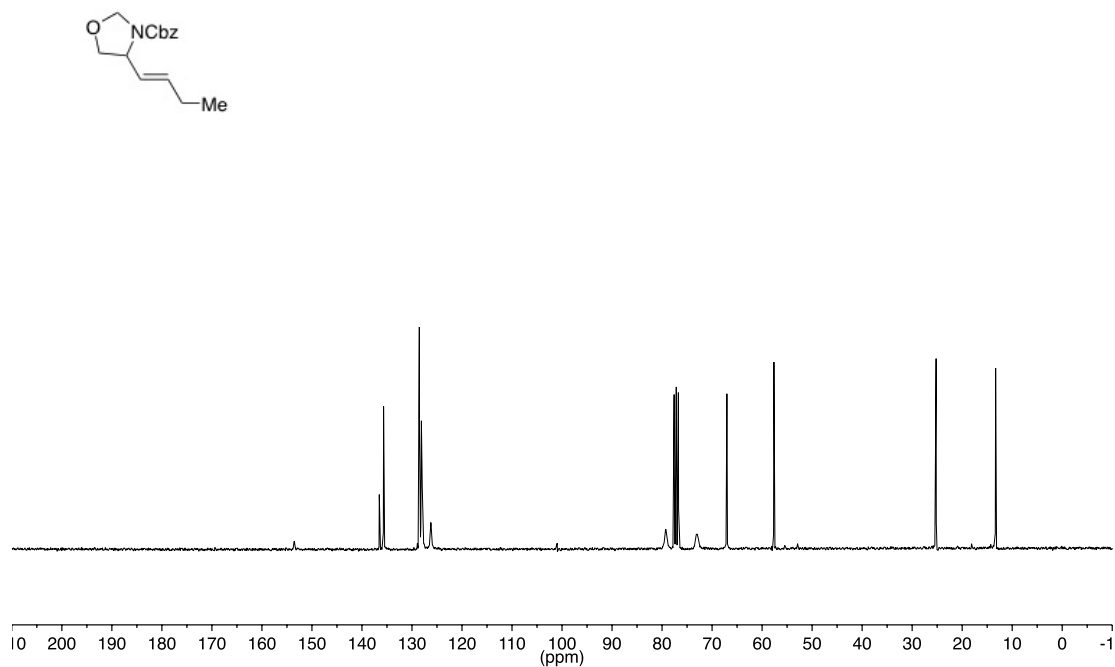
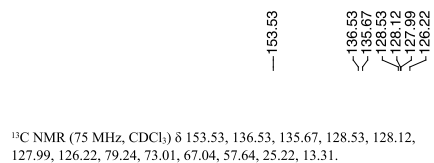
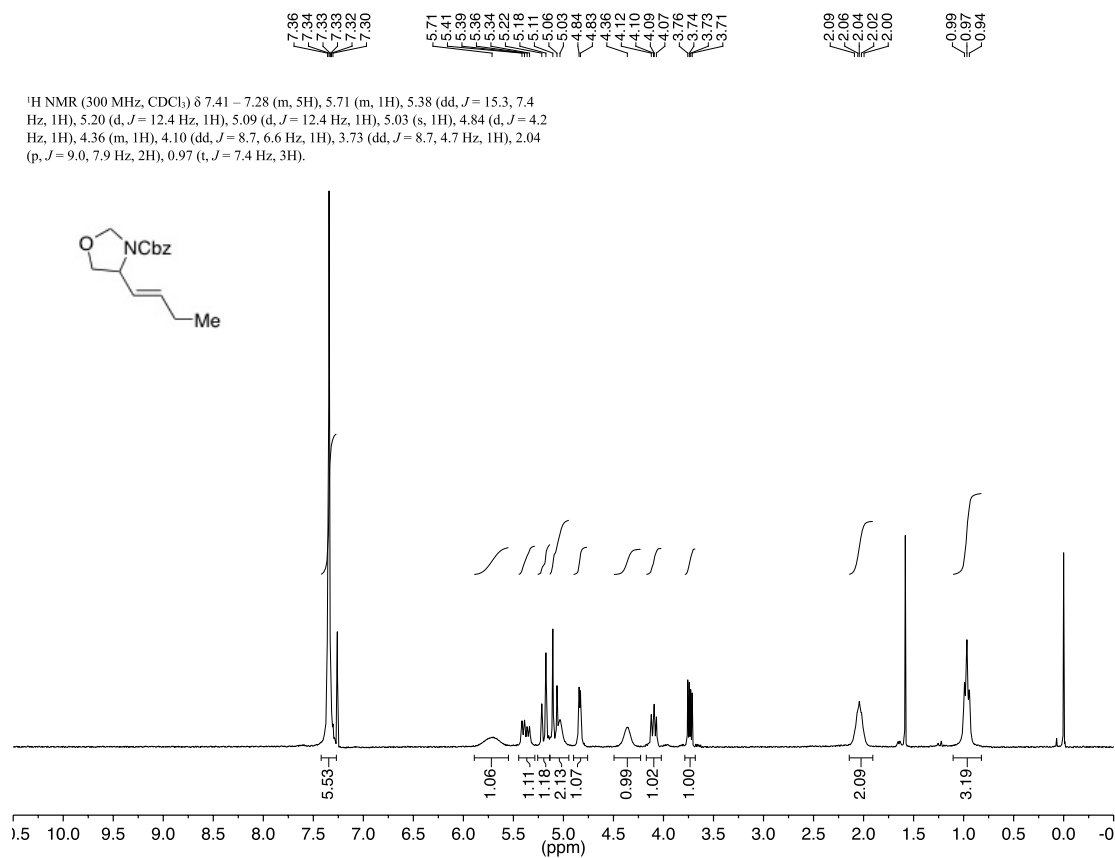


153.55
136.37
132.80
128.64
128.59
128.16
128.12
127.99
126.68
79.58
72.96
67.26
57.90

^{13}C NMR (75 MHz, CDCl_3) δ 153.55, 136.37, 132.80, 128.64, 128.59, 128.16, 128.12, 127.99, 126.68, 79.58, 72.96, 67.26, 57.90.

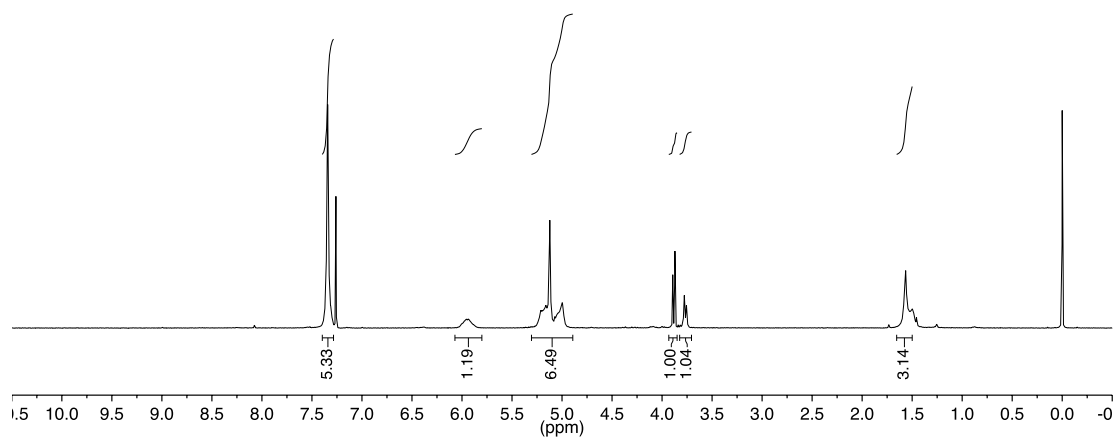
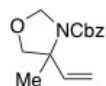




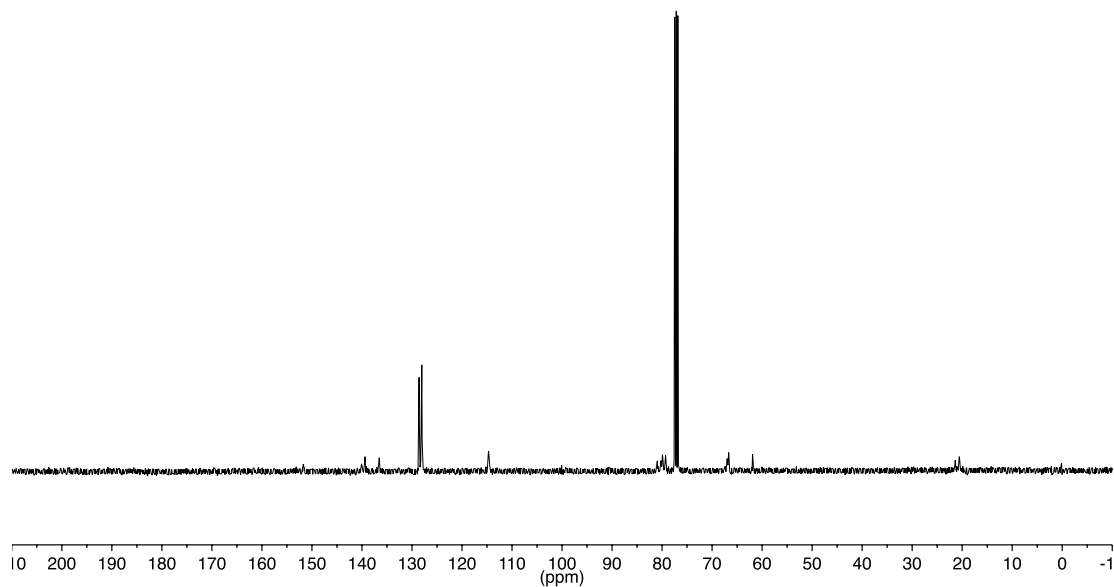
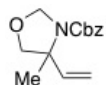


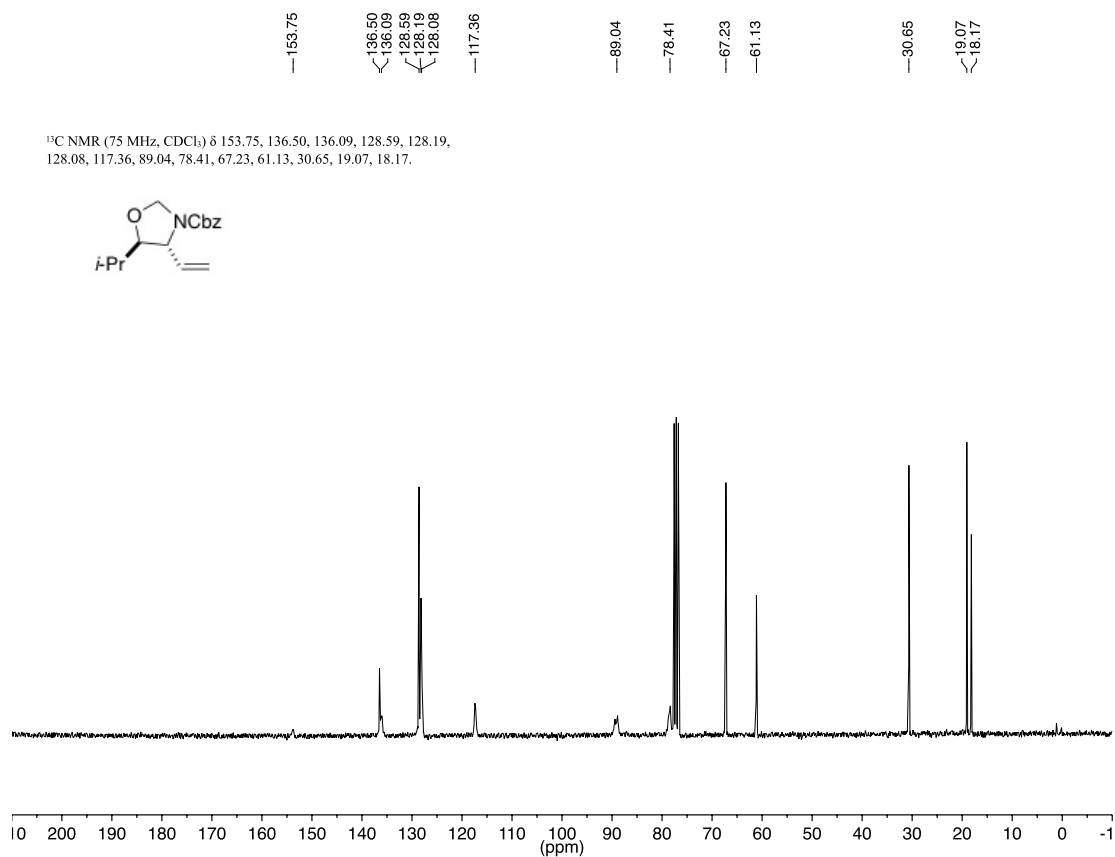
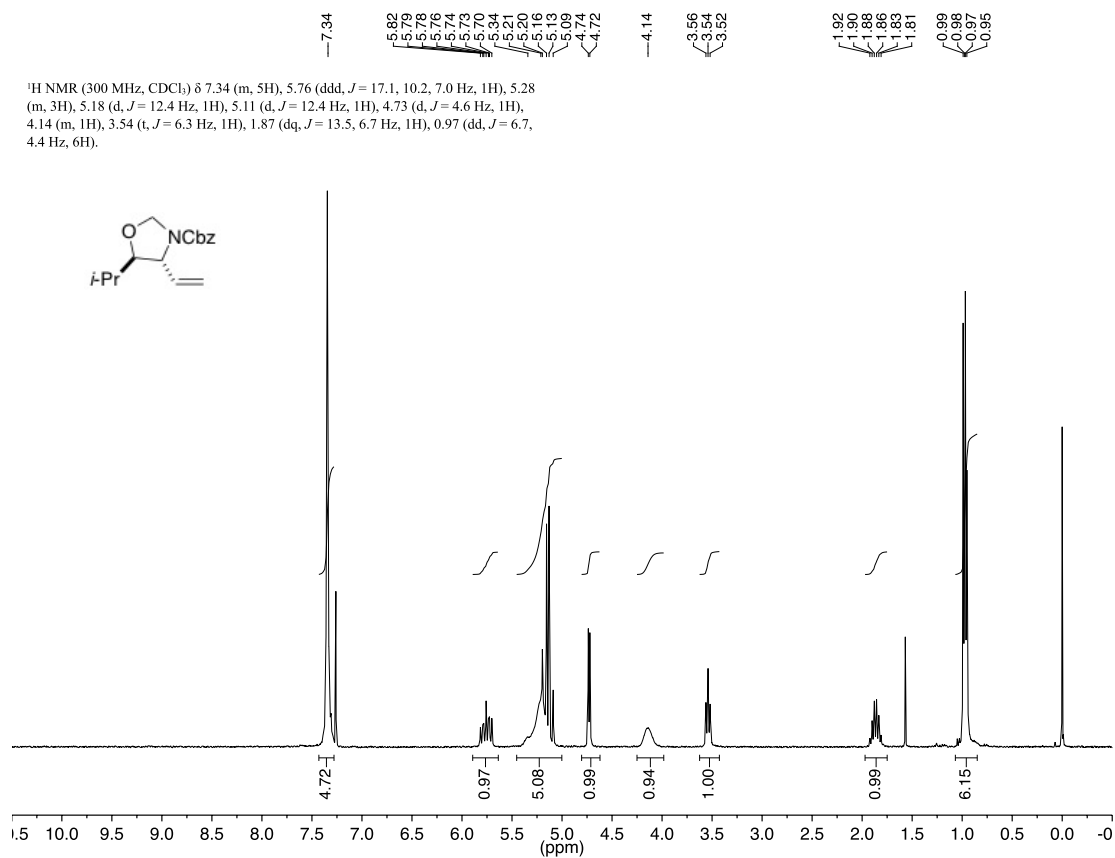


^1H NMR (400 MHz, CDCl_3) δ 7.35 (m, 5H), 5.94 (m, 1H), 5.26 – 4.90 (m, 6H), 3.88 (d, J = 8.6 Hz, 1H), 3.77 (d, J = 8.7 Hz, 1H), 1.56 (s, 3H).



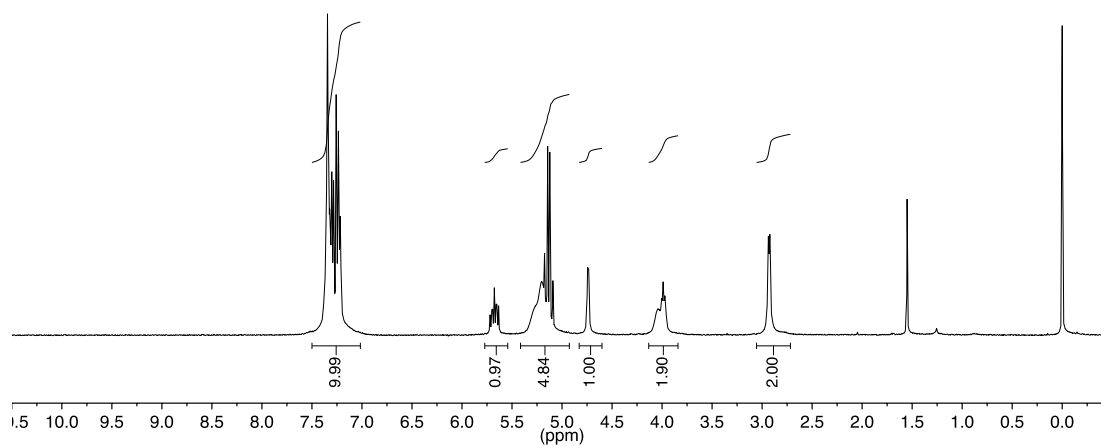
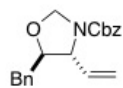
^{13}C NMR (101 MHz, CDCl_3) δ 151.74, 140.04, 139.39, 136.55, 128.58, 128.13, 128.03, 114.68, 80.95, 80.25, 79.92, 79.31, 67.02, 66.68, 61.91, 21.36, 20.55.



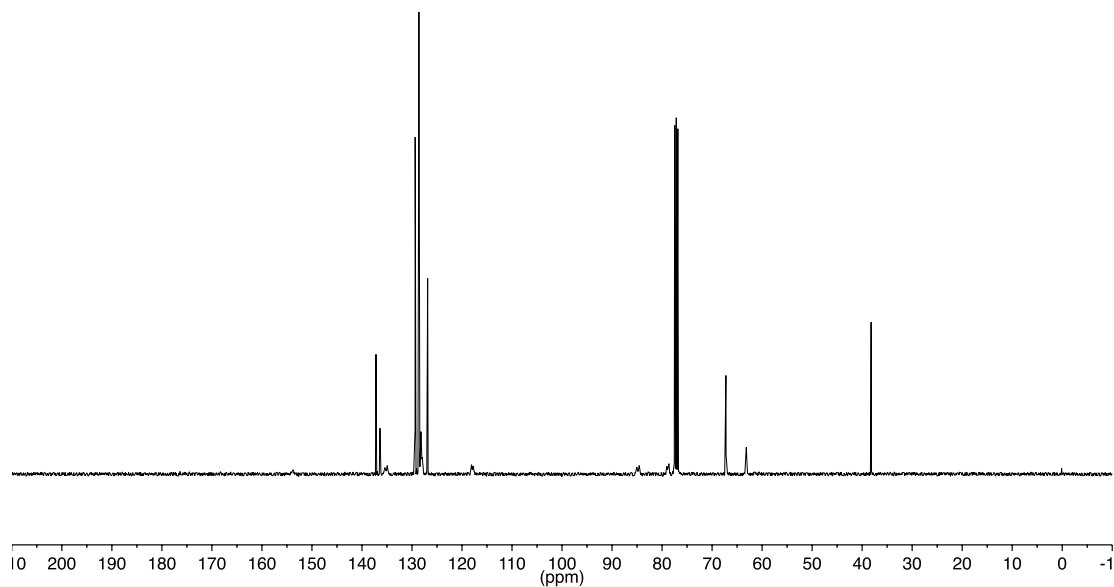
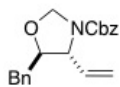


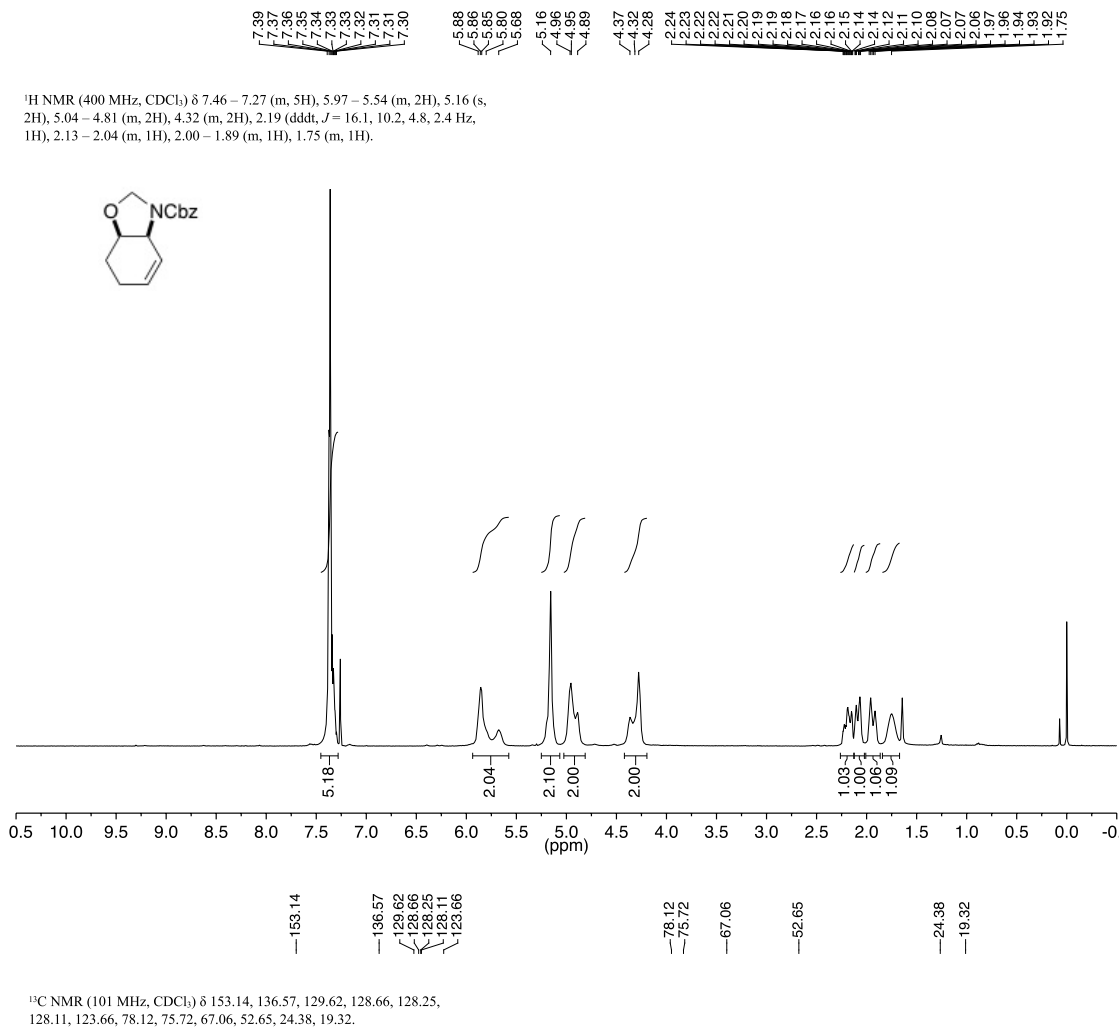


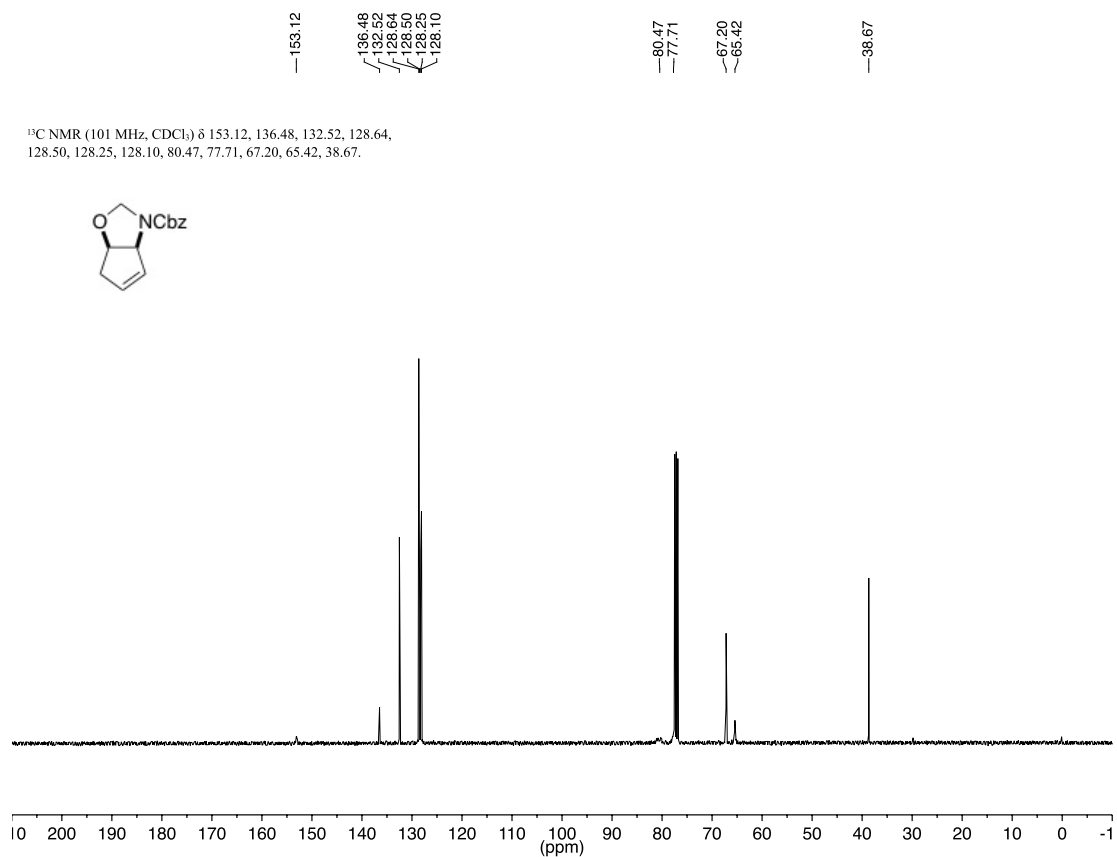
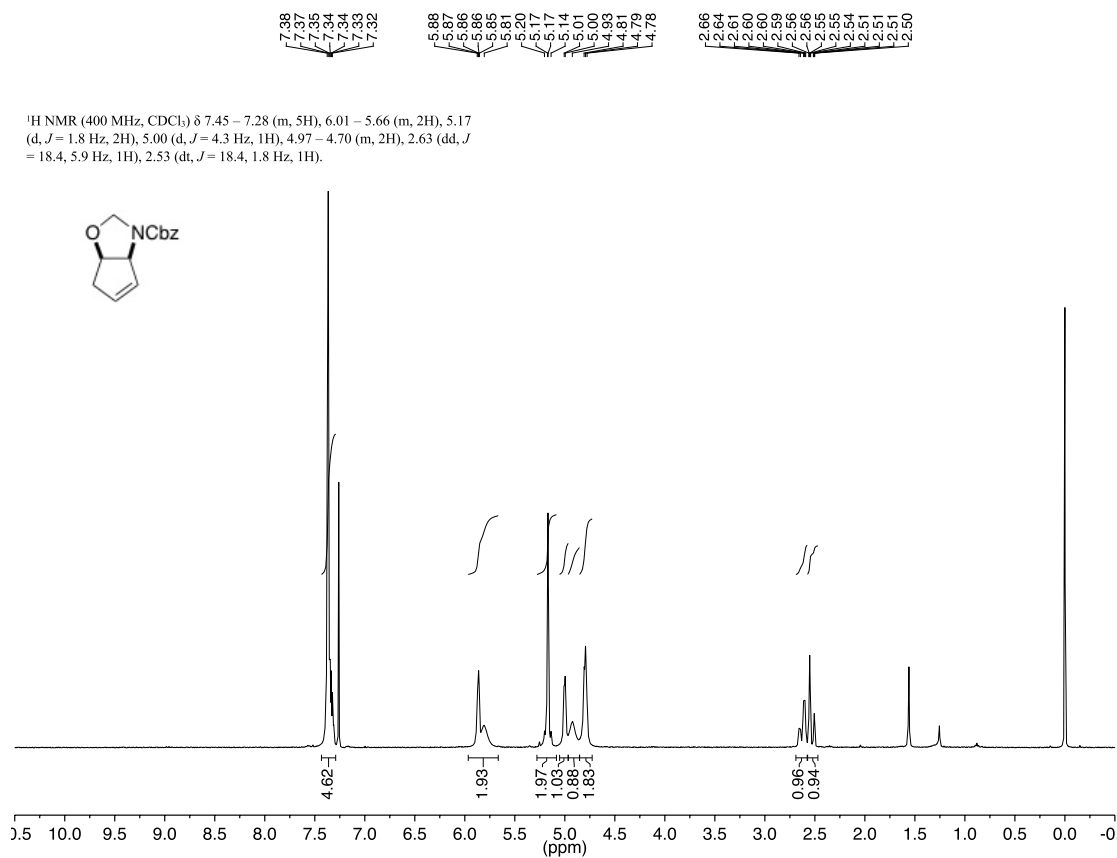
^1H NMR (400 MHz, CDCl_3) δ 7.53–7.05 (m, 10H), 5.68 (ddd, $J = 17.1, 10.2, 7.0$ Hz, 1H), 5.24 (m, 3H), 5.16 (d, $J = 12.4$ Hz, 1H), 5.11 (d, $J = 12.4$ Hz, 1H), 4.74 (d, $J = 4.7$ Hz, 1H), 4.00 (dd, $J = 16.4, 10.5$ Hz, 2H), 2.93 (d, $J = 6.2$ Hz, 2H).

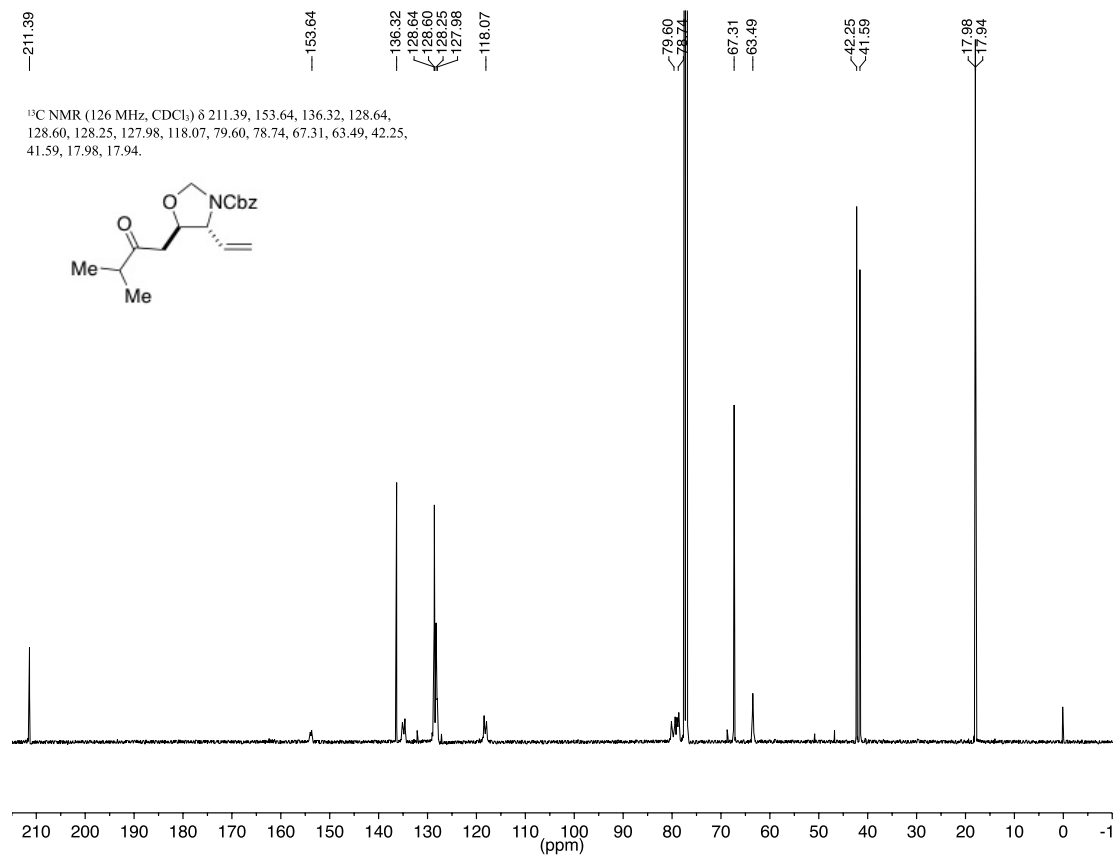
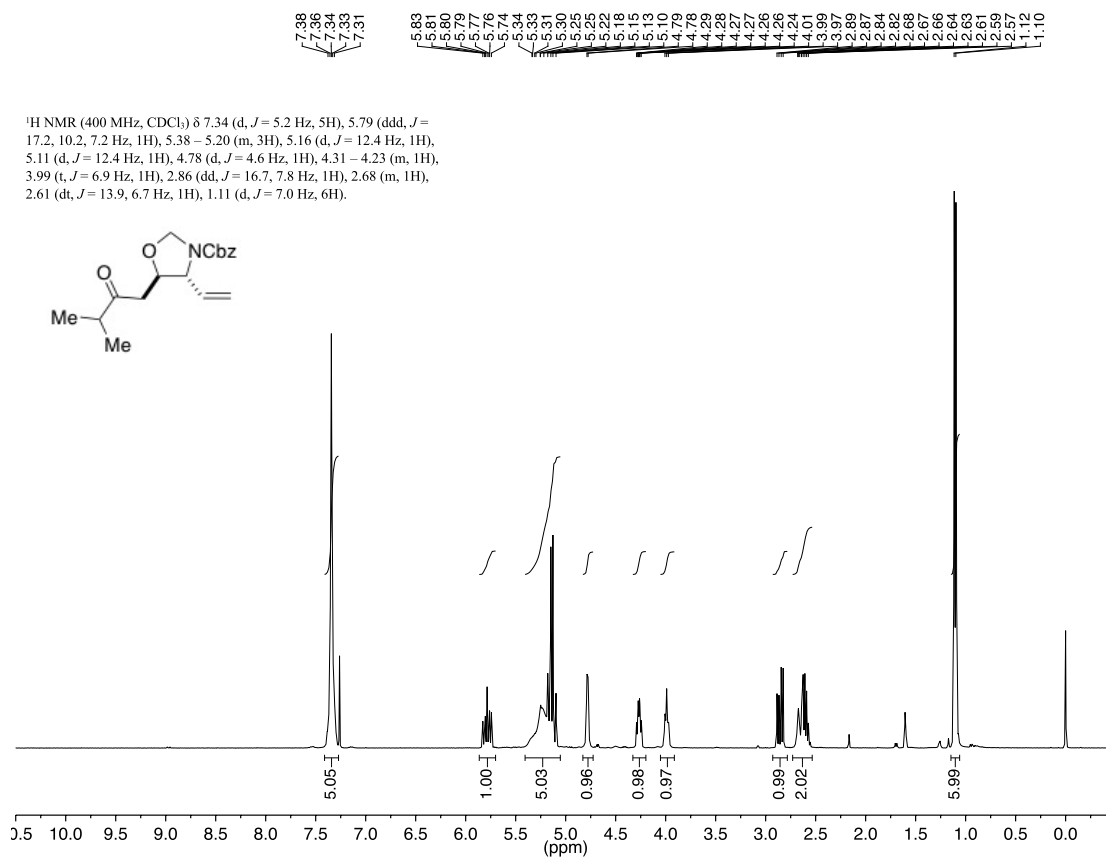


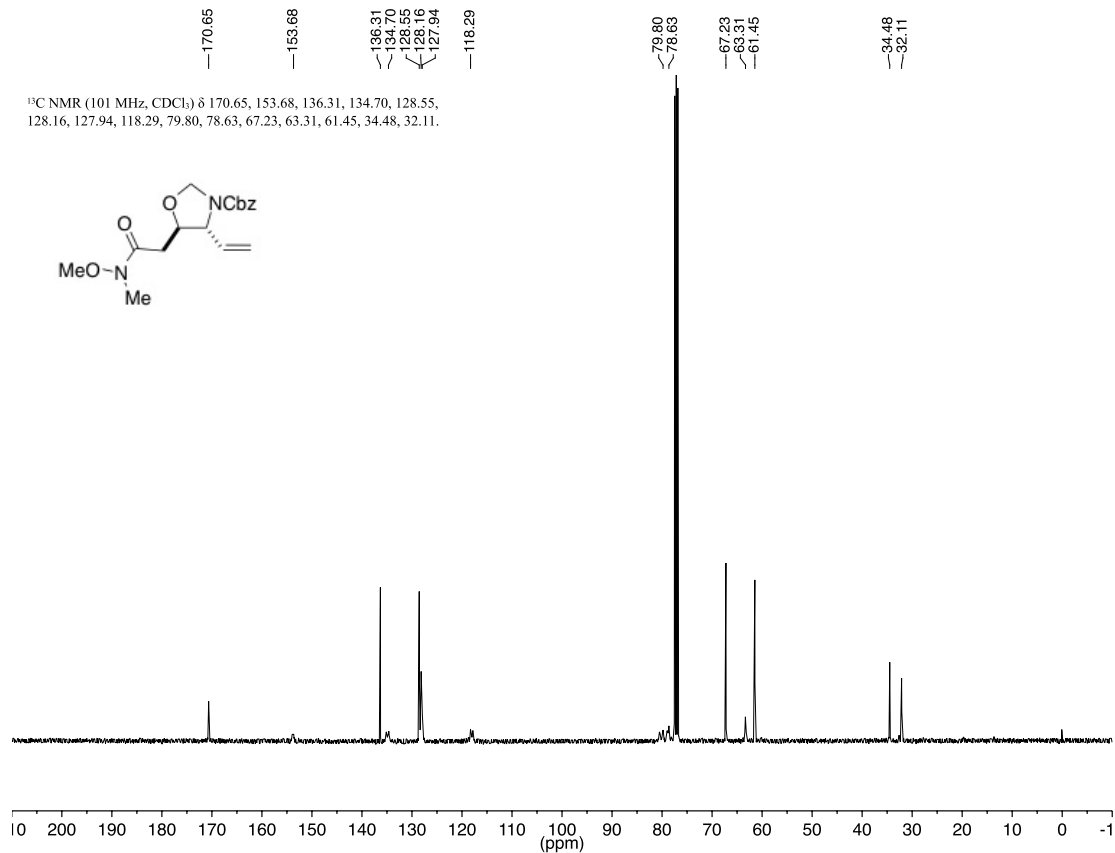
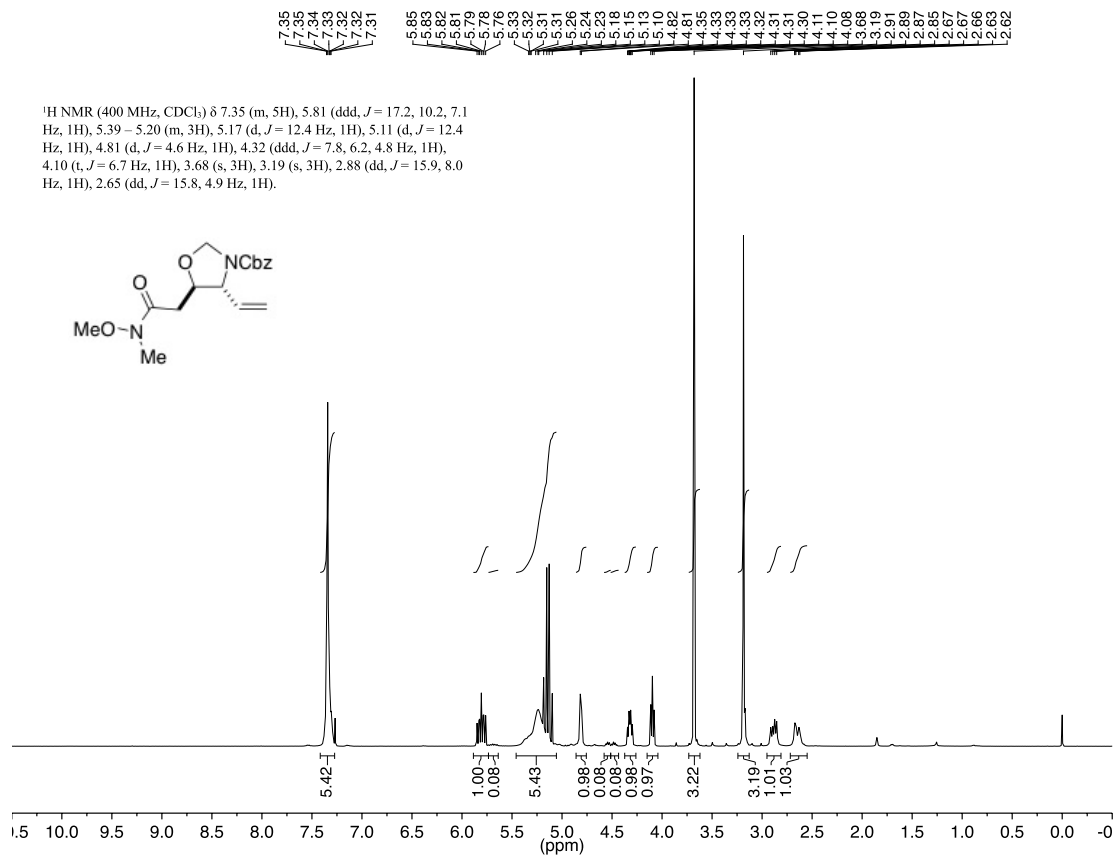
^{13}C NMR (101 MHz, CDCl_3) δ 153.90, 137.20, 136.41, 135.09, 129.36, 128.61, 128.58, 128.20, 127.93, 126.87, 117.88, 84.92, 78.75, 67.23, 63.16, 38.21.

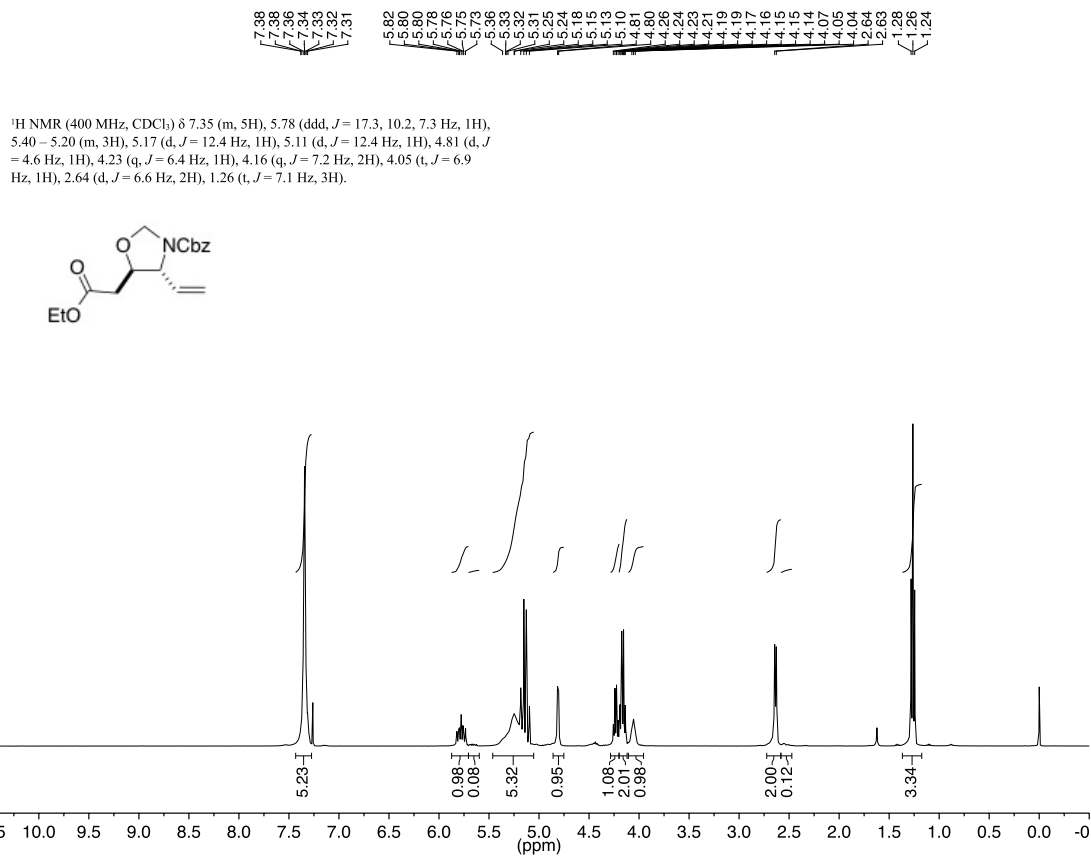




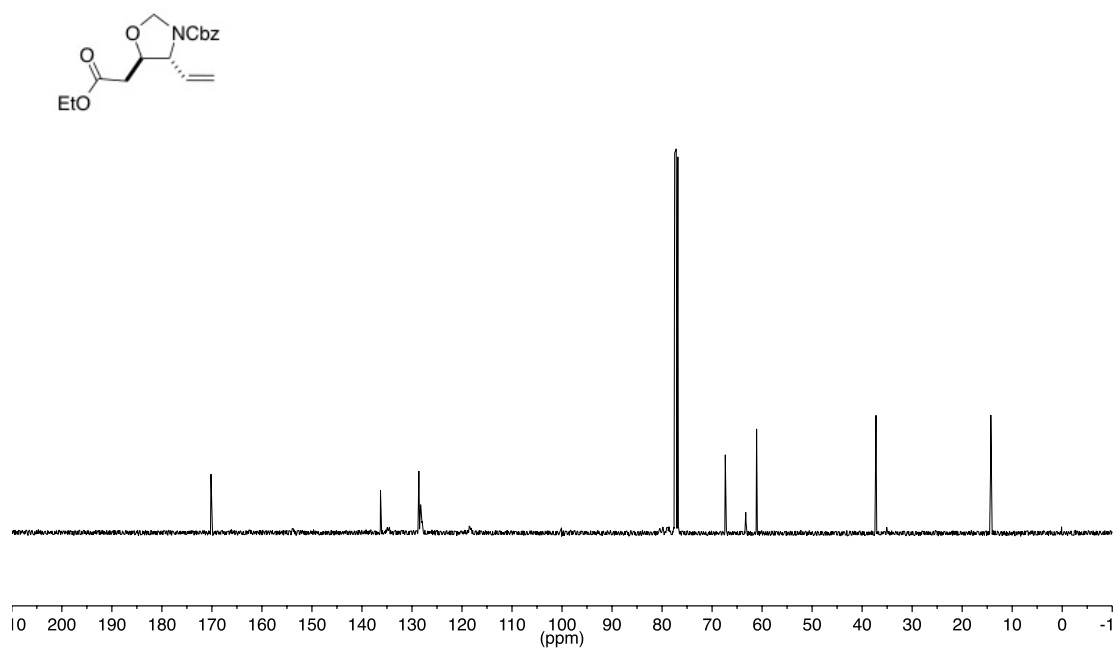


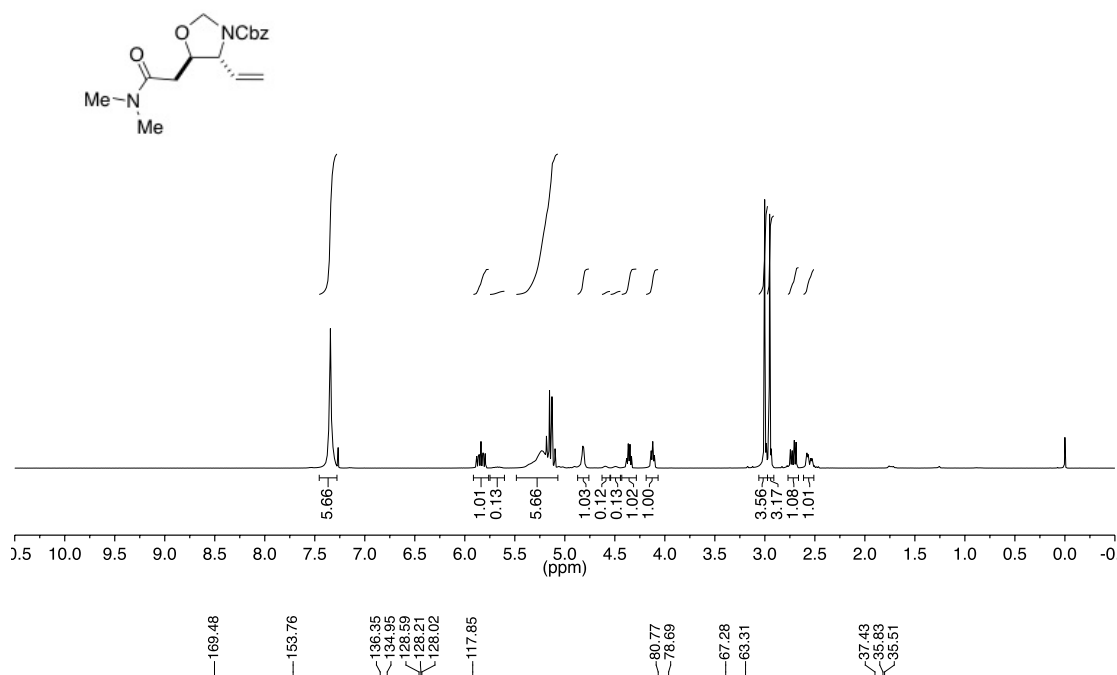
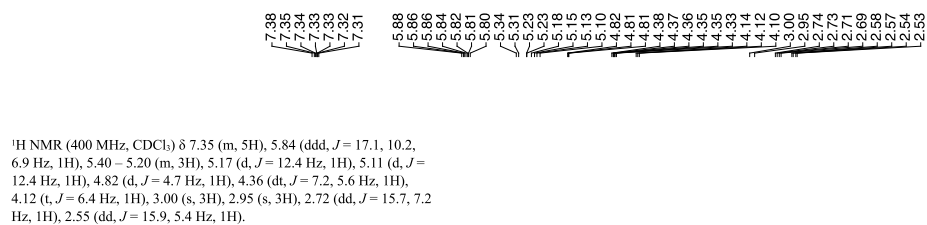




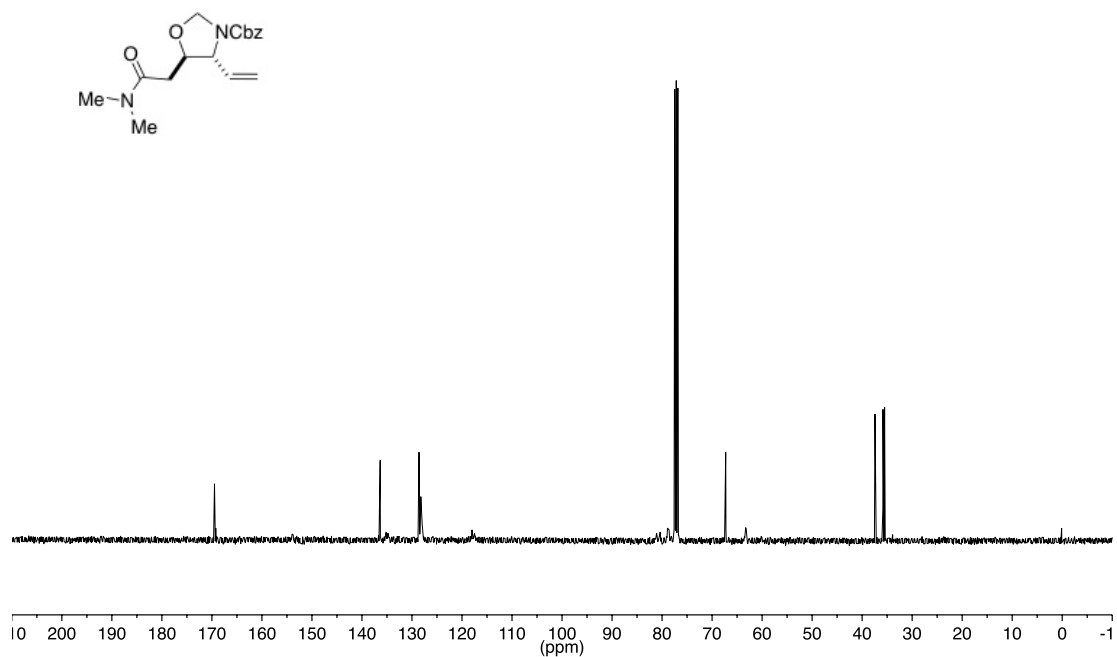


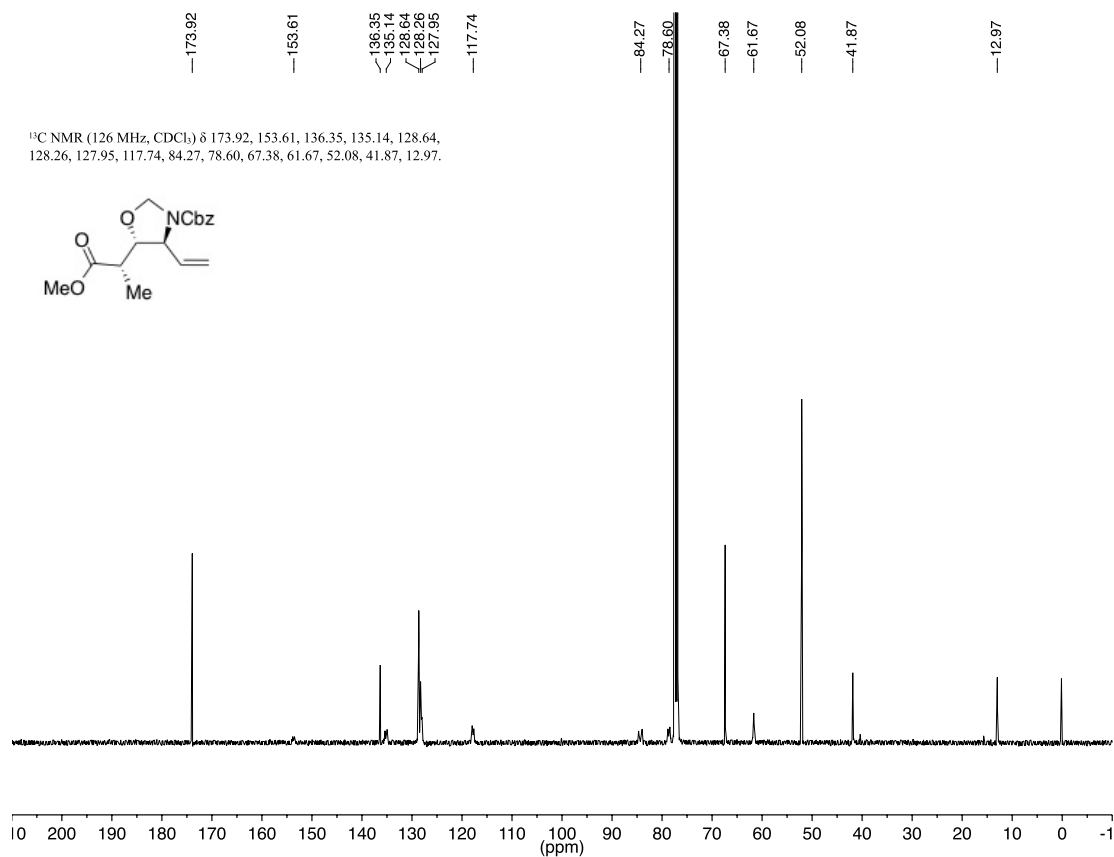
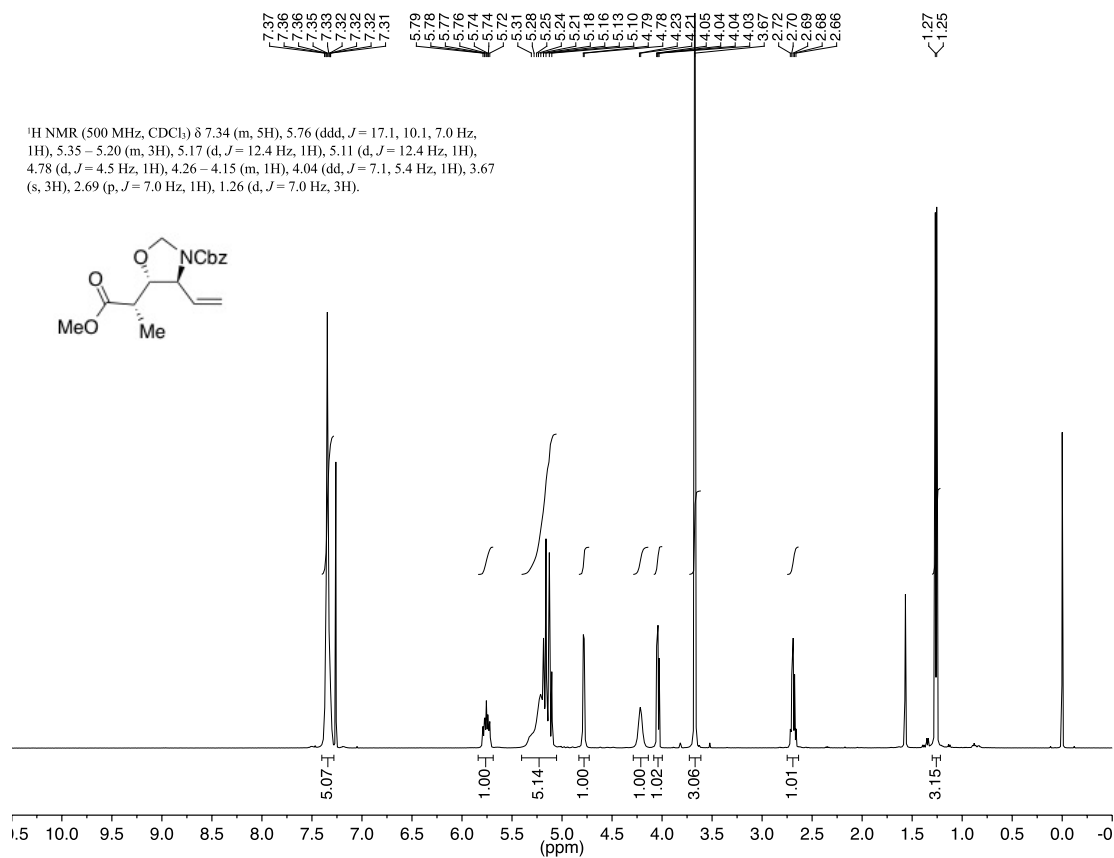
¹³C NMR (101 MHz, CDCl₃) δ 170.18, 153.70, 136.30, 134.73, 128.62, 128.26, 128.02, 118.26, 80.13, 78.83, 67.36, 63.26, 61.10, 37.23, 14.27.

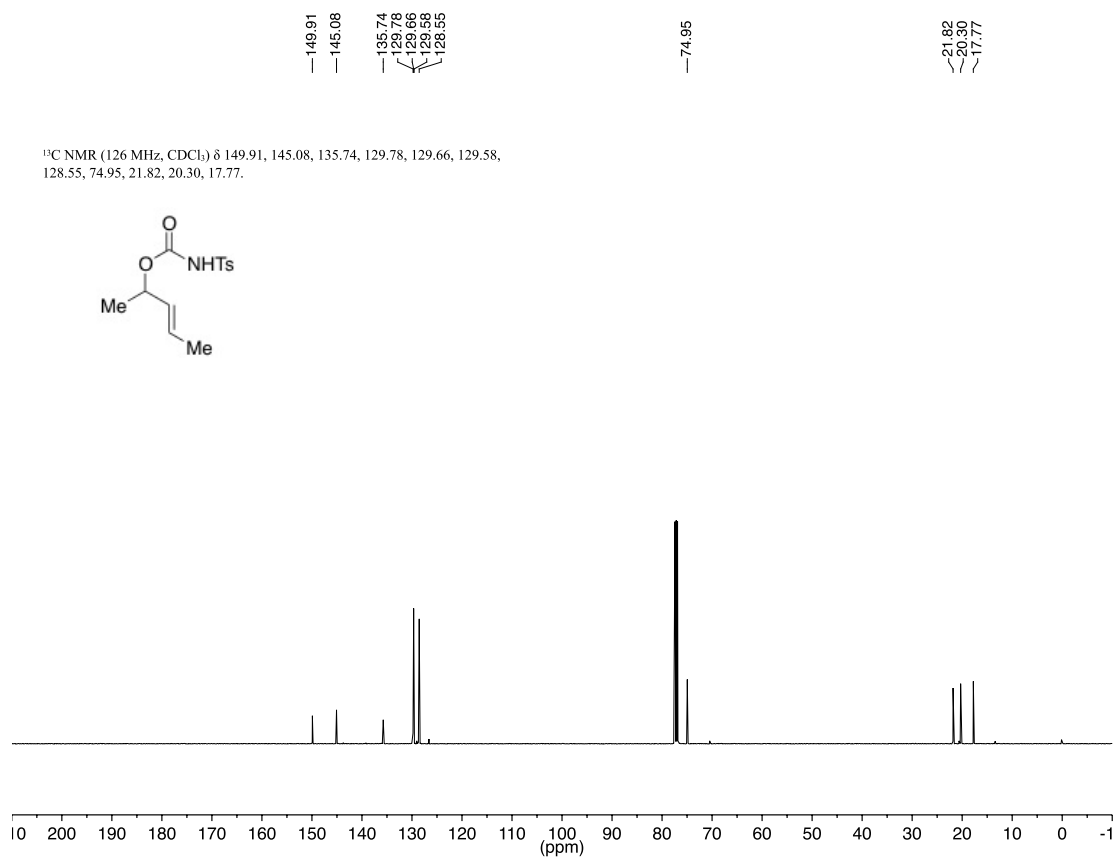
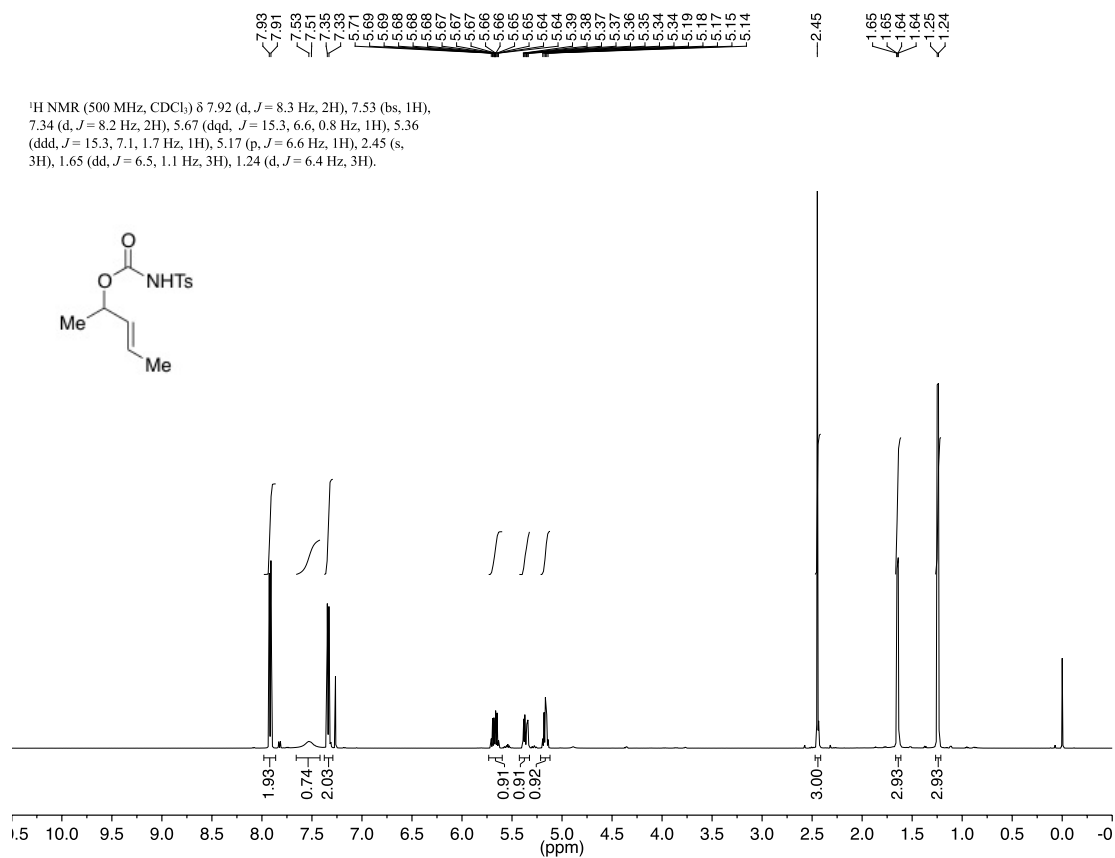


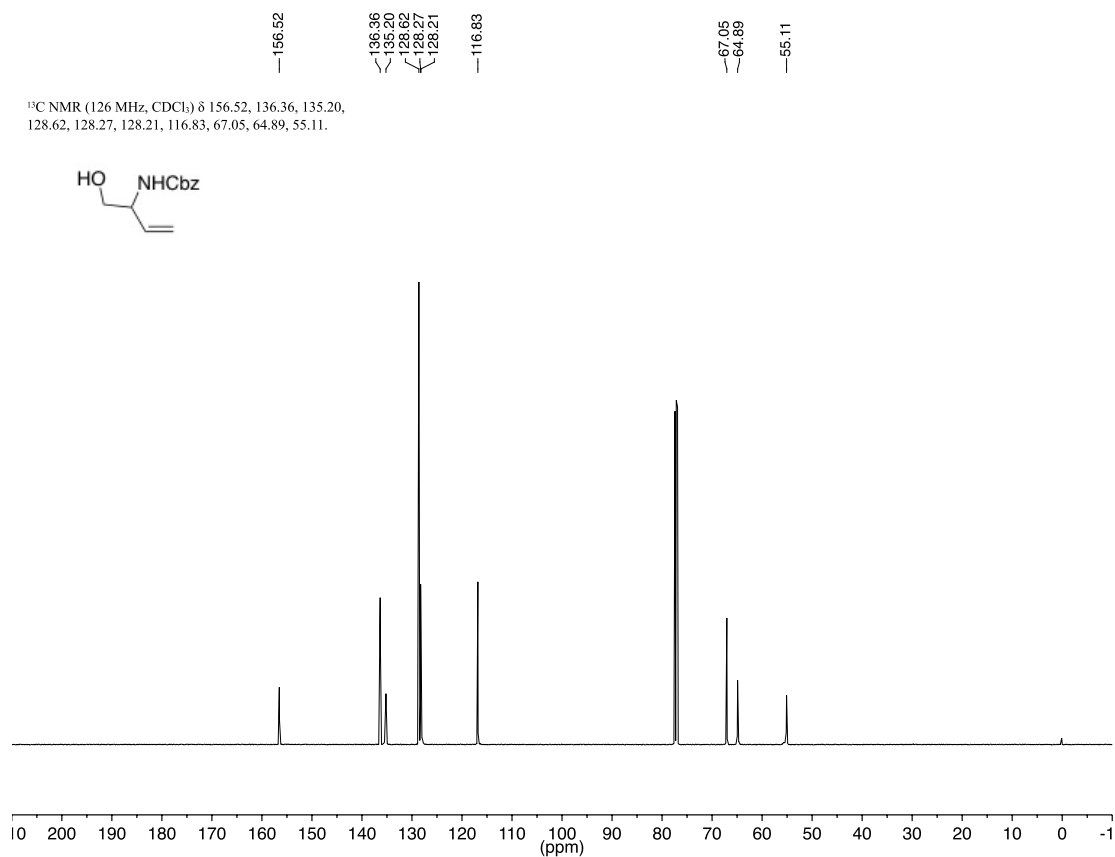
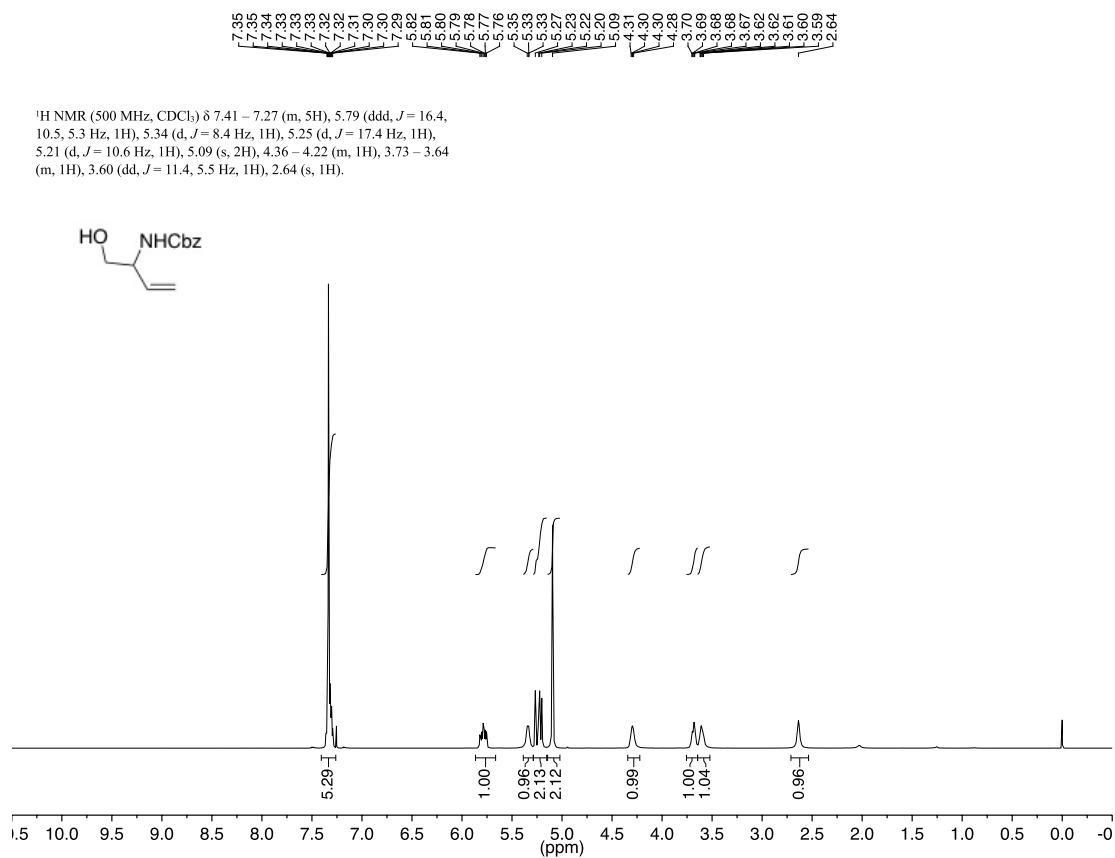


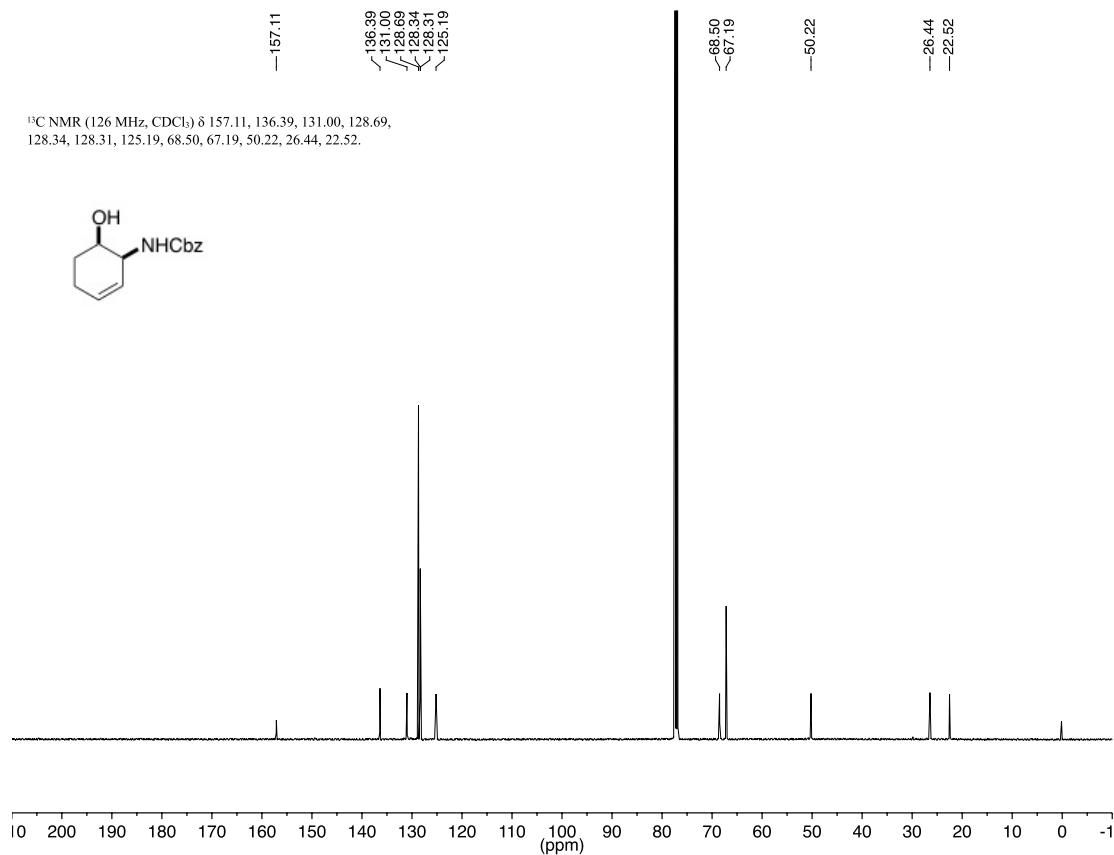
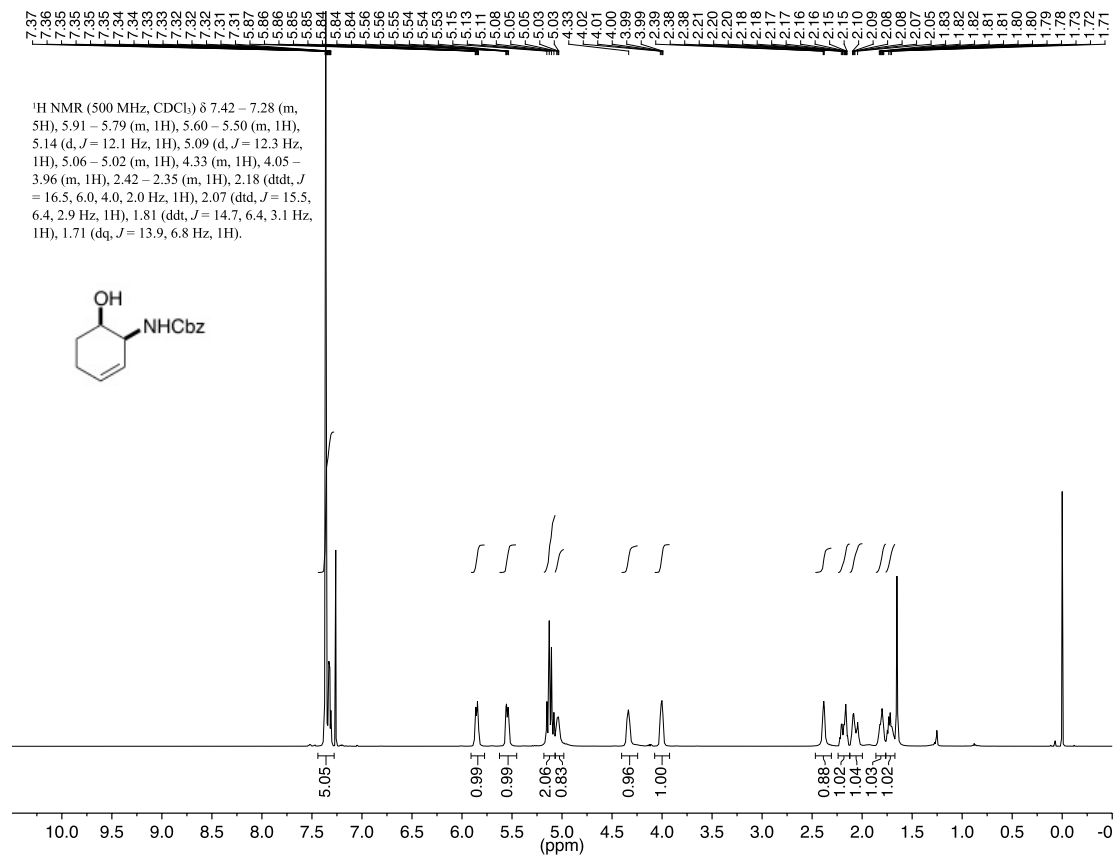
¹³C NMR (101 MHz, CDCl₃) δ 169.48, 153.76, 136.35, 134.95, 128.59, 128.21, 128.02, 117.85, 80.77, 78.69, 67.28, 63.31, 37.43, 35.83, 35.51.

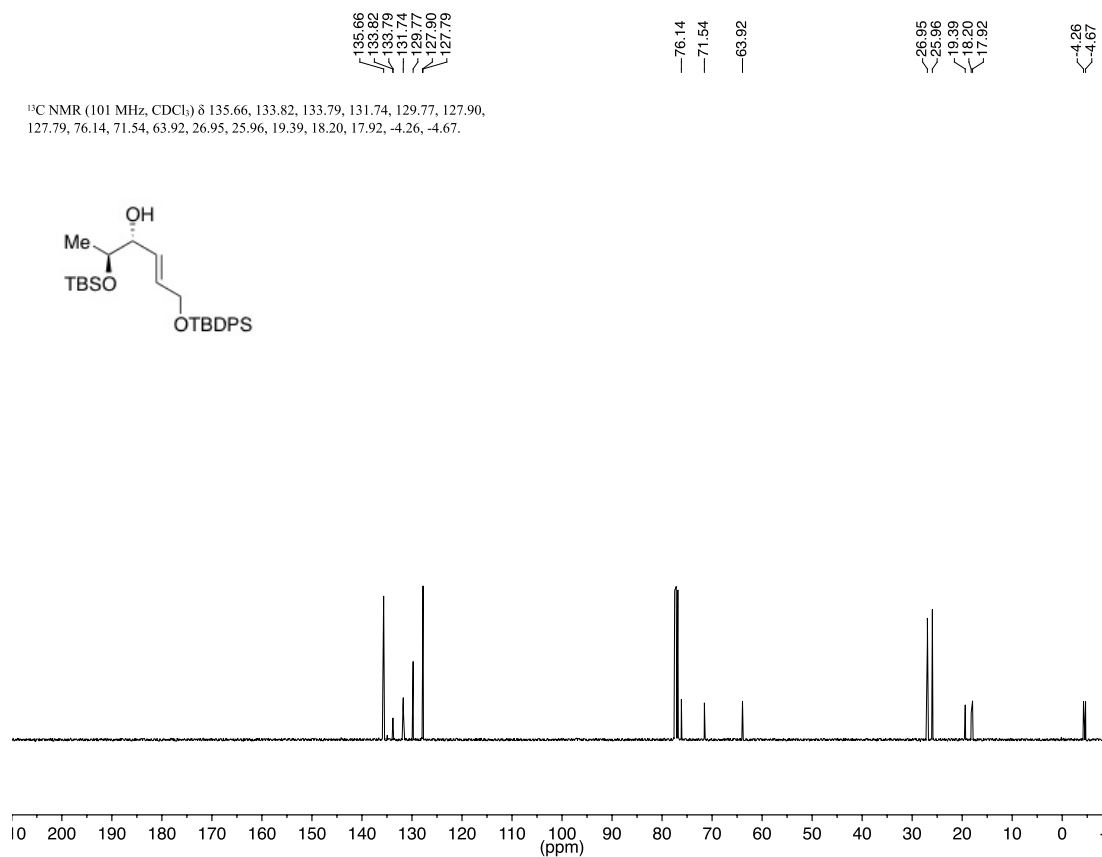
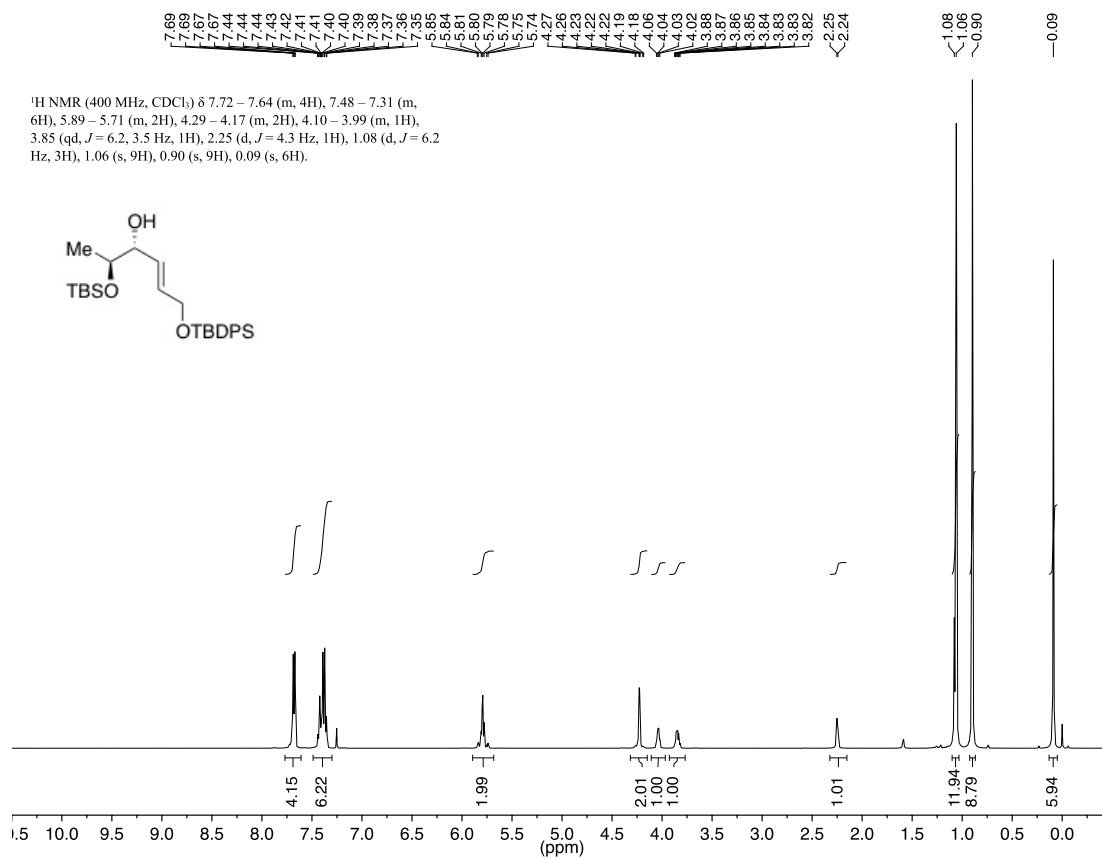


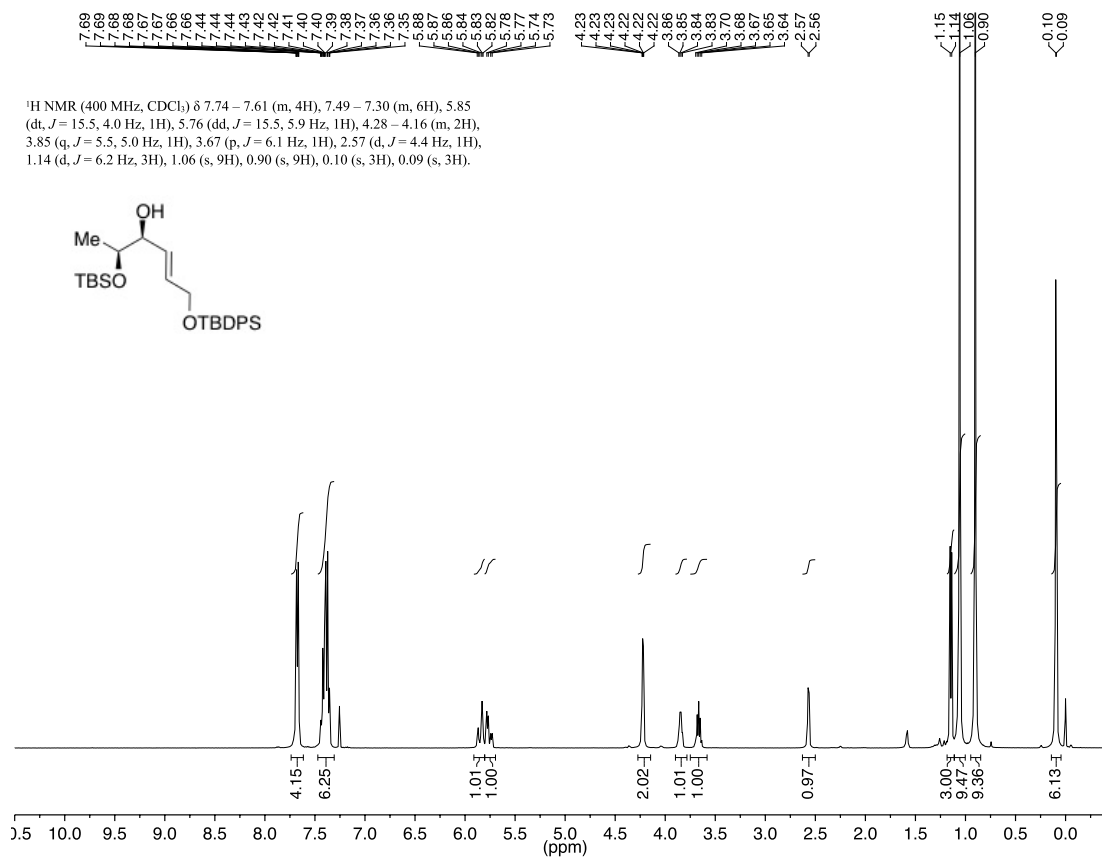
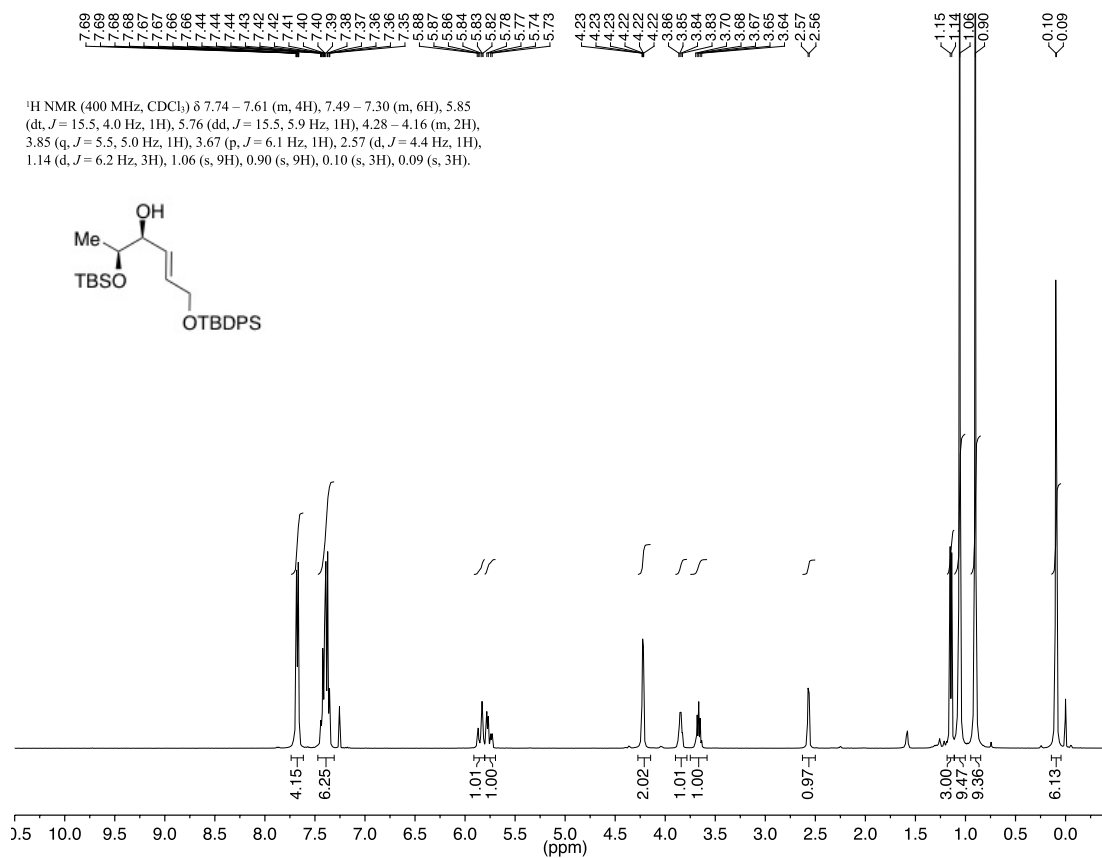


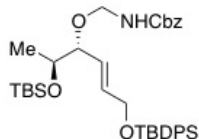
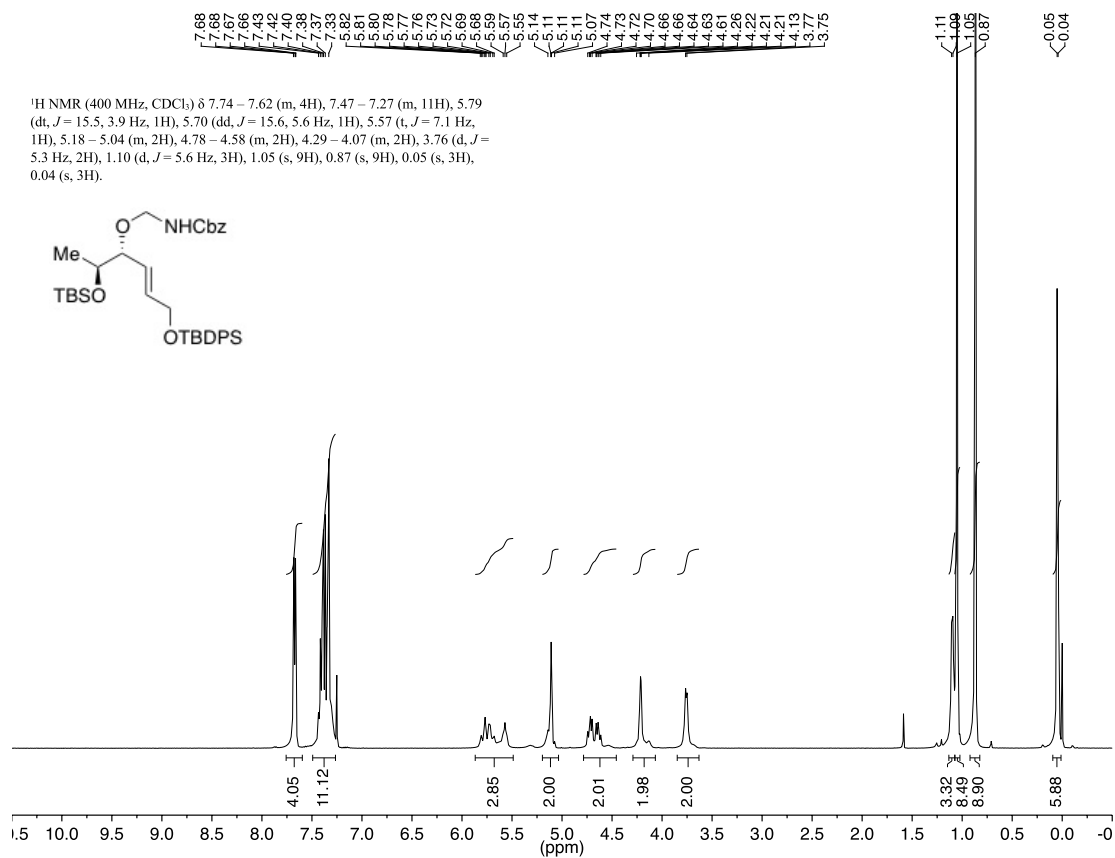




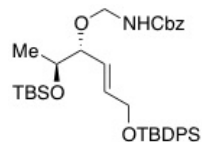
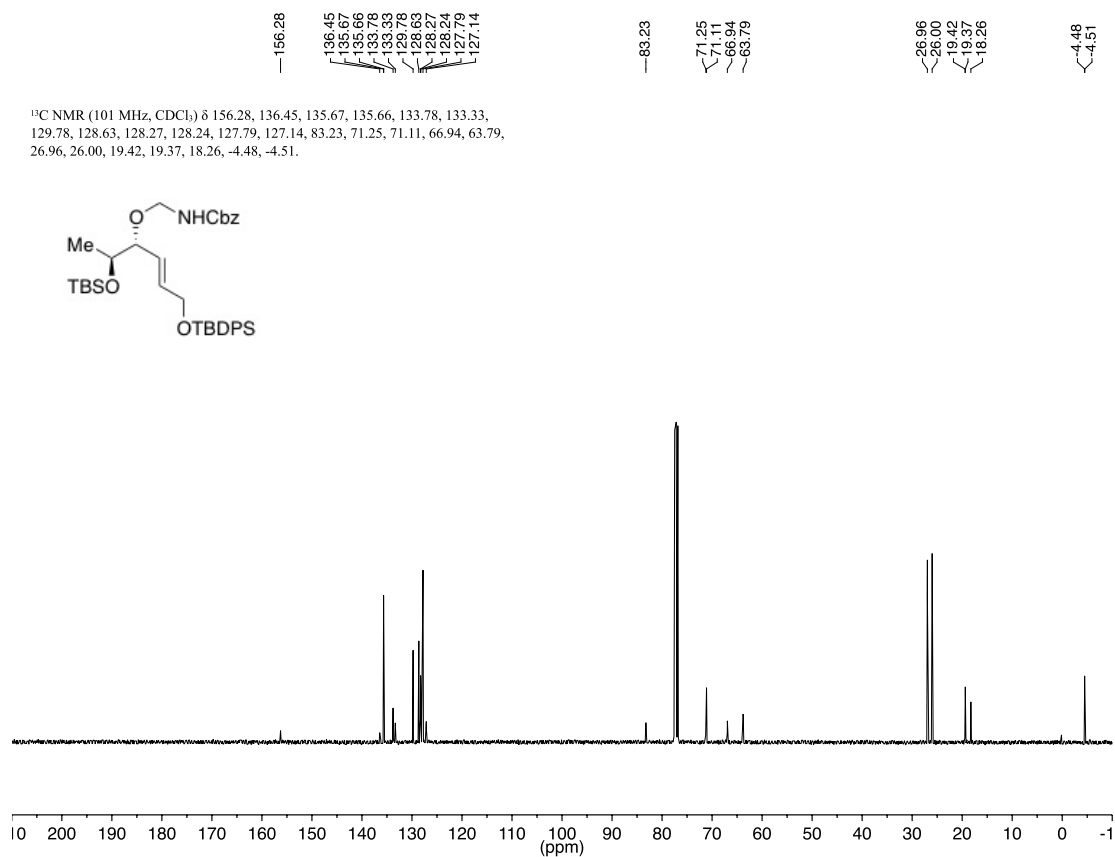


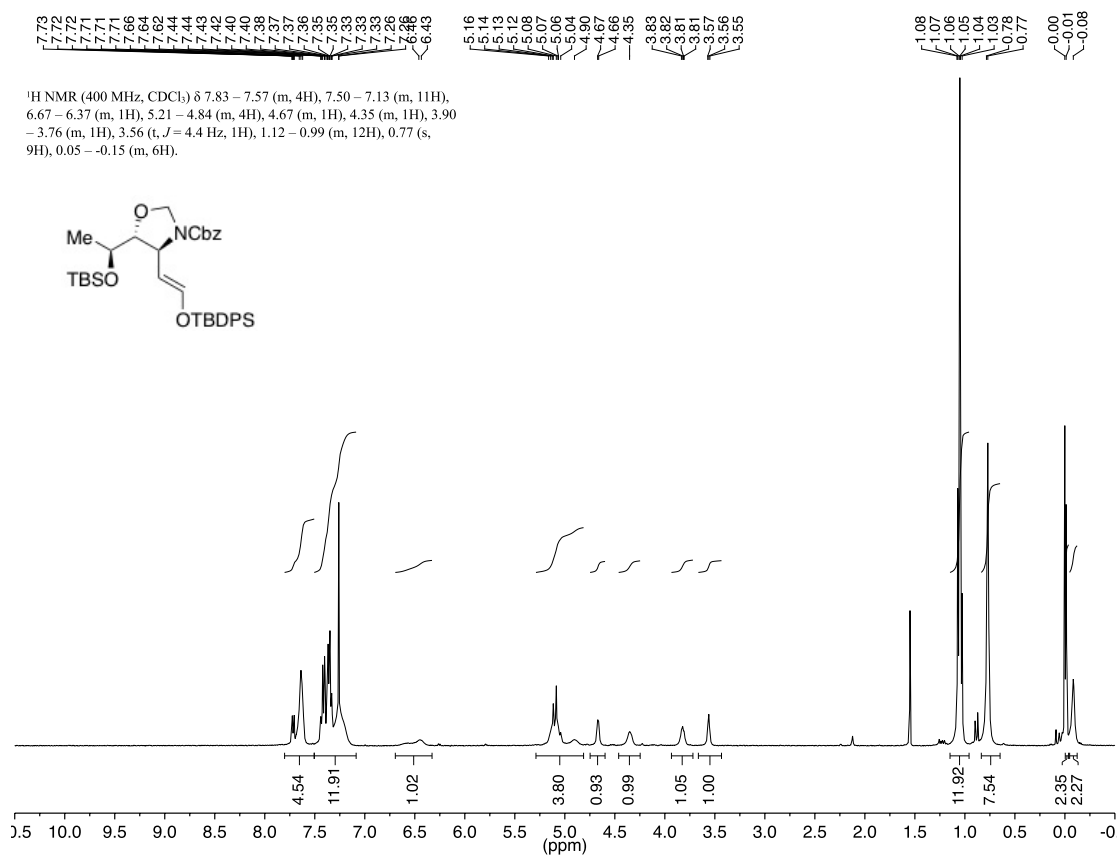




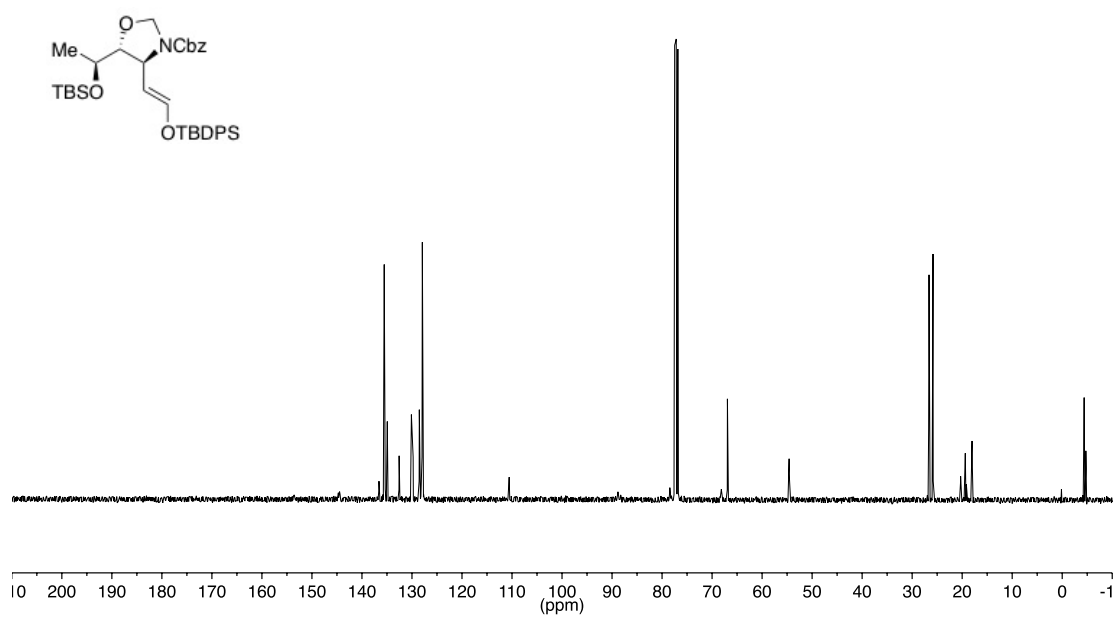


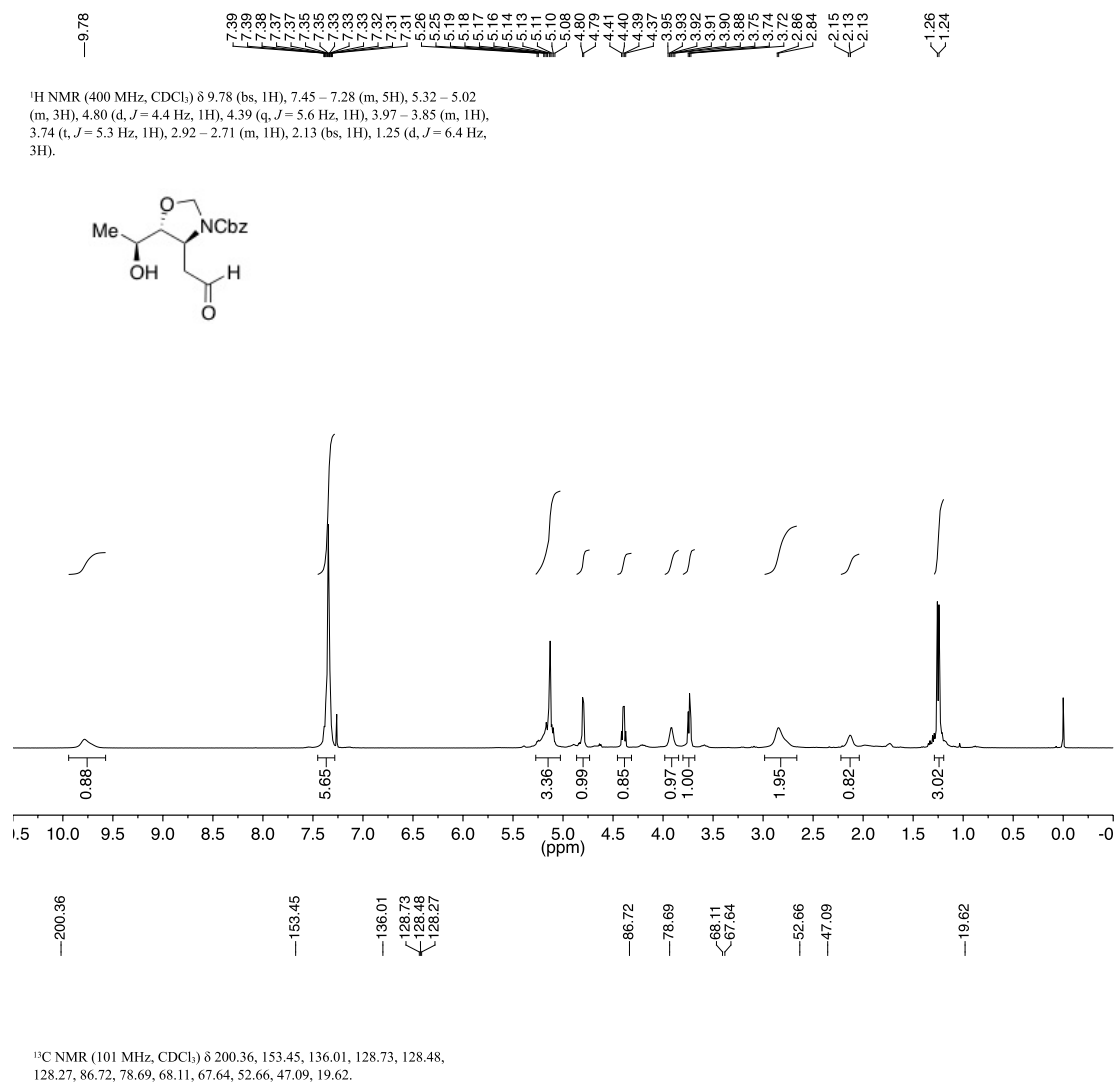
¹³C NMR (101 MHz, CDCl₃) δ 156.28, 136.45, 135.67, 135.66, 133.78, 133.33, 129.78, 128.63, 128.27, 128.24, 127.79, 127.14, 83.23, 71.25, 71.11, 66.94, 63.79, 26.96, 26.00, 19.42, 19.37, 18.26, -4.48, -4.51.

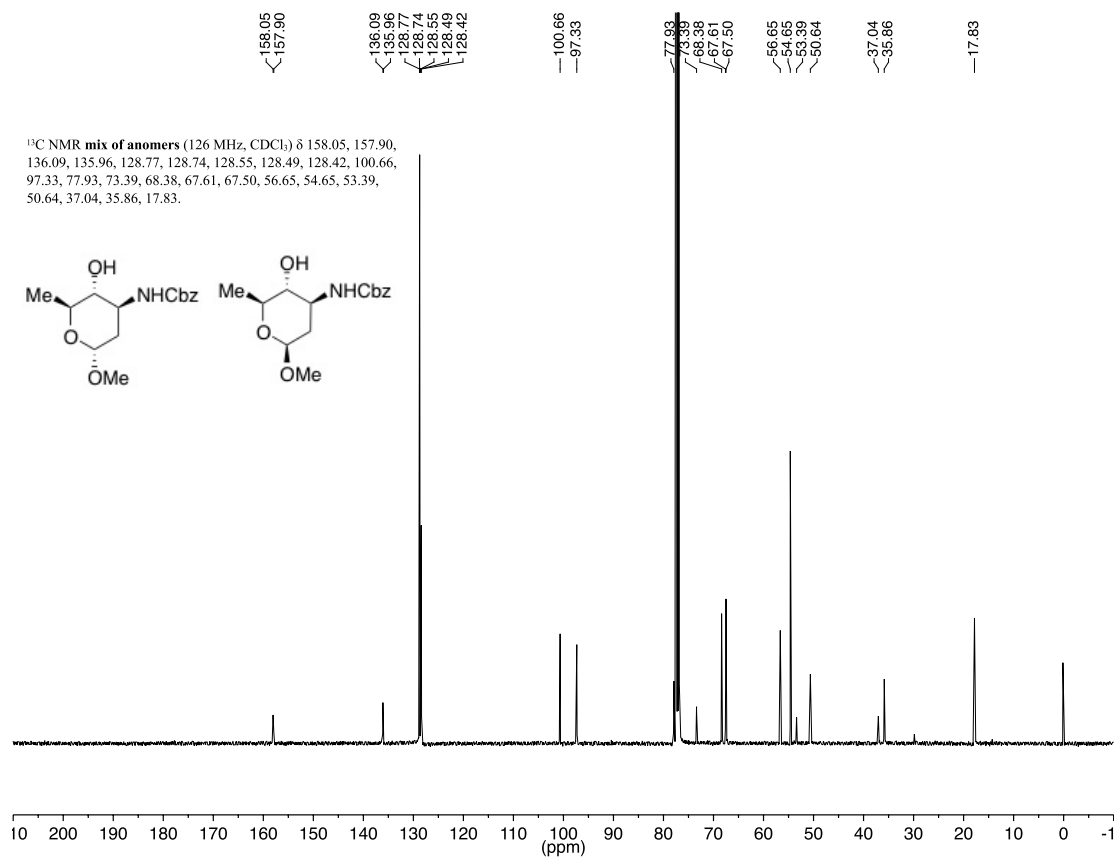
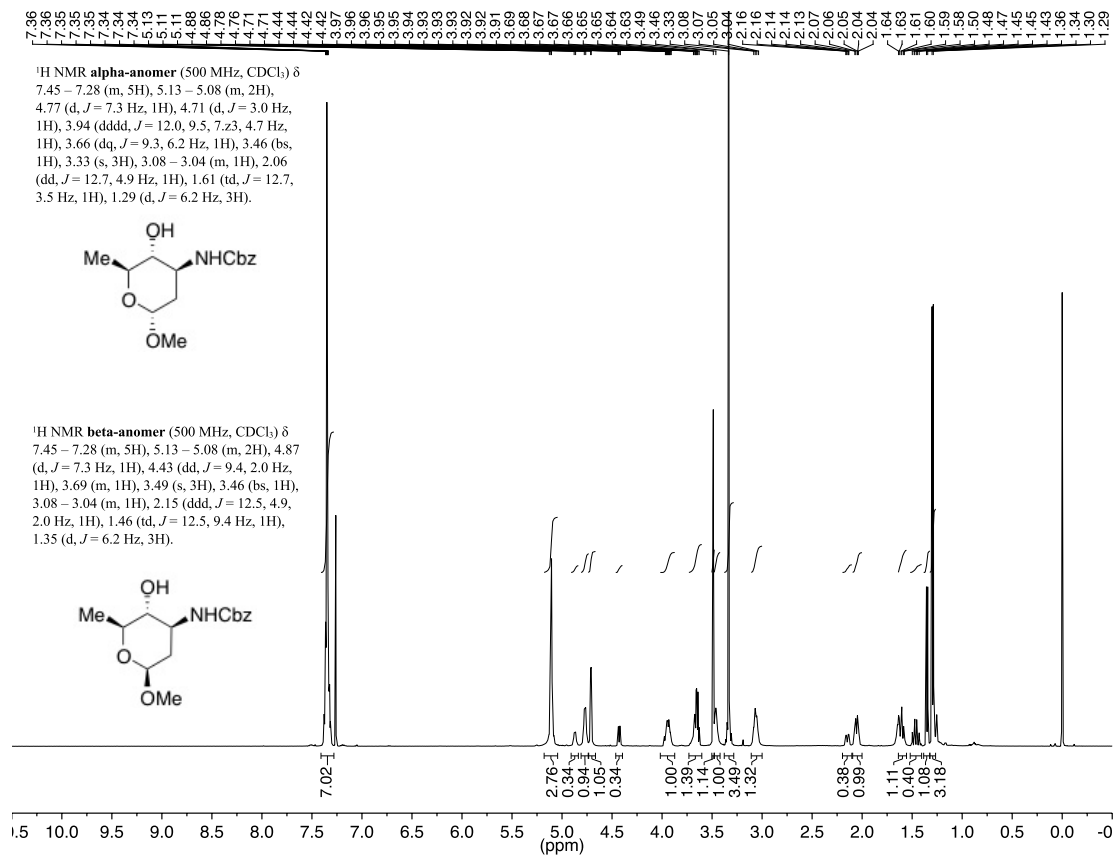




¹³C NMR (101 MHz, CDCl₃) δ 144.53, 136.60, 135.55, 134.94, 132.57, 130.11, 129.77, 128.53, 127.99, 127.93, 127.90, 127.85, 110.57, 88.79, 78.42, 68.10, 66.94, 54.60, 26.63, 25.83, 20.30, 19.38, 18.03, -4.39, -4.73.



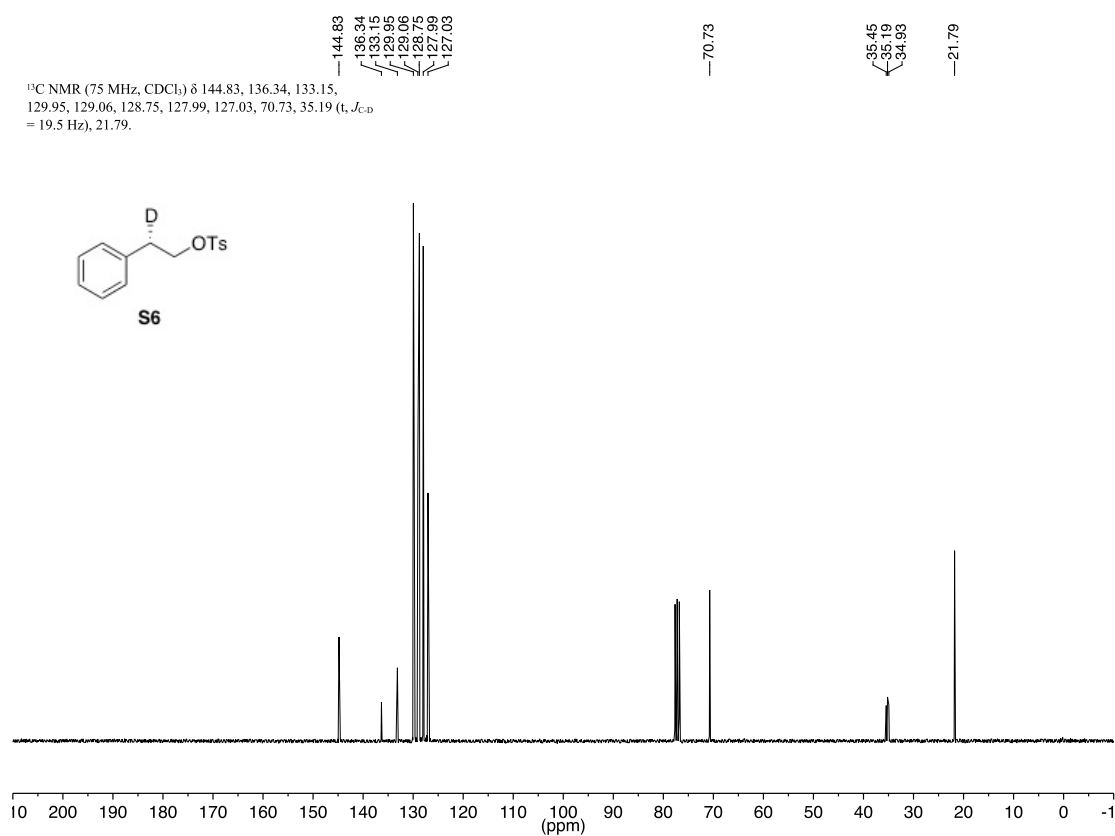
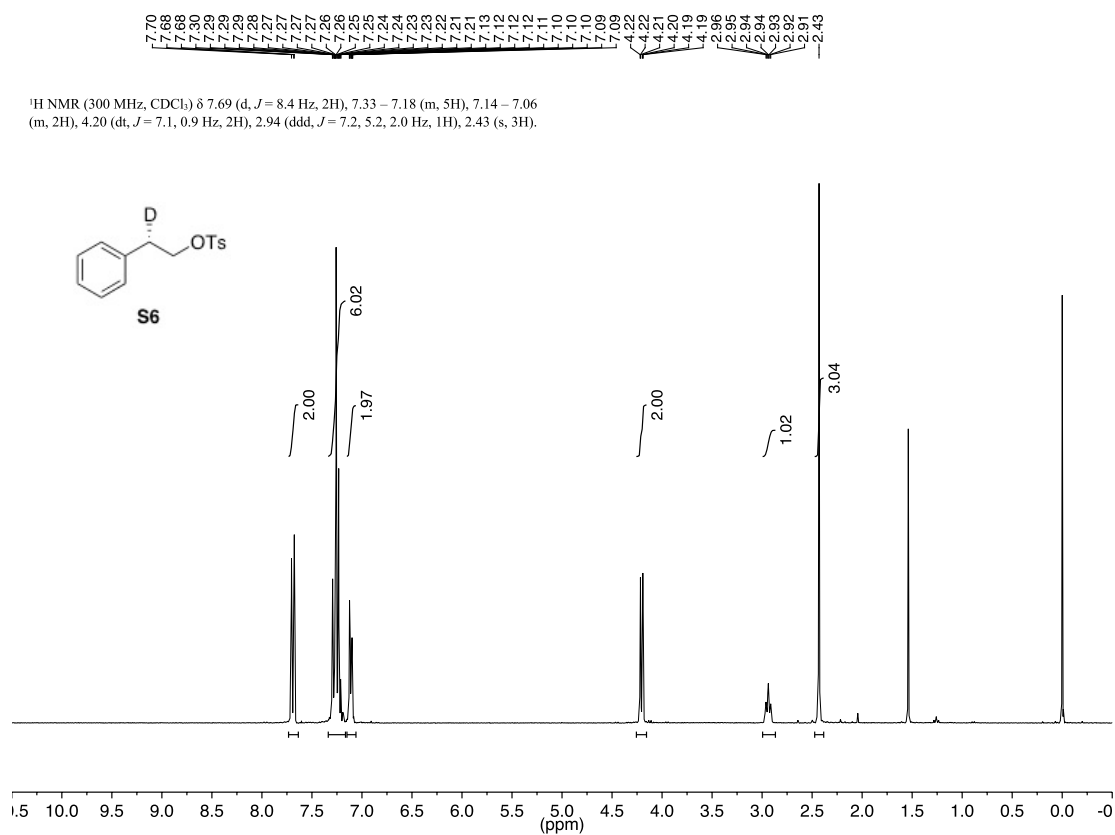


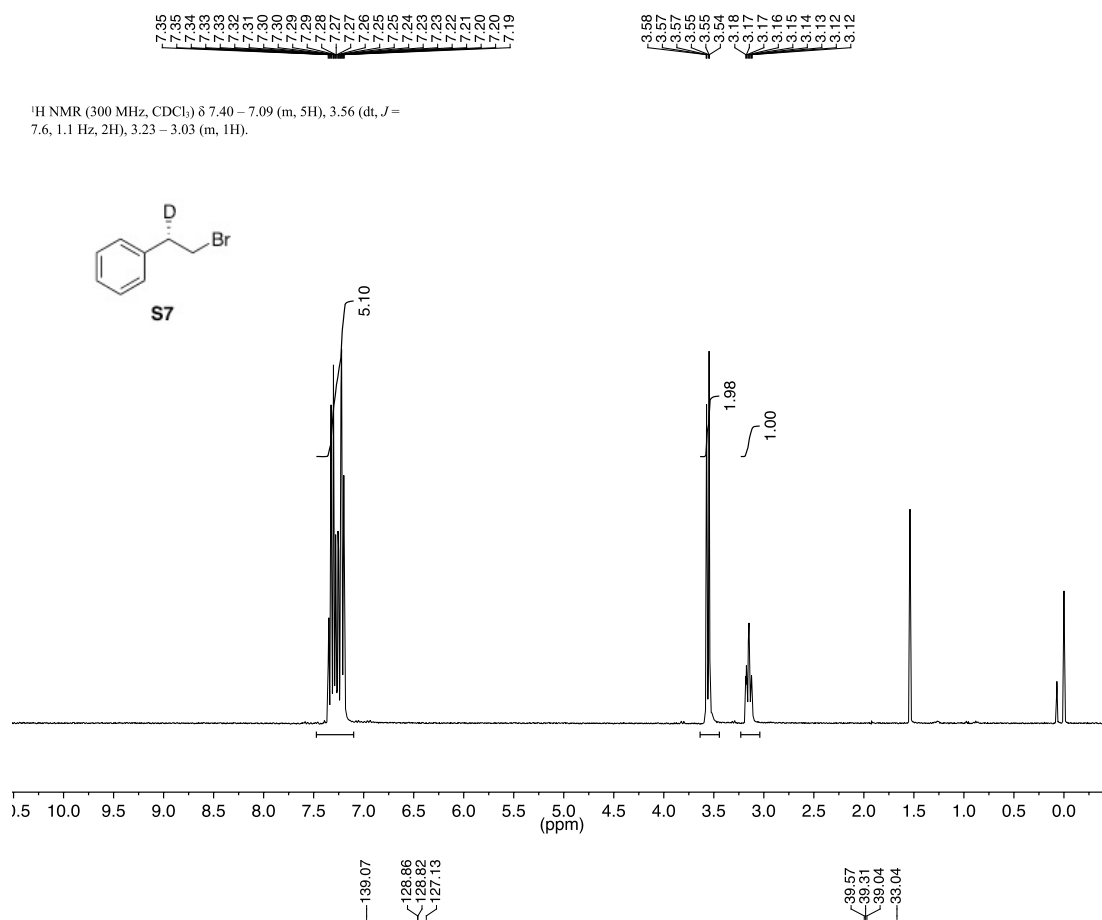


Appendix 2

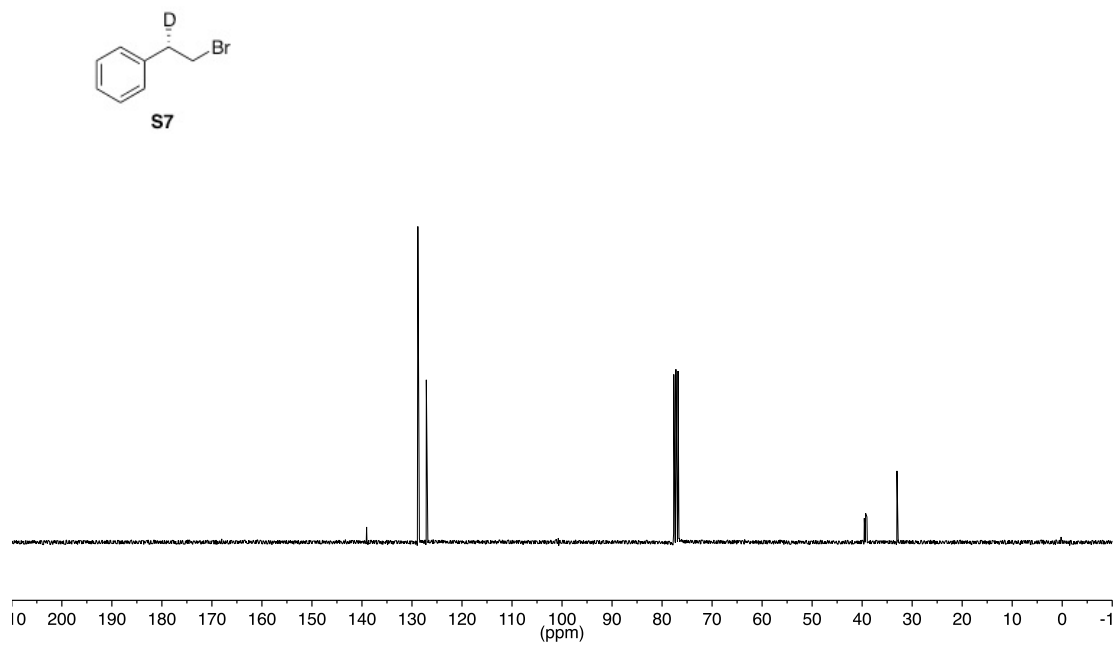
NMR Spectra for Chapter 3

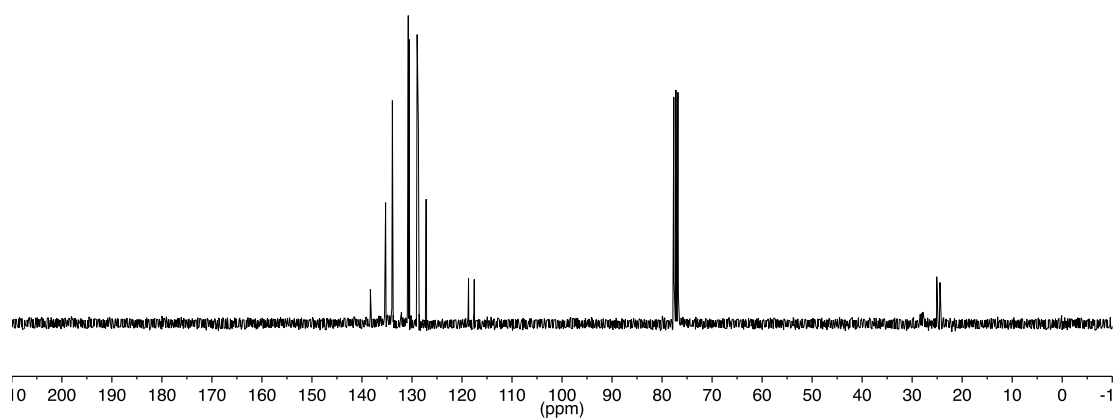
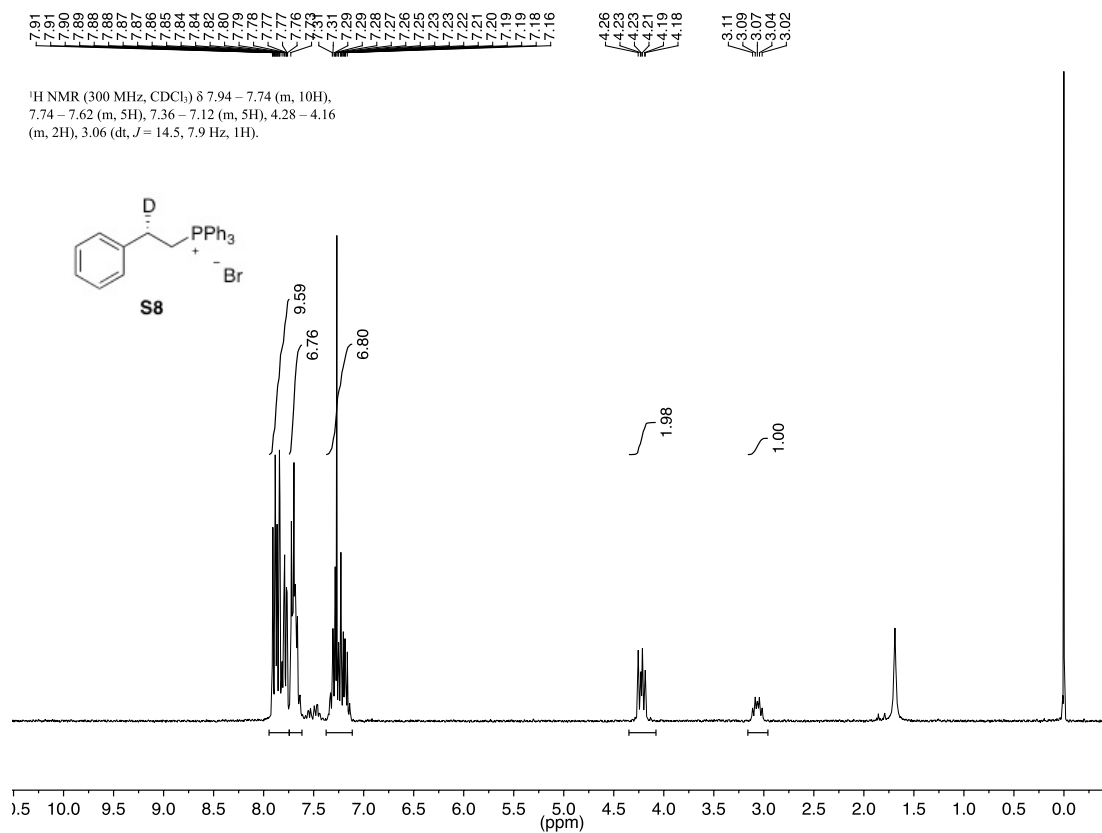
This work has been published: Weinstein, A. B.; Stahl, S. S. *Angew. Chem. Int. Ed.* **2012**, *51*, 11505–11509.

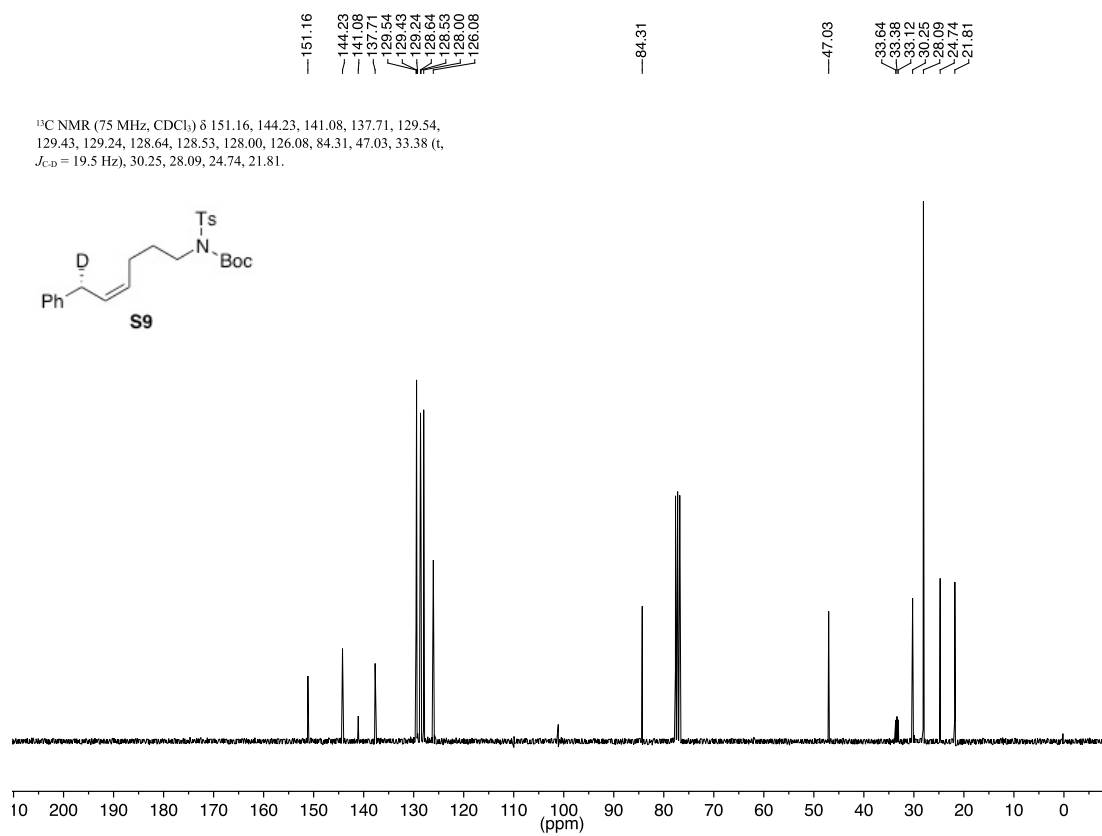
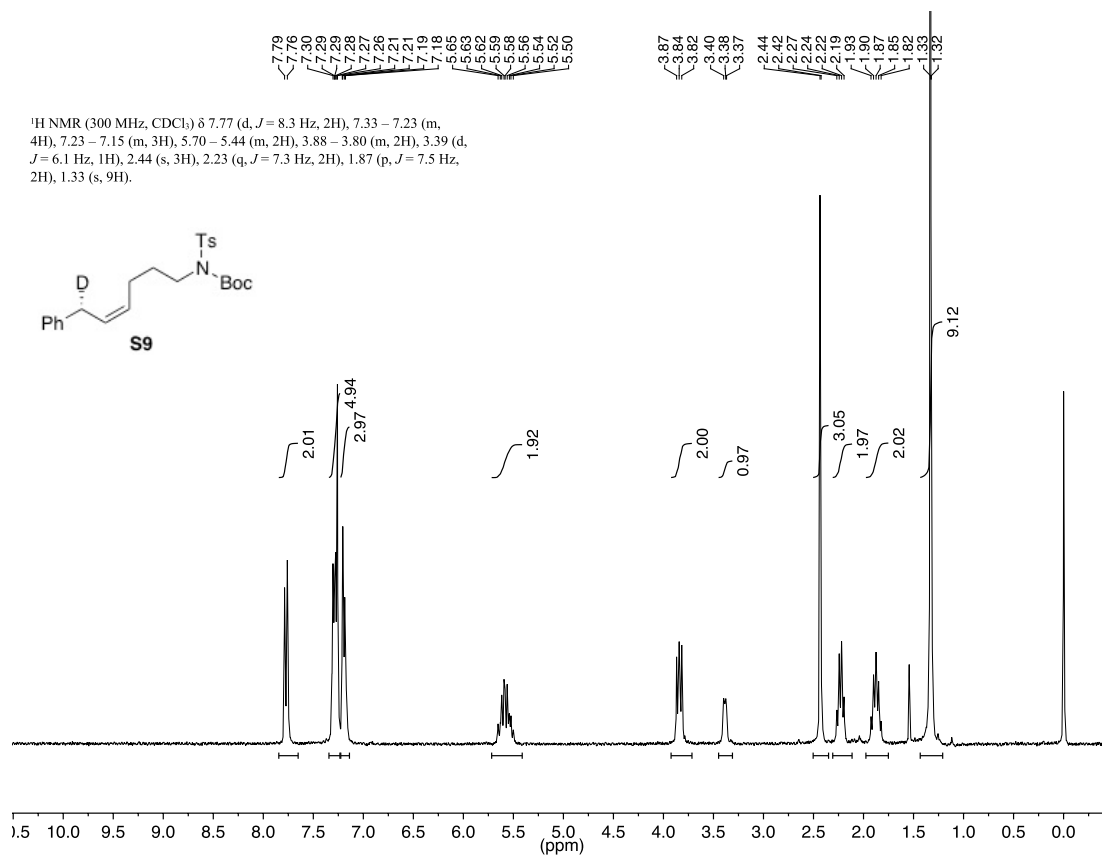




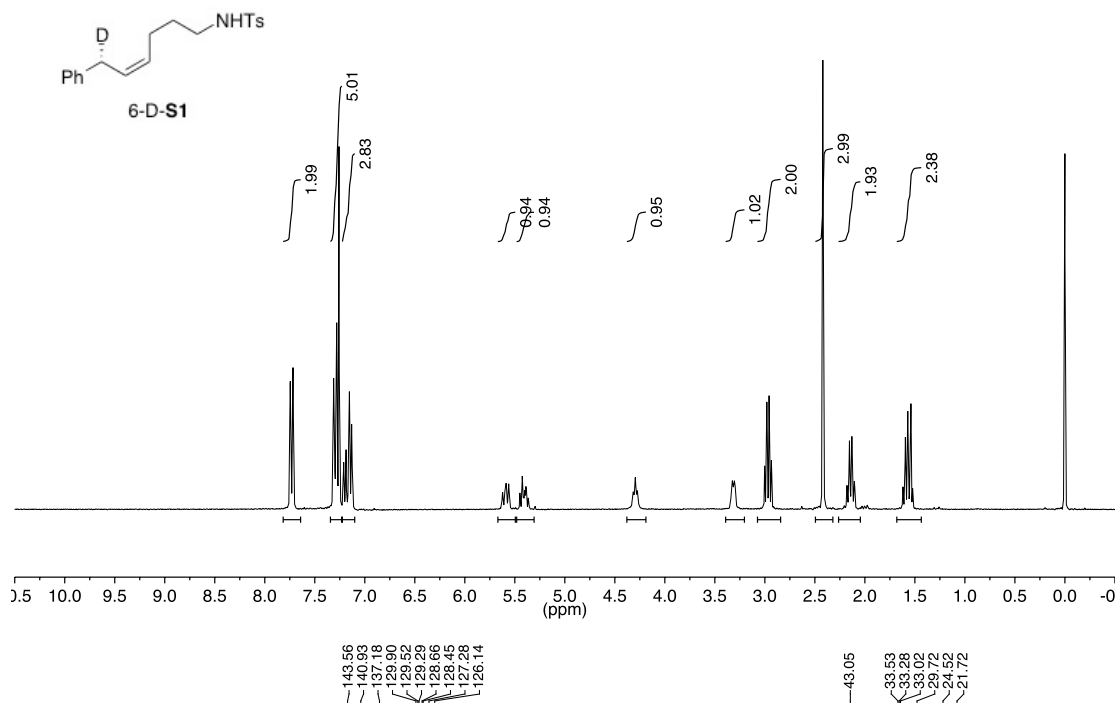
¹³C NMR (75 MHz, CDCl₃) δ 139.07, 128.86, 128.82, 127.13, 39.31 (t, *J*_{C-D} = 19.5 Hz), 33.04.



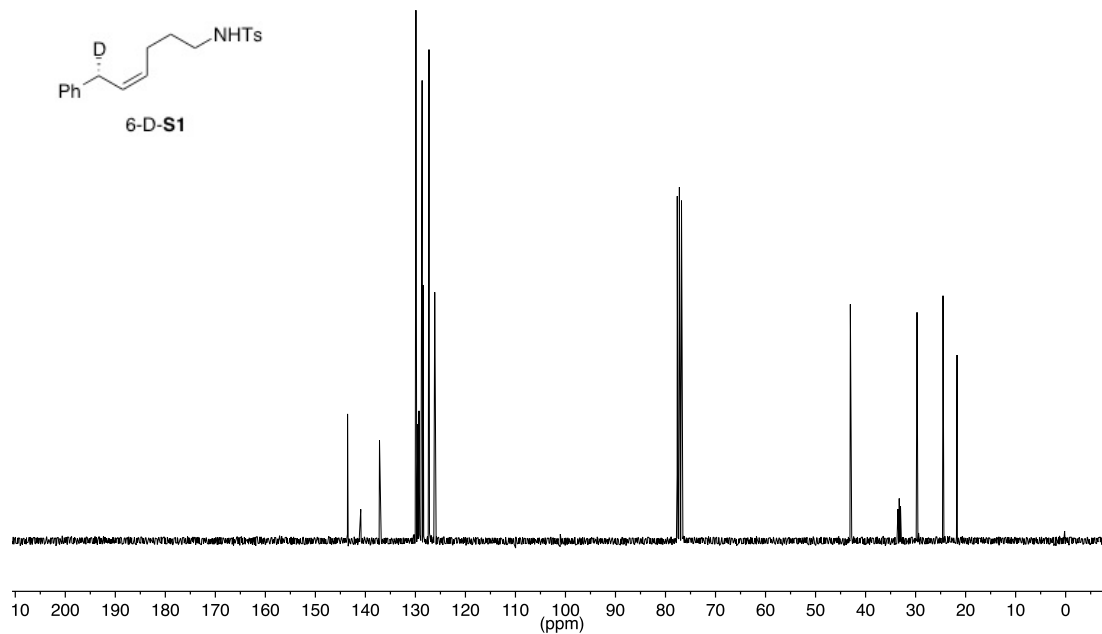


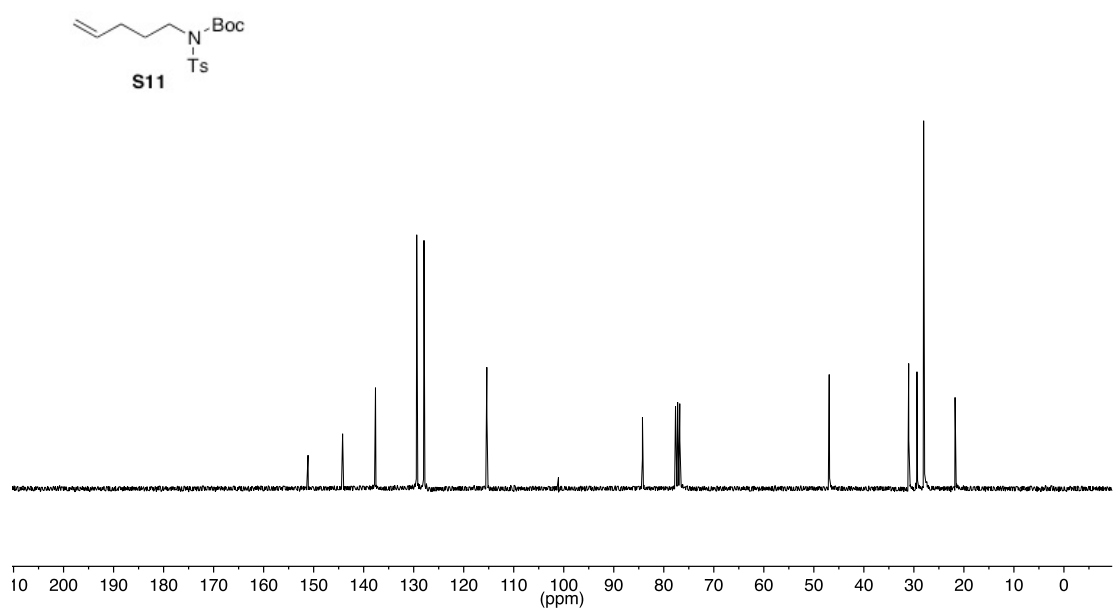
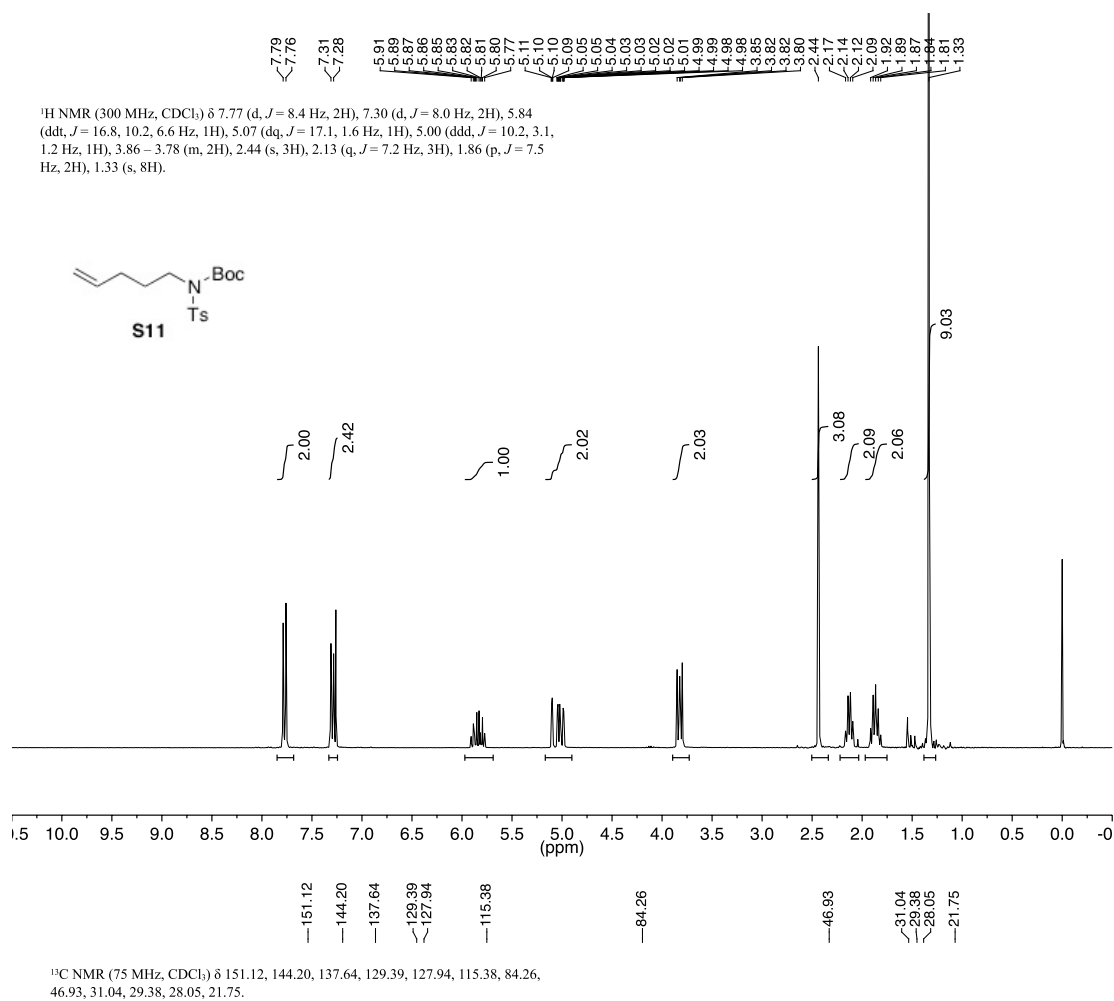


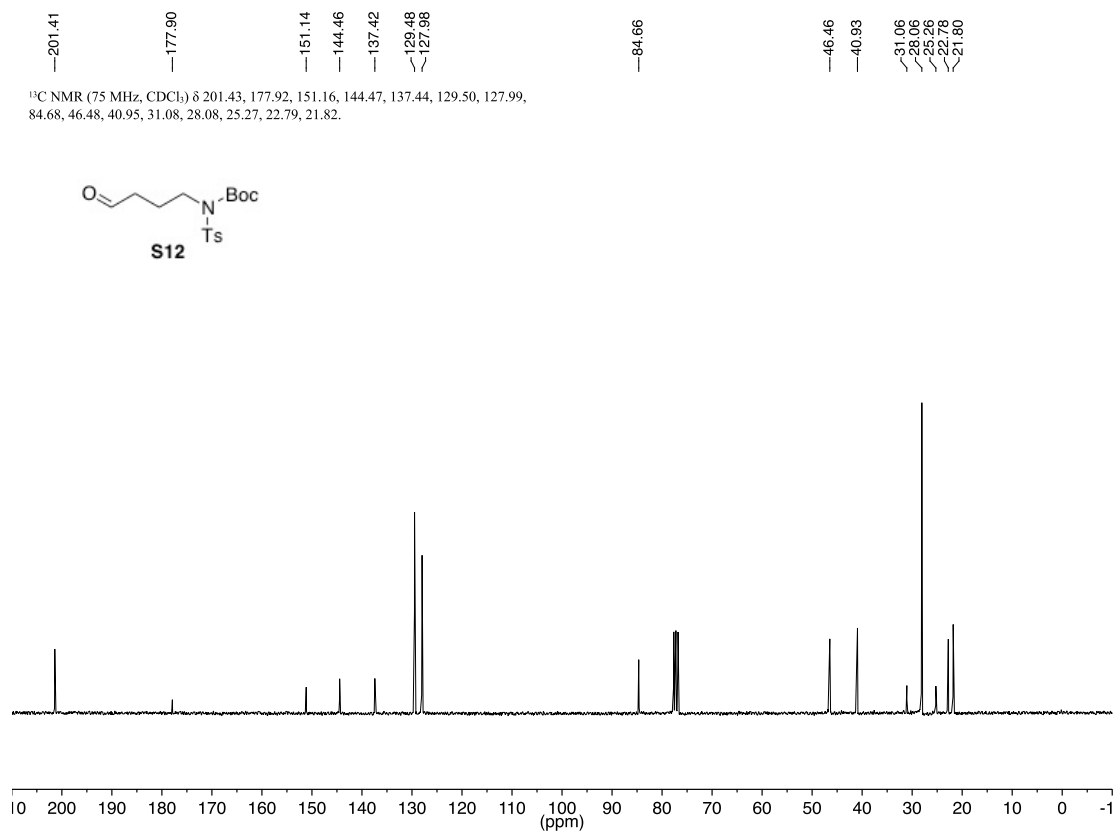
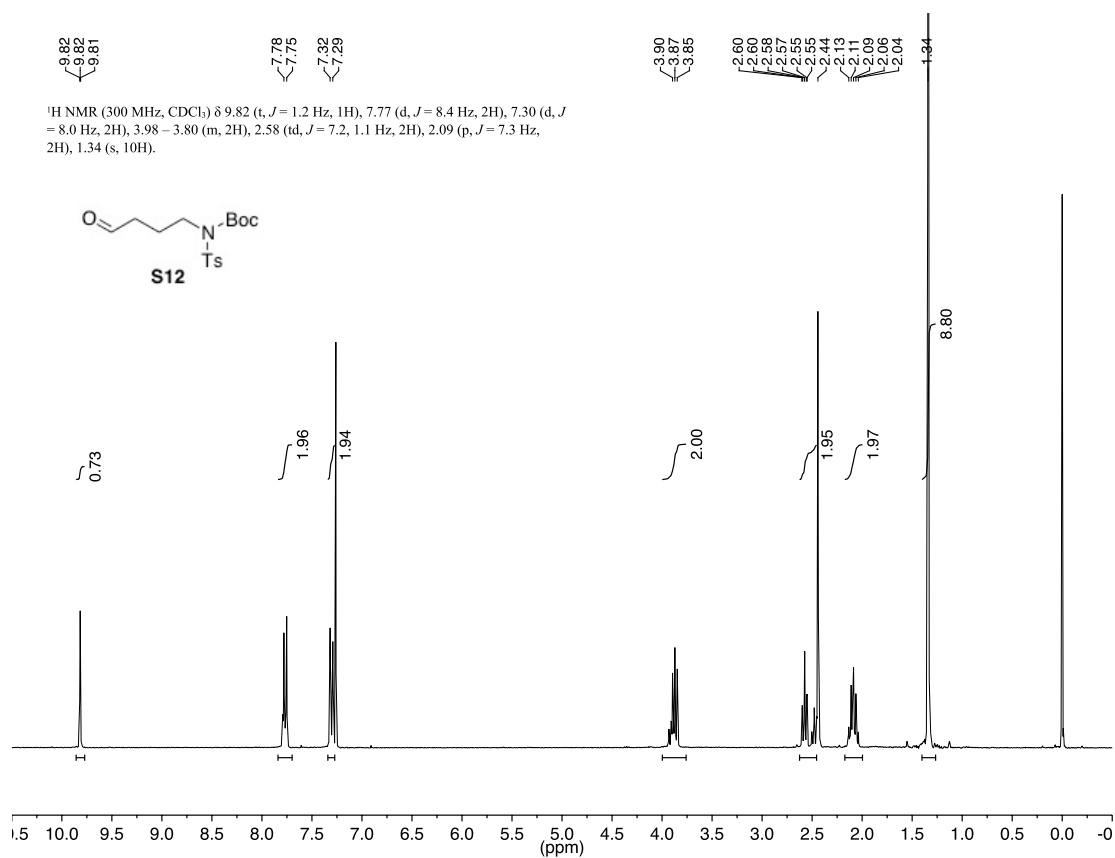
¹H NMR (300 MHz, CDCl₃) δ 7.73 (d, *J* = 8.2 Hz, 2H), 7.33 – 7.23 (m, 4H), 7.23 – 7.10 (m, 3H), 5.59 (dd, *J* = 10.6, 7.7 Hz, 1H), 5.41 (dddd, *J* = 10.8, 8.8, 6.9, 1.5 Hz, 1H), 4.30 (t, *J* = 6.3 Hz, 1H), 3.32 (d, *J* = 6.9 Hz, 1H), 2.97 (q, *J* = 6.8 Hz, 2H), 2.42 (s, 3H), 2.14 (q, *J* = 6.9 Hz, 2H), 1.57 (p, *J* = 7.2 Hz, 2H).

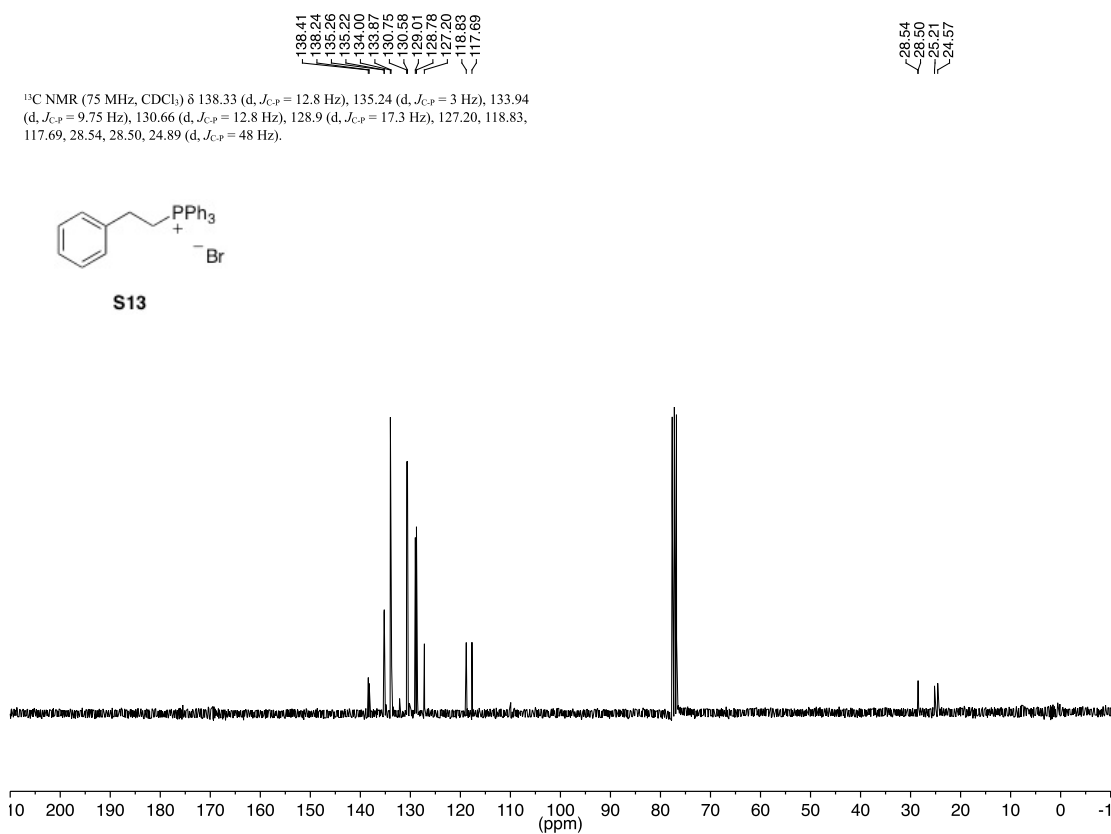
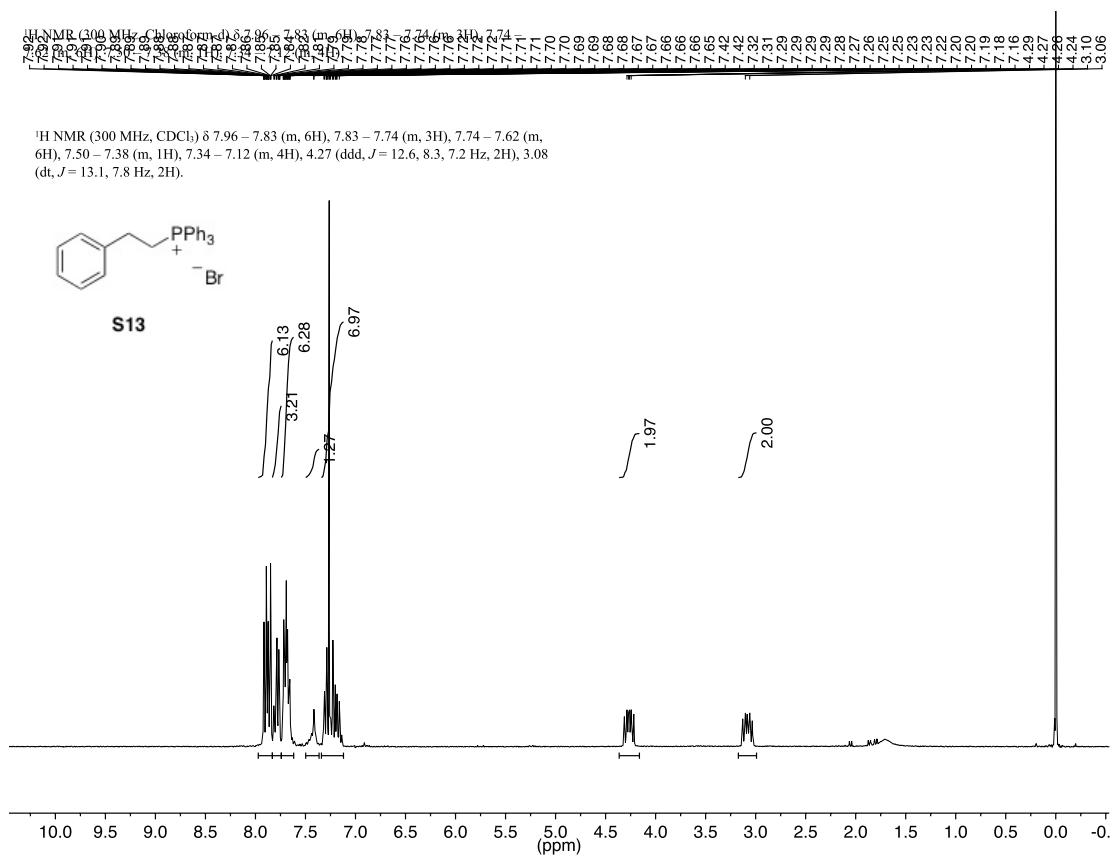


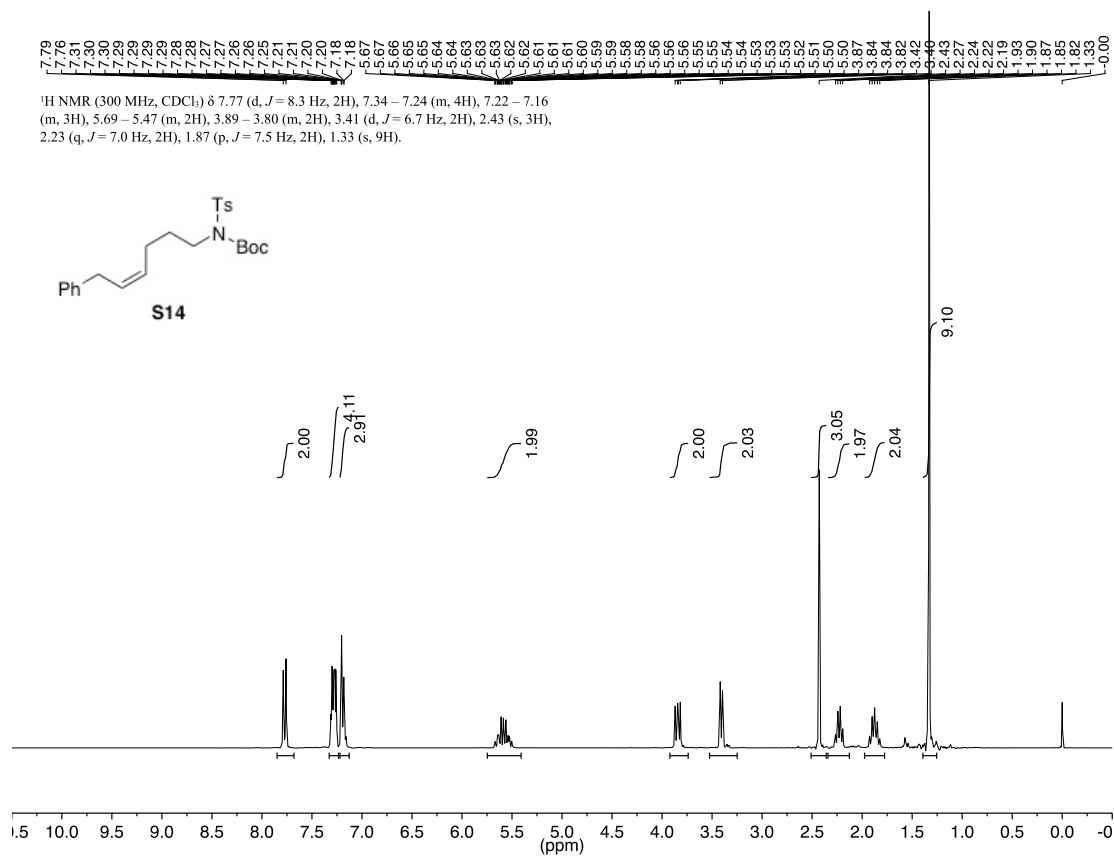
¹³C NMR (75 MHz, CDCl₃) δ 143.56, 140.93, 137.18, 129.90, 129.52, 129.29, 128.66, 128.45, 127.28, 126.14, 43.05, 33.28 (t, *J*_{C-D} = 19.5 Hz), 29.72, 24.52, 21.72.



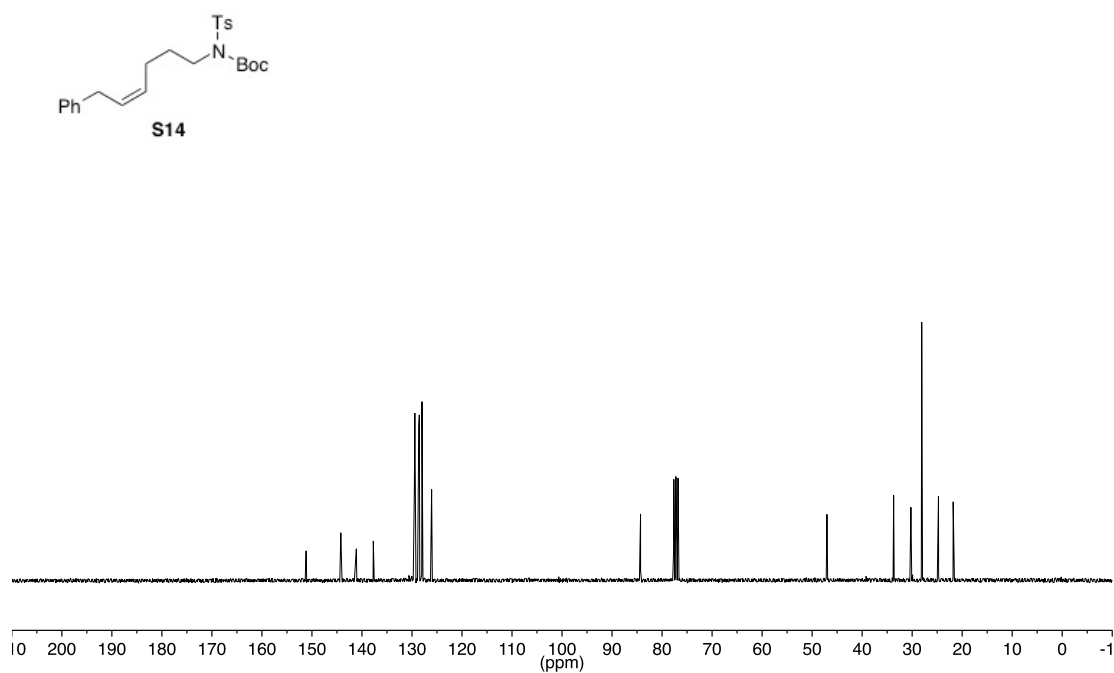


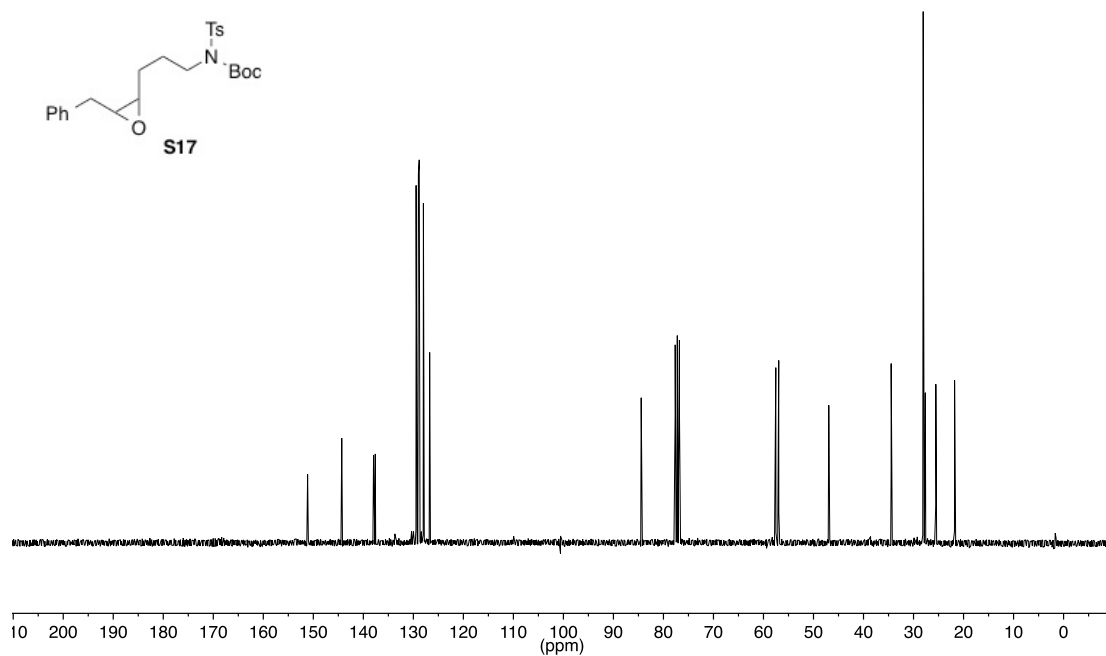
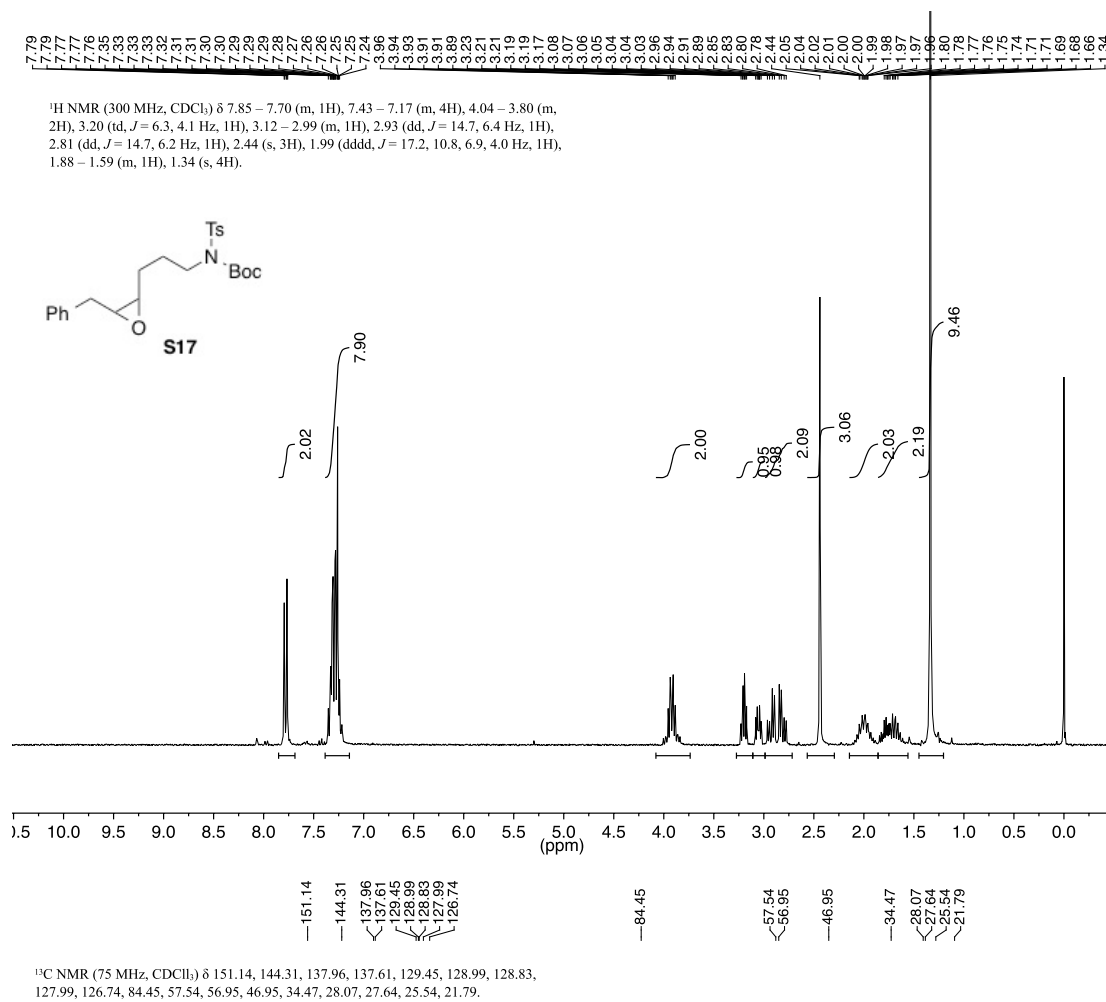


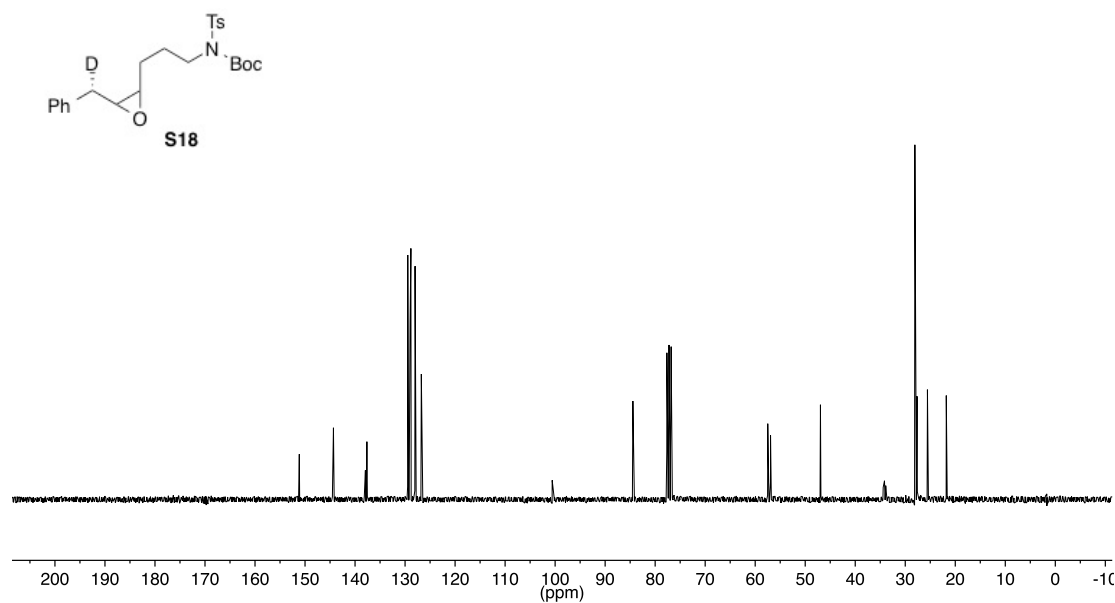
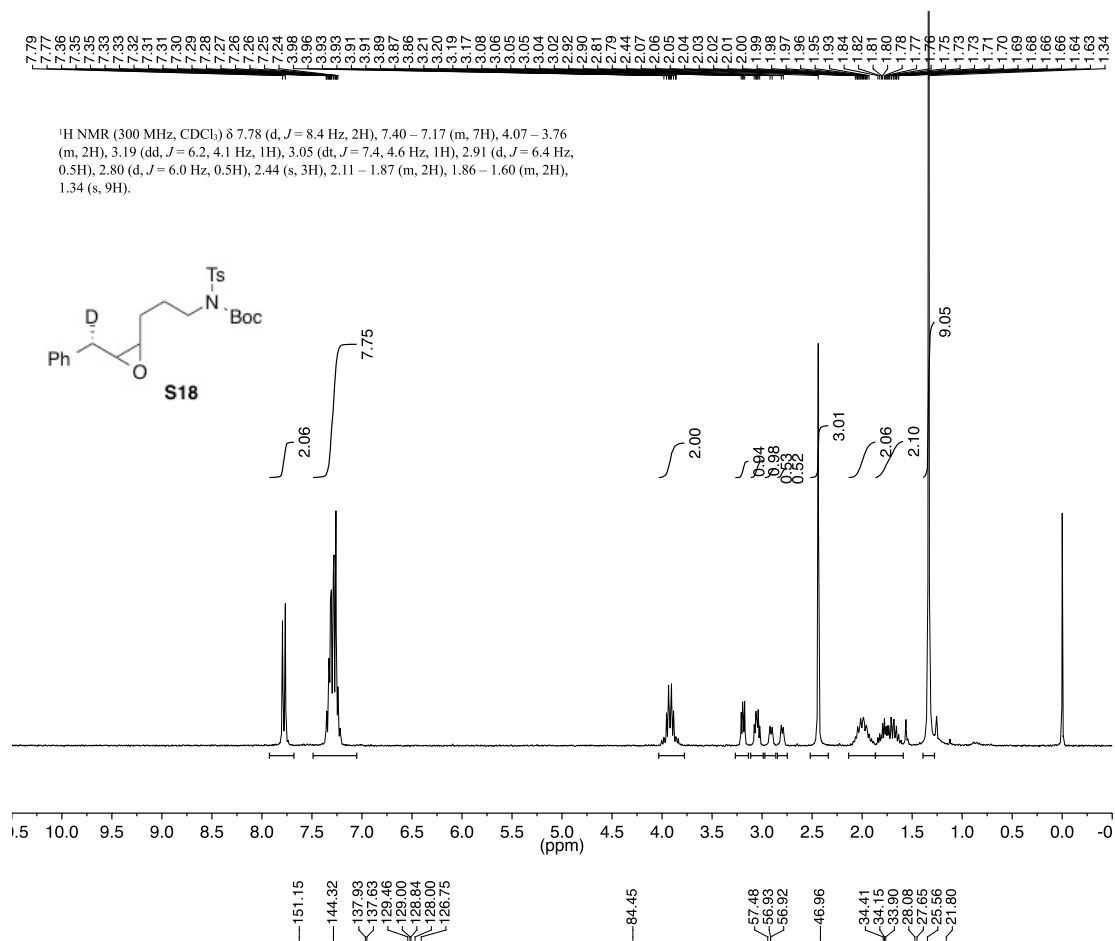


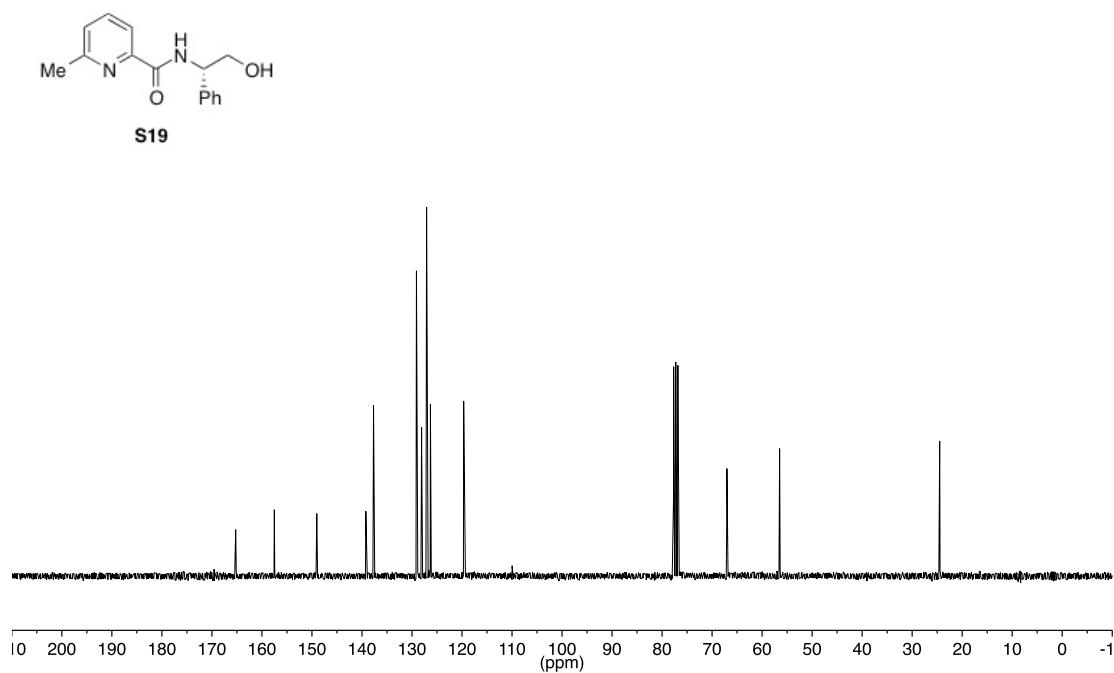
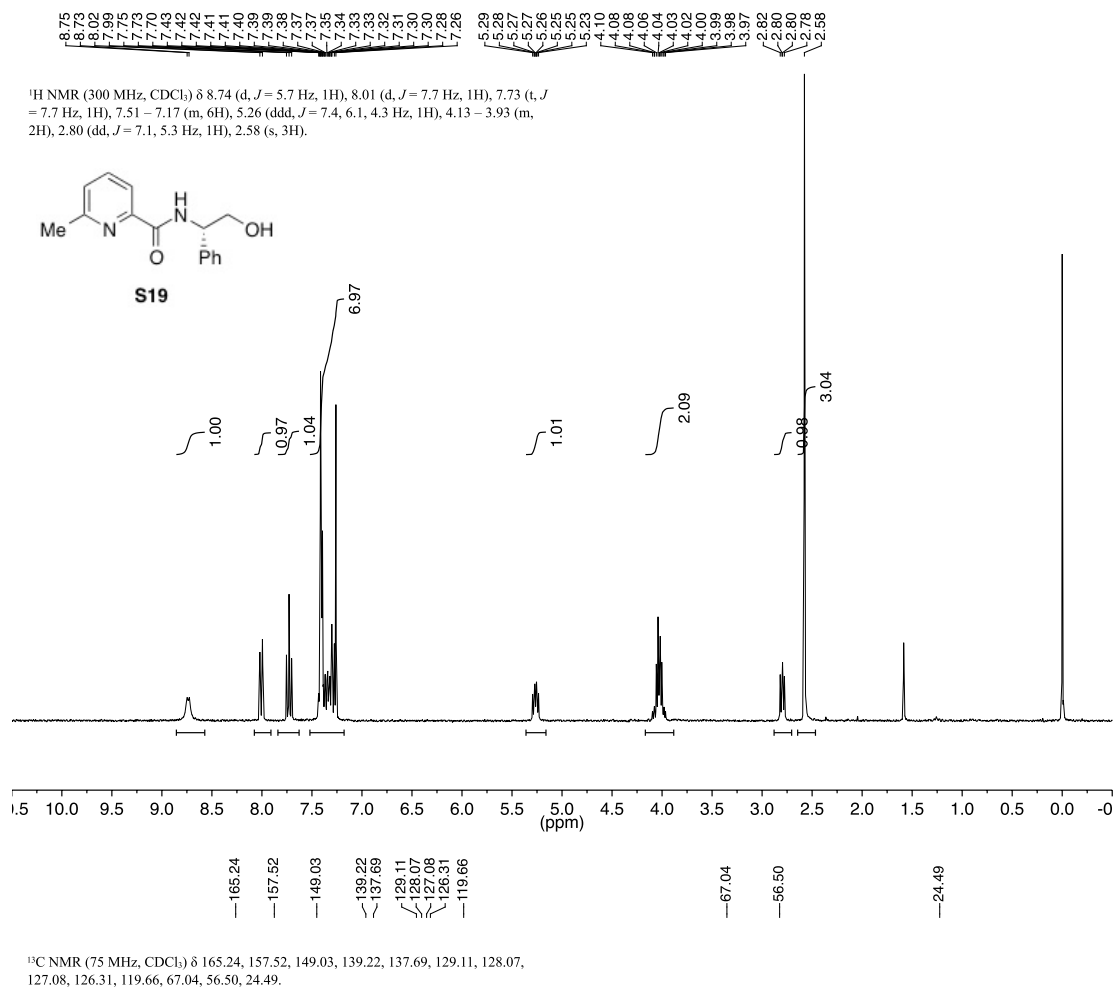


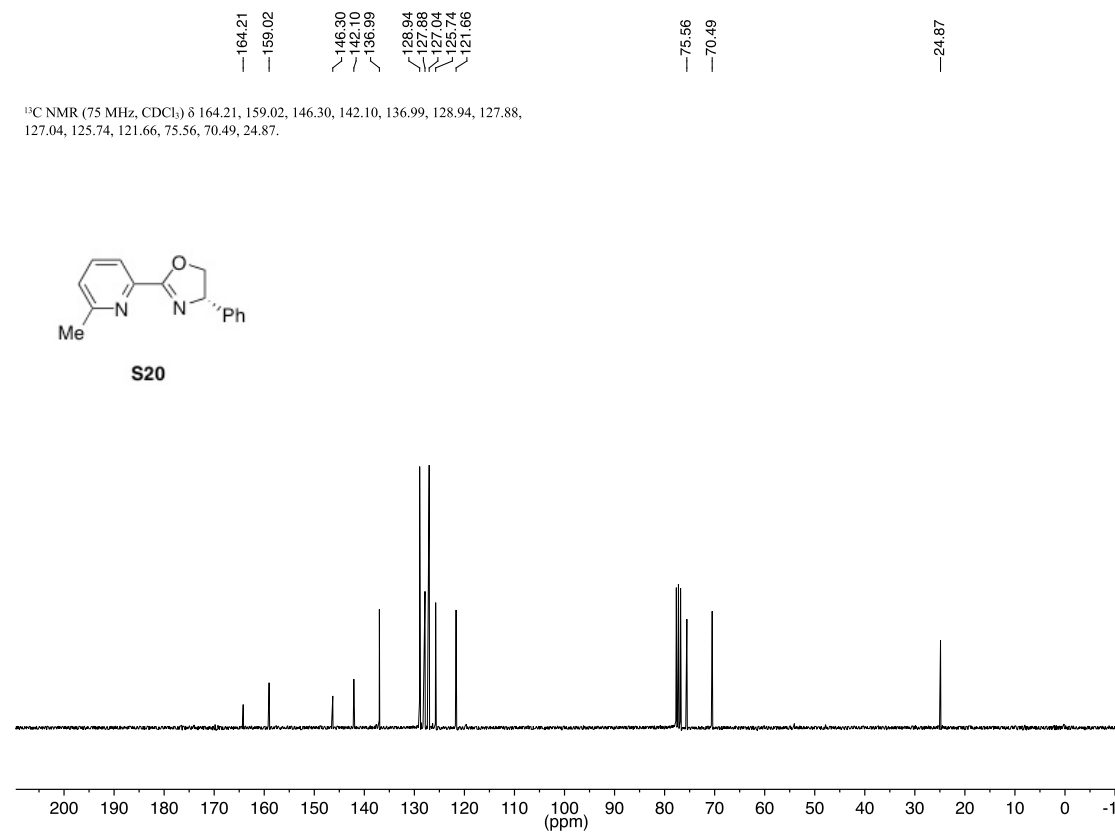
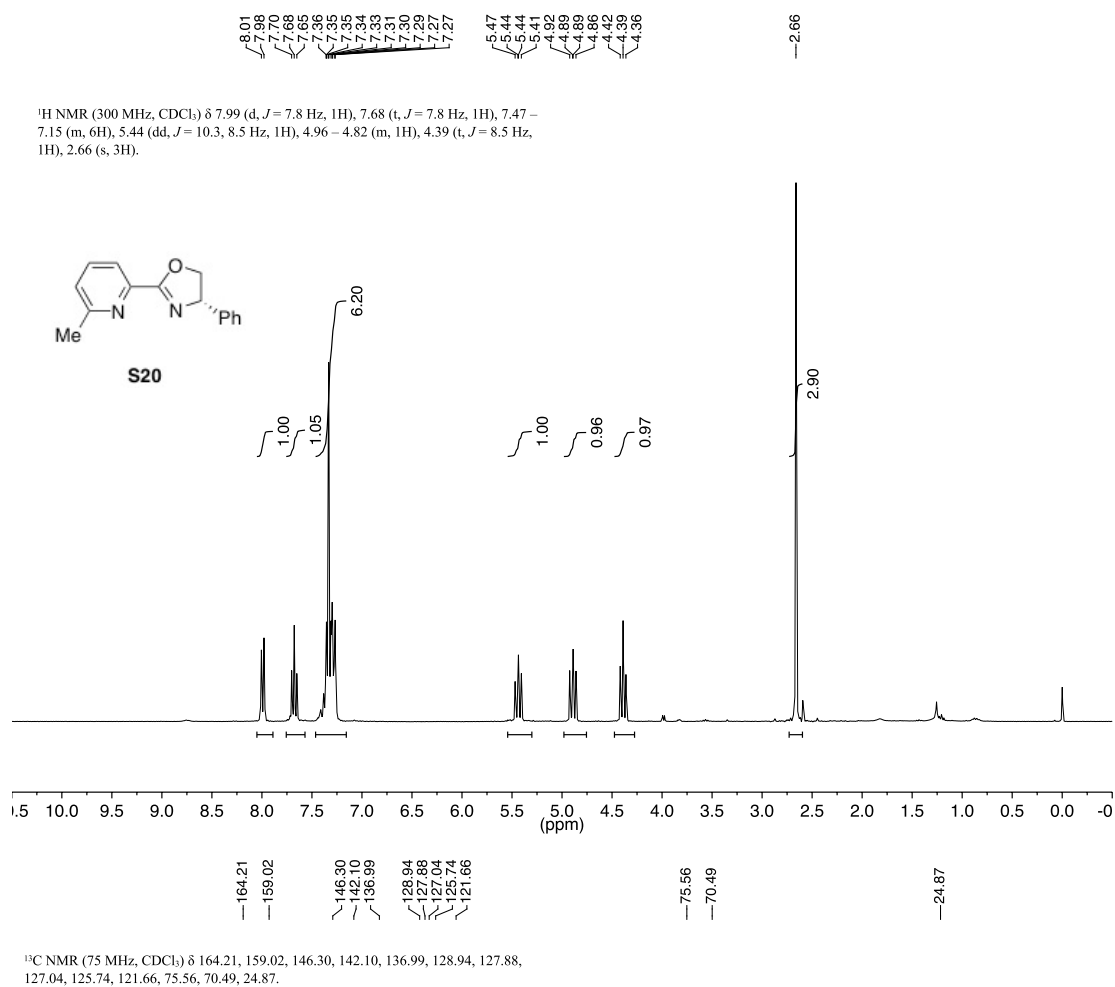
¹³C NMR (75 MHz, CDCl₃) δ 151.16, 144.23, 141.12, 137.73, 129.53, 129.43, 129.28, 128.63, 128.53, 128.00, 126.07, 84.30, 47.04, 33.70, 30.25, 28.09, 24.74, 21.80.







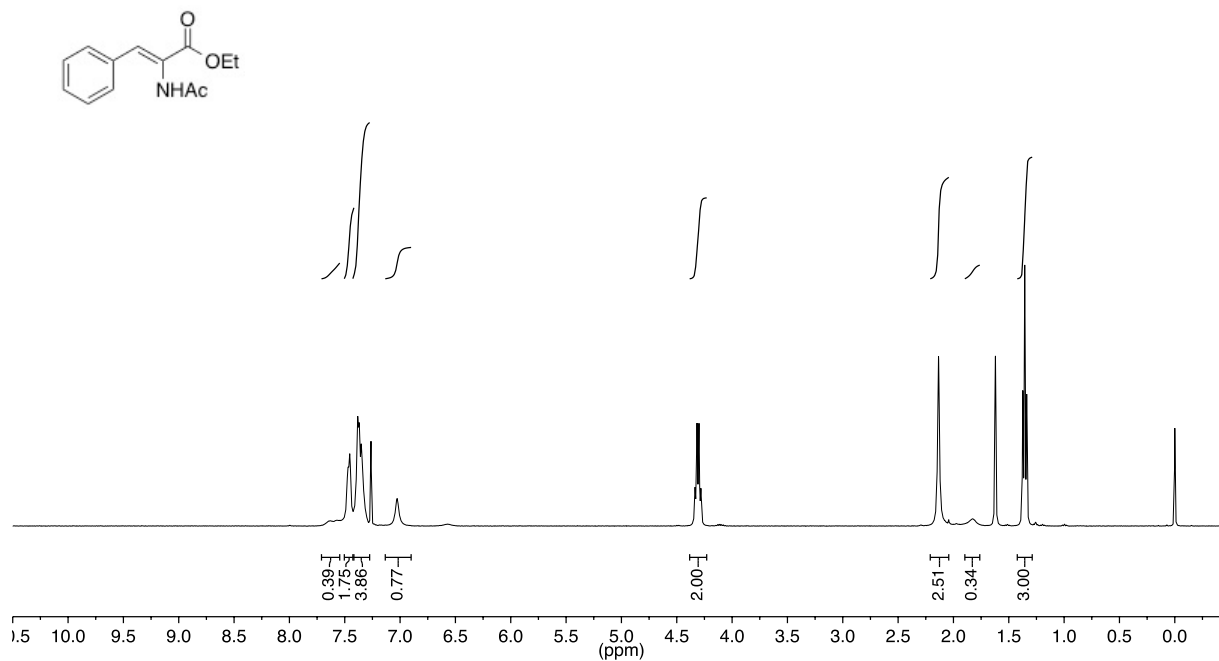




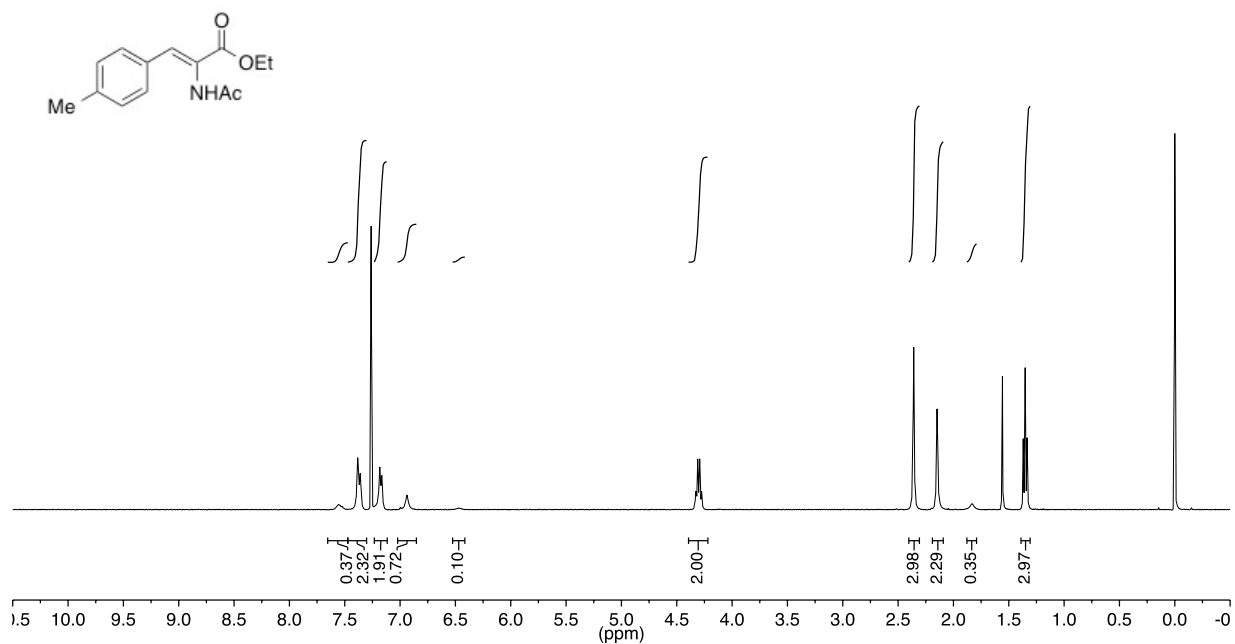
Appendix 3

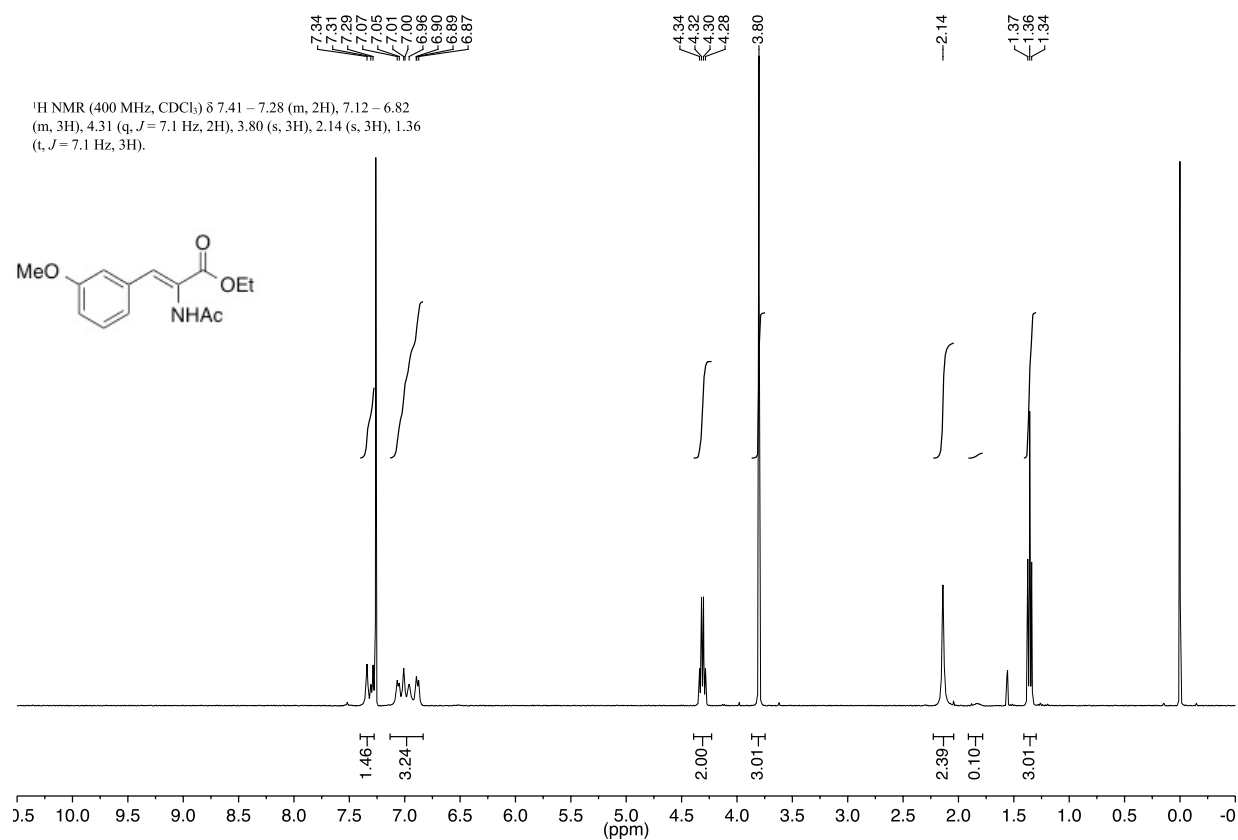
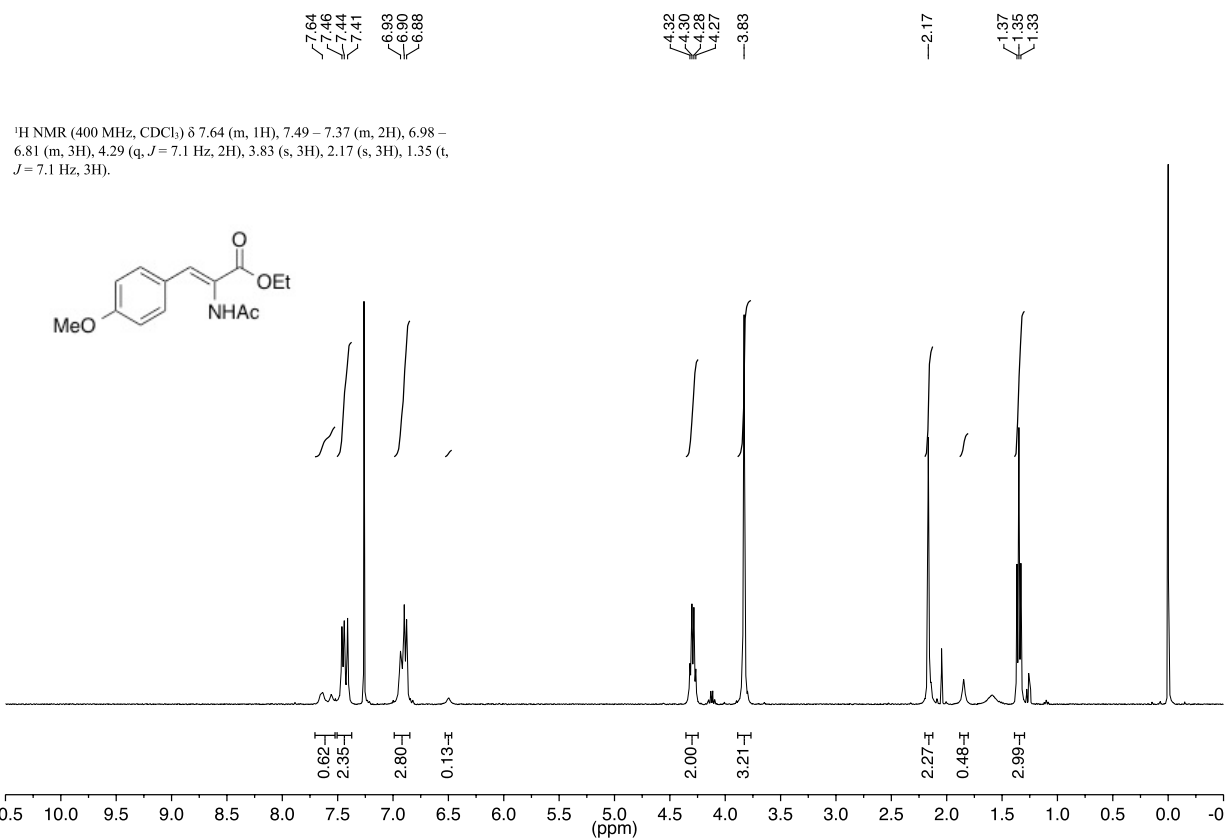
NMR Spectra for Chapter 4

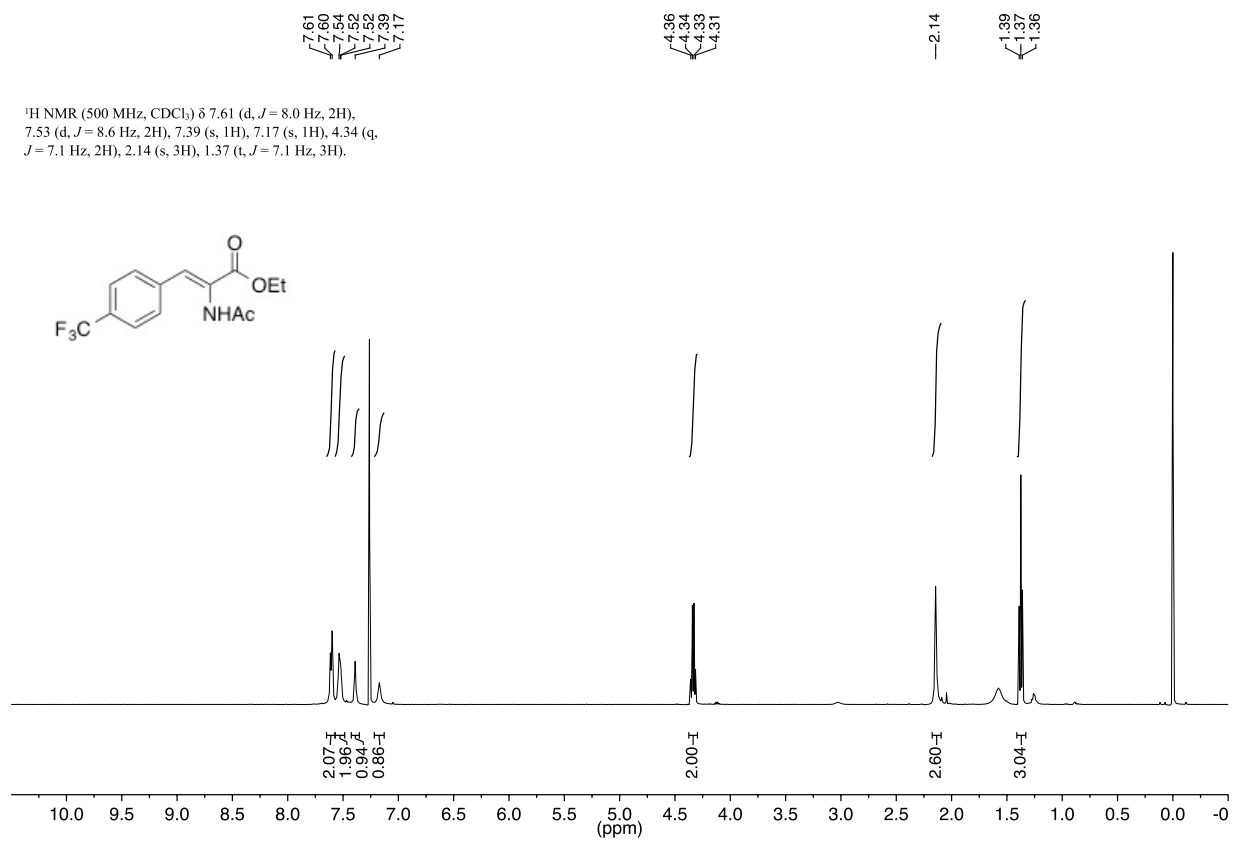
¹H NMR (400 MHz, CDCl₃) δ 7.70 – 7.29 (m, 6H), 7.03 (s, 1H), 4.31 (q, *J* = 7.1 Hz, 2H), 2.13 (s, 3H), 1.36 (t, *J* = 7.1 Hz, 3H).



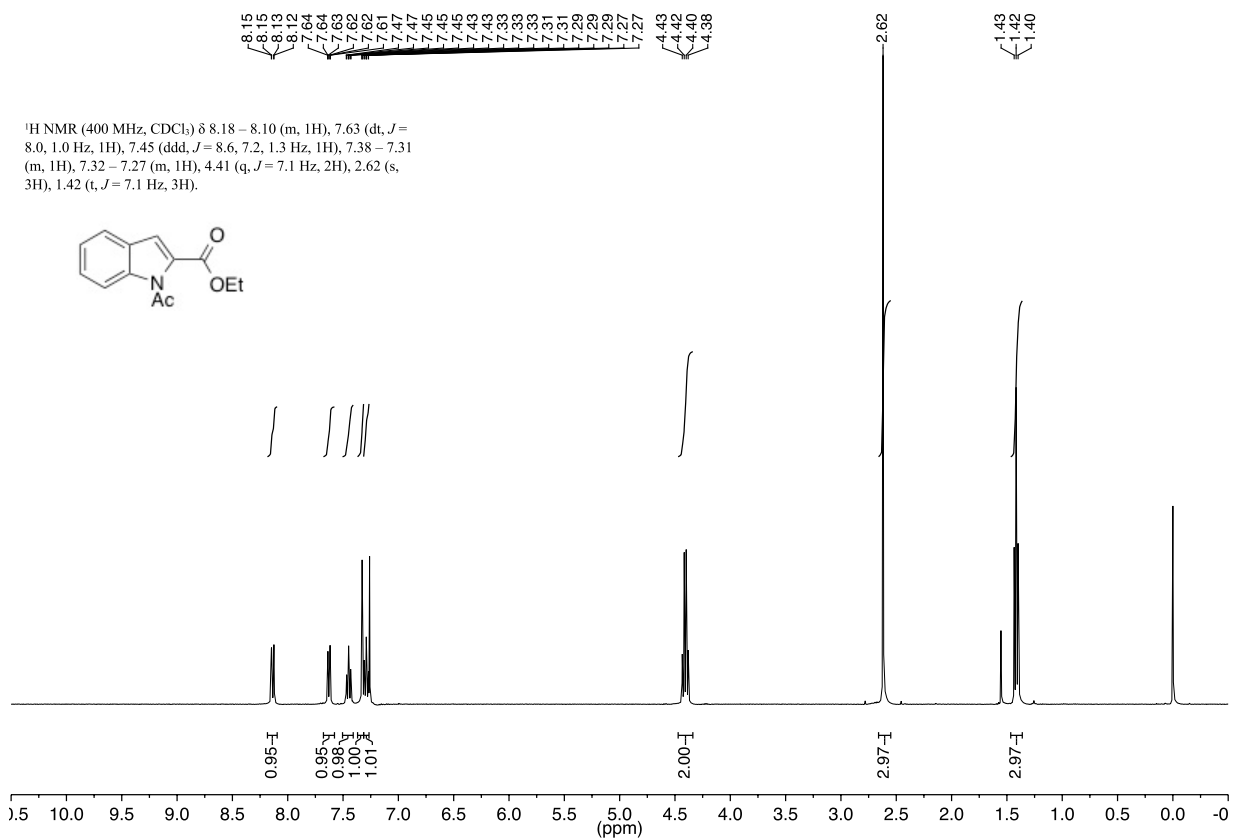
¹H NMR (400 MHz, CDCl₃) δ 7.55 (m, 1H), 7.37 (d, *J* = 8.9 Hz, 2H), 7.22 – 7.14 (m, 2H), 6.94 (s, 1H), 4.30 (q, *J* = 7.1 Hz, 2H), 2.36 (s, 3H), 2.15 (s, 3H), 1.35 (t, *J* = 7.1 Hz, 3H).



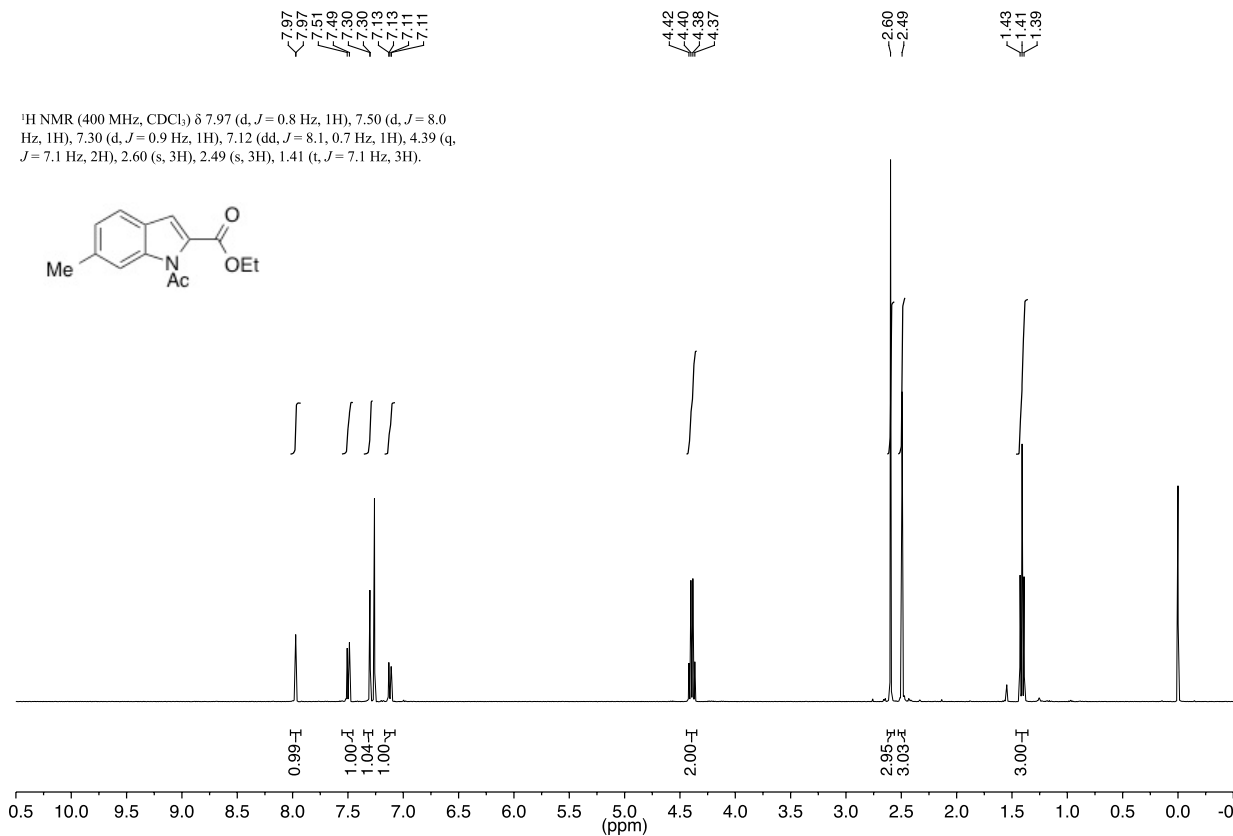




¹H NMR (400 MHz, CDCl₃) δ 8.18 – 8.10 (m, 1H), 7.63 (dt, *J* = 8.0, 1.0 Hz, 1H), 7.45 (ddd, *J* = 8.6, 7.2, 1.3 Hz, 1H), 7.38 – 7.31 (m, 1H), 7.32 – 7.27 (m, 1H), 4.41 (q, *J* = 7.1 Hz, 2H), 2.62 (s, 3H), 1.42 (t, *J* = 7.1 Hz, 3H).



¹H NMR (400 MHz, CDCl₃) δ 7.97 (d, *J* = 0.8 Hz, 1H), 7.50 (d, *J* = 8.0 Hz, 1H), 7.30 (d, *J* = 0.9 Hz, 1H), 7.12 (dd, *J* = 8.1, 0.7 Hz, 1H), 4.39 (q, *J* = 7.1 Hz, 2H), 2.60 (s, 3H), 2.49 (s, 3H), 1.41 (t, *J* = 7.1 Hz, 3H).

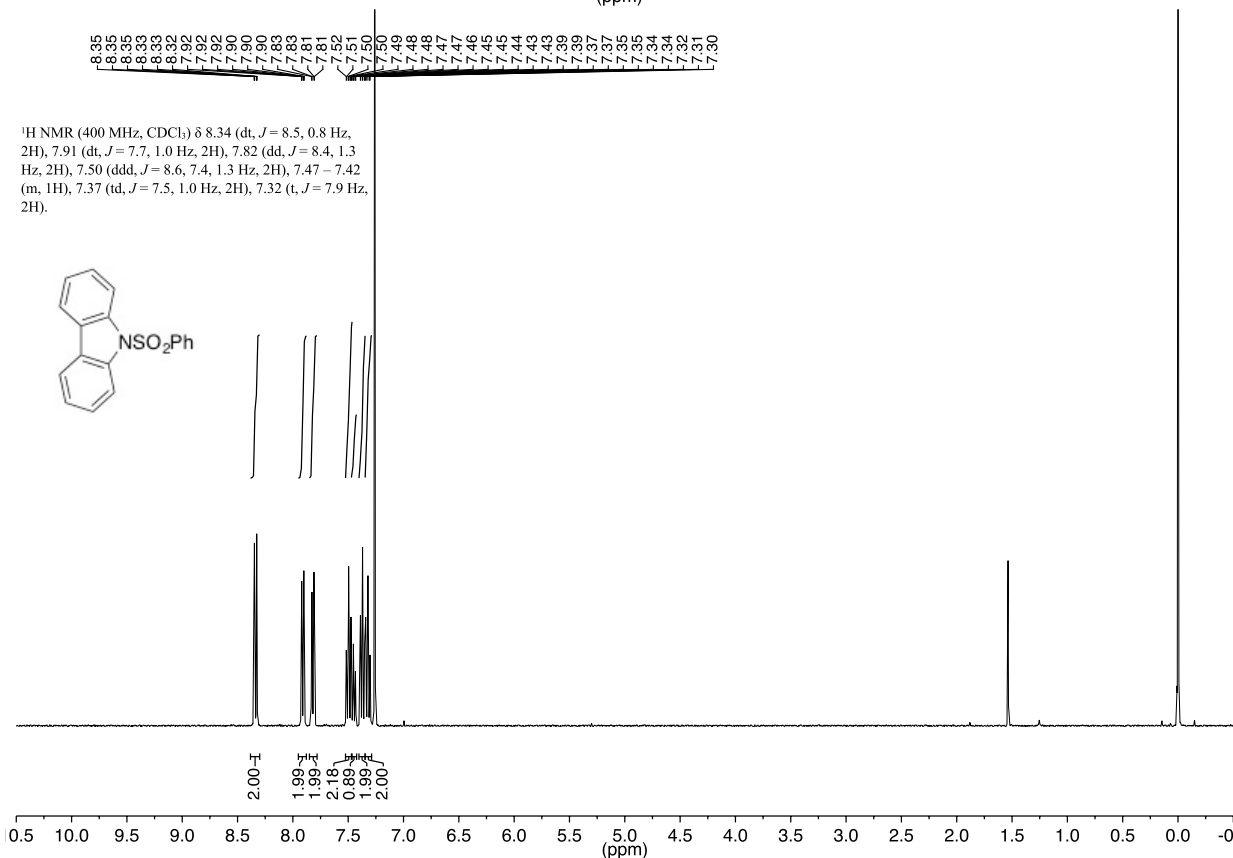
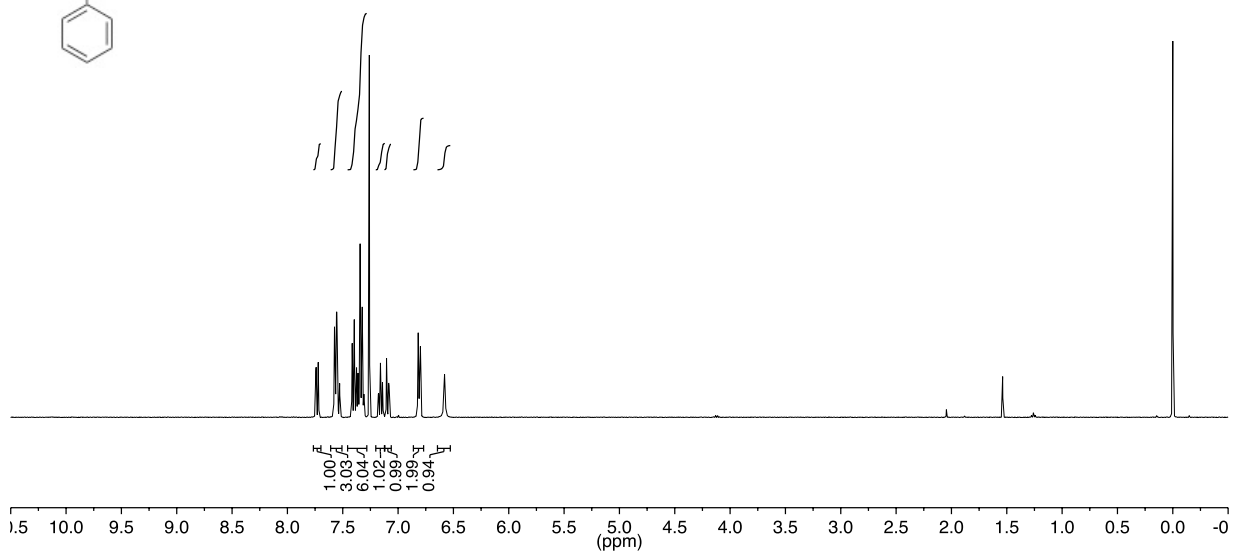
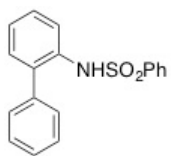


Appendix 4

NMR Spectra for Chapter 5

7.74
7.74
7.72
7.72
7.69
7.69
7.57
7.57
7.56
7.56
7.55
7.55
7.53
7.53
7.42
7.42
7.41
7.41
7.40
7.40
7.39
7.39
7.38
7.38
7.37
7.37
7.36
7.36
7.35
7.35
7.34
7.34
7.33
7.33
7.32
7.32
7.31
7.31
7.30
7.30
7.18
7.18
7.16
7.16
7.14
7.14
7.10
7.10
7.09
7.09
6.82
6.82
6.80
6.80
6.58
6.58

¹H NMR (400 MHz, CDCl₃) δ 7.73 (dd, *J* = 8.3, 1.2 Hz, 1H), 7.61
– 7.51 (m, 3H), 7.45 – 7.29 (m, 6H), 7.16 (td, *J* = 7.5, 1.2 Hz,
1H), 7.09 (dd, *J* = 7.6, 1.7 Hz, 1H), 6.81 (dd, *J* = 7.7, 1.8 Hz, 2H),
6.58 (s, 1H).



¹H NMR (400 MHz, CDCl₃) δ 8.34 (dt, *J* = 8.5, 0.8 Hz,
2H), 7.91 (dt, *J* = 7.7, 1.0 Hz, 2H), 7.82 (dd, *J* = 8.4, 1.3
Hz, 2H), 7.50 (ddd, *J* = 8.6, 7.4, 1.3 Hz, 2H), 7.47 – 7.42
(m, 1H), 7.37 (td, *J* = 7.5, 1.0 Hz, 2H), 7.32 (t, *J* = 7.9 Hz,
2H).

